Subsurface Barrier Validation with the SEAtrace™ System

Option 1 (Phase II) Topical Report

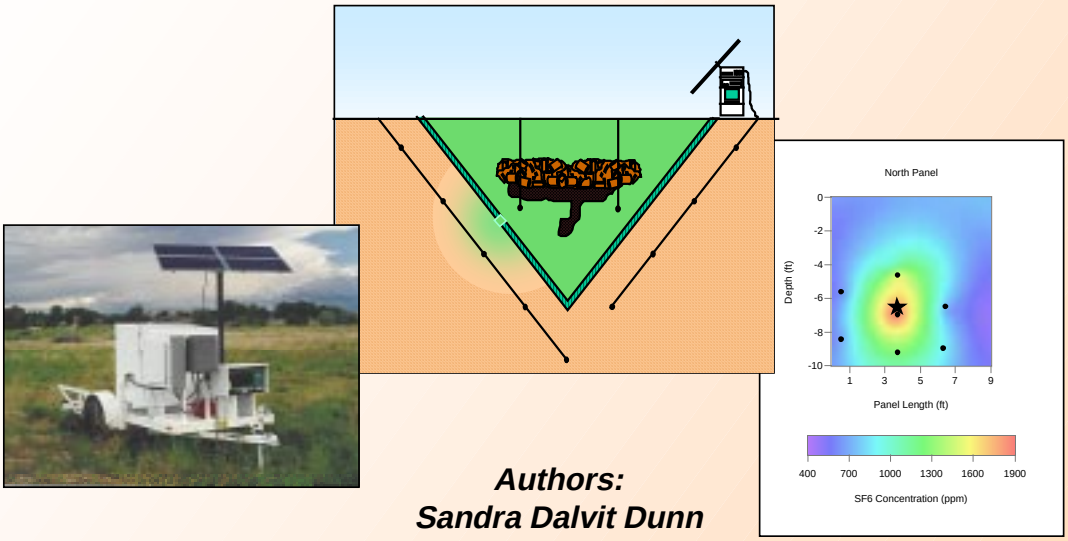

Authors:
Sandra Dalvit Dunn
William Lowry
Veraun Chipman

September 1999

SEASF-FR-99-232

Submitted to:

Karen Cohen

DOE Federal Energy Technology Center

FETC Contract DE-AC21-96MC33125

Science & Engineering Associates, Inc.

3205 Richards Lane, Suite A
Santa Fe, NM 87505
Phone (505) 424-6955

DISCLAIMER

This report was prepared as an account of work sponsored by an agency of the United States Government. Neither the United States Government nor any agency thereof, nor any of their employees, makes any warranty, express or implied, or assumes any legal liability of responsibility for the accuracy, completeness, or usefulness of any information, apparatus, product, or process disclosed, or represents that its use would not infringe privately owned rights. The reference herein to any specific commercial product, process, or service by trade name, trademark, manufacturer, or otherwise does not necessarily constitute or imply its endorsement, recommendation, or favoring by the United States Government or any agency thereof. The views and opinions of authors expressed herein do not necessarily state or reflect those of the United States Government or any agency thereof.

TABLE OF CONTENTS

LIST OF FIGURES

LIST OF TABLES

ABSTRACT

Under contract to the Department of Energy, Science & Engineering Associates has completed development and testing of a subsurface barrier verification and monitoring system. This system, called SEAtrace™, is able to locate and size leaks with a high degree of accuracy in subsurface barriers that are emplaced in an unsaturated medium. It uses gaseous tracer injection, in-field real-time monitoring, and real time data analysis to evaluate barrier integrity. The approach is:

- Conservative as it measures vapor leaks in a containment system whose greatest risk is posed by liquid leaks
- Applicable to any impermeable type of barrier emplacement technology in the unsaturated zone
- Inexpensive as it uses readily available, non-toxic, nonhazardous gaseous tracers, does not require an inordinately large number of sampling points, and injection and sampling points can be emplaced by direct push techniques
- Capable of assessing not only a barriers' initial integrity, but can also provide long-term monitoring

To date, six demonstrations of the system have been completed. Results from two of the demonstrations are detailed in this report. They include the final developmental demonstration of the SEAtrace™ system and a comparison demonstration of two tracer based verification technologies.

The final developmental demonstration of SEAtrace™ was completed at a naval facility in Brunswick, Maine. The demonstration was funded solely by the DOE and was performed in cooperation with the U.S. Navy, the Environmental Protection Agency, and the Maine Department of Environmental Protection.

A 2,300 lineal foot, nominally 3-feet thick, U-shaped soil bentonite slurry wall existed at the site. The slurry wall provides a subsurface barrier to prevent groundwater from flowing through subsurface contaminants contained within the landfill area. All indications show that the barrier is successfully meeting this criterion. The barrier varies in depth from 50 to 80 feet, while the distance to the water table varies from approximately 5 to 20 feet. The SEAtrace™ system tested a 100-ft. section of the barrier, in an area where the depth to the water table was the greatest. Seven injection wells/ports were spaced inside the barrier to provide a constant tracer source concentration. A total of 18 monitoring wells were installed outside the barrier, each with 3 ports (for a total of 54 ports). Installation of the SEAtrace™ system, including well installation, locating and connecting ports to the scanning system, and the initial performance checks of the ports and scanning system, was completed in one week. Scanning system hardware/software issues discovered during background checks were problematic, and caused a delay in the start of the test. Problems were primarily caused by the weather conditions and uptake of water through a number of the sampling lines. Once these issues were resolved, the test proceeded with no difficulties. Tracer gas injection and subsequent diffusion over the top of the barrier wall closely followed model predictions. The scanning system was able to complete one scan per day. The inversion code ran successfully after each scan. Results

of the demonstration clearly indicated a gap between the top of the barrier wall and the bottom of the cap. No breaches through the barrier were detected.

A comparison demonstration of two tracer verification technologies was performed at a barrier test facility near Waldo, NM. These technologies included the SEAtrace™ system and Brookhaven National Laboratories perfluorocarbon tracers. The basic physical principles of the two methodologies are similar. However, SEAtrace™ provides autonomous real-time data collection and analysis. Relatively high concentrations of a single tracer (sulfur hexafluoride) are used. The system is capable of producing locations and size estimates of breaches very quickly (within 12 – 24 hours) after injection of the tracer gas. This quick turn around time would allow for the initial verification of the barrier to be completed prior to equipment removal by the installation vendor, resulting in significant cost savings if breaches are found and need to be repaired. Conversely, BNL's focus has been predominantly concerned with the tracer gas and detection equipment. Perfluorocarbons can be detected in very low concentrations, requiring very little tracer to be injected into the contained barrier volume. Because there are numerous types of perfluorocarbon tracers (PFTs) that can be used, multiple verification tests can be completed either simultaneously or over time. The key advantages of the PFTs are multiple tracers, regulatory acceptance, extreme sensitivity, and proven technology with commercial acceptance and use.

SEAtrace™ data was collected automatically. One or two scans per day were recorded over a 25 day period. During this time, over 2,400 individual gas samples were collected and analyzed by the system, providing excellent concentration histories at each monitoring port. Data reduction of each scan was available within several hours of data collection. The PFT samples were collected manually using the SEAtrace™ scanning system manifold, at a rate of one scan per day for 13 days. Samples were shipped to BNL for PFT analysis. A total of 846 samples were taken during the data collection phase of this study. Analysis of the data was performed by examining over 100 contour plots of the data. Both technologies were able to detect all six of the engineered breeches in the barrier with reasonable positional accuracy.

EXECUTIVE SUMMARY

Impermeable subsurface barrier materials and emplacement technologies are being developed to contain high-risk contaminants in soils. These containment technologies are being applied to contaminated sites which are either posing immediate threats to public safety or are too difficult/costly to remediate with current practice. Using techniques derived from mining and construction ground stabilization industries, highly viscous materials and cementitious materials are being injected into soils to form walls and floors of very low permeability media to restrict transport of contaminants to the water table. Since these barriers are applied in high-risk circumstances, knowledge of their emplaced integrity is critical.

Barriers placed in the unsaturated zone pose a particularly difficult verification and monitoring challenge. They cannot be tested with water fill to determine if they are flawed, since doing so would mobilize the contaminants they are intended to contain. Geophysical techniques can image the barrier installation but cannot attain adequate spatial resolution to detect small flaws. Gaseous tracer testing, on the other hand, can detect breaches in barrier structures without risking mobilization of the contaminants, and can, with rigorous analysis, determine both the size and location of the flaws.

The SEAtrace™ system is an integrated, real time gaseous tracer system developed specifically for barrier verification and monitoring. The methodology incorporates gaseous tracer injection inside the contained volume of soil with analysis of tracer arrival at sampling points outside of the barrier walls. Solar powered, remotely accessible, and capable of multimonth standalone operation, SEAtrace™ collects soil gas samples with an automated multipoint soil gas sampling and analysis system, then immediately analyzes this data to locate and size flaws in the barrier construction. Since the approach uses real time analysis to characterize flaws, immediate repair of the barrier may be conducted with the appropriate remedial method. The gas analyzer used by the SEAtrace™ system is capable of measuring volatile organic compounds in the gas phase, so the system is also well suited to long term monitoring of the barrier's integrity.

The Department of Energy funded SEAtrace™ development. The initial proof-of-concept work was completed in 1996. Engineering development and testing occurred the following year. Two demonstrations were performed in the summer of 1997. Results were positive, and DOE chose to complete the engineering development and demonstrate the system at a real site. This demonstration was the primary thrust of this effort. Additionally, a comparison test between SEAtrace™ and another diffusion based verification methodology was completed at the SEA barrier test facility.

Finding a suitable host site to demonstrate the SEAtrace™ system proved problematic. There are multiple working barriers within the DOE complex, but most are emplaced in areas where the depth to the water table is too shallow to deploy the system. Other sites have tentative plans for emplacing barriers in the vadose zone, but anticipated installation dates would have required significant postponement of the demonstration. Private barrier owners were reluctant to allow a verification technology to be demonstrated at their site

because of liability issues and fear that results could have a negative impact at the site in the form of increased regulatory requirements. Once a site was found (the Naval Air Station in Brunswick, Maine - NASB), extensive negotiations were required. Delays caused by the negotiations pushed the start of the test into January 1999, causing weather conditions for the field test to be inhospitable. Installation of the system was difficult and short days of little solar gain were incapable of providing the energy needed to the system. Modifications to the software were undertaken to reduce the time (power) required to complete a full scan with the system.

Upon completion of the installation and collection of background measurements, it was discovered that water was being pulled in a number of the subsurface ports. Instrumentation in the scanning system could not function properly under these conditions, and required hardware modifications to assure water could not enter the unit. Software and hardware modifications were tested, the monitoring system was returned to the demonstration site, and tests were started in April 1999. The demonstration itself went very smoothly. The solar panels were able to provide ample power for the system, the monitoring system performed one or two scans per day, and the leak detection code performed as expected. While no breaches were found in the barrier, the gap between the impermeable layer in the cap and the top of the barrier wall allowed tracer to "spill" over the top of the barrier and be detected by the monitoring ports.

While negotiations were ongoing with NASB to perform the demonstration, a comparison test between SEAtrace™ and another diffusion based verification methodology (Brookhaven National Laboratories perfluorocarbon tracers) was completed at the SEA barrier test facility near Waldo, NM. The SEAtrace™ system performed very well. All six of the engineered breaches within the barrier were located (ranging in size from 7/16" to 15" in diameter), including a small leak (1" diameter) that was not opened until the test was underway and there was a significant background concentration of the tracer in the medium. Breaches not influenced by other leaks in the barrier were found to within 1 ½ feet (0.5 m) of the true location. The system also found four non-engineered breeches. One discreet leak was found on the corner of the north and east walls about half way down the corner. Another breach was on the south panel. It was near the surface and within several feet of the west panel barrier. The other two non-engineered breeches were located at the bottom of the barrier. These breaches were not discreet leaks, but rather long fractures.

The Brookhaven National Laboratory PFT tests identified a total of seven flaws. This included the six engineered flaws and one non-engineered flaw at a seam between the north and east walls. Multiple flaws were detected on the east (three flaws) and north (two flaws) walls. The use of multiple tracers provided simultaneous and independent confirmation of flaw locations and allowed monitoring of transport around the barrier. This permitted differentiation between tracers originating from flaws on the other sides of the barrier moving underneath the barrier and flaws in seams of the barrier. The PFT data were used to accurately determine the relative size of the flaws in each barrier. The east wall clearly had the largest flaw, the south and west walls had similar size flaws, and the north wall had the smallest flaws. Numerical modeling of the hole sizes and locations

was beyond the scope of work for this project. However, it is needed to improve definition of flaw size and location.

1. INTRODUCTION

The Department of Energy (DOE) is currently developing in-situ barrier emplacement techniques and materials for the containment of high-risk contaminants in soils. These include slurry walls, grout barriers, soil-mixed walls, cryogenic barriers, and other forms of impermeable barriers. Because of their relatively high cost, barriers are intended for use in high-risk circumstances. These include cases where the risk is too great to remove the contaminants, the contaminants are too difficult to remove with current technologies, or the potential for movement of the contaminants to the water table is so high that immediate action needs to be taken to reduce health risks. Consequently, barriers are primarily intended for use in the high-risk sites where few viable alternatives exist to stop the movement of contaminants in the near term. Assessing the integrity of the barrier once it is emplaced, and during its anticipated life, is a very difficult but necessary requirement. Existing surface-based and borehole geophysical techniques do not provide the degree of resolution required to ensure the formation of an integral in-situ barrier.

Many different construction methods and materials are available to create subsurface containment barriers (Rumer and Mitchell 1995). These include but are not limited to:

- Slurry trench cutoff walls (soil-bentonite, cement-bentonite, or composite materials used in a continuous trench typically created by a backhoe, clamshell or dragline)
- Plastic or diaphragm cutoff walls (typically excavated in panels using a clamshell, dragline or rotary drill)
- Thin panel cutoff walls (thin grout wall created with a vibrating beam or a steel sheet pile wall)
- Column barriers (vertical, slant, or directional walls created by soil mixing, permeation grouting or jet grouting)
- Naturally occurring low permeability geologic formation (often used as the bottom of a barrier containment system)

The types of, and potential for, defects in the containment barrier system are dependent on the barrier type and shape, the construction quality control, and the geologic characteristics of the specific site. The configuration of these flaws can be in the form of non-continuous panels at mismatched joints, soil regions with no barrier backfill material due to incomplete emplacement or grouting, open fractures, or thinned areas of the panels. The sources of defects can be grouped into two categories: construction defects and defects due to degradation of the barrier with time.

Construction defects include:

- Heterogeneous backfill due to improper mixing, entrapped slurry pockets, or material falling from the trench wall during construction / curing
- Inferior quality of the backfill material
- Trapped sediments at the bottom of the trench, inadequate excavation of the trench key, or incomplete coupling between the bottom and sides of a barrier
- Inadequate bonding between sections of backfill

- Inadequate placement between sections of backfill - especially as depth increases
- Hydrofracture of the soil during barrier construction

Barrier degradation with time occurs due to the following processes:

- Ground freezing and thawing cycles;
- Wetting and drying cycles in the near surface soils;
- Desiccation of the backfill material
- Chemical incompatibility between the barrier and contaminants; and
- Adjacent ground deformations and backfill stresses.

Barrier construction technology has evolved from the construction industry and mining practices, where structural strength is a greater driving criterion than resistance to fluid and contaminant transport. Consequently, validation of these emplacements has been primarily through construction QA practices (grout material balance, surface survey of the installation, materials QA testing, etc.), which do not provide sufficient assurance of emplaced integrity and resistance to contaminant transport.

The most common barrier emplaced to date is the slurry wall, in which a trench is excavated down to an impermeable layer (such as bedrock or clay) and backfilled with a heavy slurry of bentonite and/or grout. These designs are inherently self-healing and have historically been applied to contain contaminated groundwater. Testing of these installations is typically accomplished by drawing down the water level inside the barrier to a constant level (referenced to the water level outside of the barrier) and measuring the water flow rate under steady state conditions. The bulk hydraulic conductivity of the barrier can be estimated by this technique, which allows calculation of the contaminant flux from the barrier. A common criterion that has evolved from this practice is a hydraulic conductivity of 10^{-7} cm/s.

Slurry walls cannot treat many applications in the DOE complex because the sites may not be conducive to such emplacements. At the Hanford tanks, for example, barriers are being considered for emplacement beneath the tanks while they are being remediated to contain accidental releases of the tank contents. No confining layer exists at a reasonable depth below the tanks to serve as the floor of a slurry wall installation, and the performance of slurry walls in the vadose zone is uncertain. Consequently, alternate barrier technologies such as jet grouted columns or panels are being considered at many sites, and suitable verification technologies have yet to be developed. Hydraulically testing these installations is not likely, since many of the sites are in the vadose zone. Introducing water to the contained volume may mobilize contaminants otherwise in an immobile state. Geophysical techniques have been tested and have been shown to be capable of imaging the emplaced barriers, but do not have the required resolution to detect flaws as small as is necessary. Cross borehole electromagnetic surveys, ground penetrating radar, and electrical resistance tomography have successfully imaged barrier material in-situ. In some cases these techniques have detected major flaws, but they are not capable of resolving the types of leaks which would cause the barrier installation to fail its performance criteria. Gaseous tracer testing of barrier installations shows the

promise of resolving large and small flaws in barrier walls, so is an attractive approach for conservative verification of barrier integrity (Heiser 1994; Betsil and Gruebel 1995).

Science and Engineering Associates, Inc. (SEA) has developed a tracer-based monitoring/verification system for these contaminant containment systems. Called SEAtrace™, the technology is able to locate and size leaks in subsurface barriers that are in an unsaturated medium. It uses gaseous tracer injection, in-field, real-time monitoring and real-time data analysis to evaluate barrier integrity. SEAtrace™ currently uses sulfur hexafluoride (SF_6) as the tracer gas because it is readily detected by field rugged infrared analysis techniques and is a non-hazardous, commonly available gas used as a tracer in ventilation and hydrologic system testing (Wilson and Mackay 1993).

The field demonstrations of the SEAtrace™ system described in this document are the completion of an ongoing engineering development effort funded by the DOE. The original proof-of-concept work was conducted for Sandia National Laboratories Albuquerque, SNL (Lowry et al. 1996). This program, supported by the Subsurface Contaminants Focus Area (SCFA), demonstrated that it was possible to monitor gaseous tracer distribution with adequate temporal and spatial resolution to detect leaks. The proof-of-concept tests also showed that a spherical diffusion model could reasonably characterize the leaks using simulated annealing to optimize the data inversion. Engineering development of the system was continued through the DOE Characterization, Monitoring, and Sensor Technology (CMST) program through the Federal Energy Technology Center (Dalvit Dunn et al. 1998). The focus of the effort was to engineer an integrated system that could operate autonomously at remote sites, automatically and in real-time characterizing barrier flaws. The integrated system was evaluated at a test facility designed to simulate field conditions. Results showed that the system was capable of locating and sizing leaks in barrier installations. Leaks as small as 0.43 in. diameter/0.15 in^2 (1.1 cm diameter/0.95 cm^2 area) could be detected with a positional accuracy of 1.3 to 4.0 feet (0.4 to 1.2 m). Relative leak size information was not as accurate, estimating leaks with actual sizes ranging from 0.43 to 4.0 inches (1.1 to 10.1 cm) diameter as 7.9 to 13.6 inches (20 to 34.5 cm) diameter. A second integrated system was built for SNL and demonstrated at two different sites in the summer of 1997 (Dalvit Dunn et al. 1998). This work was funded through SCFA. The first demonstration was completed at the Dover Air Force Base in Delaware. This site was the test bed for development of a thin-wall jet grouted barrier. Two test barriers plus a separate engineered leak were tested. The second demonstration was completed at Brookhaven National Laboratory, New York. Here the DOE installed a small-scale viscous liquid barrier. Results at both sites were compelling. SEAtrace™ was able to detect breaches in all barriers tested. Breaches were found quickly, within days of injecting the tracer gas. Test results were corroborated with installation logs, other technologies, and/or excavation. At the Dover site, there were two breaches of known location. The system found both of these breaches within 1 foot (0.3 m) of the true location.

Given the positive results of the SEAtrace™ demonstrations, DOE chose to continue development of the system. Through FETC contract DE-AC21-96MC33125, SEA was tasked with completing the engineering development and demonstrating the system at a

real barrier installation. Additionally, DOE opted to perform a side-by-side comparison of two different tracer technologies, the SEAtrace™ system and BNL's perfluorocarbon tracers, at the test facility constructed under the first phase of this contract. This report describes the results of this effort.

2. OBJECTIVE

As stated in the contract statement of work, the overall objective of the effort was to "develop and demonstrate an integrated methodology and field system to evaluate the integrity of in situ, impermeable barriers constructed in the vadose zone." In the base contract the inverse modeling code was constructed, tested and integrated with the data acquisition and control computer of the monitoring system. A monitoring system was designed and tested. A mock barrier test facility was constructed. Finally a field evaluation of the integrated system was conducted at the barrier test facility (Dalvit Dunn et al. 1998). DOE evaluated the merits of the project and decided to exercise Option 1. This option included designing a field installation, installing the system, and conducting a field demonstration. DOE also chose to fund a parallel task that included using the mock barrier test facility to perform side-by-side comparison testing of two different tracer technologies, SEAtrace™ and Brookhaven National Laboratories perfluorocarbon tracers.

The contractual objectives have been met. This report details the work that was performed and the results of that work. The report is organized into several sections. Section 3 provides a description of the SEAtrace™ system. Section 4 describes the side-by-side comparison of the SEAtrace™ system with BNL's perfluorocarbon tracers at the SEA test facility. Section 5 describes the field demonstration performed. Finally, a section on issues, costs, and applicability of SEAtrace™ is presented. Extensive supporting information is included in the appendices.

3. DESCRIPTION OF THE SEATRACE™ SYSTEM

SEAtrace™ is predicated on the relatively simple and predictable transport process of gaseous diffusion in a porous media. Diffusion is an attractive process to utilize for leak detection because the tracer concentration histories measured at locations distant from the source are highly sensitive to both the size of the breach and the distance from the leak source. This sensitivity allows a global optimization modeling methodology to iterate to a leak geometry and location by minimizing the difference between measured data and that predicted using a relatively simple transport model. Thus, SEAtrace™ is composed of two distinct functional components: a monitoring system and an optimization code.

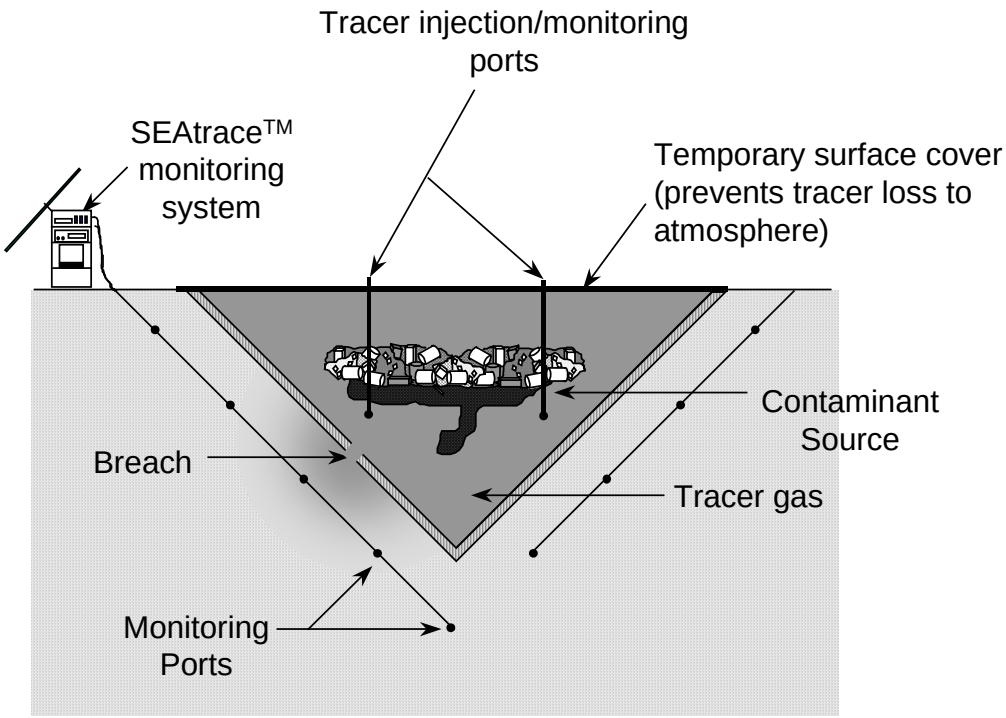

Figure 1. Schematic of a SEAtrace™ system installation.

A schematic of the SEAtrace™ system is shown in figure 1. Multiple sample points are located outside the barrier, as well as one or more injection and sample ports inside the barrier. These ports are connected to a stand-alone data acquisition and analysis system. A non-hazardous tracer gas (sulfur hexafluoride) is injected into the barrier, creating a large source volume of the tracer. If the barrier has a breach open to gas phase transport, the tracer will diffuse into the surrounding medium and the exterior sample ports will measure the amount of tracer in the soil gas with time. These concentration histories can then be provided (along with the sample locations, medium properties, and the source concentration) to the global optimization code. The code iterates to find a best-fit solution given the input parameters. This sequence is depicted in the general flow diagram of figure 2. Components of the integrated system are described in the following sections.

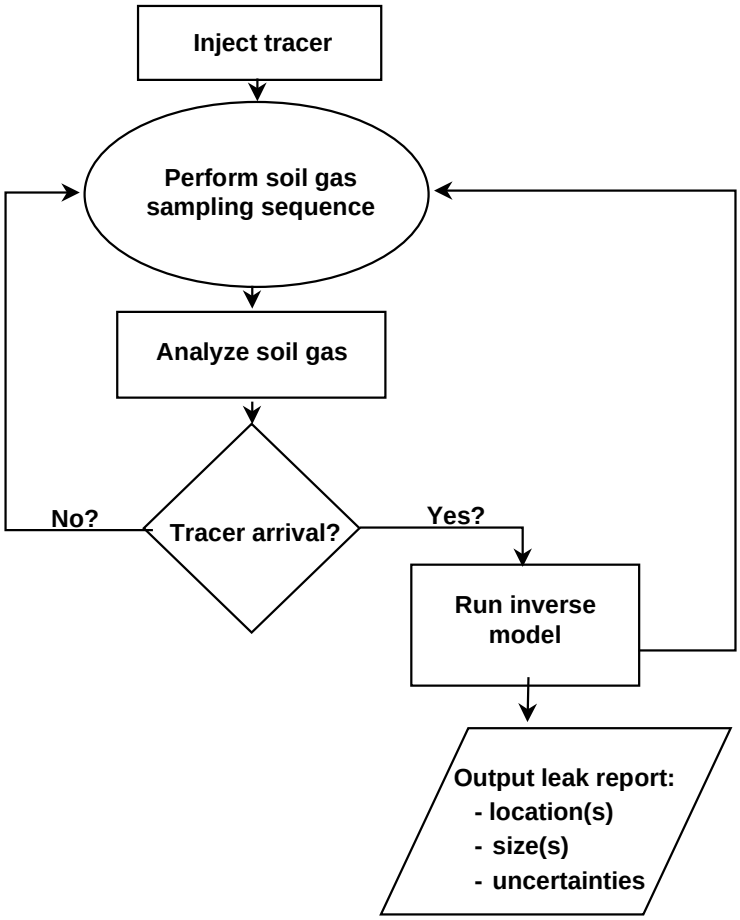

Figure 2. General sequence of SEAtrace™ system operational flow.

3.1 Sampling and Analysis System

A key feature of the SEAtrace™ system is its ability to automatically sample and analyze soil gas samples from a large number of sampling locations around the barrier. The monitoring system used is the SEA MultiScan™ scanning system. MultiScan™ is a stand-alone autonomous sampling system that can monitor soil gas composition and atmospheric related subsurface properties in real time by sampling up to 64 soil gas lines. Some of the features of the system include:

- A rigorous, fault tolerant acquisition and control code that operates on an embedded PC platform
- Self checking of software and hardware, to ensure sample manifold integrity, intermediate sample bag integrity, thorough purging of the sampling system between soil gas samples, and to identify gas sample lines that may be plugged
- A rugged, field portable gas analyzer
- Remote access
- Low power consumption devices
- Back-up power capability
- Protective, environmentally controlling enclosure

The original power load that the solar system was designed to accommodate was based on a much shorter scanning time due primarily to design specifications where a flow through gas analyzer was to be used (MSA Model 7000 LIRA analyzer). It was determined that the analyzer was very sensitive to minor temperature variations and to being turned on and off. For accurate readings, the instrument required daily recalibration, making it unacceptable for the scanning system, and was replaced with a photoacoustic analyzer. This change required reconfiguring of the sampling plumbing to incorporate an intermediate sample bag, recoding the control software, and physically installing the photoacoustic analyzer in the enclosure. Switching between a flow through device and one that required a sample to be drawn into a volume (which then had to be purged) significantly increased the time (and hence the power load) required to complete a scan. The design load was based on a 2 hour scanning interval, but the adjusted system required approximately 8 hours to complete a full 64-port scan. This increased power load stressed the solar system capacity. Time delays in finding a suitable demonstration site (pushing the test period into the winter/spring timeframe), coupled with the site chosen (Brunswick, Maine) required that either the time to complete a scan be shortened or scans be taken every other day rather than once per day. An aggressive effort was made to restructure the control software to minimize the time required to complete a scan. Delays in the code, needed to allow adequate time for various steps in the analysis, were examined and minimized as possible; different methods to purge the sample tubing / sample bag were developed and tested; and intelligence on what ports to sample and when purging of the chamber in the gas analyzer was necessary was added and tested. The final result was a 25% decrease in the amount of time required to complete a full scan.

After installation of the scanning system at the Brunswick demonstration site, a number of the monitoring ports pulled water into the system. While a water trap prevented the gas analyzer from being severely damaged, solenoid valves throughout the manifold system became corroded, preventing them from forming a complete seal when closed. Modifications were made to eliminate the possibility of water entering the system again. Individual float valves were added to each monitoring line. These valves allow air to flow through unimpeded until the valve fills with water. As water enters into the bottom of the valve, a float is lifted. If enough water enters the valve, the float seals the outlet, plugging the line. Addition of the valves was a major undertaking. In addition to physically adding the valves into an area already tight for space, tests had to be performed and the control code changed to assure adequate purging of the sample lines prior to collection of a sample.

3.1.1 Soil Gas Scanning System

The general system schematic is shown in figure 3. The system controller is a low power consumption i486 embedded industrial computer operating at 33 mhz when at full operation. This industrial PC has many features needed for this application: very low power consumption when in the inactive state between sampling operations; fault tolerance through a timer that senses lock-ups and can reboot the computer; and a versatile I/O bus that accommodates a multitude of devices (modems, digital I/O, analog/digital conversion, video displays, etc.). Communication with the analog/digital

converters and gas analyzer is accomplished through standard RS232 and RS485 serial lines. A cellular-capable modem is attached to the computer through its native PC/104 bus. Cellular communication is enabled for defined periods of the day so that the computer can be accessed remotely to change operational parameters and download data.

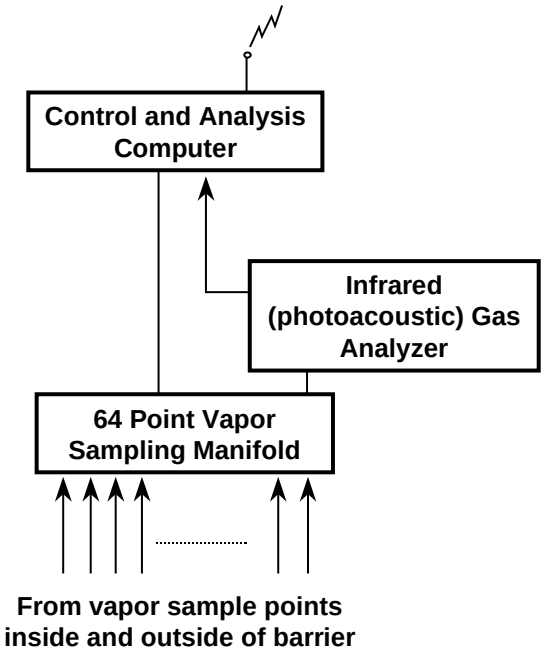

Figure 3. General monitoring system schematic.

The computer activates sampling sequences at defined times of the day, controls the sampling operation, and stores the analysis data. Two types of operations are executed. One is simply measuring the soil gas pressure at the sampling locations, and the other is the complete sampling and analysis of soil gas composition at each port. After the soil gas analysis data has been collected, the control code passes the data to the inversion code for leak characterization, which then returns the leak information for storage. The unit used for this project is capable of sampling up to 64 sample lines in the soil. Typical time requirements for the different operations are:

- Soil gas pressure measurement: less than 6 minutes
- Soil gas sampling and analysis: 6 hours
- Inversion code operation after completion of the soil gas analysis: 20 minutes

The sampling manifold consists of an array of small, low power electric solenoid valves controlled by a corresponding array of relays (see figures 4 and 5). An individual solenoid valve to the common manifold connects each sample line. A DC sample pump draws the gas sample through the valve, into the manifold, and transfers it to an intermediate Tedlar sample bag. The pump internal to the gas analyzer then samples the bag. The use of the intermediate sample bag is required because the flow rates attained through the sample line are too low to satisfy the gas analyzer flow requirements. This configuration allows purging and acquisition of the next sample in the sequence while the gas analyzer is evaluating the previous sample.

Purging of the sample manifold and lines occurs prior to acquisition of the next sample, using a network of solenoid valves and the sampling pump. Complete purging of the gas analyzer filter chamber is ensured by analyzing a sample of gas obtained from the interior of the instrument enclosure if the prior sample measurement was high. If the purge sample shows concentration of the tracer gas above a predefined level, the system is purged again until the criteria is satisfied. Atmospheric gas samples are analyzed both before and after a sampling run to ensure total system purge.

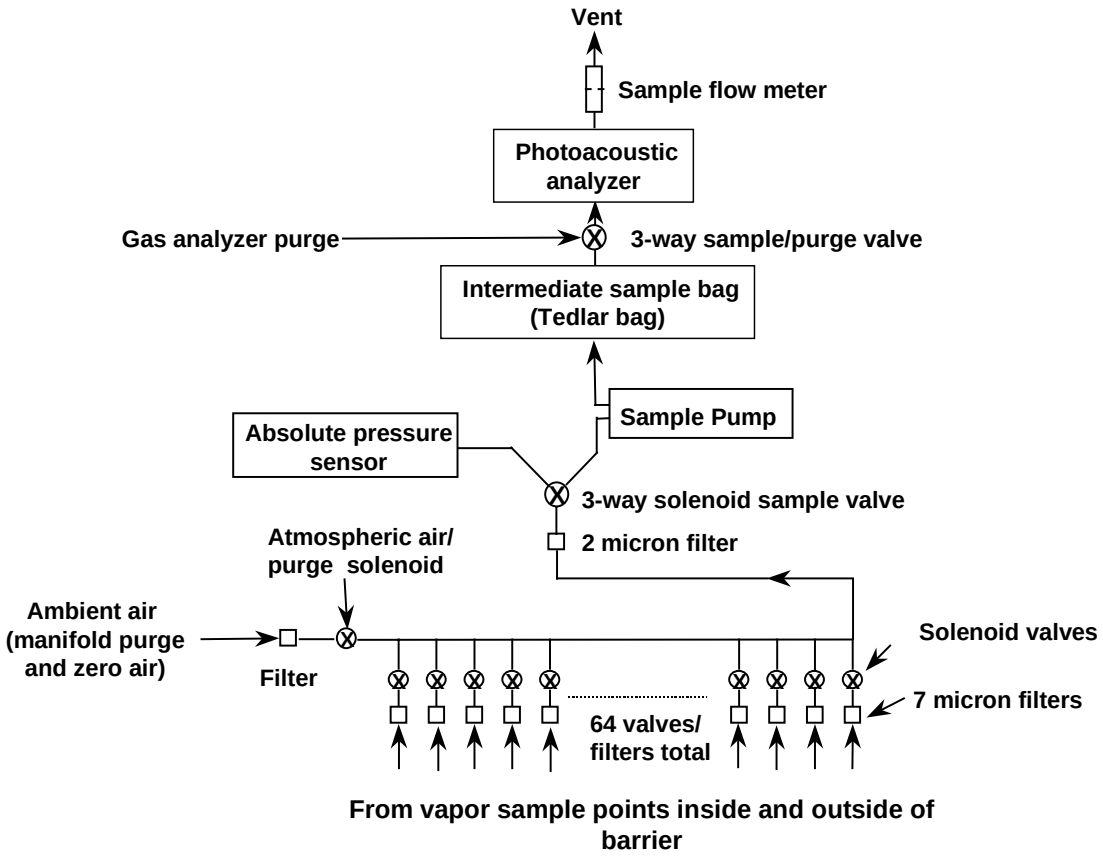

Figure 4. Sampling and analysis system.

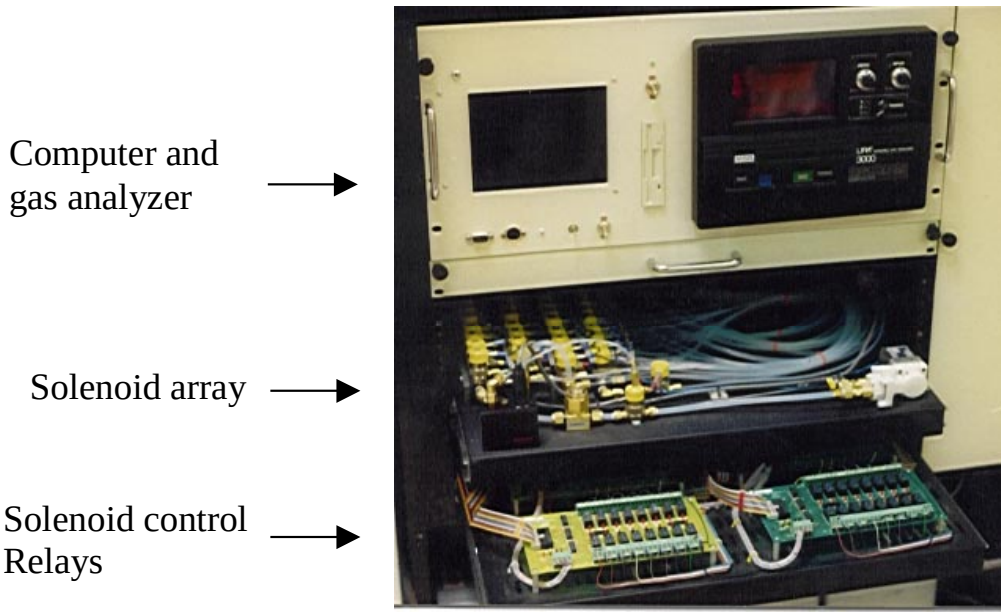

Figure 5. Control computer, gas analyzer, and solenoid valve system (prior to replacement of the NDIR analyzer with the photoacoustic analyzer and addition of the float valves).

3.1.2 Gas Analyzer

The gas analyzer used in this system is the Innova Instruments Model 1302 photoacoustic analyzer (former Bruel & Kjaer Model 1302). This is an infrared absorption device capable of quantifying the presence of up to five compounds (plus water vapor) in the soil gas. Photoacoustic analysis occurs by capturing a sample of the soil gas inside a chamber, pulsing the gas with a very precisely filtered infrared source at a wavelength corresponding to a unique absorption band of the compound, and sensing the magnitude of the absorbed energy (via pressure changes in the chamber) by a set of microphones. This device is capable of cost effective, reliable measurements in environments unsuitable for most other instruments. Reliability of the analyzer's results is ensured by regular self-tests. These test check software, data integrity, and hardware components of the unit to ensure they are functioning properly. Accuracy is ensured by the analyzer's ability to compensate any measurement for temperature fluctuations, water vapor interference and interference between other measured gases. The unit requires no warm-up time or recalibration after moving, making it ideal for use in the MultiScan™ system.

The analyzer was field tested in the U.S. EPA's Environmental Technology Verification (ETV) program (U.S. EPA, 1998). In this test, the analytical performance of the gas analyzer was evaluated using headspace analyses of ground water samples collected at two different sites. Performing multiple analyses on the samples checked the instrument's precision and accuracy. Additionally, results were compared to standard

laboratory analyses on the samples. Results of the study showed the photoacoustic gas analyzer was able to provide cost-effective data for routine monitoring when appropriate filters for the analyzer were chosen.

3.1.3 Power and Environmental Control

Standalone operation of the scanning system is necessary because at many remediation sites power is not accessible, and when it is, it is frequently unreliable. Protection from the elements was also crucial, as was moderating the temperature rise encountered due to the internal heat generation of the system components (the gas analyzer is the greatest contributor to the thermal load, at nominally 100 Watts during its operation). A Cool Cell system (from Zomeworks Corporation, Albuquerque, NM) provides an enclosure for the MultiScan™ instrumentation that integrates remote power, protection from the elements, and thermal control. This system satisfies the enclosure thermal performance requirements through use of a large water heat sink and a passive cooling cycle. A 30-gallon reservoir is located near the top of the enclosure. During operation of the heat generating components (and also during the day due to heat gain by solar exposure) the water will absorb heat energy and moderate the temperature rise inside the enclosure. At night, a passive thermosyphon action initiates in the circulation loop. The water reservoir is connected to a radiator on the top of the enclosure with a supply and return line (see figure 6). During the day circulation of water through the loop is prevented because the radiator water is at a temperature higher than that in the reservoir, and insufficient density gradients exist to induce natural thermosyphon circulation. At night, however, the radiator will cool below the reservoir temperature, resulting in a density gradient that causes recirculation of the water as heat is rejected from the radiator. If the temperature of the water in the reservoir drops below 40°F, the temperature/density relationship of water is such that thermosyphon action will no longer occur at night. Hence, in the winter the system tends to retain the generated heat instead of rejecting it, which helps maintain the instruments at temperatures above freezing. Temperature data is plotted in figure 7 showing the heat rejection and temperature moderating effect of the Cool Cell design.

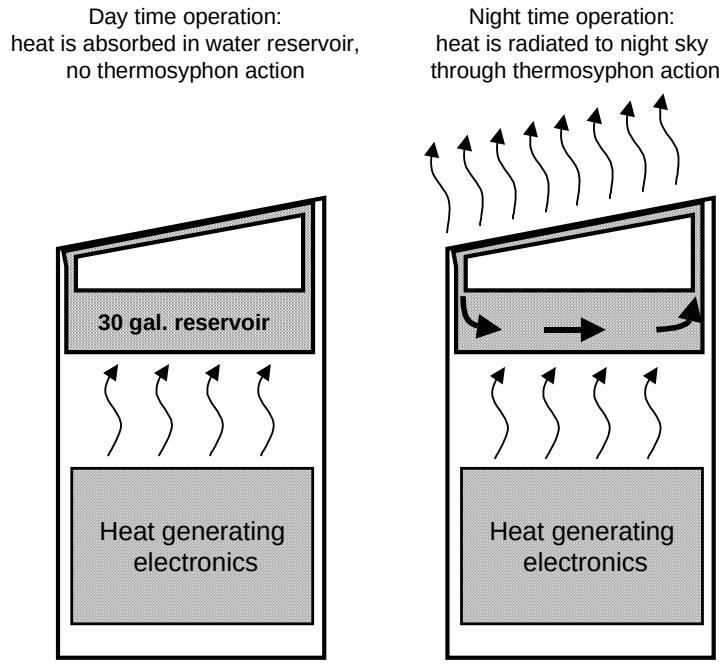

Figure 6. Instrument enclosure passive thermal control system.

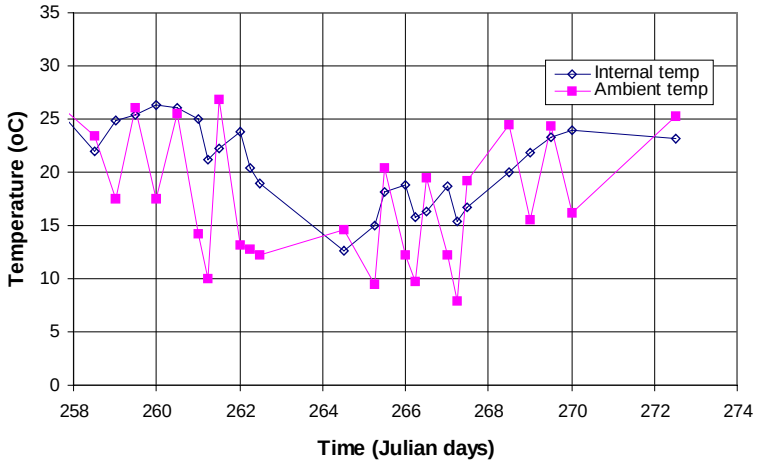

Figure 7. Record of internal enclosure and ambient air temperature showing the moderating effect of the passive thermal control system

The solar electric portion of the system is a conventional photovoltaic panel/gel cell battery system. It is designed to provide 30 Watts of continuous power, using four solar panels and eight batteries. An integral charge controller prevents both overcharging and discharging of the batteries to unacceptable levels. The assembled system is shown in figure 8. Additional information on the scanning system can be found in the Phase I topical report (Dalvit Dunn et al. 1998).

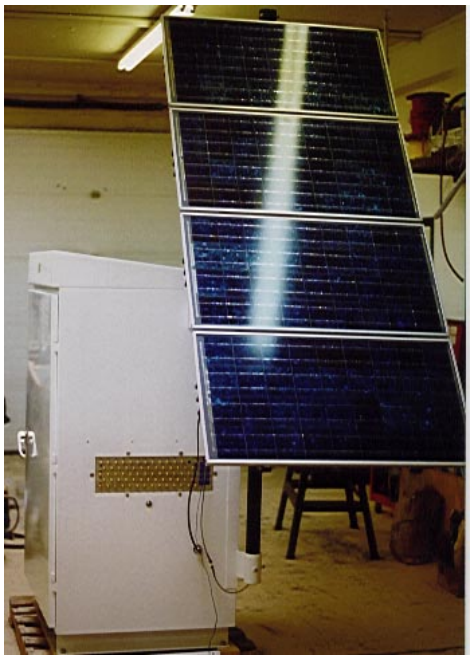

Figure 8. Monitoring system enclosure, showing the solar panels and sample tubing connection plate.

3.2 Data Inversion Methodology

Once concentration history data has been collected, it must be analyzed if any tracer gas was detected outside the barrier. This type of posttest analysis is typically performed by manually trying to match field results to results from forward diffusion models through an iterative process. This is a time consuming, artful process as the leak geometry, dimensions, and location are variable, the medium properties are often not well characterized, and the source concentration is variable. To overcome the difficulties of manual analysis, SEAtrace™ uses a global optimization technique to effectively search multidimensional "space" to simultaneously find the best fit solution based on all of the input parameters.

3.2.1 General Methodology

The general methodology of this approach rigorously searches for a set of parameters that will best characterize the leak. It requires a diffusion model that calculates concentration histories from the multiparameter "space." These calculated concentrations are compared to the measured concentrations using an objective function. For this project, the objective function was defined as the sum of the squares of the differences between the

predicted and measured tracer concentrations. A stochastic method is then employed to minimize the objective function, thus finding a best fit to the data given a range of defined parameters. The stochastic method chosen is called Simulated Annealing (Ouenes 1992). The technique selects points from the given input ranges for each parameter at random. Using these values, the objective function is evaluated. The process is repeated, the two values for the objective functions are compared, and the code chooses which is more accurate. This point is remembered and the process repeated with a new set of parameter values. The parameter values are chosen using a probability distribution that relies on the objective function of previous points in a complex way. The accuracy of the results is dependent on how well the chosen leakage model matches the monitoring data, the number and ranges of the unknown input parameters, and how the model parameters physically interact with one another. Appendix A describes the methodology in detail.

3.2.2 Forward Models

Presently, two different forward models have been incorporated into the inversion code. The first is the model used in the original prototype system. It is a simple one-dimensional spherical diffusion model (see figure 9), which assumes the following:

- A constant source concentration is maintained inside the barrier
- The flux exiting the leak is not restricted by diffusion through the leak (a function of the barrier thickness, source concentration, and the leak's dimension and flow properties)
- The region of the barrier under evaluation is a plane surface
- The medium outside the barrier is homogenous (e.g., that the diffusivity of the tracer gas through the soil pores is constant)
- It neglects gravity, advective flow, and adsorption/desorption of the tracer

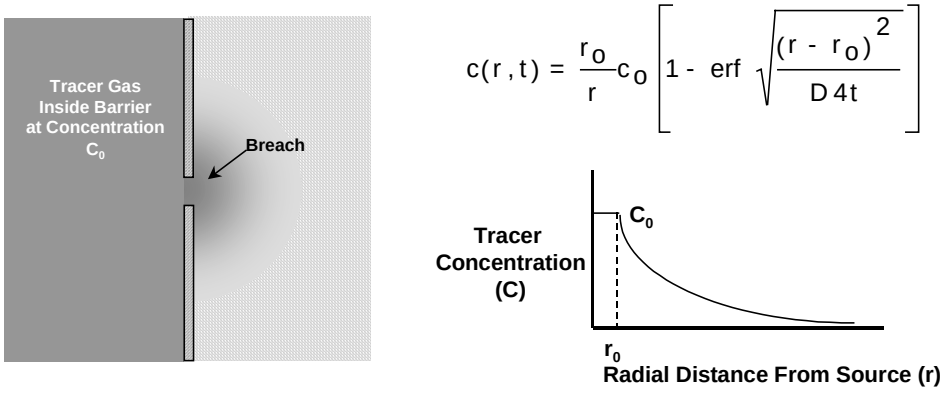

Figure 9. One-dimensional spherical model used as the forward model for SEAtrace™ data inversion.

While this diffusion model is simplistic, to a first-order it is realistic. If the area of the barrier wall is much greater than the area of the leak, at some distance from the leak the

gas will approach spherical diffusion regardless of the true geometry of the leak. Additionally, the barrier wall will act as a flat no-flow boundary and the medium that the tracer gas is diffusing into can be assumed to be semi-infinite. The partial differential equation describing this transient process is:

$$\frac{\partial c}{\partial t} = \frac{D}{r^2}\frac{\partial}{\partial r}\left(r^2 \frac{\partial c}{\partial r}\right)$$

where c is the concentration at radial position r and time t. The controlling parameter in this process is the diffusivity of the tracer in the soil gas, D, which is inclusive of the effects of porosity and soil tortuosity. If the barrier is well constructed (e.g., there are only a limited number of breaches in the barrier walls), the mass of tracer gas that can be injected into the internal pore volume of the barrier will be very large when compared to the mass of tracer gas that can diffuse through the leak area(s). Thus, the barrier will serve as an infinitely large reservoir of tracer gas at a fixed concentration (once the injected tracer gas has been completely injected and reached a state of equilibrium). Boundary conditions can be set as:

$$c(r_o, t) = c_o \text{ at } t \geq 0 \text{ and } c(r, t) = 0 \text{ at } t \geq 0$$

Solving the differential equation results in a straightforward expression of:

$$c\left(\underline{p}; x, t\right) = \frac{r_o}{r} c_o \operatorname{erfc}\left(\sqrt{\frac{(r - r_o)^2}{4D(t - t_o)}}\right), \; r > r_o, \; t > t_o$$

where:

$r^2 = (x-x_o)^2 + (y-y_o)^2 + (z-z_o)^2$,
$y_o = a\, x_o + b$ (the barrier surface is a plane described by $y = ax + b$),
(x_o, y_o, z_o) is the location of the leak,
(x, y, z) is the location of the sampling point,
t_o is the time that the leak began, and
r_o is the constant radius of the leak after time t_o

As with any model, it is important to understand how the assumptions used may effect the predicted results. In predicting the location of the leak, only the assumption of spherical isopleths must be true. Gravity and a heterogeneous medium are the two main factors that will influence the shape of the isopleths. Initial numerical calculations performed using T2VOC, a finite difference transport code (Falta et al. 1995), have shown that given the expected concentrations of the tracer in the surrounding medium outside the barrier, gravity will not be significant (S. Dalvit Dunn et al. 1998). The effects of a heterogeneous medium were also modeled. Results are included in appendix C. The conditions analyzed were found to have no significant effect on the results of the SEAtrace™ system operation.

Prediction of the leak size is more difficult. For the forward model to accurately calculate this parameter, in addition to maintaining spherical isopleths, the source concentration must be constant and flow through the breach must not be more restrictive than flow into the surrounding medium. The barrier thickness, leak geometry, or leak-flow properties could easily cause the flow of the tracer gas to be flux, rather than diffusion, limited. Figure 10 schematically depicts how barrier thickness would influence

concentration profiles in the medium. A second forward model was developed to account for this.

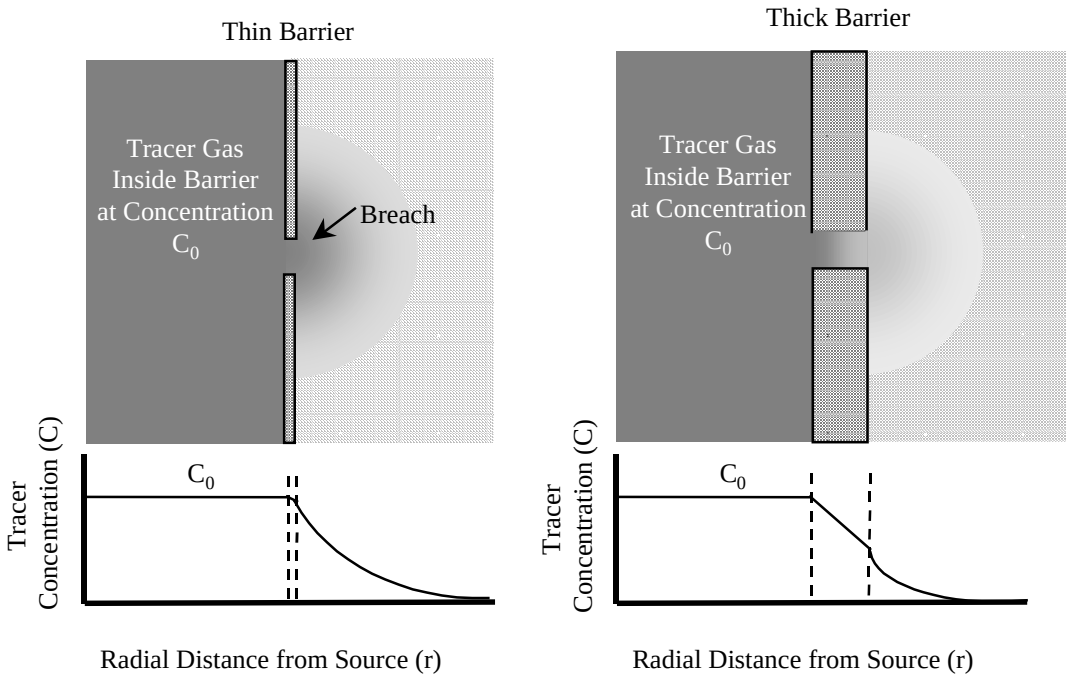

Figure 10. Schematic of how barrier thickness will effect the resulting concentrations of the tracer gas in the medium outside the barrier.

Numerical calculations were performed on a barrier configuration that would create flux-limited diffusion through the leak. Calculated concentrations of the tracer gas in the region outside the barrier were significantly (orders of magnitude) lower than those predicted with the one-dimensional spherical model first used with the inversion code. Given these results, a more accurate analytical model was developed to predict tracer concentrations outside the barrier for flux limited flow (Dalvit Dunn et al. 1998). The problem was split into two parts: the leak through the barrier, and the medium outside the barrier. A separate solution was developed for each part of the problem. The solution is presented below.

3.2.3 The Leak through the Barrier

Diffusion of the tracer through the hole in the barrier was modeled using a two dimensional cylindrical model. The T2VOC runs suggested that the hole through the barrier acts as a conduit, allowing diffusion of gas from the source concentration within the barrier, C_o, to a much lower concentration in the soil immediately outside the barrier, C_{exit}. T2VOC results showed the concentration along the axis of the mesh (e.g., across the thickness of the barrier) rapidly (within hours) approached a steady state condition. At steady state, the tracer concentration varied linearly along the length of the leak. The diffusive mass flux through the leak also reached its steady state value within hours from the start of the leak. Further, the concentration gradient across the diameter of any section

of the leak was very small after steady state conditions were achieved (e.g., flow was predominantly one dimensional).

A one-dimensional analytical model describing this geometry can be described by the following governing equation.

$$\frac{1}{r}\frac{\partial^2(rc)}{\partial r^2} = \frac{1}{D}\frac{\partial c}{\partial t}$$

Using the boundary and initial conditions of:

$c = c_o$ @ $z = 0$ and $t > 0$
$c = c_{exit}$ @ $z = L_h$ and $t > 0$
$c = 0$ @ $t = 0$ and $0 \le z \le L_h$

The equation can be solved to provide the following models for concentration profiles and mass fluxes:

$$c(x,t) = c_o + (c_{exit} - co)\frac{z}{L_h} - \frac{2}{L_h}\sum_{m=1}^{\infty} e^{-D\beta_m^2 t}\,\frac{\sin(\beta_m z)}{\beta_m}$$

$$q''(x,t) = \frac{D(c_o - c_{exit})}{L_h}\left[1 + 2\sum_{m=1}^{\infty} e^{-D\beta_m^2 t}\cos(\beta_m z)\right]$$

where:

$c(x,t)$	=	the concentration within the leak at a given distance from the leak entrance and time
c_o	=	source concentration
c_{exit}	=	concentration at the exit of the leak
L_h	=	thickness of the barrier
$q''(x,t)$	=	flux through the leak
D	=	diffusivity within the leak

As mentioned above, results from T2VOC simulations showed steady state conditions were reached very quickly within the leak. If only steady state conditions are of concern, the above equations can be reduced to:

$$C(x) = C_o + (C_{exit} - Co)\frac{z}{L_h}$$

$$q''(x) = \frac{D(C_o - C_{exit})}{L_h}$$

These analytical equations were able to match results from T2VOC within ± 10% if C_{exit} could be accurately estimated. Modeling work completed during the initial phase of this contract (Dalvit Dunn et al. 1998) showed that using the equation:

$$c_{exit}/c_0 = 0.7 - 5{,}714D$$

provided a good estimate of the exit concentration in barriers greater than 6-in. thick if the effective diffusivity within the leak was the same as that in the medium outside the barrier.

3.2.4 Medium Outside the Barrier

If the medium is homogeneous, the region outside the barrier can be described as 1-D spherical diffusion of the flux moving through the leak into a semi-infinite medium of effective diffusivity D_m. Such a process can be described by the following governing equation:

$$\frac{1}{r}\frac{\partial^2 (rc)}{\partial r^2} = \frac{1}{D}\frac{\partial c}{\partial t}$$

Subjected to boundary conditions:

$c = 0,$	$@\ t = 0$ and $0 \le r \le \infty$
$-D\,(\partial c/\partial r) = q''$	$@\ r = r_h$ and $t > 0$
$c = 0$	$@\ r = \infty$ and $t > 0$

Using several transformations and employing the Laplace transformation technique, the solution to this set of equations was obtained to be:

$$c(r,t) = \frac{q'' r_h^2}{Dr}\left[\operatorname{erfc}\left(\frac{r}{\sqrt{4Dt}}\right) - e^{-Hz+H^2Dt} \bullet \operatorname{erfc}\left(H\sqrt{Dt} + \frac{r}{\sqrt{4Dt}}\right)\right]$$

This equation predicts that very close to the leak exit, the concentrations reach a steady state value very quickly. Thus in anything but highly transient phenomena, the equation can be reduced to:

$$c\ (R,t) = \frac{q''\ r_h^{\ 2}}{Dr}\left[\operatorname{erfc}\left(\frac{r}{\sqrt{4Dt}}\right)\right]$$

where:

- $c(r,t)$ = the concentration within the leak at a given radial distance from the leak exit and time;
- q'' = steady state flux through the leak
- r_h = radius of the leak
- r = radial distance from the leak
- D = diffusivity in the medium outside the leak
- t = time

To assess the accuracy of the derived analytical equations, results were compared to the original T2VOC runs. It was found that the equations compared reasonably well with T2VOC predictions. The analytical model consistently over-predicted the tracer

concentrations in the medium outside the barrier at early times. This was expected, as assumptions made with the analytical model ignored early transient phenomena. Figure 11 shows typical results.

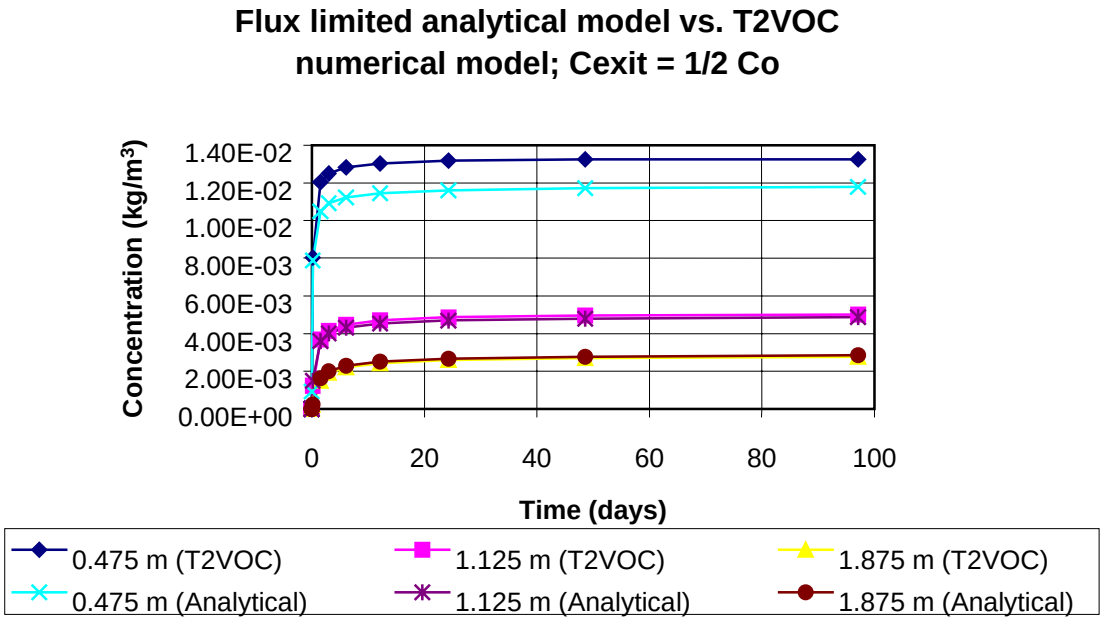

Figure 11. Comparison of the flux limited analytical model and the T2VOC numerical model.

A major factor in the accuracy of the inversion codes' results is how well the chosen leakage model matches the monitoring data. To help determine how the different assumptions made in developing the forward models effects the system, numerical modeling has been performed. Effects of a non-constant source concentration and non-constant diffusivity, gravity, and heterogeneous soil properties have all been modeled. Results have shown that these assumptions are valid in general, and will not cause significant errors in the SEAtrace™ system's results. Summaries of the modeling work can be found in appendix C.

3.2.5 Inversion Code Design and Testing

The inversion code, called SEAIM™, was designed to be a general tool for inverse modeling. It has the ability to search for the leak in a volume rather than a plane (allowing the system to be used for barriers of any shape with panels at any orientation, as well as to be used for other applications, such as locating leaks in underground pipe systems) and the ability to accommodate future developments in the forward model.

Simulated annealing is a global optimization method. An optimization method is a method which optimizes some norm (parameter, function, or functional). For the SEAtrace™ system, simulated annealing is used to optimize the error functional, or the sum of squared differences between the measured and synthetic data set. The error

functional is considered optimized when it is minimized. Because there are so many model parameters in the forward model (seven in the one-dimensional model and ten in the flux-limited model), the linear space in which this error functional exists is a seven or ten dimensional space. Because of the many dimensions, and because the interaction between each of the model parameters is not readily apparent, there may be multiple local minima in the error functional. Local minima are minima within the multi dimensional error functional space to which the inversion algorithm may converge but are in fact incorrect answers. The nature of the simulated annealing algorithm allows it to sample many of these local minima without being trapped by them. In this way, the algorithm has a significantly improved chance of locating the desired absolute minima, which corresponds to the true answer, even in the presence of many local minima.

Benchmarking of the SEAIM code involved evaluating its ability to invert a synthetic data set to find the model parameters. This process is multi faceted, as each model parameter and each algorithm parameter interact with the others in a very complex way. As a way to better understand how the parameters interact, a large matrix of cases was run. They involved:

- Letting all parameters vary
- Setting one or more of the parameters at fixed values (which may or may not be their true values)
- Evaluating the effect of different constants on the mathematical scheme (in particular varying the number of independent searches, the number of iterations per search, a cooling factor and probability of acceptance constant)
- Evaluating the number of time sequences to be inverted

Synthetic data sets were generated using both the forward models and the T2VOC finite difference modeling code. Because of the stochastic nature of the simulated annealing algorithm, the complicated and unclear interactions among the model parameters, and the choice of error metric, exercising the code proved difficult. In particular, the interactions among the model parameters were the most difficult to understand and exploit.

A series of studies was performed to gain insight into the performance characteristics and abilities of the code with the forward models described in the previous sections. These studies examined the ability of SEAIM to return accurate estimates of the model parameters for various settings of parameters and locations of leaks. For these studies, input concentrations for the inversion code were generated in two ways. First, the forward models were used to generate concentrations at points in space given certain input parameters. The concentrations generated were then randomly adjusted from -30 to +30% of the true value. These adjusted concentrations were input into the inversion code. Second, a finite element code, T2VOC, was used to generate concentrations at points in space given certain input parameters. In these cases, the medium surrounding the barrier was heterogeneous.

To summarize the results of the studies, SEAIM was able to return accurate estimates of the x_o, y_o, and z_o model parameters (the location of the leak in space) using either forward model, regardless of whether the input parameters were based on thick or thin barriers.

The radius of the leak, r_o, and the source concentration were strongly coupled for both models. For the flux limited model, these values were also coupled with the barrier thickness. In general, SEAIM was able to return reasonable relative leak sizes. The diffusivity of the soil, D, was usually estimated within an acceptable range (half an order of magnitude). Details of the studies can be found in appendix B.

In an effort to understand the inversion code's sensitivity to model parameters, a parametric study was conducted using the spherical diffusion forward model. For each parameter studied, it was allowed to vary while all the other model parameters were set at their true values. The shape of each of these plots is particularly important. In order for the inversion algorithm to be able to accurately find the desired value of the model parameter, there must be a well-defined minimum or trough in the vicinity of the answer. The resulting plots are shown in figure 12.

As can be seen, for x_o, y_o, and z_o in particular, there is a very pronounced minima at the location of the true value for the model parameters. Note that for y_o, the double minima are present due to the search range specified and the fact that the simulated monitoring point array was planar in nature. This resulted in two identical answers, one on either side of the monitoring array. This result demonstrates the necessity to either avoid planar monitoring point configurations or define the search range to avoid the incorrect minima (i.e., define the search range to be toward the barrier from the monitoring point location). Because the search range over these parameters are typically bounded to within several meters of the actual leak location, the inversion algorithm has a very defined minima on which to converge. Model parameters r_o and D likewise have very well defined minima at the location of the true values. The source concentration, c_o, however, has very broad minima. The implications here are that there are many values of c_o in the vicinity of the true value that may be chosen by the inverse algorithm. And finally, the start time model parameter, t_o, also has a very broad minima, which accounts for the inability of the inverse algorithm to determine an accurate value for t_o.

While the design of the code allowed solution for seven parameters (x_o, y_o, z_o, r_o, D, c_o, T_o), it is important to recognize that accurate solution for the leak location (x_o, y_o, z_o) and radius (r_o) are important and the other parameters are less significant.

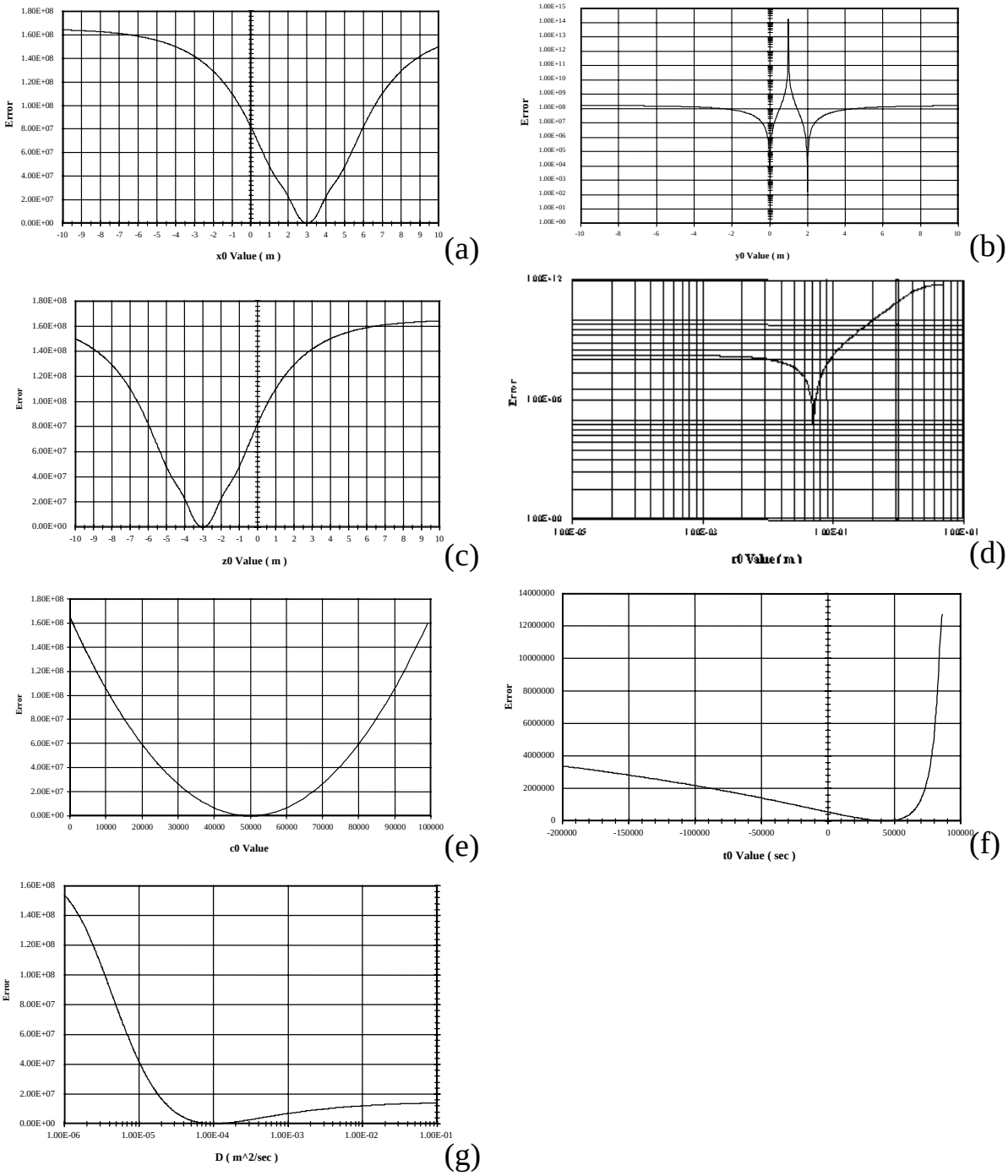

Figure 12. Error functional versus model parameter where all other parameters are held to their true value. (a) x position varied; (b) y position varied; (c) z position varied; (d) radius varied; (e) source concentration varied; (f) start time varied; (g) diffusivity varied.

4. COMPARISON TESTING AT THE WALDO TEST FACILITY

Because of the importance of the containment integrity of subsurface barriers, the DOE has funded multiple verification / validation demonstrations, including geophysical, tracer, geotechnical, and hydraulic methodologies. The maturation of many of the innovative technologies tested varies, as did the results from the demonstrations. To date, no direct comparisons have been made between the different technologies. However, gaseous tracer testing has proved to be both a mature and effective method in verifying barrier integrity in unsaturated media. In an effort to better understand the difference between the two different tracer technologies funded, DOE chose to have a side by side demonstration performed. The study included SEA's SEAtrace™ system and Brookhaven National Laboratory (BNL) perfluorocarbon/detection equipment. Tests were performed at the Waldo test facility near Santa Fe, NM. While the purpose of these tests was to allow the two tracer technologies to be tested under the same conditions, a comprehensive comparison of the technologies will not be addressed in this report. A comparison of this sort could only be completed by an independent party, and only if system costs, ease of use, timeliness of the systems results, and overall accuracy of the systems were reviewed. However, data will be represented in a similar format by both vendors such that the DOE can make an evaluation of the accuracy with which each technology/type of tracer can detect the location and size of the flaws. The SEAtrace™ system results are presented below. The topical report produced by BNL is included as appendix D.

4.1 Description/Preparation of the Test Facility

4.1.1 General Description of the Waldo Test Facility

The test facility was originally designed to exercise the SEAtrace™ system under conditions similar to those that would be encountered at a "real" barrier. Extensive testing at this facility had been conducted under the initial phase of this contract (S. Dalvit Dunn et al. 1998). The test volume consisted of a small-scale barrier with monitoring points both internal and external to the barrier. The shape and the dimensions of the barrier were chosen to be realistic, easily constructed, and capable of allowing a multitude of leak combinations to be tested. A V-shaped trench roughly 5 meters deep and 15 meters long was excavated (figure 13). The side walls and ends of the trench were sloped roughly 45^{o} from horizontal - a slope shallow enough to minimize construction hazards but steep enough that it would be economically viable to use at a real site. The trench was excavated using a trackhoe. Inspection of the trench afterward revealed three distinct geologic layers. The upper layer (approximately one third of the total depth) was an alluvial deposit; the middle layer (approximately one third of the total depth) a clay layer, and the bottom third was a dense but highly fractured shale. A vertical wall was formed at one end of the trench after the trench had been excavated. The three sloped walls of the trench were sprayed with a 3-4 in. layer of gunnite concrete. The gunnite stabilized the trench walls, held the flanges for the valves (part of the engineered leaks) in place, and provided a smooth surface for the membrane to lay against. A 30 mil plasticized polyvinylchloride geomembrane composed the primary barrier to gas migration. A professional landfill company installed the membrane. After the liner was in place, the valves were attached to the flanges to act as controllable,

known leak sources of various sizes. Figure 14 is a schematic of a typical valve assembly, and figure 15 is a photograph of two of the valves after they were emplaced. The different lengths of soil-filled pipes incorporated in each valve assembly simulate various barrier thicknesses. Boots of the liner material were used to seal around the valve assemblies. The barrier was then backfilled. Finally, the trench area was covered with a surface seal (40 mil high density polyethylene plastic sheeting) to prevent both excessive loss of the tracer to the atmosphere and water infiltration. The surface seal was covered with a 2-3 in. layer of native soil for protection. Figure 16 is a schematic of the completed test barrier.

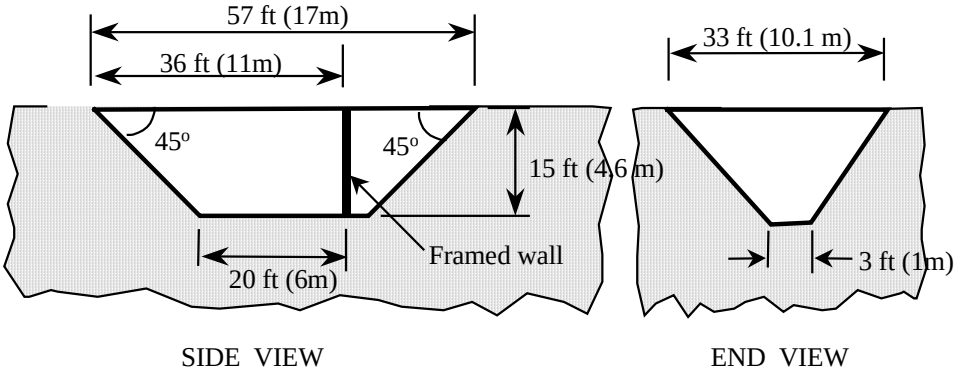

Figure 13. Approximate dimensions of the test facility at the Waldo site.

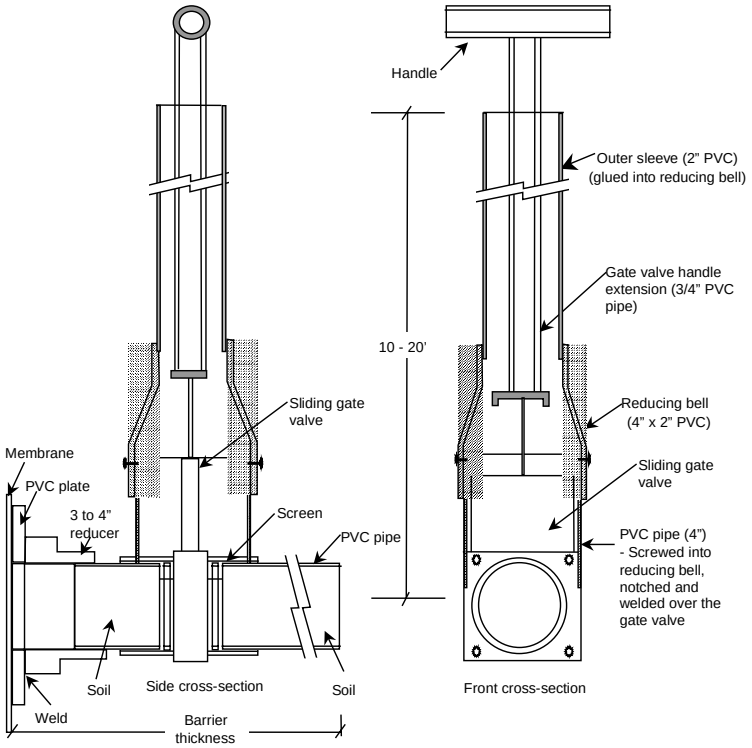

Figure 14. Typical gate valve assembly used to define the engineered leaks at the Waldo site test barrier. Note the barrier "thickness" is defined by the valve assembly, not the thickness of the concrete or the impermeable liner.

Figure 15. Photograph of engineered leak valve assemblies. Assembly in the foreground simulates a 15-in. diameter leak, in a 2 ft. thick barrier. Assembly in the background simulates a 4-in. diameter leak in a 2 ft. thick barrier.

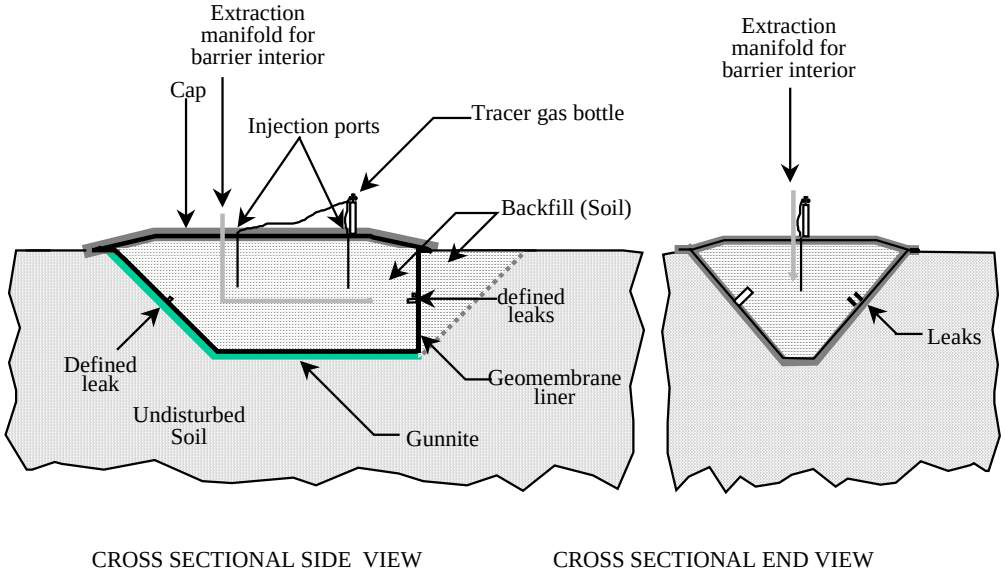

Figure 16. Sketch of the completed test facility at the Waldo site.

There were six engineered leaks within the test barrier. Table 1 lists the leak radius and corresponding wall thickness along with other pertinent information of each defect. It is important to note that the design of the engineered leaks allows for all but the smallest leak (on the north panel) to be closed.

4.1.2 Preparation of the Waldo Test Facility for the Side-by-Side Tracer Tests

From a test standpoint, two problems needed to be overcome prior to using the Waldo test facility for this series of tests. First, there was some damage to the monitoring port tubing at the facility, and second, there was a significant amount of tracer gas, sulfur hexafluoride, in the medium outside the barrier remaining from the initial testing performed there.

Table 1. Properties of the engineered leaks in the Waldo test barrier.

	Location		**Leak Radius**		**Leak Diameter**		**Leak Area**		**Barrier Thickness**	
Panel	lateral, relative to panel	depth, relative to panel	(in)	(cm)	(in)	(cm)	(in^2)	(cm^2)	(ft)	(m)
East	closest to north panel	center	7.5	19.1	15.0	38.1	176.7	1140.1	2	0.6
East	closest to south panel	center	2.0	5.1	4.0	10.2	12.6	81.1	4	1.2
South	closest to west panel	center	0.5	1.3	1.0	2.5	0.8	5.1	0	0
West	closest to south panel	center	1.5	3.8	3.0	7.6	7.1	45.6	2	0.6
North	closest to east panel	center	0.5	1.3	1	2.5	0.79	5.07	0	0
North	Closest to west panel	center	0.22	0.56	0.44	1.20	0.15	0.97	0	0

4.1.2.1 Repair of the Waldo Test Facility. Between the time that the original work at the test facility was completed (October 1997) and the time that the DOE opted to perform the comparison tests (July 1998) some damage was incurred at the test facility. Cattle grazing around the facility damaged or moved much of the protective pipe around the sample tubing, leaving the tubing exposed. Rodents then chewed through the tubing. Rather than try to repair the tubing and then deduce what port it was connected to, the decision was made to install new ports around the barrier. Figure 17 shows the designed

monitoring port locations. Ports on the east, west and south panels were spaced on 6 foot (1.8 meter) intervals on a plane parallel to and 2 feet (0.61 meters) from the barrier panels. Rows of ports were offset 3 feet (0.9 meters) from one another. The port spacing on the north panel was slightly different from the other panels. This panel was smaller than the others, and the spacing used on the other panels did not provide the best coverage for the number of ports available. The ports were emplaced as shown in figure 17.

Boreholes were formed with a 4" hollow stem auger. Ports were connected to the monitoring system via 1/8-inch od, 1/16-inch id colored polyethylene tubing. The ports/tubing emplaced in each well were bundled prior to emplacement. Tubing in the bundle was held apart from one another with T-clips. The clips provide a defined space that allowed backfill material to flow between the tubes, forming a more complete vertical seal. After the tubes were lowered into place, the borehole was backfilled using a mixture of 2 parts bentonite flour to 5 parts silica sand by weight. Under the first phase of this contract, the effective air permeability of the different geologic layers at the site and the proposed backfill material were measured. Results are given in table 2. The permeability of the backfill material was equal to or lower than the medium surrounding the ports, which minimized preferential removal of pore gas from the borehole during sample collection. Note that permeability data was not obtained for the fractured shale layer as it was not possible to obtain a representative sample for the laboratory tests. Subsequent air extraction from this layer showed that soil gas could move easily through this layer, presumably through the fractures. As such, the backfill material used provided adequate protection against creation of a short circuit pathway along the borehole during sample collection. Figure 18 roughly shows the different geologic layers at the sites, the engineered leak locations, and the as-installed port locations. The sketch shows the panels as if they were rotated around the bottom panel and laid flat. Port locations were then superimposed over the panels.

Table 2. Laboratory measured effective air permeabilities of the different soils at the barrier test facility in Waldo, NM.

Medium Description	**Measured Permeability (darcies)**
Alluvium (top geologic layer)	10
Clay (middle geologic layer)	4
Crusher fines (backfill behind north wall)	25 – 40
Backfill (5:2 silica sand/bentonite flour)	3

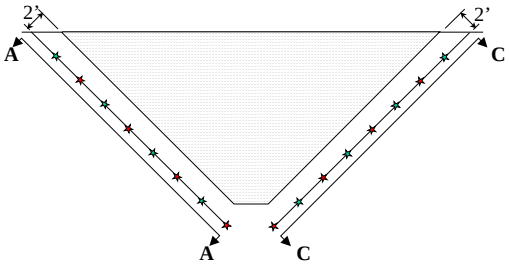

End view (from south) showing ports on East and West panels

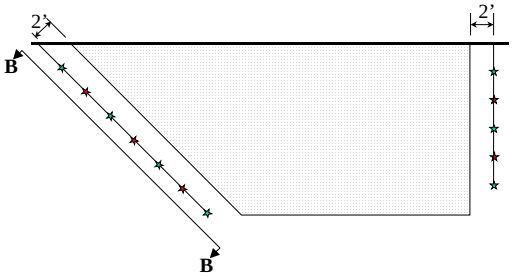

Side view showing ports on North and South panels

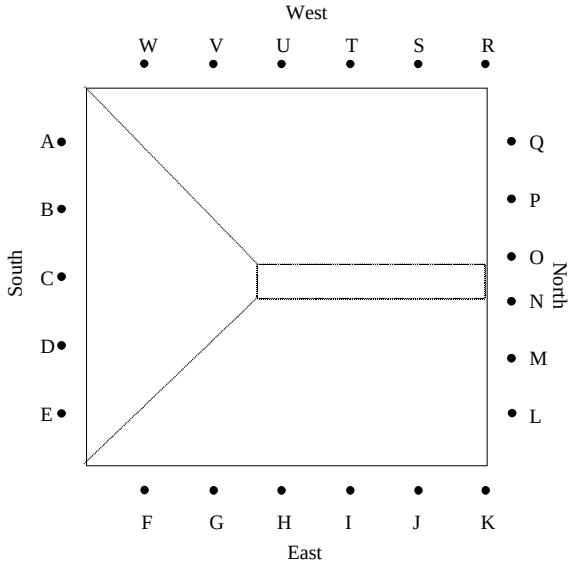

Plan view

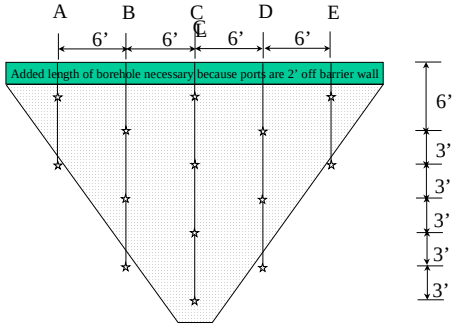

Cross sectional view B-B (South panel)

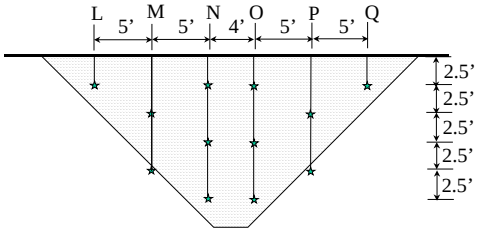

End view (facing North wall)

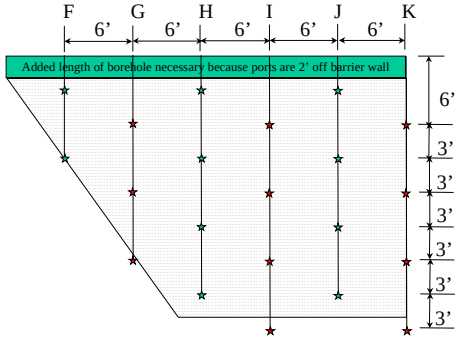

Cross sectional view C-C (East panel)

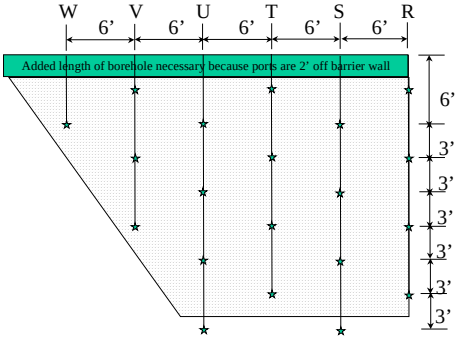

Cross sectional view A-A (West panel)

Figure 17. Scaled drawings of the designed well / monitoring port locations for the Waldo test facility.

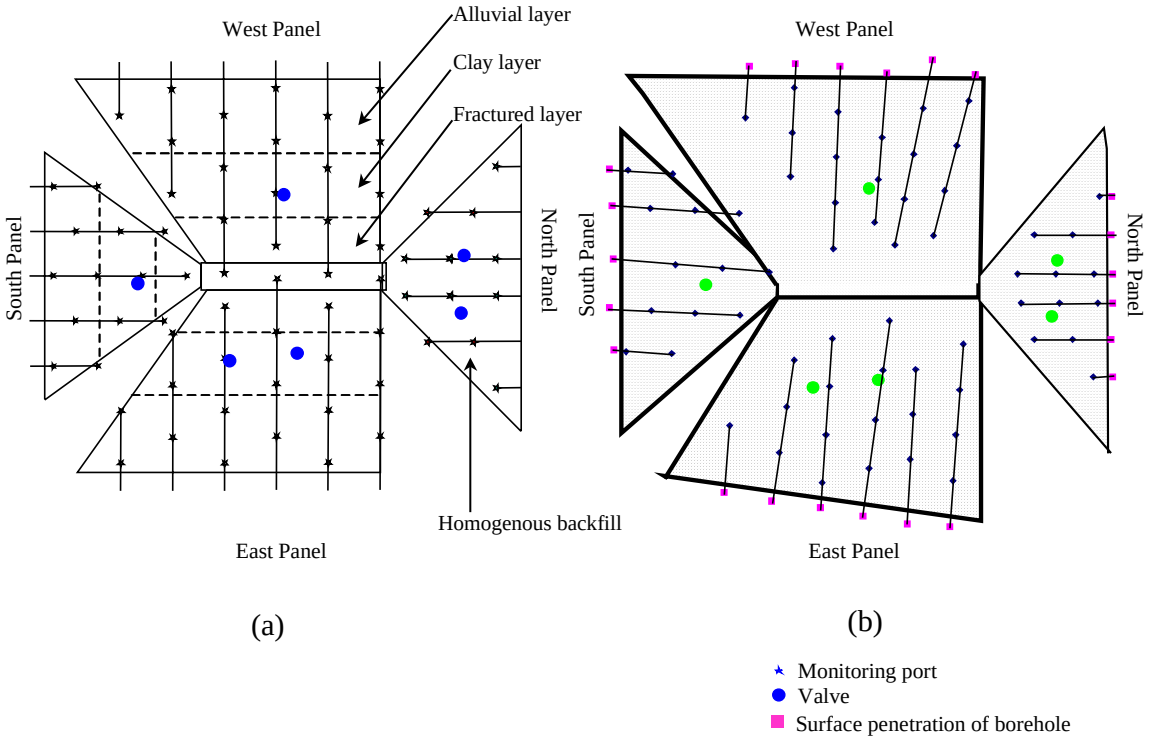

Figure 18. Locations of the monitoring ports and engineered leaks (shown as stars and circles on the schematic, respectively), viewed as if the panels were opened around the bottom of the barrier. Ports were then superimposed over the panels. (a) shows the designed port locations, (b) shows the as-built locations.

Tubing was routed from individual monitoring wells into a common 2" pvc pipe. The pipe terminated at the scanning system. The pipe protected the tubing from ultraviolet light and other forms of damage during the test.

4.1.2.2 Removal of Background Tracer at the Waldo Test Facility. As soon as the use of the Waldo test facility was confirmed for further tests, a manual gas analysis was performed on all of the monitoring ports. Results from undamaged ports showed concentrations of the tracer gas as high as 200 ppm. While it is possible for the SEAtrace™ system to operate with background concentrations that high (Dalvit Dunn, et al. 1998), it is not desired. An effort was made to reduce the residual tracer by extracting soil gas from the medium. This was done after the new monitoring wells had been drilled, but before the monitoring ports were installed. PVC pipe was placed in each well after it was drilled. The top three feet of the annulus between the pipe and the well was plugged, and the pipes were connected to form a manifold. Blowers were used to extract soil vapor. Soil gas samples were collected from numerous ports during the extraction. The majority of the ports sampled showed a very quick response. After extracting for less than a week, most measured concentrations were below 10 ppm. However, there was one section of the barrier, the southwest corner, where concentrations remained as high as 60 ppm. Vapor extraction was continued on this area of the barrier.

Concentrations were reduced to between 14 and 45 ppm. The vapor extraction was discontinued and the monitoring ports were installed. Once the ports were connected to the scanning system, background measurements were collected over a 10-day period. Those ports in the fractured region (the bottom third of the barrier) began to increase. This was not unexpected, as results from the initial tracer tests showed large non-engineered leaks in the bottom of the barrier. The tracer injected into the barrier for the first series of tests diffused through these breeches, preferentially moving through the fractured layer via the fractures. As the source concentration was not removed after the completion of the initial tests, tracer diffused into the medium over a considerable period of time. Once the vapor extraction process began, soil gas was drawn from the entire length of the boreholes, flushing clean surface air through the medium. Once the extraction was stopped, tracer in the medium away from the barrier diffused back towards the barrier. These results were seen not only in the recorded tracer histories, but also in the carbon dioxide records. The start of the test (injection of the tracer into the barrier) was postponed as long as possible, until the background concentrations approached a constant value. Recorded data is shown in section 4.3. Experimental Results.

4.2 Experiment Design

A detailed description of the experiment design can be found in appendix E, *Subsurface Barrier Validation with Gaseous Tracers, draft Phase II Test Plan for Gaseous Tracer Comparative Tests Conducted at the Waldo Subscale Barrier Test facility*. As such, this section will only provide highlights of the experiment design.

The basic design for the SEAtrace™ system installation is driven by the size of the leak that must be detected given the various parameters that influence that value. The design includes:

- Determining the monitoring port locations and method of emplacement
- Determining the injection port placements and the overall injection scheme
- Determining a means to verify that the monitoring system is functioning properly

4.2.1 Monitoring Port Spacing and Locations for the Demonstration

The primary design issues in the application of SEAtrace™ are the gas sample port locations and spacing. In general, more closely spaced monitoring ports have the advantages of:

- Detecting a leak more quickly
- Detecting smaller leaks over a given test period, and
- Finding multiple closely spaced leaks on the barrier with greater resolution

Conversely, the disadvantages of closely spaced ports are:

- The area that can be monitored with a single 64 port scanning system decreases
- The cost to verify the barrier increases (primarily because more monitoring wells need to be drilled)

Determining the optimum port spacing for a given site depends on a large number of variables. First, there are the uncontrollable variables (from the system's viewpoint). These include:

- The properties of the medium in which the barrier is emplaced (diffusivity, porosity, tortuosity, permeability).
- The properties of the material of which the barrier is made (diffusivity, porosity, tortuosity, permeability).
- The physical dimensions of the barrier - thickness as well as the overall area(s) that must be verified. In general, large panels require fewer ports to monitor on a square footage basis than small discreet panels. This is due to the number of data points required for the inversion code.
- The way the barrier was constructed (e.g., overlapping panels can interfere with the way the tracer diffuses).
- How quickly the verification is to be completed after the barrier is emplaced (materials high in water content will create a saturated halo around the barrier, effectively reducing the diffusivity in the region for some period of time after the barrier is installed).

There are also some controlled variables that influence port spacing, including:

- The tracer source concentration (which is limited only by the amount of soil gas that could realistically be replaced with the tracer)
- The time frame available to complete the verification
- The minimum size of the leak that is desired to be detected

For the tests at the Waldo test facility, the barrier was small enough that all of the panels could easily be monitored with the 64 available monitoring ports, even though the shape of the barrier panels required monitoring ports to be placed below or near the edges of each panel. A fairly dense port layout was chosen to minimize the time required to complete the tests. Calculations were performed using a flux limited numerical model and a spherical diffusion model to conservatively estimate the minimum leak size that could be detected given certain assumptions. In particular, calculations were completed for several combinations of source concentration, barrier thickness and the minimum detectable concentration required to be recorded at the maximum distance between a leak anywhere on the barrier and at least three monitoring ports. Details of the calculations can be found in appendix E. The assumptions and the numerical model used in the calculations are also described in the appendix. Table 3 is a summary of the results. The table shows the smallest leak that could be found for the various cases. The highlighted cells show when, during the test sequence, the system would detect the different engineered leaks given a maximum test duration of one week for each source concentration. If the measured background concentration of the tracer gas, SF_6, is very low, then any measured tracer at the exterior monitoring ports can be assumed to be from a leak in the barrier. Under these conditions, all of the engineered leaks except the 2-in. diameter, 4-ft. thick leak on the East panel would be seen after the initial low concentration source injection (2500 ppm). That leak would only be seen after the second stepped injection (7500 ppm). If the measured background concentrations at the monitoring ports are not zero, then the SEAtrace™ system will "see" a leak as the

concentrations at the ports exceed the background concentration. The maximum anticipated background value of the tracer at any of the ports was assumed to be 10 ppm for the calculations (for most areas of the barrier this assumption proved to be valid). Using this value as the minimum assumed detection limit, none of the engineered leaks would be seen after the initial low concentration source injections (2,500 ppm and 7,500 ppm). The small diameter leaks on the north wall would be seen after the source concentration is increased to 20,000 ppm. The remaining engineered leaks would not be seen until the source concentration was stepped up to the maximum target concentration. Results of the calculations proved to be conservative. All of the engineered breaches were detected by the time the source concentration was increased to 20,000 ppm. This is due to the effects of injecting the tracer in the barrier (calculation models assume a constant source concentration). This phenomena is discussed in more detail in appendix C.

Table 3. Summary of the calculational results completed with the forward diffusion models for the Waldo demonstration. Values were calculated for a port grid of 6 ft. horizontal by 6 ft. vertical grid, where adjacent columns of ports are skewed 3 ft. from one another. The plane of the sampling ports is 2 ft. from the barrier wall. The minimum distance the tracer must be able to be detected for this port spacing is slightly less than 6.6 ft (2.0 m).

Assumed detection limit (ppm)	Barrier thickness (feet)	Min. leak radius that could be seen given a source concentration of:							
		2500 ppm, 7 day test		7500 ppm, 7 day test		20,000 ppm, 7 day test		100,000 ppm, 7 day test	
		(cm)	(in)	(cm)	(in)	(cm)	(in)	(cm)	(in)
1	0	2.0e-1	7.8e-2	7.0e-2	2.8e-2	2.5e-2	1.0e-2		
1	2	6.0	2.4	3.5	1.4	2.2	0.9		
1	4	8.5	3.4	5.0	2.0	3.0	1.2		
10	0	2.0	7.0e-1	6.5e-1	2.6e-1	2.5e-1	1.0e-1		
10	2	19.0	7.5	11.0	4.3	5.7	2.3	3.0	1.2
10	4	27.0	10.6	15.5	6.1	9.5	3.7	4.2	1.7

Initial results from the SEAtrace™ system were calculated based on concentration measurements recorded at all of the exterior monitoring ports. However, analyses were also performed on subsets of the measured data (sets where data from every other well was removed, which doubled the horizontal grid spacing) to determine how a much coarser grid of monitoring ports would effect the results of the system (section 4.3 Experimental Results).

4.2.2 Injection Port Spacing and Locations for the Demonstration

Tests completed under the initial phase of this contract coupled with research of typical "real" barrier installations showed a need for a more structured injection scheme for the tracer gas than initially used. During the initial testing of the system, emphasis was placed on injecting the tracer gas through a limited number of centrally located ports in the barrier interior. The assumption with this approach was that the tracer would equilibrate rapidly within the contained volume creating a constant source concentration. Research showed that barriers are often emplaced around tens to hundreds of acres at a contaminated site. The volume contained by these barriers would make creating a constant source concentration throughout the entire volume prohibitive, both from cost and time standpoints. Additionally, field results showed that it was possible (probable) that immediate injection of the tracer to a high target concentration would result in exterior medium concentrations from large leaks high enough at distant monitoring ports that smaller leaks in the barrier would be masked. Thus the most complete verification of barriers would include multiple injection steps that would create a relatively constant concentration at the barrier wall for a given period of time. Multiple injection ports would be needed, with each port generating a source concentration over a defined area of the barrier wall. The initial injection would be a low concentration to check for large leaks. Areas of the barrier where leaks are found would be maintained at the low source concentration until adequate data is collected. The source concentration at other areas of the barrier would be increased incrementally until the target concentration is achieved. This method of injection would increase the detail of SEAtrace™ results without flooding the medium with the tracer and without the need to maintain a constant concentration throughout the entire barrier volume.

Numerical calculations were performed with T2VOC to establish a relationship between the mass of tracer / injection port location/equilibration time / duration of the “constant” concentration. These calculations are discussed in appendix E.

Testing the new injection scheme at the Waldo test facility was difficult due to the small size of the barrier. Numerical calculations showed injection ports could be spaced on 18 foot centers under typical test conditions. However, this spacing at the Waldo facility would result in creating a constant concentration throughout the entire barrier volume. Placement of the injection ports was scaled down to 9 foot centers.

4.2.3 Leak Anomaly

Acceptance of the SEAtrace™ systems results by regulators will be dependent on the belief that the system is working as designed. Testing a controlled leak best validates this, particularly if actual validation testing shows a barrier to be integral. Thus, SEA has adopted the practice of installing an engineered leak (leak anomaly) near any barrier that is to be tested. The leak anomaly will typically be located in close proximity (within 50 ft.) to the barrier. A small container (pipe) is buried to a shallow depth (5 to 10 ft below ground surface). The container acts as the source volume. A gate valve attached to the container forms the “leak.” A 1.5-inch diameter valve was used for this test. Small diameter tubing from the surface to the center of the container is used to inject the tracer gas into the source volume, while tracer is being injected the gate valve is closed so gas

will not be advectively forced into the medium. Prior to opening the valve, a bleed line is used to allow the pressure in the container to equilibrate with atmospheric pressure (at shallow depths this is very close to the soil gas pressure). Figure 19 shows a schematic of the leak anomaly used for this demonstration. The test commences with the opening of the "leak." Monitoring ports are installed near the leak anomaly, at the same spacing used to monitor the barrier. The leak anomaly was tested immediately after completion of the barrier test. Results of the test were almost ideal. The leak was found within 24 hours of injection. The inversion code calculated the leak to be within 1 ft. (0.3 m) of the true position. Calculations of the x (horizontal) and z (depth) coordinates were exact. The code predicted the leak was closer to the monitoring ports than in reality.

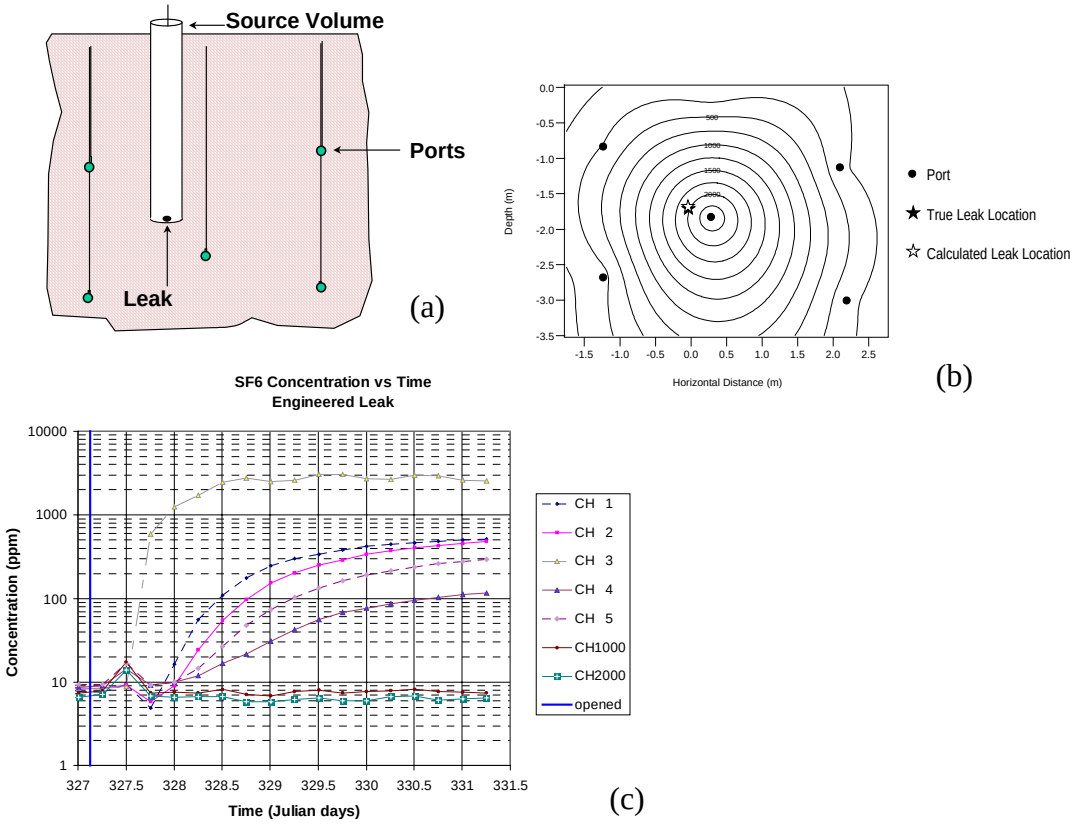

Figure 19. (a) Schematic of the leak anomaly (b) contour plot of measured concentrations (c) measured tracer concentrations.

4.3 Experimental Results

The tests were conducted between October 16, 1998 and November 29, 1998. Background data was collected for a number of days prior to injecting tracer. Tracer injections were performed in steps. In each step, small amounts of tracer were injected into a each of the twelve injection ports. Each port generated a source concentration over a defined area of the barrier wall. The initial injection concentration was low (2500 ppm) to check for large breaches in the barrier. In the afternoon of October 27, 1998, 0.2 lb of

tracer was injected into each of the interior ports. Exterior ports were monitored over a three-day period. During this time, modest increases (over and above increases due to rebound of the tracer from the prior active venting of the region near the barrier) in the recorded tracer concentrations were seen in the bottom most ports of the barrier. On October 30, 1998 another 0.4 lbs of tracer gas was injected into each of the injection ports to obtain a nominally 7500 ppm source concentration at the barrier wall. The leaks (fractures) at the bottom of the barrier were more clearly delineated. These areas of the barrier were then maintained at the low source concentration. The source concentration throughout the rest of the barrier was increased to 20,000 ppm on November 4, 1998, by injecting 1.0 lb of the tracer gas into the ports in these areas (7 total). Over the next 14 days the data collected clearly showed the presence of all 6 engineered leaks plus numerous non-engineered leaks. On November 23, 1998, the scanning system was reconfigured to perform the leak anomaly test. Background data for this test was collected for a 24 hour period, and tracer was injected into the contained volume on November 24, 1998. Within 24 hours SEAtrace™ detected the leak. Over the next four days, data was collected and analyzed. After the test was completed (November 28, 1998), the scanning system set-up was again switched over to monitor the main barrier. Data was collected until the equipment arrived to abandon the site, on November 30, 1998.

Figures 20 and 21 show the measured concentration histories of the tracer gas at the monitoring ports. Ports are divided by the four panels of the barrier. Injection times are noted on the graphs. Scans were completed once or twice per day through November 23, 1998 (Julian day 325). Gaps in the data between Julian days 325 and 330 are when the system was reconfigured to perform the leak anomaly test. The data was well behaved. A clear response in the data is seen after the third (main) injection. In general measured concentrations increase in time. The exception to this being ports very near a breach. These ports saw a more pronounced increase immediately after the injection, then a drop and subsequent increase in the concentration. This is expected. While the forward model(s) assume a constant source concentration, in reality the tracer is injected into the barrier. The injection of the gas into a point source creates spherical diffusion/advective movement from the injection point out into the source volume. When the concentration front reaches the barrier it can not continue to expand in that direction. The concentration at the barrier wall increases very rapidly. If there is a leak in this area of the barrier, a pulse of tracer will diffuse through the leak. As the tracer begins to equilibrate along the barrier wall, the concentration at the leak entrance will diminish, causing less tracer to diffuse through the leak and a subsequent decay in the tracer concentration in the medium (appendix C). Equilibration along the barrier wall requires 5 to 7 days (appendix E, attachment C). The magnitude of the increased concentration in the medium is a function of how close the injection port is to the leak.

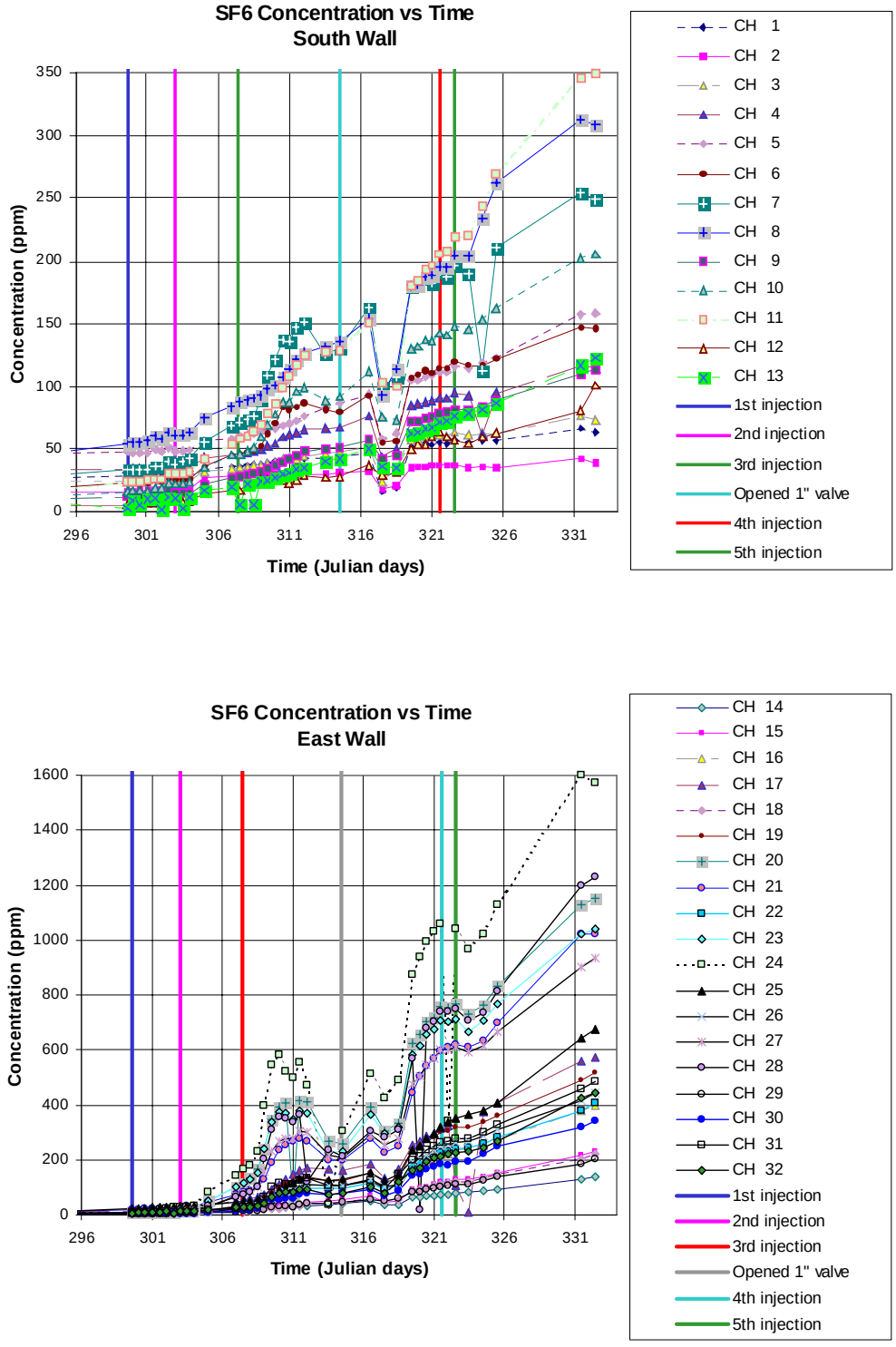

Figure 20. Measured concentration histories of the tracer gas for monitoring ports at the Waldo SEAtrace™ demonstration site.

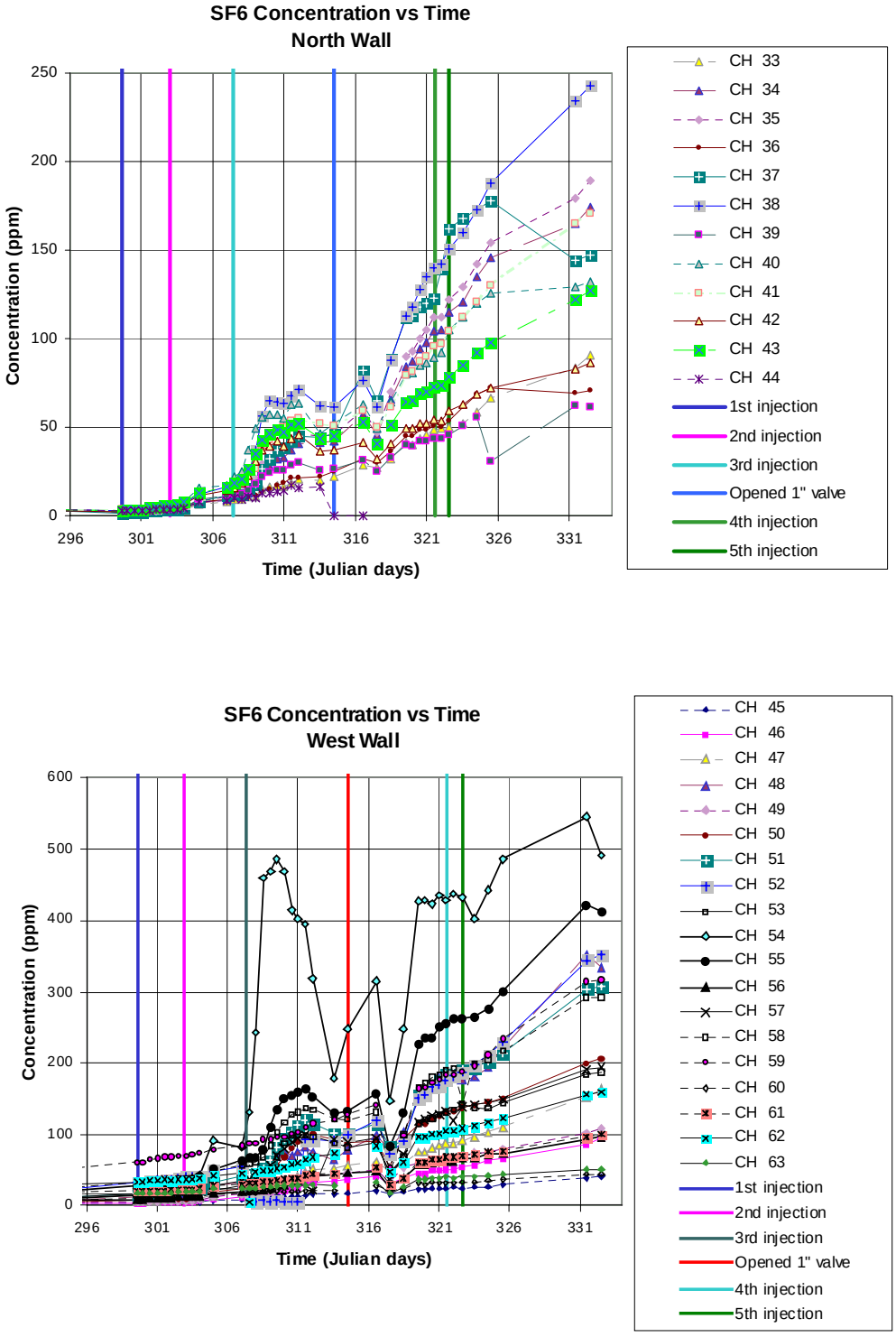

Figure 21. Measured concentration histories of the tracer gas for monitoring ports at the Waldo SEAtrace™ demonstration site.

Figures 22 and 23 show the measured concentrations of carbon dioxide during the test. This data proved to be very useful. It provided corroborating data that showed the rebound of soil gas into the volume of soil that was effected during the vapor extraction (note the increased concentrations through Julian day 304). This helped to determine when to start the test and when increased concentrations in the SF_6 data could be construed as being from a breach in the barrier rather than from vapor rebound. The data clearly shows the different medium beyond the north panel (the area that was backfilled with crusher fines during construction of the test facility. Ports along the north panel recorded CO_2 concentrations much higher than ports in the native soil (nominally35,000 vs 6,000 ppm). Diffusion of the CO_2 from the medium around the north panel into adjacent native soil on the west and east panels (i.e., ports 46-48 and 30-32) is evident. The data is also useful in determining if the tubing to the ports are damaged. The CO_2 concentration in air is considerably less than that in the medium. If recorded values dropped to levels near atmospheric it would be a clear indication that the tube had been damaged and samples were not being drawn from the subsurface port. No tubes were damaged during the demonstration.

Figures 24 and 25 show the measured concentration histories for water vapor. Measured concentrations of other gases are cross compensated for water vapor. These values are recorded to see if liquid is potentially being pulled into the sample lines. Figure 26 shows the time histories required to fill the sample bag. These histories can be used to determine which ports are becoming plugged.

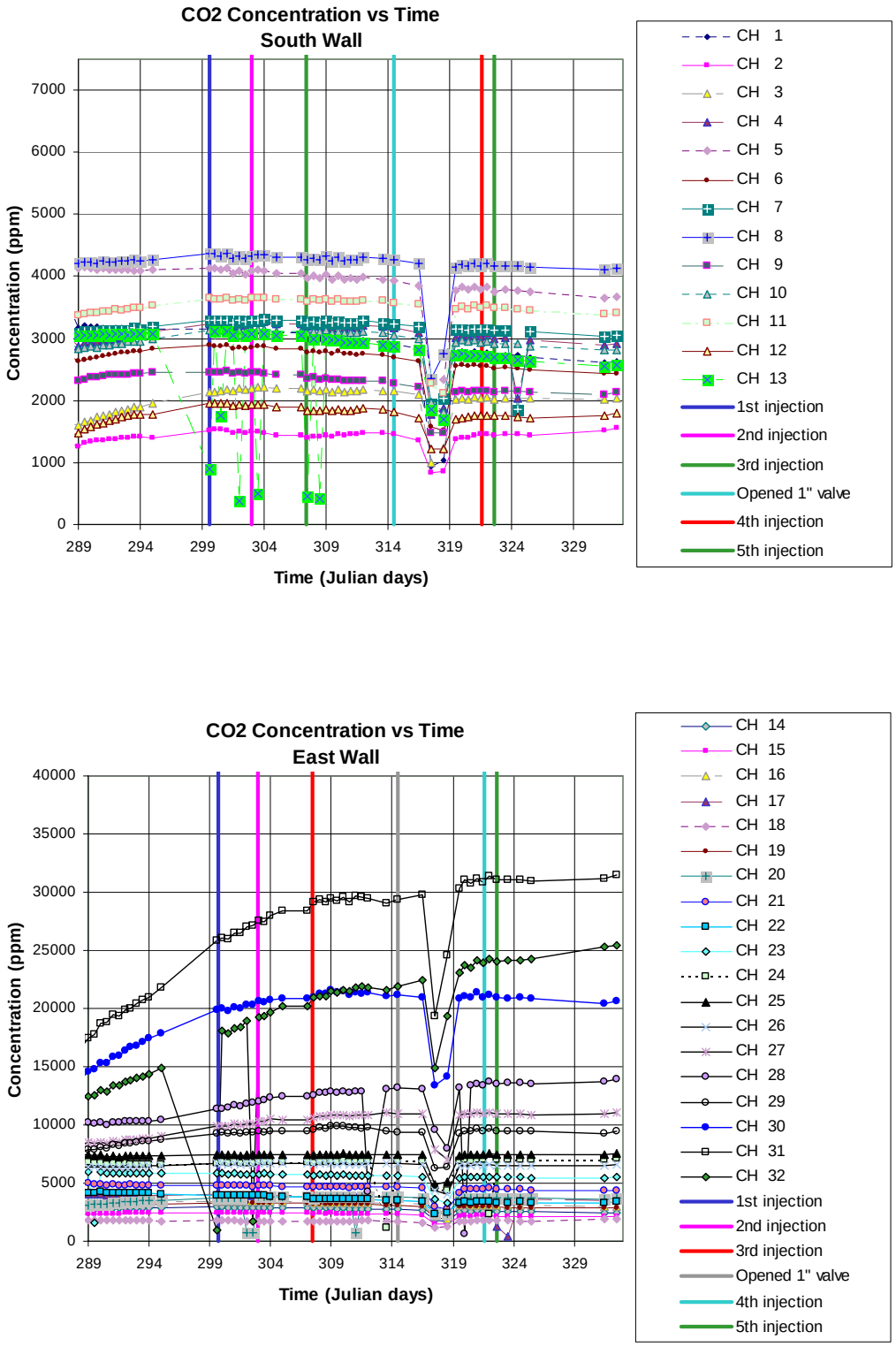

Figure 22. Measured concentration histories of the carbon dioxide for monitoring ports at the Waldo SEAtrace™ demonstration site.

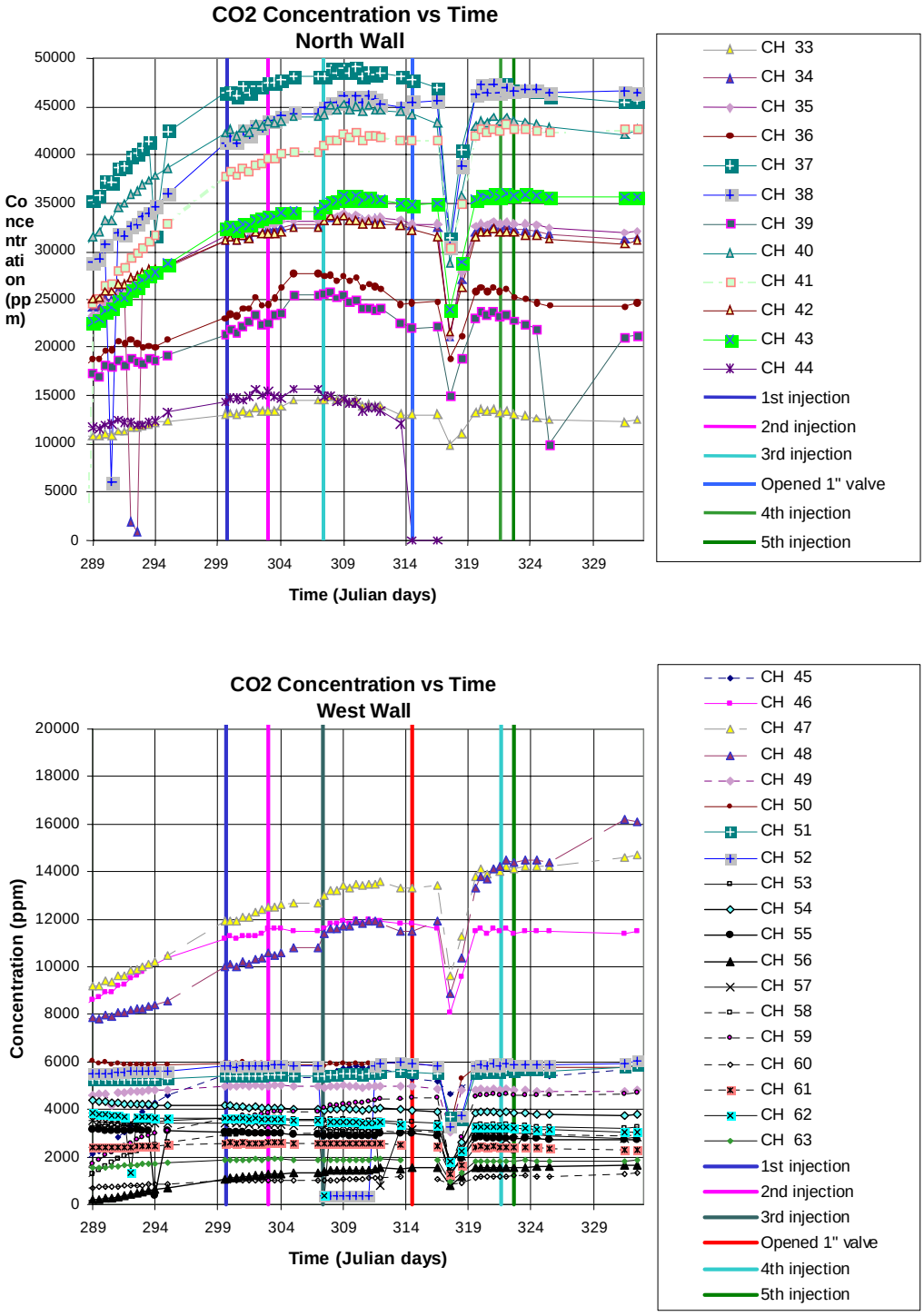

Figure 23. Measured concentration histories of the carbon dioxide for monitoring ports at the Waldo SEAtrace™ demonstration site.

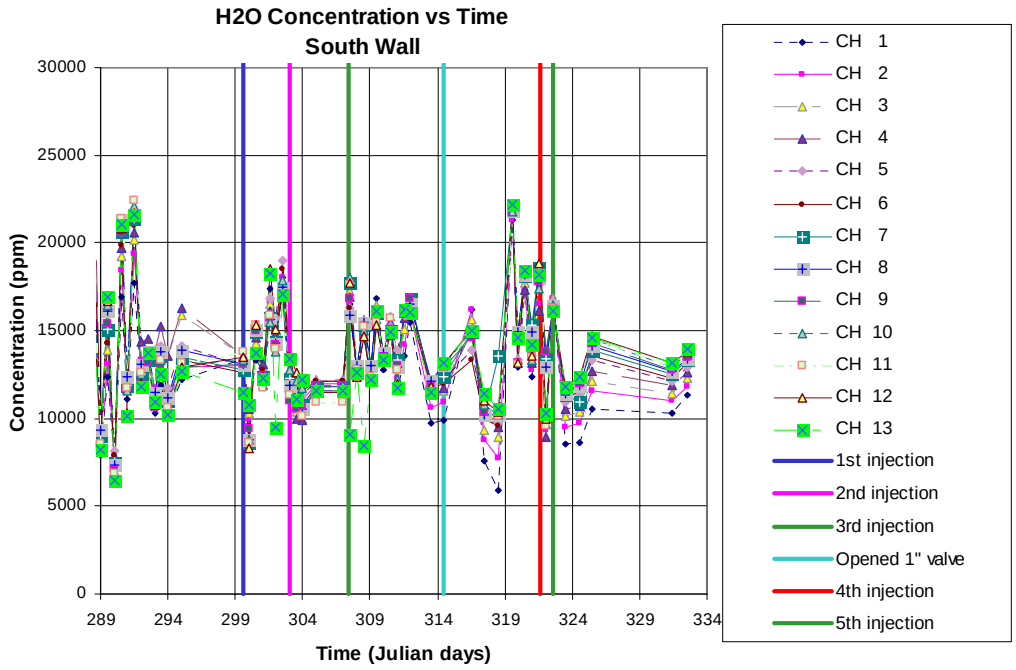

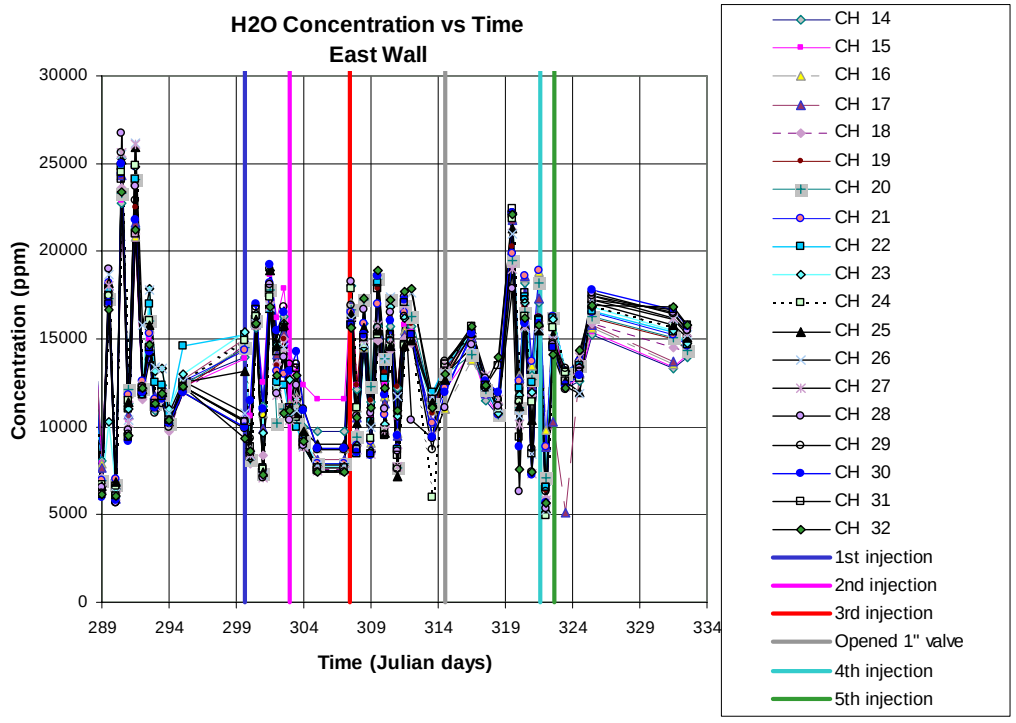

Figure 24. Measured concentration histories of water vapor for monitoring ports at the Waldo SEAtrace™ demonstration site.

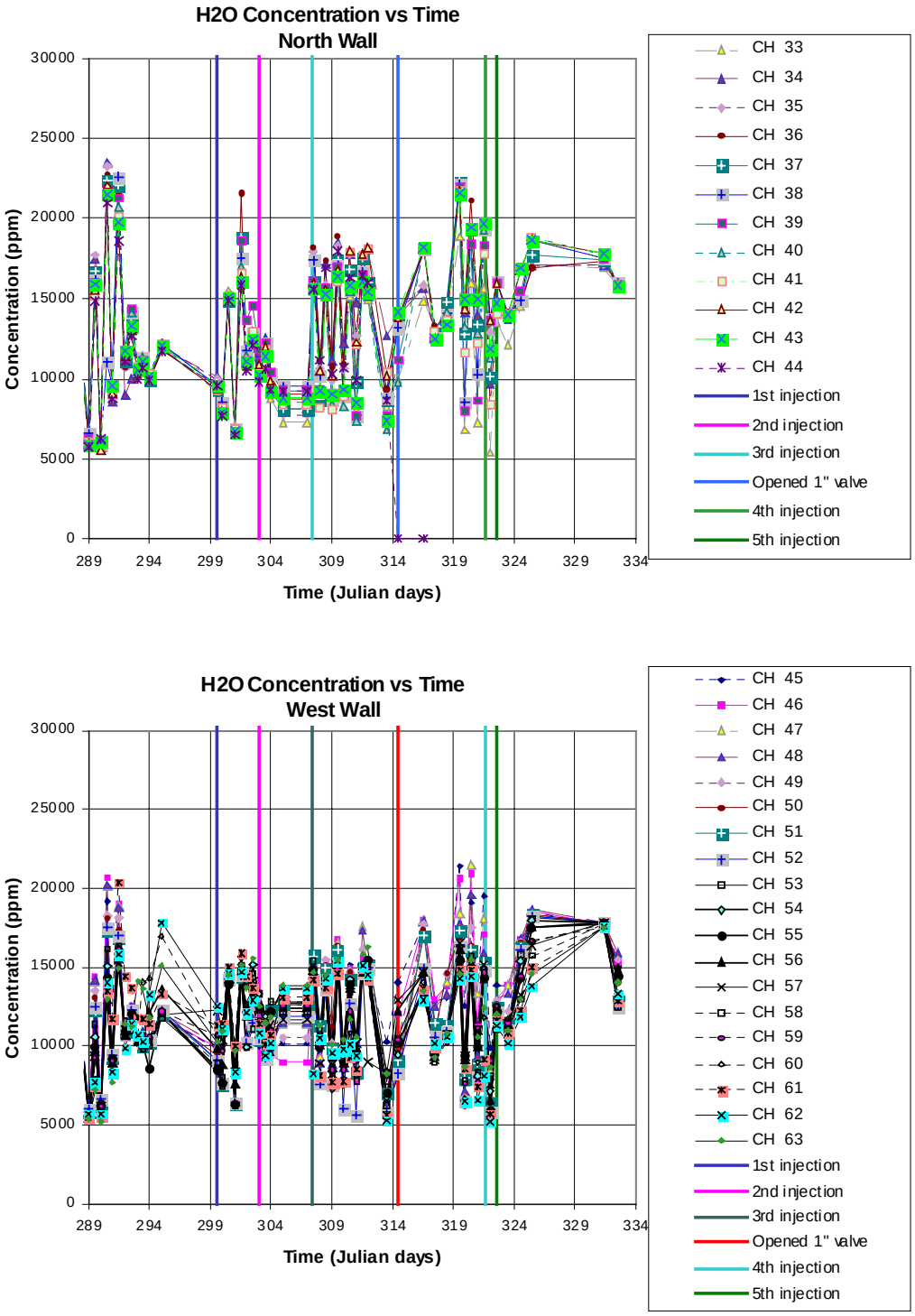

Figure 25. Measured concentration histories of water vapor for monitoring ports at the Waldo SEAtrace™ demonstration site.

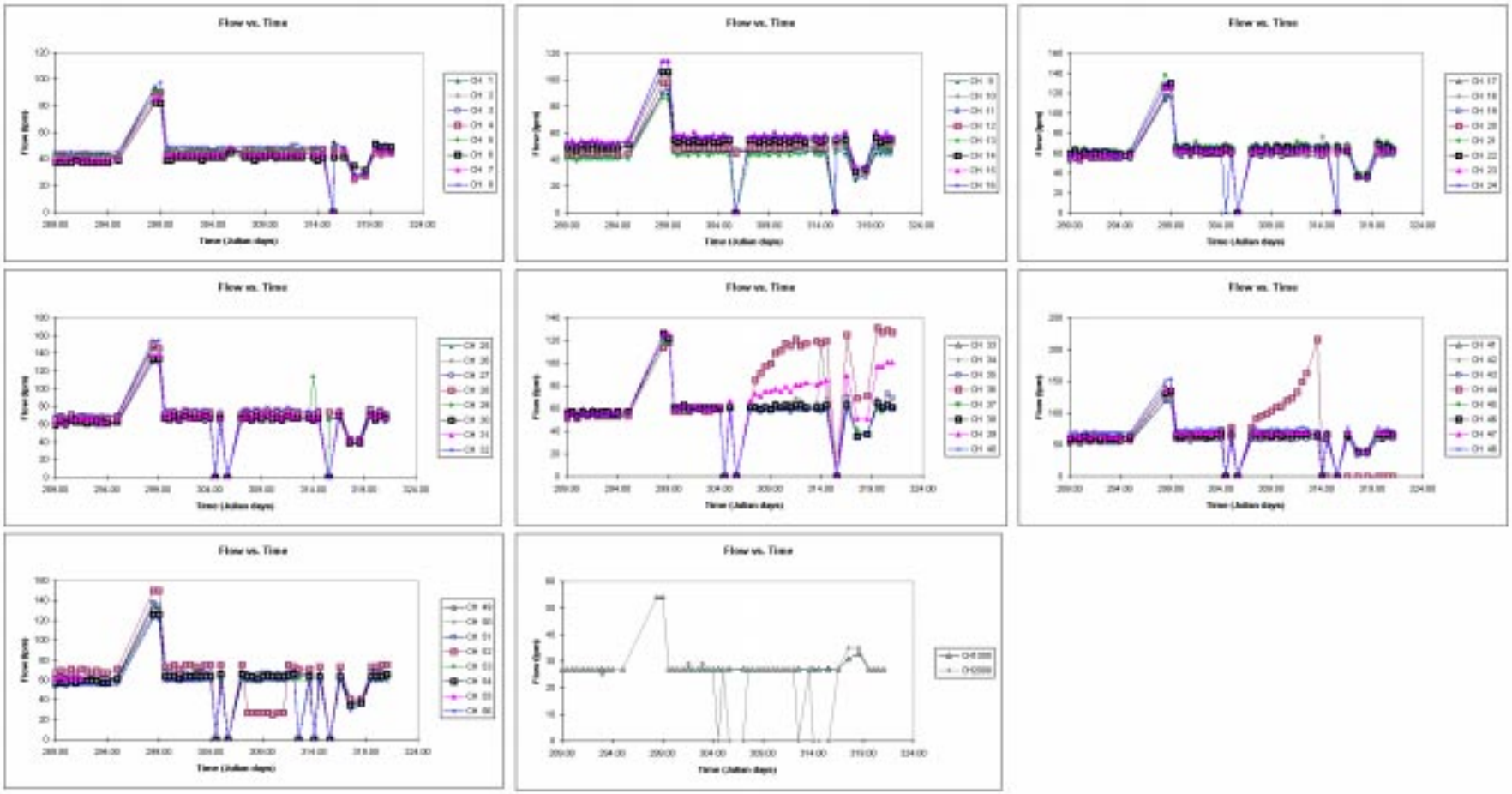

Figure 26. Time (seconds) required to fill the monitoring ports at the Waldo SEAtrace™ demonstration site.

SEAtrace™ was able to find multiple leaks on the barrier, even under adverse conditions including pre-existing, spatially variable background concentrations, a heterogeneous medium and multiple unplanned breaches. The system located a total of six engineered and four non-engineered leaks on the barrier, plus accurately detected an independent test leak, which was located away from the barrier. The large non-engineered leaks (a fracture along the length of the bottom of the barrier and another in the bottom corner of the intersection between the south and east panels) were detected within a day of the preliminary injection. These leaks were monitored throughout the initial two low-concentration injections. Four of the five engineered leaks that were open at the start of the test were found within five days of the initial injection. The remaining engineered leak that was opened at the test start was found two days after the source concentration was boosted to the target concentration of 20,000 ppm (eight days into the test). The remaining engineered leak was opened eight days after the test began. This leak was found within two days after the valve was opened, even with the existing background concentrations created by other nearby leaks. Table 4 summarizes the leak locations and radii of the engineered leaks as calculated automatically by the SEAtrace™ system (using the datum shown in figure 16). True locations of the leaks are included, as is the distance between the calculated and the true positions. Detected leaks ranged from 1.1 cm to 38 cm (7/16 in. to 15 in.) in diameter. The locations of the leaks that the system found were consistent with time (inversions of sequential leak data sets produced similar results – figure 27). The calculated location of the engineered leaks was typically within 0.7 to 2.3 feet (0.2 to 0.7 m) of the true positions. The most accurate results were found for leaks distant enough from other leaks such that the measured concentrations at the monitoring ports were due to a single leak. The single engineered leak that was not affected by another leak was detected to within 8 inches (0.2 m) of the true position, while leaks near adjacent leaks were typically found to within 2.3 feet (0.7 m). The leaks most influenced by the non-engineered fractures at the bottom of the barrier were found less accurately, to within 6 feet (1.9 m). In each of these cases, results varied more in time and the leaks were not located on the surface of the barrier, indicating that the measured concentration profiles did not match the assumed spherical diffusion model. Review of the contour plots confirmed this deduction. Contour plots of select time steps are shown in figures 28 through 31.

The calculated radii of the leaks were less accurate. The accuracy of the leak size determination is affected by the forward model used in the SEAIM code, the correlation between leak radius and start time of the leak as seen in the inversion code, and the injection method of the source concentration. The system characterized the leaks as ranging from 4.3 to 12.2 inches (11 cm to 31 cm) in radius, while the actual sizes ranged from 0.25 to 7.5 inches (0.6 to 19 cm) in radius.

Table 4. Results of the SEAtrace™ demonstration at the Waldo test facility.

Description of Engineered Leak	X (m)	Y (m)	Z (m)	Difference between true and calculated position (m)_	radius (m)
3" diamter, 2'long valve on West Panel actual position of the valve	8.41 +/- 0.29 8.42	7.91 +/- 0.15 8.07	-2.56 +/- 0.14 -2.45	0.19	0.23 +/- 0.07 0.04
15" diamter, 2'thick valve on East Panel actual position of the valve	8.46 +/- 0.12 8.80	3.26 +/- 0.38 3.27	-2.68 +/- 0.20 -2.56	0.36	0.34 +/- 0.05 0.19
4" diamter, 4'thick valve on East Panel actual position of the valve	7.80 +/- 0.16 6.16	3.00 +/- 0.17 3.33	-3.30 +/- 0.14 -2.34	1.93	0.31 +/- 0.05 0.05
1" diameter, valve on North Panel actual position of the valve	12.09 +/- 0.06 12.15	4.29 +/- 0.01 4.06	-2.02 +/- 0.06 -1.60	0.49	0.20 +/- 0.07 0.013
7/16" diameter valve on North Panel actual position of the valve	12.29 +/- 0.03 12.34	6.30 +/- 0.23 6.35	-2.12 +/- 0.15 -1.40	0.72	0.11 +/- 0.04 0.006
4" diameter, 0'thick valve on South Panel actual position of the valve	3.99 +/- 0.26 3.36	5.45 +/- 0.13 5.34	-2.57 +/- 0.27 -2.08	0.81	0.18 +/- 0.03 0.05

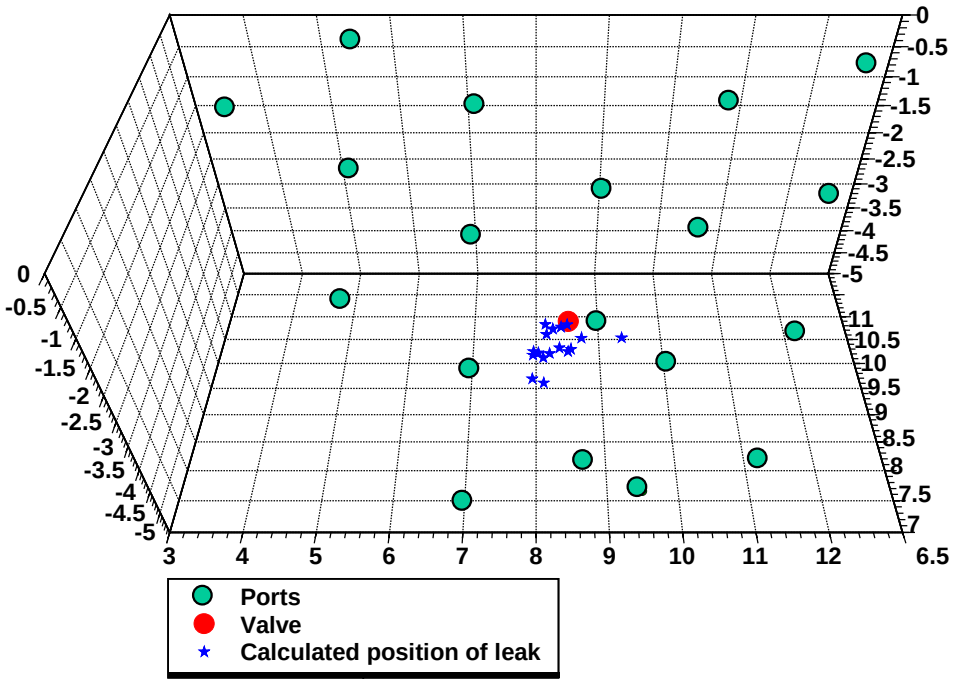

Figure 27. Sequential results for one of the leaks in the Waldo demonstration. Calculated position of the leaks with time were very well behaved.

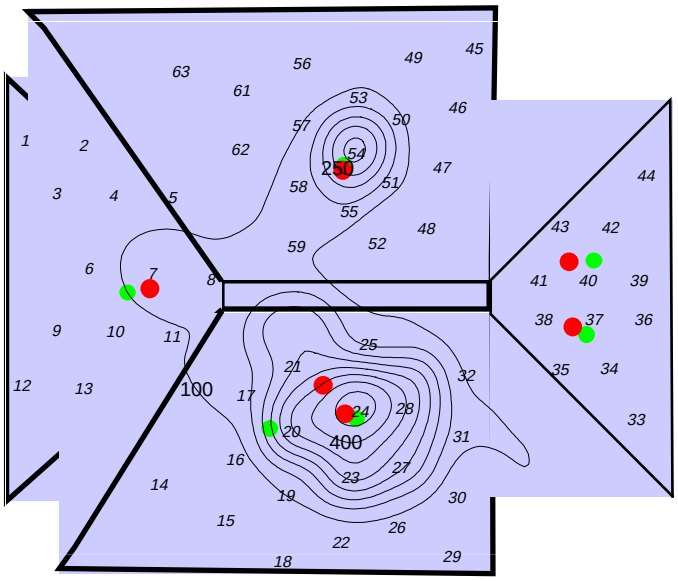

Figure 28. Contour plot of data taken on November 7, 1998. Plots were created by generating a 2-D grid of the data ports (ports were rotated around the bottom of the barrier into a plane). Leak locations (lighter dots) and the calculated position of the leaks (darker dots) are superimposed over the grid.

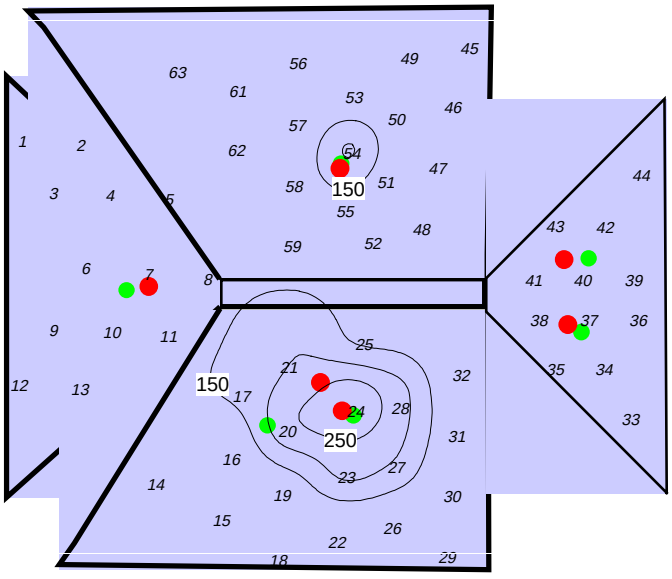

Figure 29. Contour plot of data taken on November 11, 1998. Plots were created by generating a 2-D grid of the data ports (ports were rotated around the bottom of the barrier into a plane). Leak locations (lighter dots) and the calculated position of the leaks (darker dots) are superimposed over the grid.

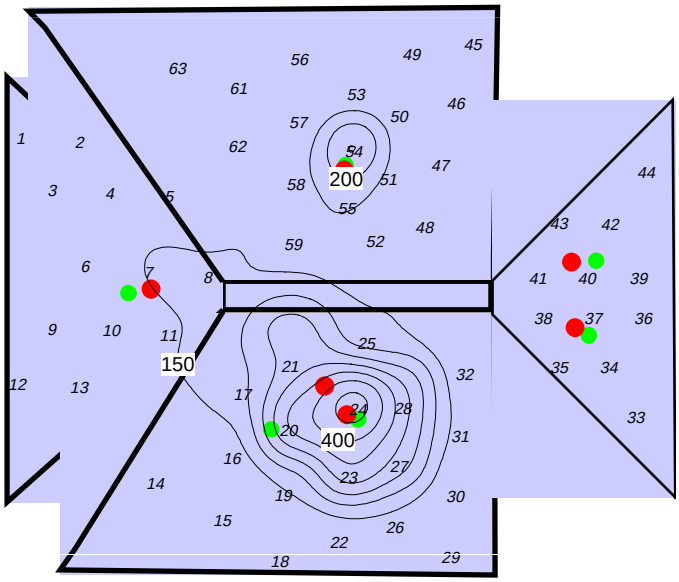

Figure 30. Contour plot of data taken on November 13, 1998. Plots were created by generating a 2-D grid of the data ports (ports were rotated around the bottom of the barrier into a plane). Leak locations (lighter dots) and the calculated position of the leaks (darker dots) are superimposed over the grid.

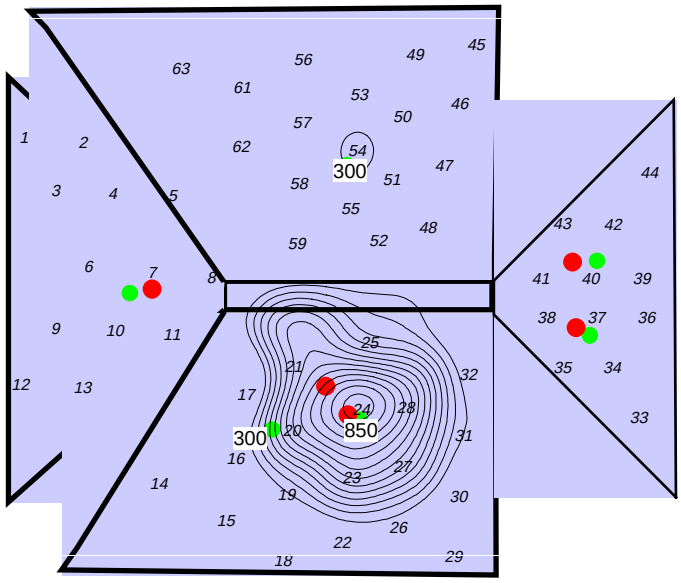

Figure 31. Contour plot of data taken on November 19, 1998. Plots were created by generating a 2-D grid of the data ports (ports were rotated around the bottom of the barrier into a plane). Leak locations (lighter dots) and the calculated position of the leaks (darker dots) are superimposed over the grid.

Of the non-engineered leaks detected, there were two large fracture type breaches in the barrier. One was along the bottom of the barrier, starting at the intersection between the bottom and the south panel and extending towards the north panel about two thirds of the total distance. The other was along the intersection of the east and south panels, starting near the bottom of the barrier and extending about one quarter of the way to the top of the barrier. The remaining breaches were more localized. One was near the intersection of the north and east panels, about half way up the barrier (coordinates in meters are 12.19, 5.27, -2.29). The final breach was on the south panel. It was near the surface and within several feet of the west panel barrier (coordinates in meters are 1.44, 9.26, -0.13).

In an effort to determine how a coarser spaced port grid would effect the results, analysis was also performed on data sets where ports from every other well around the barrier were removed. Breaches were not found quite as accurately, however in most cases the results were acceptable. The analysis found four of the six engineered leaks. The smallest leaks, those on the north panel, were masked by the much higher concentrations from other leaks. The leaks that were larger or that were not close to other leaks were found to within 0.75 m of the true leak location. Those breaches that were influenced by other leaks were found less accurately, although results were very similar to the analysis using all the ports (see table 4). Results are summarized in table 5.

The BNL tests were performed in series with the SEAtrace™ test. Between the second and third SF_6 injections (October 30, and November 4,1998), BNL injected the PFT tracers. Details on the BNL tests are given in appendix D.

Table 5. Results of the SEAtrace™ inversion code on a subset of the data (data from every other well around the barrier were removed).

Description of Engineered Leak	X (m)	Y (m)	Z (m)	Difference between true and calculated position (m)_	radius (m)
3" diamter, 2'long valve on West Panel	8.67 +/- 0.17	8.09 +/- 0.05	-3.10 +/- 0.10		0.23 +/- 0.06
actual position of the valve	8.42	8.07	-2.45	0.69	0.04
15" diamter, 2'thick valve on East Panel	8.70 +/- 0.12	2.68 +/- 0.12	-3.01 +/- 0.11		0.32 +/- 0.07
actual position of the valve	8.80	3.27	-2.56	0.75	0.19
4" diamter, 4'thick valve on East Panel	4.17 +/- 0.02	3.50 +/- 0.14	-3.48 +/- 0.21		0.27 +/- 0.03
actual position of the valve	6.16	3.33	-2.34	2.30	0.05
1" diameter, valve on North Panel					
actual position of the valve	12.15	4.06	-1.60		0.013
7/16" diameter valve on North Panel					
actual position of the valve	12.34	6.35	-1.40		0.006
4" diameter, 0'thick valve on South Panel	3.91 +/- 0.12	5.33 +/- 0.07	-3.23 +/- 0.09		0.27 +/- 0.05
actual position of the valve	3.36	5.34	-2.08	1.27	0.05

To demonstrate the SEAtrace™ inversion code's ability to work with any tracer, a single time series of data collected by BNL (data collected November 9, 1998) was analyzed with the SEAIM code. Each of the four perfluorocarbons injected into the barrier was analyzed independently. Results were similar to those found with the SF_6 with one notable exception. The largest leak, the 15-in. diameter leak on the east panel, was not located (recorded concentrations showed there was a leak there, but the highest concentration in the area was recorded closest to port no. 23 whereas the closest port to the leak was port no. 24). As such, SEAIM found a leak in the area, but it was not deemed an engineered leak. The leak on the south panel was not calculated by SEAIM. The maximum concentration in this area was detected at the port closest to the breach in the area. However, it was less than 5 ppm, which was below the minimum limit input for the run. This is an artifact of the different ranges used for the different tracers. If PFT tracers were to be used with the code as the primary tracer, this value could be lowered to eliminate the problem. Finally, when this data set was taken, the 1-in. valve on the north wall was unopened. A summary of the results is given in table 6.

Table 6. Results of the SEAtrace™ inversion code on a single set of perfluorocarbon data (a single sample time containing data from all four PFT's injected into the barrier).

Description of Engineered Leak	X (m)	Y (m)	Z (m)	Difference between true and calculated position (m)_	radius (m)
3" diamter, 2' long valve on West Panel	8.04	8.13	-2.04		0.17
actual position of the valve	8.42	8.07	-2.45	0.57	0.04
15" diamter, 2' thick valve on East Panel	Recorded data showed leak closer to another port (port 23)				
actual position of the valve	8.80	3.27	-2.56		0.19
4" diamter, 4' thick valve on East Panel	7.19	2.96	-2.93		0.05
actual position of the valve	6.16	3.33	-2.34	1.27	0.05
1" diameter, valve on North Panel	This valve was not opened at time of data collection				
actual position of the valve	12.15	4.06	-1.60		0.013
7/16" diameter valve on North Panel	12.97	6.39	-1.59		0.01
actual position of the valve	12.34	6.35	-1.40	0.67	0.006
4" diameter, 0' thick valve on South Panel	Concentrations recorded at this location were below set limit for code				
actual position of the valve	3.36	5.34	-2.08		0.05

4.4 Experimental Conclusions

The Waldo demonstration provided an excellent test of the SEAtrace™ subsurface barrier verification and monitoring system. SEAtrace™ was able to find multiple leaks on the barrier, even under adverse conditions including pre-existing, spatially variable background concentrations, a heterogeneous medium and multiple unplanned breaches.

The system located a total of 6 engineered and 4 non-engineered leaks on the barrier, plus accurately detected an independent test leak, which was located away from the barrier. SEAtrace™ data was collected automatically. One or two scans per day were recorded over a 25-day period. During this time, over 2,400 individual gas samples were collected and analyzed by the system, providing excellent concentration histories at each monitoring port. Data reduction of each scan was available within several hours of data collection.

A staged/stepped injection scheme was designed and implemented. This scheme provided a constant concentration along the barrier wall to be attained rapidly and with great control. The initial injection produced a low concentration meant to detect gross leaks in the barrier. Areas where breaches were defined were then maintained at the low concentration while the concentrations over the remainder of the barrier were increased. This method of injection increases the detail of SEAtrace™ results without flooding the medium with the tracer and without the need to maintain a constant concentration throughout the entire barrier volume.

Using this injection method, two large non-engineered breeches were detected at the bottom of the barrier. These breaches (a fracture along the length of the bottom of the barrier and another in the bottom corner of the intersection between the south and east panels) were detected within a day of the preliminary injection. They were monitored throughout the initial two low concentration injections (spanning a four day period). The six engineered breaches and two other non-engineered breaches were detected after the third injection sequence. At this point, the source concentration in those areas where there were not gross defects was near 20,000 ppm. All five of the engineered leaks that were open at the time of the third injection were found within three days of the injection. The remaining engineered leak was opened 8 days into the test period, after the target source concentration had been reached. This leak was found within 2 days after the valve was opened, even with the existing background concentrations created by other nearby leaks. The engineered leaks ranged from 1.1 cm to 38 cm (7/16 in. to 15in.) in diameter. The calculated location of the engineered leaks was typically within 0.7 to 2.3 feet (0.2 to 0.7 m) of the true positions. The most accurate results were found for leaks distant enough from other leaks such that the measured concentrations at the monitoring ports were due to a single leak. The single engineered leak that was not affected by another leak was detected to within 8 inches (0.2 m) of the true position, while leaks near adjacent leaks were typically found to within 2.3 feet (0.7 m). The leaks most influenced by the non-engineered fractures at the bottom of the barrier were found less accurately, to within 6 feet (1.9 m). The system characterized the leaks as ranging from 4.3 to 12.2 inches (11 cm to 31 cm) in radius, while the actual sizes ranged from 0.25 to 7.5 inches (0.6 to 19 cm) in radius. Two discreet non-engineered breeches were found. One was near the intersection of the north and east panels, about half way up the barrier. The other was on the south panel. It was near the surface and within several feet of the west panel barrier.

To demonstrate the SEAtrace™ system's ability to work with any tracer, a single time series of data collected by BNL was analyzed with the system. Each of the four

perfluorocarbons injected into the barrier was analyzed independently. Results were similar to those given above.

In an effort to determine how a coarser spaced port grid would effect the results, analysis was also performed on data sets where ports from every other well around the barrier were removed. Breaches were not found quite as accurately, however the results were acceptable. The analysis found four of the six engineered leaks. The smallest leaks, those on the north panel, were masked by the much higher concentrations from other leaks. The leaks that were large or that were not close to other leaks were found to within 0.75 m of the true leak location. Those breaches that were influenced by other leaks were found less accurately, although results were very similar to those using all the ports.
To verify the integrity of the system itself, an independent leak test was performed. The leak anomaly was tested immediately after completion of the barrier test. Results of the test were almost ideal. The leak was found within 24 hours of injection. The inversion code calculated the leak to be within 1 foot (0.3 m) of the true position. Calculations of the x (horizontal) and z (depth) coordinates were exact. The code predicted the leak was closer to the monitoring ports than in reality.

5. DEMONSTRATION

5.1 Finding the Demonstration Site

Finding an acceptable host site for the demonstration proved to be difficult. While there are numerous working barriers throughout the DOE complex none were found to be ideal. The majority of the barriers were emplaced in areas where the depth to the water table was very shallow (on the order of 1-5 feet below ground surface). Other sites had tentative plans for emplacing barriers, but the anticipated dates of installation would have required a significant postponement of the demonstration. Once finding a host site within the DOE complex was ruled out, other sites were researched. Finding where barriers have been emplaced was in itself not easy. Vendors were typically unwilling to divulge specific information on barriers they had installed, and most sites do not publish information on barriers that have been installed for them. The best source found for information proved to be the regional Environmental Protection Agency (EPA) offices. Records of Decisions at contaminated sites (in particular Superfund sites) included references to barriers emplaced at those sites, and became starting points in the search for a host site. Table 7 is a compilation of the barriers that were found while searching for a demonstration site. The vast majority of the sites (except for sites where the description of the geology / depth to the water table was such that they were not considered suitable for the demonstration) were contacted. Most sites were not interested in participating in the demonstration. Reasons listed for not wanting to participate included:

- Fear of regulatory agencies requiring additional work at the site should the demonstration show there was a breach in the barrier.
- Increased liability incurred by the host site during the demonstration.
- Hidden costs to the host site.
- Difficulty in gaining approval for the demonstration from all parties involved (typically there were multiple responsible parties for clean-up of the site, the EPA, and a state environmental agency involved).
- Fear of having the demonstration damage the integrity of the containment system. Of particular concern were penetrations through the surface cap required to emplace the injection ports within the barrier volume, and the possibility of drilling through the barrier while drilling wells for port emplacement. Many of the barriers are very large (extending around the perimeter of sites that are 10s to 100s of acres in size), and the exact location of the barrier was not known.
- A lack of a clear benefit to the host site for participating in the demonstration.

Table 7. Information on barriers deemed potential candidates for the SEAtrace™ demonstration.

Site Name(s)	State	Contaminants	size	dimensions	description	cap	water table info.	general info
Brunswick Naval Air Station; Sites 1 & 3; Orion Street Landfill North and Hazardous Waste Burial Area	Maine	voc's	12 ac	2220 ft	slurry wall	double barrier landfill cap	h2o has dropped below a significant amount of the landfill waste	
Gilson Road Superfund Site	Massachusetts		20 ac		slurry wall	impermeable cap		cap and slurry wall completed 1982; groundwater treatment facilit operated from 86-96.
Solvents Recovery Service of New England	Connecticut	voc's, pcb's, DNAPLs, LNAPLs	2 ac		slurry wall		500' from Quinnipiac River	presently extending groundwater treatment system
Old Springfield Landfill Site	Vermont	voc's, pcb's, pah's	27 ac					ROD of 1988 said were looking at installation of a slurry wall
Sylvester Hazardous Waste Dump	New Hampshire	voc's	6 ac		slurry wall around 20 ac.	impermeable cap		cleanup completed, monitoring now to at least 2001.
Diamond Alkali Site (aka Diamond Shamrock Site)	New Jersey	dioxin, ddt	3.4 ac		slurry wall	RCRA cap		
Florence Land Recontouring (FLR) Landfill	New Jersey	phthalates, heavy metals, vinyl chloride monomers, voc's	60 ac		perimeter soil/bentonite slurry wall	clay cover initially, later a synthetic membrane and clay composite cap		all major phases completed in 1994
GE Moreau	New York	voc's, pcb's	40 ac		soil/bentonite cutoff wall	cap		completed in 1990, upgraded in 1994 (reduce migration of contaminated groundwater by creating an inward hydraulic gradient
Helen Kramer Landfill	New Jersey	voc's, heavy metals	66 ac		slurry wall around entire site, 3' wide, varies from 20-70' deep	multi-layer cap (over 81.5 ac)		originally site clean-up done by federal government; in1994 transferred O&M to New Jersey Departmnet o f environmental Protection
Hooker (102nd street) Landfill	New York	voc's, semi volitale organics, pesticides, heavy metals	22 ac		slurry wall around perimeter of site	synthetic lined cap		next to the Niagara River (part of the love canel site)
Lipari Landfill	New Jersey	organic compounds, heavy metals	6 ac		bentonite/soil slurry wall encircling 16 ac area, keyed into the underaying aquitard	bentonite clay cap		Army Corp of Engineers oversaw construction
Pollution Abatement Services (PAS) Facility	New York	heavy metals, voc's, pcbs	15.5 ac		perimeter slurry wall	clay cap, topsoil, vegitation (later states cap as being impermeable -RCRA)		Work performed by EPA and New York State Department of Environmental Conservation
Scientific Chemical Processing Site	New Jersey	voc's, pcb's, pah's, heavy metals	6 ac		perimeter slurry wall (an interim measure only), 15-20' deep	temporary infiltration barrier		Located in a coastal wetlands area, bordered on by Peach Island Creek, a tidal waterway

Table 7 (cont). Information on barriers deemed potential candidates for the SEAtrace™ demonstration.

Site Name(s)	State	Contaminants	size	dimensions	description	cap	water table info.	general info
South Brunswick Landfill, aka BrowningFerris Industries	New Jersey	voc's, heavy metals	68 ac		perimeter slurry wall	clay cap		major components completed in 1985
Volney Landfill	New York	vinyl chlorid, benzene, arsenic, voc's and metals	55 ac		slurry wall (original landfill was not lined)	cap		
Brodhead Creek Superfund Site	Pennsylvania	pooled coal tar			slurry wall			
Delaware Sand & Gravel Landfill	Delaware	organics and inorganic compounds	27 ac total, .75 ac drum disposal area		slurry wall around drum disposal area	multi-layer cap over drum disposal area		4 mj disposal areas; in the drum disposal area a soil vapor extraction/bioremediating system is installed, so probably a significant amount of the slurry wall is in the vadose zone. Treatment (removal) completed in 1996.
Douglassville Disposal Site	Pennsylvania		50 ac		slurry wall may have been constructed		Next to Schuylkill river	
El Dupont, Newport Site	Delaware				barrier wall around the south landfill	cap	Next to Christina River	
Kane & Lombard Street Drums	Maryland	voc's, pcb's, pah's phthalates, lead	10 ac		slurry wall encircles waste disposal area	multi-layer cap	no mention of bodies of water near the site	
Lord-Shope Landfill	Pennsylvania	voc's, arsenic, copper	5 ac		slurry wall used to divert grounwater	PVC liner cap		Removed voc's from landfill soils through in-place vapor stripping; completed 1996
Osborne Landfill	Pennsylvania	voc's pcp heavy metals pcb's	15 ac		slurry wall around perimeter of landfill	clay cap, revegitated	property surrounded by wetlands and woods	completed in 1997
Rentokil Virginia Wood Preserving dvision Site	Virginia	vods, dioxin, PAHs, phenols, metals			will be constructing a slurry wall, but doesn't say where		site includes woodlands and wetlands, a pond and a floodplain	
Standard Chlorine of Delaware, Inc. Site	Delaware	chlorobenzenes	46 ac		interim action includes construction of barrier, beginning in 1999			
Tybouts Corner Landfill	Delaware	1,2-dichloroethane, vinyl chloride, benzene, etc	47 ac	5 to 40' thick	slurry wall (does not say surrounds landfill)	multi-layered cap		

Table 7 (cont). Information on barriers deemed potential candidates for the SEAtrace™ demonstration.

Site Name(s)	State	Contaminants	size	dimensions	description	cap	water table info.	general info
Union Gas Site	Pennsylvania	voc's PAHs, metals	12 ac		slurry wall constructed to mitigate onsite coal tar migration toward brodhead creek			
Agrico Chemical Co. Site	Florida	fluoride, lead, arsenic	30 ac		slurry wall	multi-media cap over affected areas	not close to body of water; bayou 1 mi downgradient from site	
Petroleum Products Corporation Superfund Site	Florida		7 ac, sludge disposal pit 0.7 ac	sludge pit 18-22' deep	alternative plan recommended did NOT include a barrier		lakes located in the trailer park south of the site; surficial water 1-10' bgs, shallow water approximately 25' bgs	
Whitehouse Waste Oil Pits Site	Florida	voc's, PCBs, phenols and metals	7 ac		slurry wall	soil cap	cypress swamp system adjacent, McGirts Creek traverses north site boundary; surficial aquifer underlies the site	
Sixty-second Street Dump	Florida		5.5 ac		permanent slurry wall around perimeter of site	entire landfill capped	80 ac marshland close by	
Sydney Mine Sludge Ponds	Florida	voc's, oil	2.1 ac (another report said 9.5 ac)		slurry wall around ponds		Turkey creek .5 mi from site	
Allied Chemical, Goldcamp Disposal Area	Ohio	cyanides, voc's, PAHs, phenols, benzene, organics	4 ac		slurry wall around disposal area fron ground surface intot he low permeability bed-rock	entire site capped w/ clay; disposal area has RCRA cap		
Waste Disposal Engineering (WDE) Site	Minnesota	voc's and organics	73 ac of a 114 ac dump		clay slurry wall	RCRA cap over the 73 ac landfill	site characterized by low relief with shallow water tables and numerous wetlands	
Forest Waste Disposal Site	Michigan	voc's, PAHs, PBBs, metals	11 ac		slurry wall containment system	RCRA cap	surrounded by woodlands and wetlands	
Fort Howard Paper CO. Sludge Lagoons	Wisconsin				slurry wall gradient control system		permeable soil and shallow ground water (5' in some cases), increases potential for contaminants to move	waste put into unlined ponds; surficial soils beneath are silty sand

Table 7 (cont). Information on barriers deemed potential candidates for the SEAtrace™ demonstration.

Site Name(s)	State	Contaminants	size	dimensions	description	cap	water table info.	general info
G&H Landfill	Michigan	voc's, PAHs PCBs, heavy metals	80 ac (second document states 70 ac)		clay barriers in the path of seepages to restrict movement of oil -- these deteriorated in the swampy areas. Later installed a partial slurry wall	capped		waste oil dumped in 2 unlined storage ponds
Gratiot County Landfill	Michigan	PBBs	40 ac		slurry wall constructed along property boundary	waste covered with clay		investigations showed slurry wall ineffective in halting groundwater flow at several locations.
Hunts Disposal Site	Wisconsin	voc's, acids, metals	84 ac w/ 35 ac landfill		slurry wall intersects the cap and a subsurface confining layer	landfill capped w/ multilayer clay and soil cover	landfill surrounded by woodlands, wetlands and a lake	
Outboard Marine Site	Illinois	PCBs			cutoff wall and slurry wall form containment cell (3 cells total)		on west shore of lake Michigan	
Lemberger Landfill (LL) Site	Wisconsin	voc's, PCBs, pesticides, metals, organics	45 ac		slurry wall around perimeter of wastes	multilayer cap w/ vegetative cover	Branch river <1 mi from site	wastes were deposited in unlined trenches
Lakeland Disposal Service, Inc	Indiana	heavy metals, voc's	39 ac		slurry wall to prevet groundwater migration from site (around perimeter of landfill)	landfill cap and gas collection system	Sloan Ditch adjacent to site, several wetlands and woodlands close,Palestine Lake 2 mi away	
Liquid Disposal, Inc (LDI) Site	Michigan	voc's, heavy metals, pesticides, PAHs, PCBs	7 ac		clay barrier to prevent dike seepage from reaching river; later constructed a slurry wall	impermeable cap containment system	site surrounded by wetlands and the Clinton River	
Motor Wheel Site	Michigan	voc's, PCBs, pesticides, metals, PAHs	24 ac		slurry wall around western and southern boundary of disposal area	14.9 ac multimedia cap		
Ninth Ave Dump	Indiana	voc's, PAHs, heavy metals, PCBs, pesticides	17 ac		soil/bentonite slurry wall around most of contaminants at site; also intermediate slurry wall was installed	capped the site after treatment (w/ RCRA cap)	low-lying and poorly drained; site adjacent to several ponds and a wetland area; prior to filling site consisteed of parallel ridtes separated by wetlands areas	

Table 7 (cont). Information on barriers deemed potential candidates for the SEAtrace™ demonstration.

Site Name(s)	State	Contaminants	size	dimensions	description	cap	water table info.	general info
Southside Sanitary Landfill or Disposal & Transfer Co., Inc	Indiana	heavy metals, PAHs	160 ac		underground slurry wall to control migration of ground water			THIS SITE IS ACTIVE and the site is being removed from the NPL list
Summit National Site	Ohio	voc's, organics, phenols, PAHs, PCBs, arsenic, chromium	11.5 ac		slurry wall around site perimeter	RCRA cap with regrading and revegetation		
Bayou Sorrel Site (consists of 4 landfills, spent lime cell, crushed drum cell, 4 covered liquid waste pones and a land farm)	Louisiana	sulfide, pesticide	50 ac		30' deep slurry wall around landfill area and shallow slurry wall around one of ponds	disposal areas coverd w/ RCRA capa top-soil/geomembrane/clay caps w/ drainage layer below cap	entire site has a marshy, buyou-type environment and is prone to flooding and poor drainage	truck driver was killed by sulfuric fumes
Eldorado Creosote Co.; Popile Site	Arkansaw	voc's, PAHs, phenols	41 ac		slurry wall implemented to ensure that at least 3' of soil remains between bottom of treatment zone and seasonal high ground water tables	lesser-contaminated soil graded and begetated;		

Two sites were identified that would at least consider hosting the demonstration. They were the Visalia Poleyard Site in southern California, and the Naval Air Station in Brunswick (NASB), Maine.

Although a private corporation (Southern California Edison, Co.) owns the Visalia Poleyard site, a DOE presence existed at the site. The site covered approximately 20 acres. In 1977, a slurry wall was built to slow contaminant migration in a shallow aquifer. Groundwater was pumped from inside the barrier and treated. Hydraulic pump tests performed at the site showed that there were breaches in the barrier. By 1994, the depth to the shallow aquifer dropped below the bottom of the slurry wall, making the slurry wall inactive. In 1995, Lawrence Livermore National Laboratory (LLNL) and the University of California at Berkeley used the site to test an innovative pilot-scale steam injection/vapor extraction system to enhance the bioremediation process. This site was considered ideal for demonstrating the SEAtrace™ system because:

- There was only a single owner of the site, and a DOE presence on site was already established
- Concerns regulatory agencies would require additional work at the site because of the demonstration were minimal (the slurry wall was no longer an integral part of the remedial plan)
- The demonstration could not damage the integrity of the containment system (there was no existing cap on the barrier, and the barrier was no longer an integral part of the site containment)
- Increased liability to the host site was minimal (the barrier was large enough to allow the demonstration to be completed away from ongoing activities, the work could be performed in conjunction with other DOE work, and the remedial action at the site was completed)

Still, Southern California Edison Co. was hesitant to host the demonstration. The lack of an immediate benefit to the company at this particular site made them unwilling to pursue use of the site.

The regional EPA office overseeing the Naval Air Station (NAS) Brunswick, Maine site was interested in pursuing using NASB as a host site for the demonstration. The office provided the names of people within the Navy who were involved with the barrier. The initial contact was very promising. However, after formally approaching NASB, those issues mentioned above became prominent. It was felt that the benefits of hosting the demonstration did not outweigh the risks, particularly the risks of:

- Having one of the regulatory agencies overseeing the site require additional work at the site based on results of the demonstration
- Damage to the existing containment system

Responses and solutions to the concerns raised were drafted. Discussions between the two regulatory agencies present at the site (the Environmental Protection Agency (EPA) and the Maine Department of Environmental Protection (MEDEP)), the Navy, the DOE, and SEA continued. These discussions resulted in tentative approval for performing the demonstration. The discussions were formalized in a memorandum of understanding

(MOU) between all participating parties and the demonstration proceeded. Initial contact with the Navy was made in June 1998. The MOU was finally signed in January 1999, after 6 plus months of negotiations. Essentially the MOU states that the demonstration at the site is a test of the verification system, not the slurry wall. As such, NAS Brunswick would not be required to complete any action solely on the results of the demonstration. There is also a list of understandings included in the MOU. These understandings 1) define the number of wells that would be installed for the demonstration and require SEA to be responsible for the installation and closure of the wells, 2) define who/how the landfill cap will be repaired, and require SEA to be responsible for the repairs, 3) require SEA to follow all NAS Brunswick policies and procedures while performing the demonstration, 4) specify that the tracer gas to be used is considered a non-hazardous substance, 5) outlines the funding source for the demonstration, and 6) specifies that the Navy can review the report prior to it being distributed. The MOU is attached as appendix F.

5.2 Description of the Naval Air Station, Brunswick Demonstration Site

NAS Brunswick is located south of the Androscoggin River between Brunswick and Bath, Maine. The topography at the site is characterized by low, undulating hills with deeply incised brooks. The ground surface elevation ranges between mean sea level to over 110 ft. A 2,220-lineal-foot, nominally 3 foot thick soil-bentonite slurry wall has been emplaced at the site. The barrier forms a U around the buried waste. The slurry wall provides a subsurface barrier to prevent groundwater from flowing through subsurface contaminants contained within the landfill area (OHM Remediation Services Corp, 1996). All indications show that the barrier is successfully meeting this criterion. The barrier varies in depth from 50 to 80 feet, while the distance to the water table varies from approximately 5 to 20 feet. The water table is higher at the bottom of the U. The ground surface and the depth to the water table drop along the sides of the U. The SEAtrace™ system was tested at an area where the depth to the water table was the greatest, near the top of the U. Figure 32a is a reproduction of a topographic view of the site showing the approximate location of the demonstration. Figure 32b shows an elevation view of the demonstration area.

5.3 Design of the Demonstration

A detailed description of the experiment design can be found in appendix G, *Subsurface Barrier Validation with the SEAtrace™ System: Proposed Test Plan of the System at the NAS Brunswick Site*. As such, this section will only provide highlights of the experiment design.

The basic design for the SEAtrace™ system installation is driven by the size of the leak that must be detected given the various parameters that influence that value. The design includes:

- Determining the injection port placements and the overall injection scheme
- Determining the monitoring port locations and method of emplacement
- Determining a means to verify that the monitoring system is functioning properly

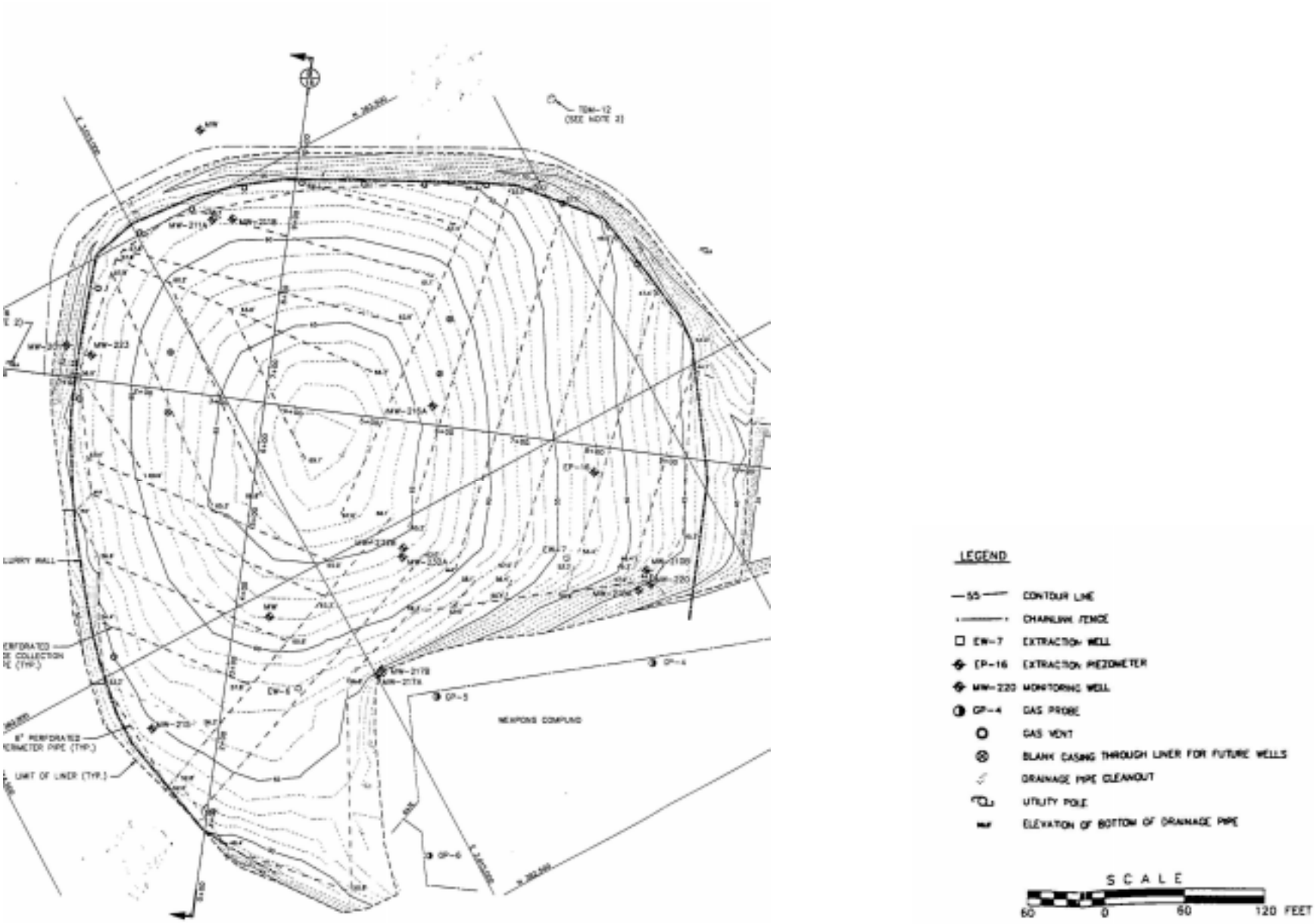

Figure 32A. Plan and elevation views of the NASB demonstration site.

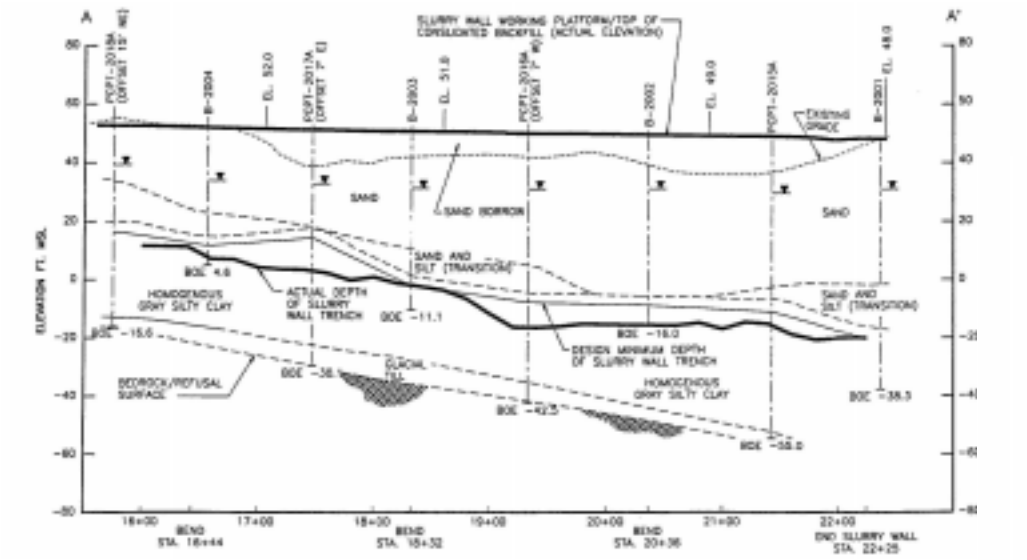

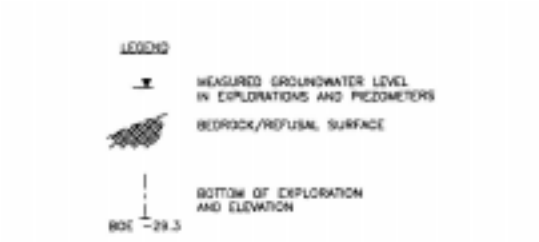

NOTES:

1. THE GENERALIZED CONDITIONS SHOWN REPRESENT INTERPRETATIONS OF CONDITIONS ENCOUNTERED IN WIDELY SPACED EXPLORATIONS. ACTUAL FIELD CONDITIONS MAY VARY FROM THOSE SHOWN.
2. THE MINIMUM SLURRY WALL WORKING PLATFORM GRADES HAVE BEEN DEVELOPED TO PERMIT SLURRY WALL CONSTRUCTION IN A SINGLE PASS. THE CONTRACTOR MAY INCREASE THE GRADE ABOVE THOSE SHOWN AT THE CONTRACTOR'S EXPENSE TO ACCOMMODATE THE CONTRACTOR'S SLURRY WALL CONSTRUCTION METHODS. HOWEVER, THE MINIMUM PLATFORM GRADES MUST BE MAINTAINED.
3. THE EXISTING ORGANIC ROOT MAT MUST BE STRIPPED AT THE "SLURRY WALL ALIGNMENT" (10'-0" WIDE) PRIOR TO CONSTRUCTION OF SLURRY WALL WORKING PLATFORM.
4. THE WORKING PLATFORM, LEADIN TRENCH, AND STATIONING HAS BEEN DEVELOPED FOR CONSTRUCTION OF THE SLURRY WALL IN A CLOCKWISE MANNER ALONG THE SLURRY WALL ALIGNMENT.
5. THE MINIMUM DEPTH OF SLURRY WALL INDICATED REPRESENTS THE ESTIMATED MINIMUM DEPTH OF TRENCH REQUIRED FOR A 3.0 FEET KEY INTO HOMOGENEOUS SILTY CLAY. THE FINAL DEPTH OF THE SLURRY WALL WILL BE DETERMINED BY EXAMINATION OF THE TRENCH CUTTINGS; HOWEVER, THE MINIMUM DEPTHS SHOWN MUST BE REACHED.

Figure 32b. Plan and elevation views of the NASB demonstration site.

5.3.1. Injection Port Spacing and Locations for the Demonstration

Injection ports were spaced inside the NAS Brunswick barrier to provide as constant a tracer source concentration along the portion of the wall used in the demonstration, using the fewest number of ports possible. Spacing from port to port, and from the port to the walls was guided by numeric modeling with T2VOC. Seven injection ports were needed. The ports were spaced 15 feet apart from one another and were installed to a depth of 11 feet below the top of the barrier wall (14 feet below ground surface). The ports were located 9 feet from the barrier wall. Figure 33 shows plan and elevation views of the design. Figures 33 and 34 schematically depict the area of influence of each injection port.

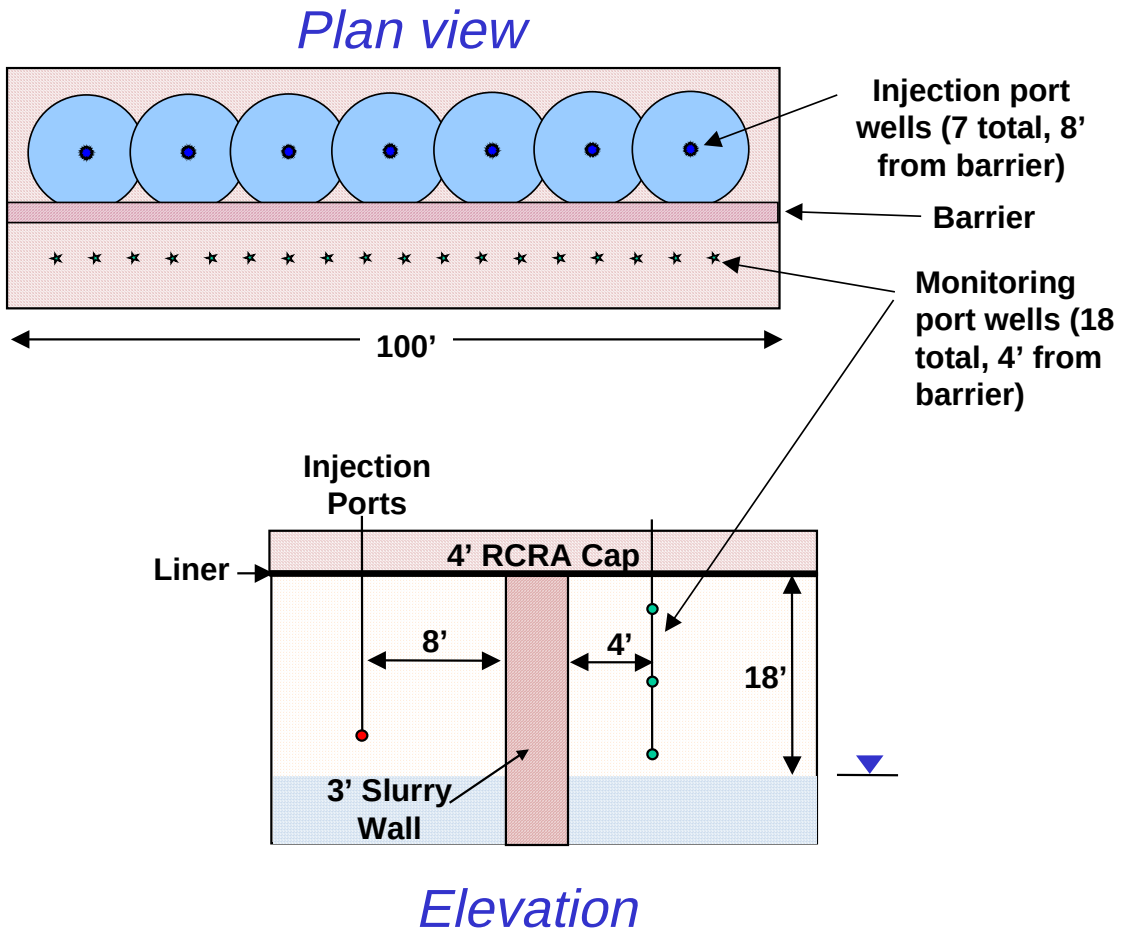

Figure 33. Plan and elevation views of the SEAtrace™ installation at the NASB demonstration site (not to scale).

The tracer gas injection scheme for the SEAtrace™ system is designed to create a uniform concentration of tracer along the barrier wall itself rather than within the volume of the enclosed soil. Injection occurs in slow, controlled staged steps. Initial injections at

one or more low concentrations allows detection of relatively large flaws, if they exist, without the possibility of flooding the medium with such high concentrations of the tracer that the maximum detection limit of the gas analyzer is exceeded. Subsequent testing at higher tracer concentrations allows the system to search for successively smaller leaks. While the typical starting concentration is 2,500 ppm, calculations showed that the overall distance between the injection and the monitoring ports for the this demonstration (15 feet) would preclude any but extremely large leaks to be seen within the allotted time. Additionally, hydraulic testing of the barrier has shown the areas of the barrier below the water table to be water tight, indicating that general construction of the barrier was sound Thus the starting concentration was increased to 20,000 ppm. After 10 days the source concentration was raised to the target demonstration concentration of 80,000 ppm.

5.3.2 Monitoring Port Spacing and Locations for the Demonstration

A maximum test period of 5 weeks was chosen for the demonstration. Given the dimensions of the section of barrier to be used in the demonstration and a general description of the geology at the site, calculations were performed to estimate what minimum size leak could be found by the system given several different test configurations, assuming a stepped injection sequence of the tracer. After reviewing the calculational results, a 6 ft. horizontal x 6 ft. vertical skewed grid of ports offset 4 ft. from the barrier was chosen (figure 34). Offsetting the ports 4 ft. from the barrier wall allowed a considerable safety zone to minimize any chance of inadvertently drilling through the barrier during port emplacement. The 6 ft. x 6 ft. grid allowed for a relatively small diameter leak (3/4 in.) to be found during the test period. The port spacing allowed for a roughly 100 foot section of the barrier to be tested. A total of 18 monitoring wells were installed, each with 3 ports (for a total of 54 ports).

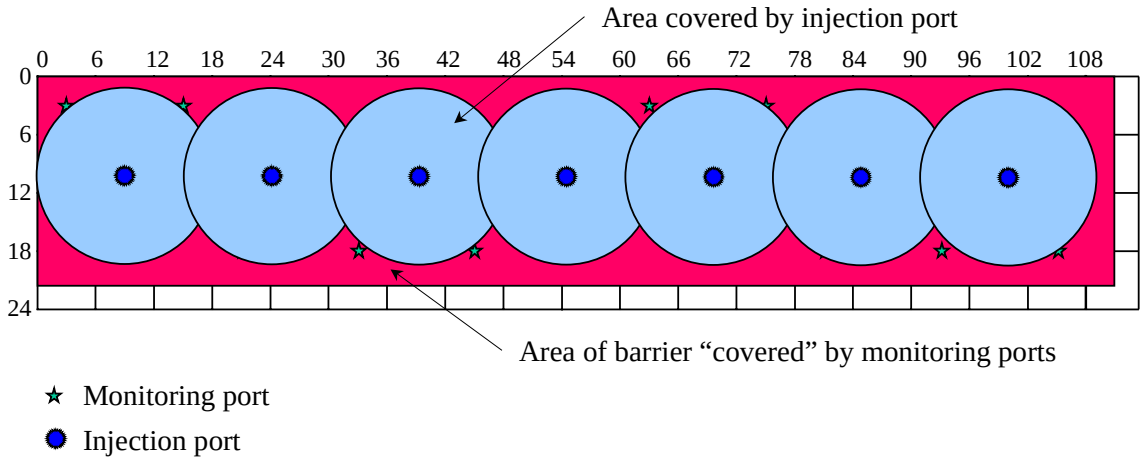

Figure 34. Schematic (elevation) of the proposed monitoring port/injection port layout for the NAS Brunswick demonstration. The monitoring ports are outside of the volume contained by the barrier. The injection ports are inside the barrier volume.

5.4 Execution of the Demonstration

A kick-off meeting was held January 6, 1999 at NASB. Plans for the demonstration were firmed up, and the necessary paperwork to obtain access to the site was initiated. The following week the section of the barrier to be used in the demonstration was staked using existing survey data. A subcontract was put in place to perform the well installation. Wells were installed between February 2 and February 4, 1999. To assure the wells were not impacting the barrier, samples were collected at a number of the wells at depths of 5, 10 and 15 feet below ground surface. While some work surface material was found at the shallowest depth, samples collected at 10 and 15 feet bgs were native soil. Wells were ported and backfilled immediately after they were drilled. Once all the ports were installed, tubing was run through pipe insulation inside schedule 40 pvc pipe. A strip of heat tape was included between the insulation and the pvc pipe in case water vapor pulled through the lines while sampling condensed and froze. Tubes were connected to the scanning system, and background data collection was begun. Installation of the SEAtrace™ system was completed in one week.

Analysis of the background data showed some problems. The vacuum integrity checks of the manifold showed there was a significant leak in the sampling system. Calibration gas checks showed the sample was being diluted prior to analysis. Scans were being prematurely aborted. Water was being pulled into the manifold. Working conditions at the site were not ideal. Freezing rains and low temperatures made it difficult to troubleshoot. The instrument enclosure was opened while work was performed, keeping the temperature within the cell from increasing enough to be within the operating range for the gas analyzer. The rubber seats in the solenoid valves wouldn't seal properly. Samples could not be drawn through numerous ports. The decision was made to suspend the test until the hardware / software issues could be resolved. Instrumentation was removed from the instrument enclosure and brought back to the SEA office. The manifold was replaced, all solenoid valves were removed and cleaned, and water stops were added on the inlet for each sample line. The stops allow air to flow unrestricted, but close the line if water is drawn into the system. Addition of the water stops necessitated additional hardware and software changes. Components had to be re-arranged/re-plumbed to physically create enough room for the water stops. These changes, along with the volumetric increase in the sample lines, required purge times and other code timing to be changed. Additionally, the code was changed so that it would recover more controllably if problems were encountered, minimizing aborted scans. The modified system was thoroughly tested. It was re-installed at the site April 5-6, 1999. Manual flow checks were performed on each of the monitoring lines. A total of twelve ports were unusable, either drawing water or plugged. These tubes were disconnected. Background data was collected April 6 through April 9, 1999. During this time, the engineered leak test was also conducted. Tracer was injected at the barrier on April 9, 1999. Twenty-six oz. (estimated source concentration of 20,000 ppm) was injected in 6 of the 7 injection ports. The seventh injection port was plugged so no tracer could be injected at that location. Data was collected between April 9 and April 20, 1999. During this time, no breaches through the barrier were detected. However, there was a gap between the top of the slurry wall and the impermeable liner in the barrier cap. Tracer was able to travel through this gap and "spill" over the barrier. On April 21, 1999 the

source concentration was boosted to the target concentration of 80,000 ppm. Seventy-eight oz. of tracer was injected in each of the 6 functioning injection ports. Figure 35 is a photograph of the system installed at the site. The engineered leak is shown in the foreground. The scanning system is seen behind and to the right of the engineered leak. The PVC pipe extending from the left side of the photo to beyond the scanning system was the manifold created to protect the sample tubing. It parallels the section of barrier wall that was tested.

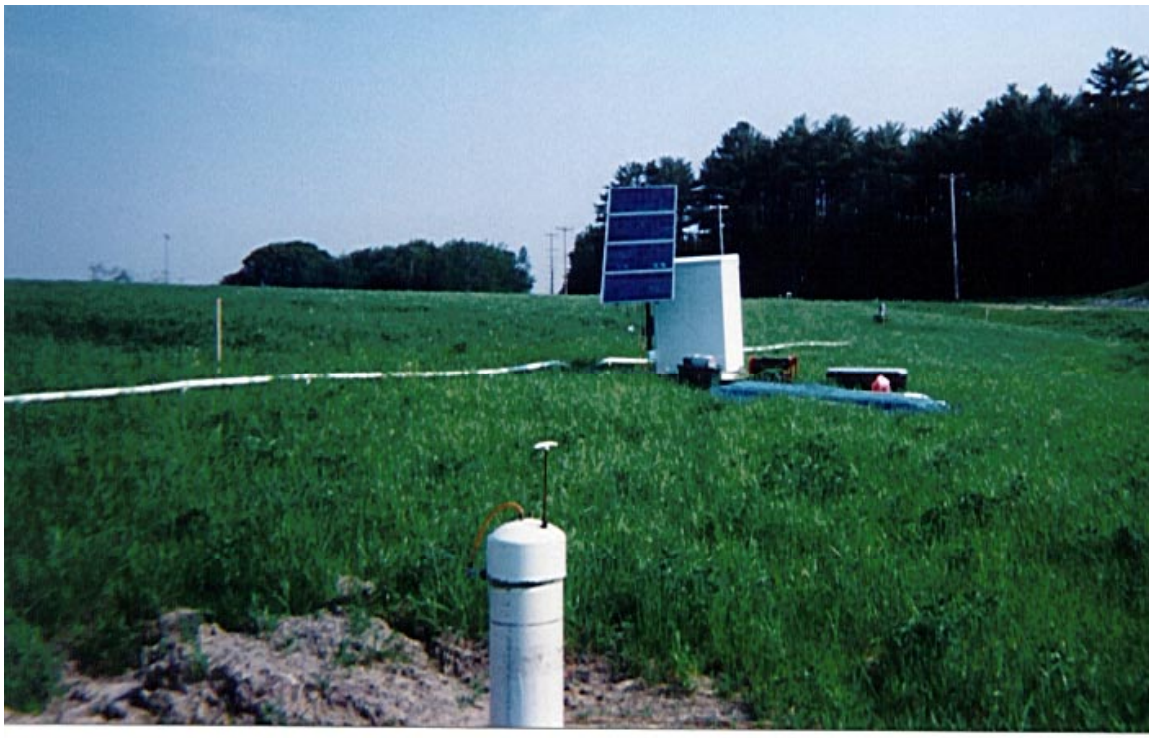

Figure 35. Photograph of the NASB SEAtrace™ demonstration. The scanning system, PVC manifold that protected the sample tubing, and the engineered leak are shown.

Abandonment work at the site was completed between June 1 and June 3, 1999. The engineered leak was removed, as was the scanning system and tubing manifold. Monitoring tubes were cut several inches below the ground surface and capped. Holes through the cap made when installing the injection wells were repaired. Overburden around each of the wells was removed to the geomembrane layer. A professional repair company repaired and tested the geomembrane per the original specifications of the cap Each of the repairs were vacuum tested. Layers above the geomembrane were reconstructed, and new material was brought in for the fine sand layer. Areas of the vegetative layer that were disturbed during the demonstration were repaired and re-seeded.

5.5 Results of the Demonstration

Measured concentration histories of the tracer gas recorded at the monitoring ports are shown in figures 36 and 37. As mentioned above, tracer was able to spill over the barrier because of the gap between the top of the slurry wall and the bottom of the cap. This effects the demonstration in two ways. First, the gap allows a large amount of tracer to diffuse away from the source, causing the source concentration to deplete. This was not considered to be of great concern, as the injection scheme was designed to create a constant source concentration just at the barrier wall, not throughout a contained volume. The second effect was more relevant. Tracer diffusing into the medium from the gap could mask a breach through the barrier. Because the barrier is thick (a minimum of 3 feet) the amount of tracer that is available to diffuse to the monitoring ports (3-d spherical diffusion) is limited by the mass of gas that can diffuse through the breach (planar diffusion) – see section 3.2.2, Forward Models. Because of this, the concentrations expected to be seen at the monitoring ports due to a breach are low (< 100 ppm, see calculations in appendix G). Modeling predicted, and the measured data at the site showed, that the tracer concentrations at the site due to the gap at the top of the barrier could be in the hundreds of ppm, making it more difficult (although not impossible) to detect a breach through the barrier. Careful review of the data showed no anomalies in the measured concentration histories from what was expected. There were no breaches detected during the demonstration period. Figure 38 shows concentration plots of the tracer at several times during the test. Note that while it appears the gap between the top of the slurry wall and the bottom of the cap is most pronounced near the center of the tested section, this is an artifact of failed ports. First, the injection port that would be furthest left on the contour plot was plugged, and tracer was not injected. Tracer seen at later times in that area of the barrier had to travel further and hence was at a lower concentration. Second, several of the surface ports in that area of the barrier were not used. Twelve ports were found to be plugged or pulled water samples prior to beginning the test (Ports 3, 5, 14, 16, 21, 23, 29, 33, 37, 38, 40 and 45). Tubing from these ports was disconnected from the scanning system (e.g. ports sampled atmospheric air). Four other ports (10, 12, 28, and 34) became blocked during the test. Table 8 lists information about these ports. Figure 39 shows the time required to fill the sample bag for the ports, a clear indicator of how ports were behaving.

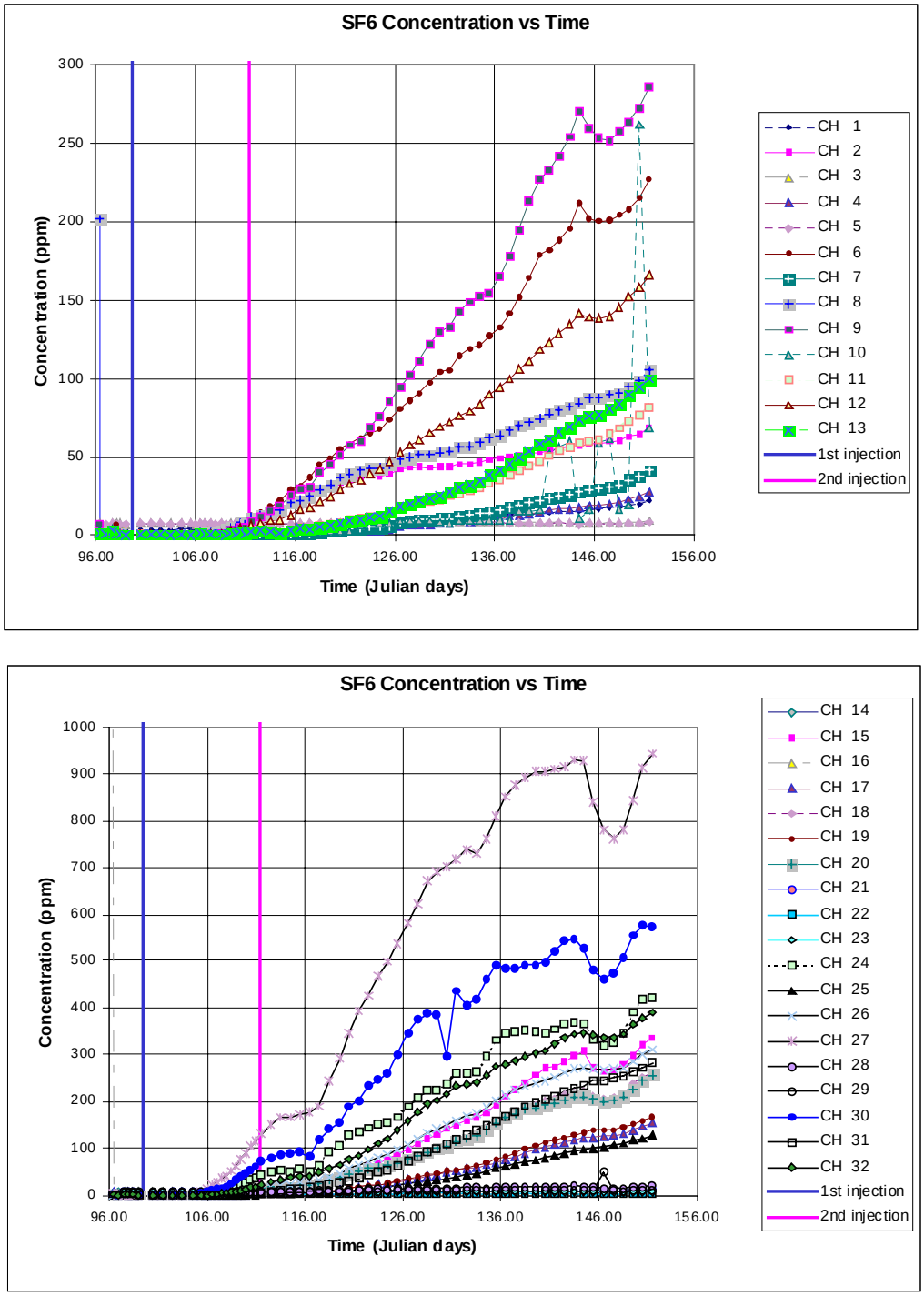

Figure 36. Measured concentration histories of the tracer gas for monitoring ports at the NASB SEAtrace™ demonstration site. Ports 1, 4, 7 etc. are the deepest ports. Ports 2, 5, 8 etc. are center ports. Ports 3, 6, 9 etc. are the ports nearest the surface. See table 8 for a list of damaged ports.

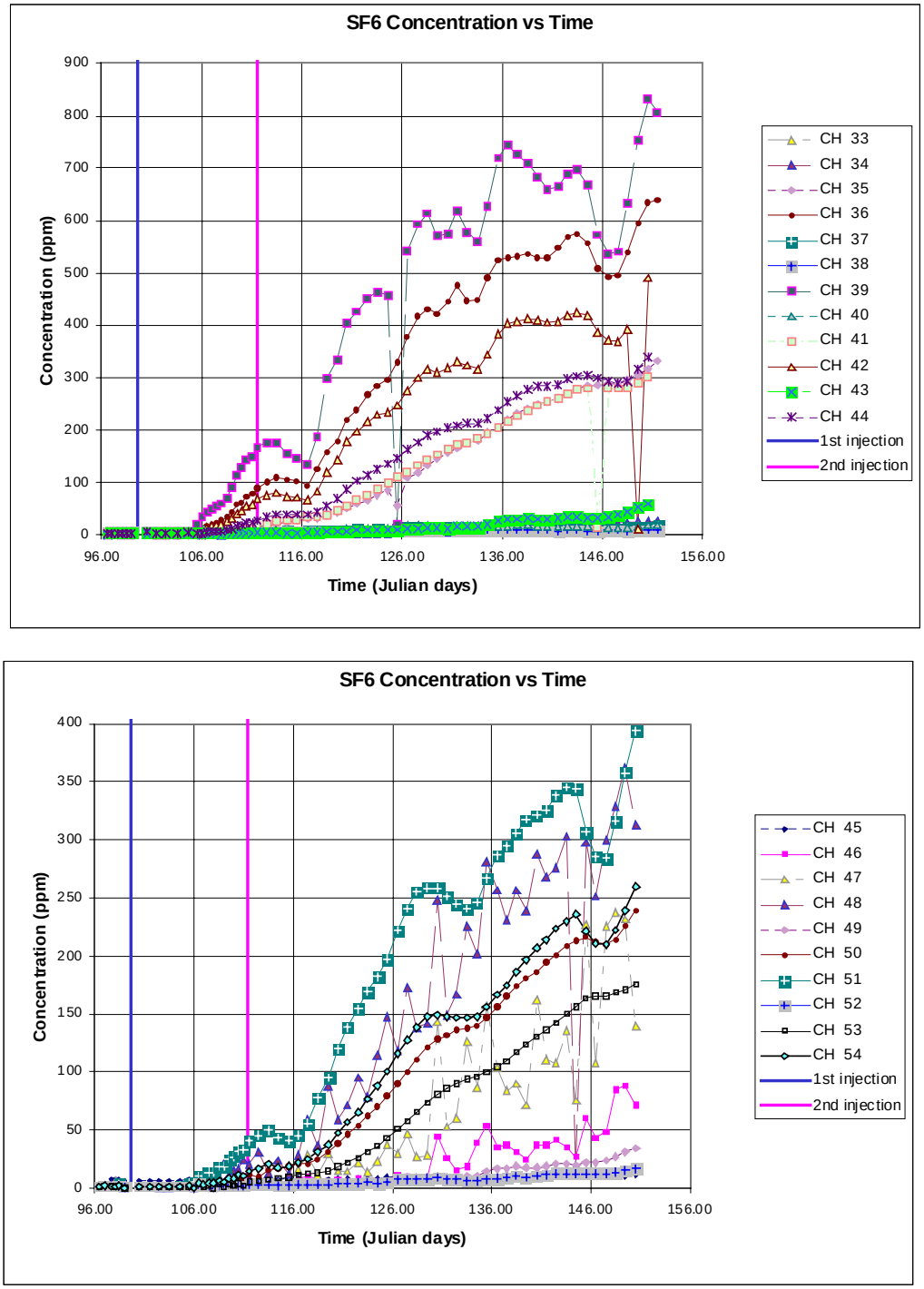

Figure 37. Measured concentration histories of the tracer gas for monitoring ports at the NASB SEAtrace™ demonstration site. Ports 1, 4, 7 etc. are the deepest ports. Ports 2, 5, 8 etc. are center ports. Ports 3, 6, 9 etc. are the ports nearest the surface. See table 8 for a list of damaged ports.

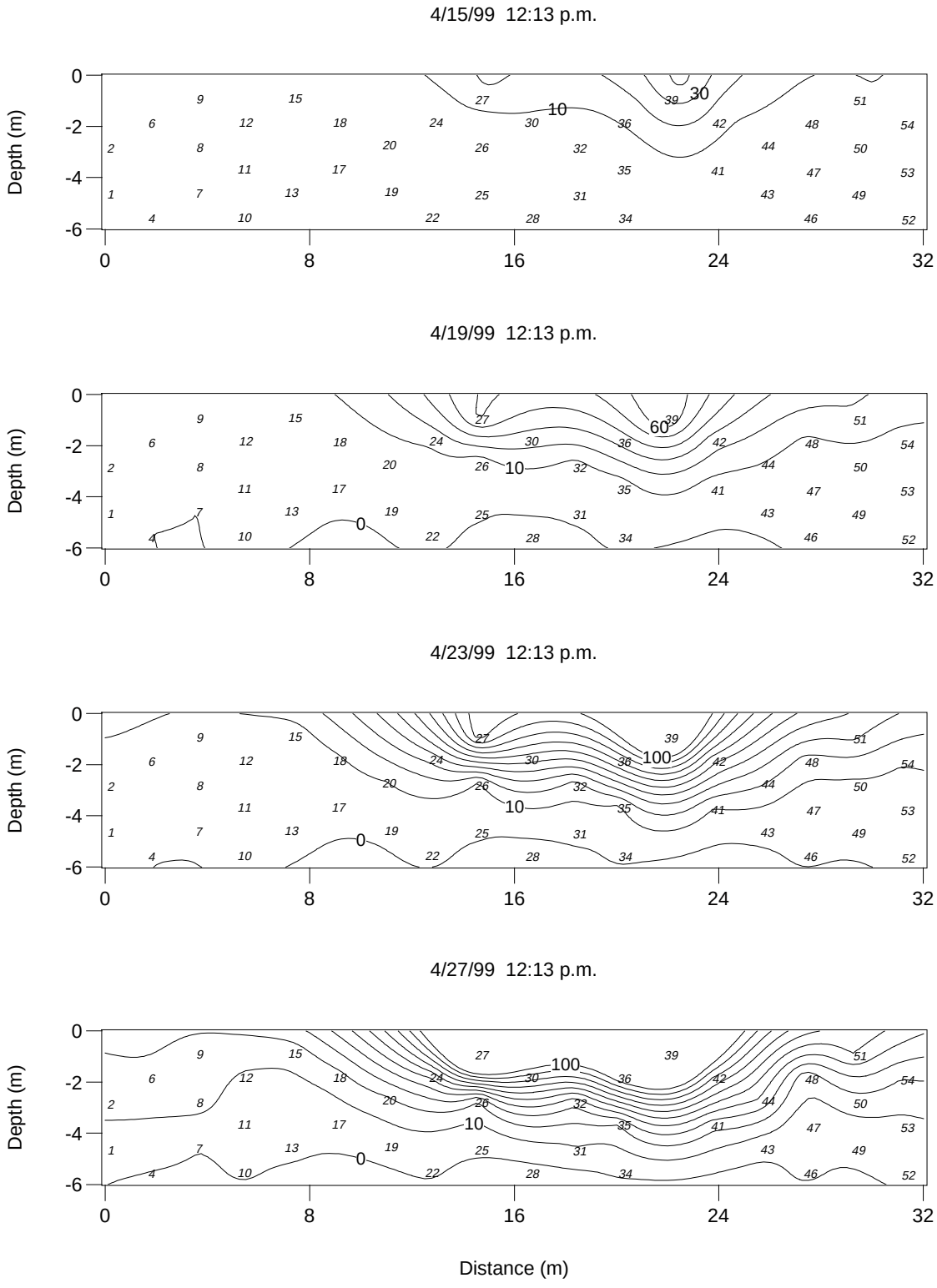

Figure 38. Contour plots of data taken at several time steps during the SEAtrace™ demonstration at the NASB. See table 8 for a list of damaged ports. Port locations are identified with numeric designators.

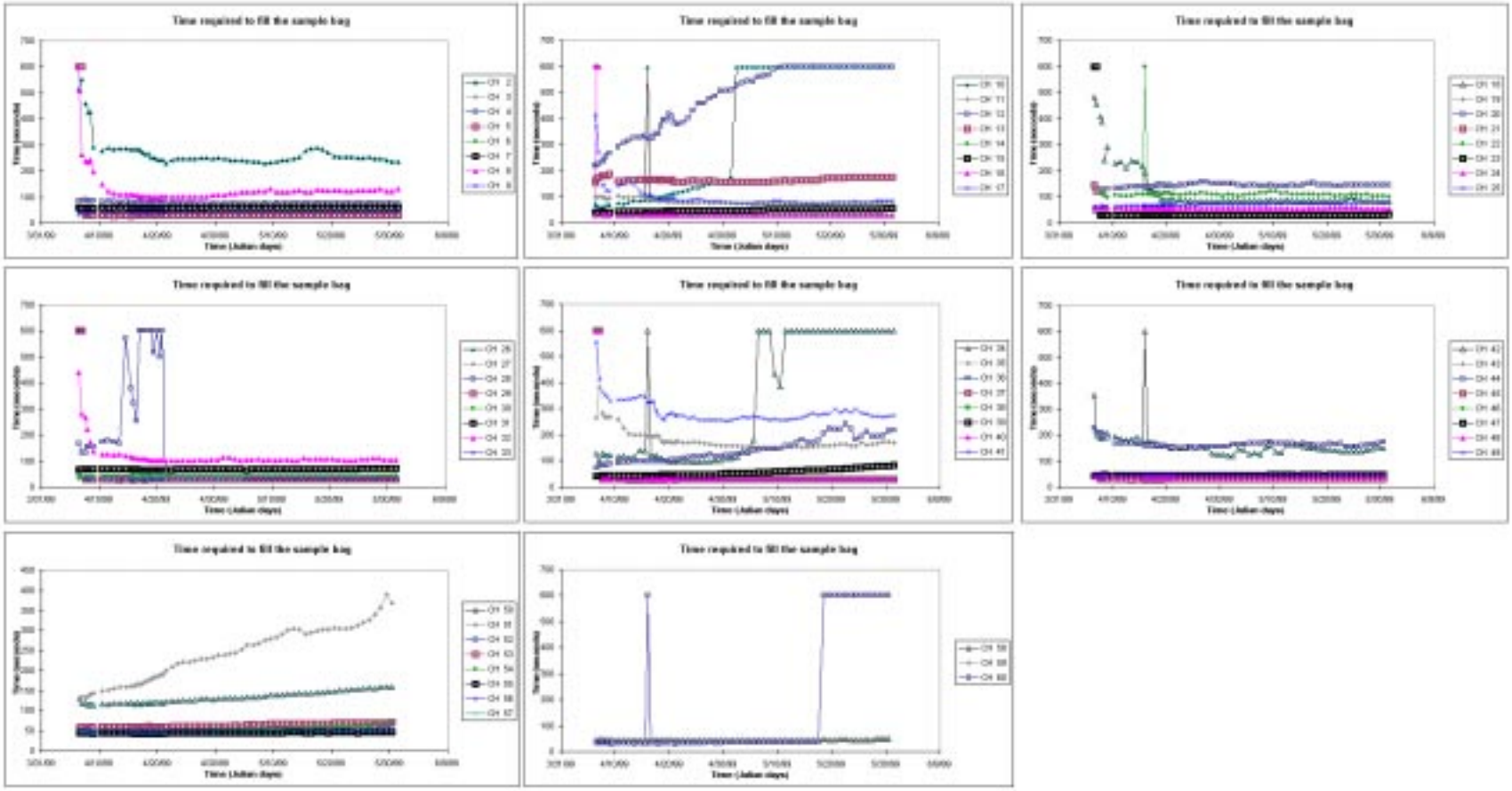

Figure 39. Time (seconds) required to fill the monitoring ports at the NASB SEAtrace™ demonstration site. Ports 1, 4, 7 etc. are the deepest ports. Ports 2, 5, 8 etc. are center ports. Ports 3, 6, 9 etc. are the ports nearest the surface. Ports 55 – 59 are near the engineered leak. Port 60 measured a calibration gas. Data clearly shows several ports failing (reduced flow capacity with time). See table 8 for a list of damaged ports.

Table 8. Failed monitoring ports at the NASB demonstration. Ports that were disconnected (e.g., tubing was disconnected from the scanning system) drew in atmospheric samples.

PORT NO.	DATE PLUGGED	DATE DISCONNECTED	RELATIVE DEPTH
3		4/6/99	SURFACE
5		4/6/99	CENTER
10		5/2/99	BOTTOM
12		5/10/99	SURFACE
14		4/6/99	CENTER
16		4/6/99	BOTTOM
21		4/6/99	SURFACE
23		4/6/99	CENTER
28	4/14/99	4/21/99	BOTTOM
29		4/6/99	CENTER
33		4/6/99	SURFACE
34	5/6/99		BOTTOM
37		4/6/99	BOTTOM
38		4/6/99	CENTER
40		4/6/99	BOTTOM
45		4/6/99	SURFACE

In addition to measuring the tracer gas, carbon dioxide and water vapor histories were recorded. These are shown in figures 40 through 43. Carbon dioxide concentrations were very high, between 70,000 and 130,000 ppm. Because the barrier cap extended well beyond the slurry wall, CO_2 generated in the soil cannot diffuse to the atmosphere. The gas was measured as a check for the scanning system – if the values remain consistent with time it is an indication that the gas analyzer is functioning properly and that there are no leaks in the scanning system plumbing. Additionally, it is an indication of the integrity of the tubing. After ports are installed, damage to the tubing will typically occur in the portion of tubing that is above ground, e.g., rodent or ultraviolet light damage. The amount of CO_2 in the atmosphere is low (600 – 800 ppm at the site). If a tube became damaged, the measured concentration of CO_2 at the port would drop significantly and remain low. This was not seen during the test in ports that were used throughout the entire test. Note, several ports were disconnected during the test (table 8) and allowed to draw atmospheric samples.

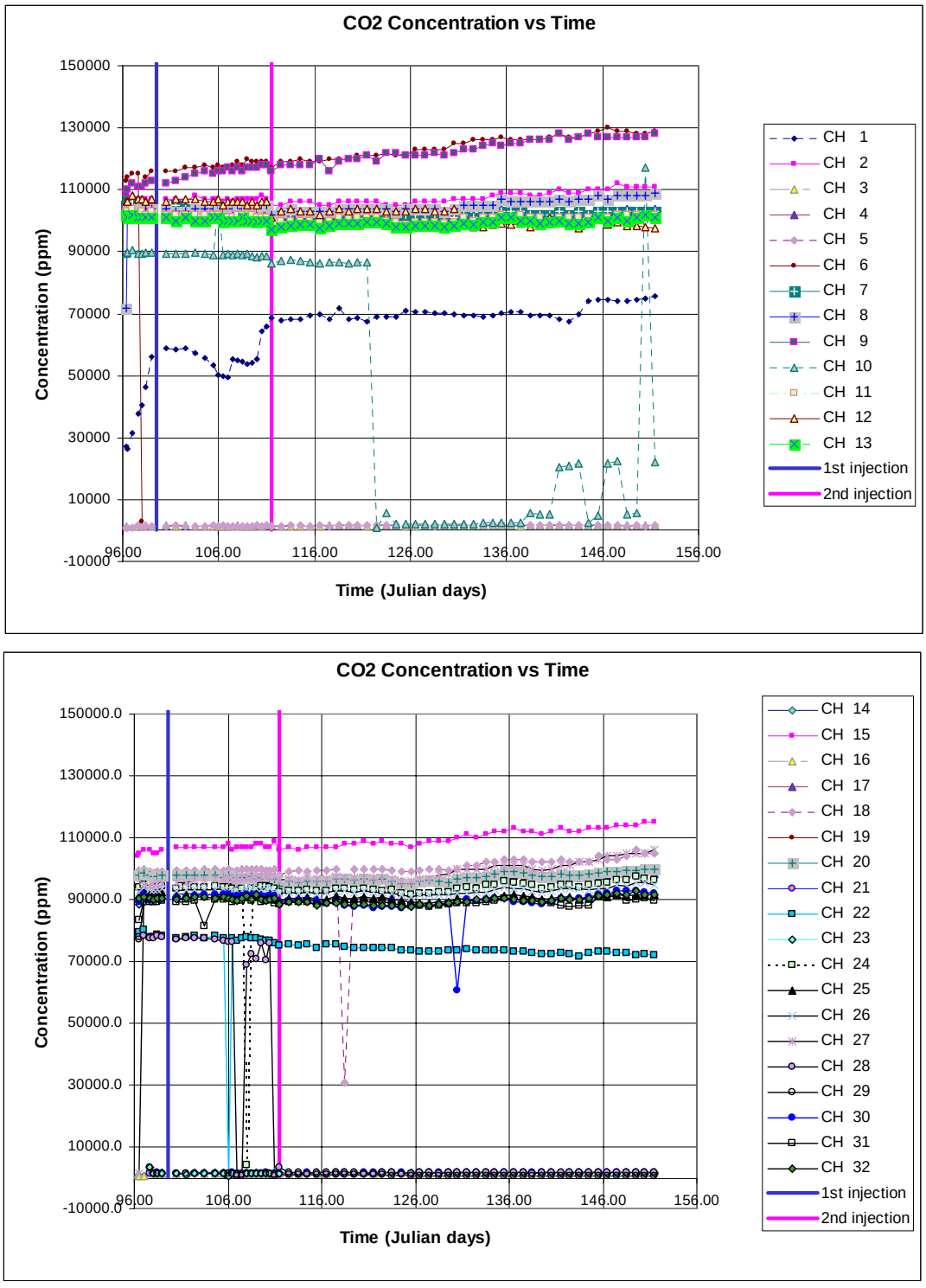

Figure 40. Measured concentration histories of carbon dioxide for monitoring ports at the NASB SEAtrace™ demonstration site. Ports 1, 4, 7 etc., are the deepest ports. Ports 2, 5, 8 etc., are center ports. Ports 3, 6, 9 etc., are the ports nearest the surface. See table 8 for a list of damaged ports.

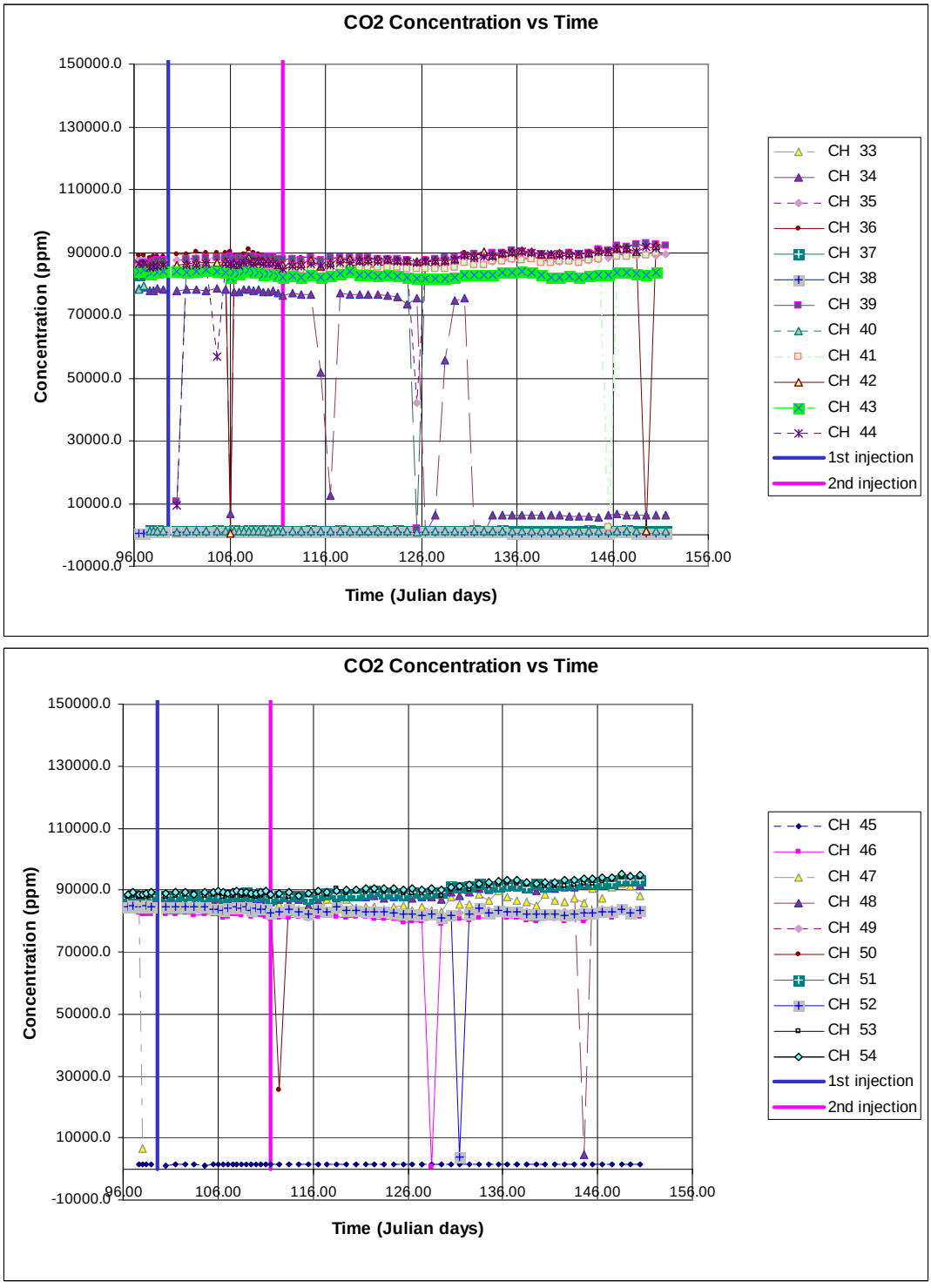

Figure 41. Measured concentration histories of carbon dioxide for monitoring ports at the NASB SEAtrace™ demonstration site. Ports 1, 4, 7 etc., are the deepest ports. Ports 2, 5, 8 etc., are center ports. Ports 3, 6, 9 etc., are the ports nearest the surface. See table 8 for a list of damaged ports.

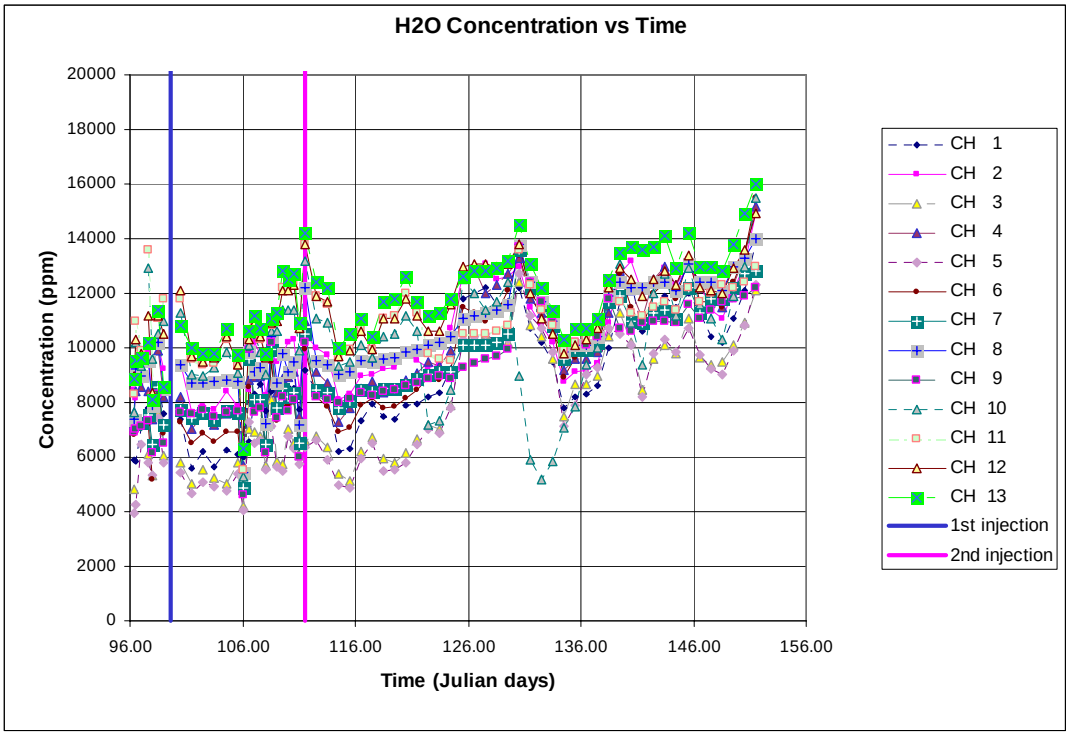

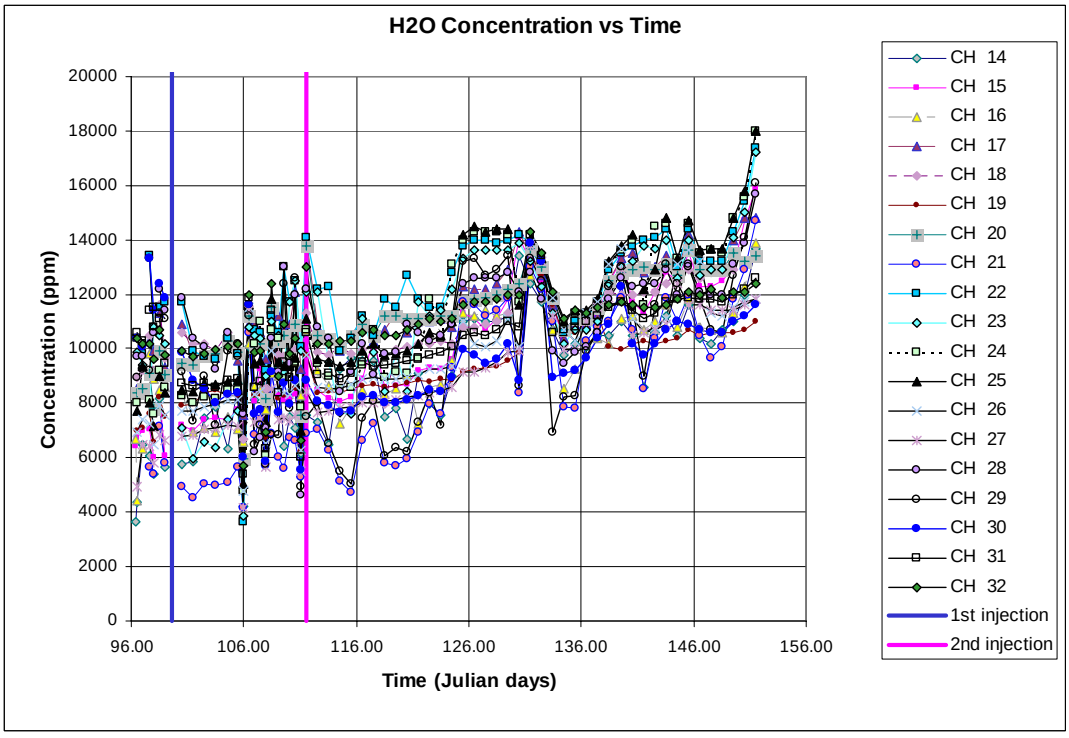

Figure 42. Measured concentration histories of soil gas water vapor for monitoring ports at the NASB SEAtrace™ demonstration site. Ports 1, 4, 7 etc., are the deepest ports. Ports 2, 5, 8 etc., are center ports. Ports 3, 6, 9 etc., are the ports nearest the surface. See table 8 for a list of damaged ports.

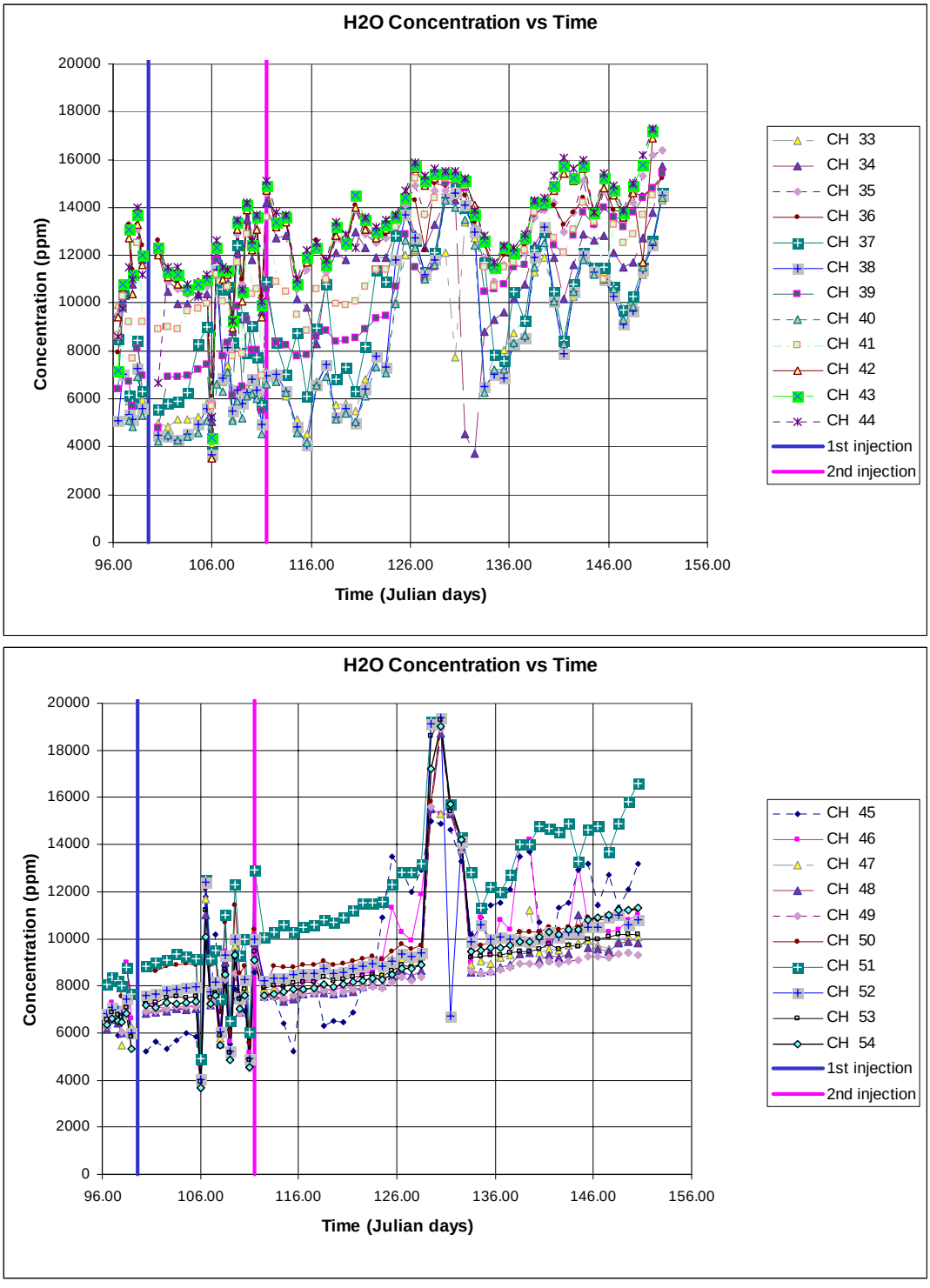

Figure 43. Measured concentration histories of soil gas water vapor for monitoring ports at the NASB SEAtrace™ demonstration site. Ports 1, 4, 7 etc., are the deepest ports. Ports 2, 5, 8 etc., are center ports. Ports 3, 6, 9 etc., are the ports nearest the surface. See table 8 for a list of damaged ports.

Water vapor is measured so that other gases measured can be compensated for interference. While it doesn't have to be recorded for this purpose, it also serves as an indicator for when lines may be starting to pull up water rather than gas samples.

A calibration gas was measured throughout most of the demonstration. The cal gas is an indicator of how the scanning system is operating. It can detect leaks in the internal plumbing of the system (by indicating a sample dilution from the known concentration) or failure of the gas analyzer (by indicating erratic or inconsistent concentrations). Calibration gas is added to a large tedlar sample bag that is connected to one of the ports on the scanning system. The bag must be refilled every 5 to 7 days. Figure 44 shows the recorded concentration histories of the cal gas as well as the pre and post scan atmospheric samples. No indication of problems was seen in the data. Recorded concentrations were consistent over time, measuring 1560 +/- 60 ppm. The exception was a six day period between Julian day 100 and Julian day 105 when the recorded concentrations were higher, averaging 6260 +/- 90 ppm. During this time it was determined that the sample bag had been filled without first thoroughly flushing the regulator. Tracer gas remaining in the regulator after an injection caused the higher concentration. The sample bag was not refilled after Julian day 131, and the bag was empty by Julian day 138.

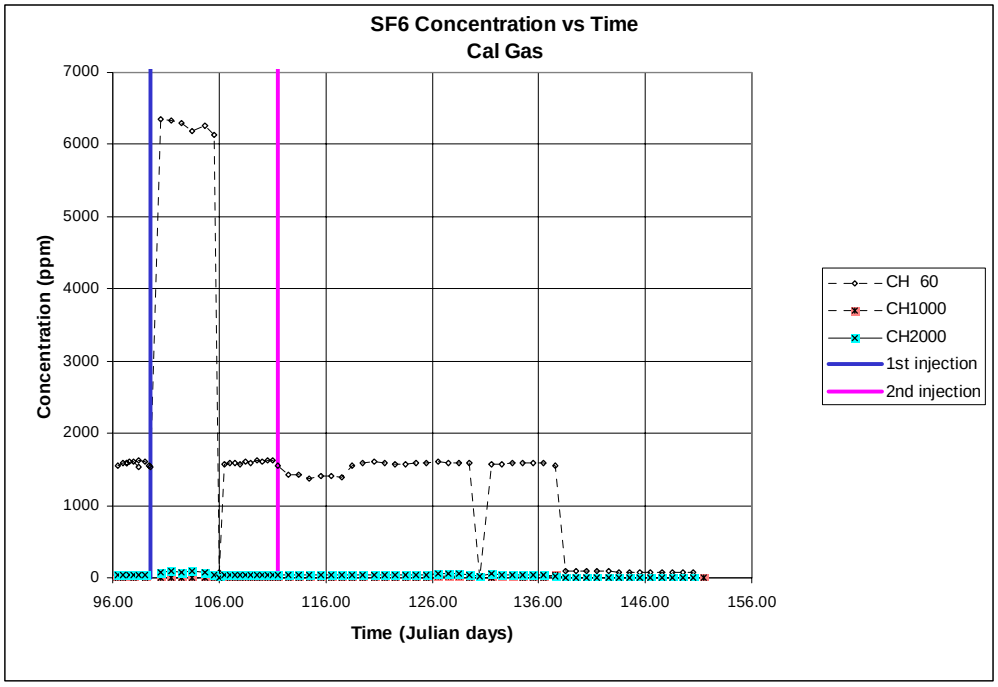

Figure 44. Measured concentration histories of the tracer gas for pre and post scan atmospheric samples (channels 1000 and 2000, respectively) and the calibration gas (CH 60).

An engineered leak was installed and tested during the course of the demonstration. The engineered leak was located approximately 50 feet from the slurry wall. A large pipe (8-in. diameter) was buried so that a valve at the bottom of the pipe was 6 feet below ground surface (figure 45). The pipe acted as the source volume for the tracer gas. The

1.5-inch diameter gate valve formed the leak. Pure tracer gas was injected into the pipe volume via a small diameter tubing that ran from the surface to the center of the container. The valve was closed while tracer was injected into the container so that gas was not advectively forced into the medium. Prior to opening the valve, a bleed line was opened to allow the pressure in the container to equilibrate with atmospheric pressure. Figure 45a shows a schematic of the leak anomaly configuration used for this demonstration. Five monitoring ports in three wells were installed in a plane perpendicular to the engineered leak volume. The horizontal and vertical grid spacing for the ports was the same as those used in the main demonstration. The monitoring ports were installed before the engineered leak volume. While the volume was being installed, it was discovered that the geomembrane of the cap extended well beyond the slurry wall, to the test area. The membrane was roughly 3 feet below ground surface in this area. Data was collected at the ports near the engineered leak throughout the entire demonstration period. Figure 45b shows the measured concentration histories of the ports. In reviewing the concentration histories, it was apparent that the two upper most monitoring ports were located above the geomembrane so were isolated from the source tracer. Measured concentrations of these ports were almost an order of magnitude lower than the other ports at approximately the same distances from the leak. These ports were removed from the input files for data analysis. The system was able to locate the leak within 3.3 feet (1 m) of its true position. Figure 45c shows the true and calculated positions of the leak.

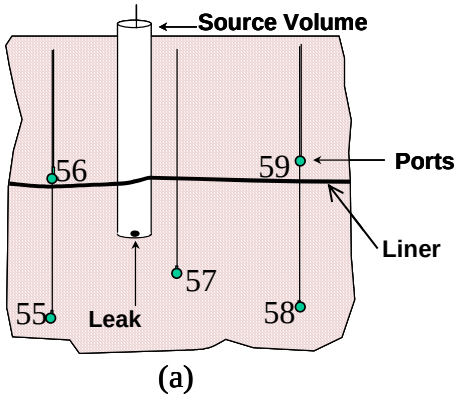

(a)

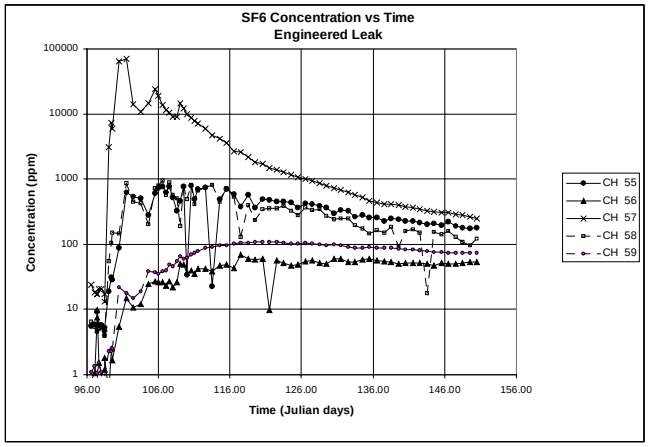

(b)

Engineered Leak	x (m)	y (m)	z (m)
Calculated position	-0.13	-0.96	-1.70
True Position	0.00	0.00	-1.83

(c)

Distance from true leak = .97 m

Figure 45. (a) Schematic of the leak anomaly (b) measured tracer concentrations. (c) table showing the true and the calculated leak locations.

5.6 Conclusion of the Demonstration

Installation of the SEAtrace™ system at the site went very smoothly, requiring only one week. Scanning system hardware / software problems discovered during background checks were problematic, and caused a delay in the start of the test. Problems were primarily caused by the weather conditions and uptake of water through a number of the sampling lines. Once these issues were resolved, the test proceeded with no difficulties. Tracer gas injection and subsequent diffusion of the gas over the top of the barrier wall closely followed model predictions. The scanning system was able to complete one scan per day. The inversion code ran successfully after each scan. Results of the demonstration clearly indicated the gap between the top of the barrier wall and the bottom of the cap. No breaches through the barrier were detected.

6. APPLICABILITY, ISSUES, AND COST ANALYSIS

The SEAtrace™ methodology, and gaseous tracer testing in general, is applicable to the verification of barrier structures emplaced above the water table. It is particularly well suited to emplacements at sites where the entire barrier is located in the unsaturated zone and it is not safe or practical to test the barrier's integrity hydraulically. The technique can assess the integrity of any impermeable barrier type. Sampling array emplacements can be accomplished by either conventional drilling or direct push techniques. Vapor sampling lines can potentially be several hundred feet deep in the soil (SEA has successfully operated its sampling systems with 300 to 400 feet of sample lines). It is unlikely that a barrier can be emplaced deeper than the SEAtrace™ system can monitor.

SEAtrace™ is capable of locating flaws with typical positional accuracy of 1.6 feet (0.5 m). If the purpose of SEAtrace™ testing is to assist remediation of barrier flaws, this positional accuracy is sufficient to guide regrouting techniques to patch the holes in the barrier. The system can detect breaches in a barrier rapidly enough (days to weeks) so that results could be available prior to demobilization of emplacement rigs, yielding significant cost savings over needing to remobilize equipment.

The system has been successfully demonstrated at a number of different sites, in some cases under severe conditions. The system can support the STCG needs for which it was developed, in particular:

- SR-3009: Develop in-situ barrier technologies for immobilization, containment, and treatment of VOCs, metals, and/or radionuclides in unconsolidated subsurface sediments; i.e., sandy/clayey soils.
- SR-3014: Performance monitoring systems for in-situ stabilization and barrier technologies using non-intrusive technologies to monitor subsurface contamination and fate and transport of remedial activities.
- RL-WT031: Surface barriers are being used over many Hanford environmental restoration and waste management sites to reduce moisture infiltration and plant and animal intrusion. Because the design life of the barrier is 1,000 years, there is a need for data on degradation to better understand the validity of the design life estimate.
- OR-BW-08: Improvements in predictive capabilities for evaluation of long-term performance of stabilization and containment technologies; advances in grouting/barrier technology, understanding of grout/barrier wastes/media interactions, and long-term barrier performance (e.g., stability and longevity); improvements in modeling capabilities to match improvements in predictive capabilities.

There are presently two fully operational SEAtrace™ scanning systems owned by the DOE. However, there is presently no DOE or commercial application for the system anticipated in the near future.

Historically, barriers have been used in environmental applications to control subsurface water migration in and around contaminants, providing a fast (compared to remediation) way to reduce both the amount of ground water being contaminated and the amount of contaminants moving off-site. Validation of these barriers has been driven by their intended purpose, so has been limited to verifying subsurface portions of the barrier below the water table. Traditional methods of testing slurry walls (materials QA, drawdown, and saturated hydraulic conductivity) are typically used. These methods are inexpensive, simple, and unambiguous. If breaches are determined to exist, sites typically will develop a positive hydraulic gradient across the barrier by pumping water out of the barrier interior, assuring that contaminant movement out of the barrier is minimized. Flawed wall sections are re-emplaced. Thus for a typical site where barriers are used only to mitigated water movement, there is no need for a vadose zone monitoring system. Existing barriers are not good candidates for the SEAtrace™ system.

Barriers are currently being considered for applications other than water control, such as beneath the Hanford tanks during their remediation (to prevent transport of accidentally released contaminants to the water table). However, they are not yet being installed. Because of the history of barrier use, there are currently no regulatory drivers that exist to require verification of sections of barriers in the vadose zone. The recently developed innovative methods required for this verification are expensive compared to what installers and end users anticipate. There is resistance to using them because of this perception, and the lack of clear regulatory drivers.

The cost of SEAtrace™ verification activities at barrier sites of various magnitudes (characterized by the square footage of barrier wall tested) have been estimated based on SEA experience to date. Several different cases are presented in table 9. The costs presented include the total cost of installation, operation, and data analysis/reporting. Note that the unit cost, indicated as dollars per square foot of barrier wall area, is highly dependent on a number of variables. An incomplete list includes:

- Size of the barrier
- Depth of the barrier
- Medium in which the barrier is emplaced
- Geographic location of the barrier
- Minimum size of the breach that must be detected
- Thickness of the barrier
- If the barrier is capped or covered

The overall square footage to be tested, the depth of the barrier, and the medium in which the barrier is emplaced are the most significant of these. As expected, the larger the barrier the less expensive the monitoring unit cost, and the deeper the barrier or the more difficult the medium is to drill the more expensive the monitoring (due to the drilling costs associated with installing the monitoring and injection ports). Examples of associated costs for three different sizes of barriers (small @ approximately 2500 sq. ft., medium @ approximately 25,000 sq. ft., and large @ approximately 250,000 sq. ft.), and three different depths of barriers (25-30 ft., 50 ft., and 100 ft.) are provided in table 9.

Table 9. Estimated costs of subsurface barrier verification using the SEAtrace™ system.

	Cost as a function of barrier depth			Cost as a function of barrier size			Cost as a function of barrier thickness		
	Medium Sized Barrier of different depths			Large, Medium and Small Barrier costs			Medium Sized Barrier of different		
Scale of Barriers	Case 1	Case 2	Case 3	Case 1	Case 2	Case 3	Case 1	Case 2	Case 3
depth (m)	8.2	14.3	29.6	8.2	8.2	7.6	8.2	8.2	8.2
(ft)	27	47	97	27	27	25	27	27	27
length (m)	262.1	152.4	76.2	2621.3	262.1	32.9	262.1	262.1	262.1
(ft)	860	500	250	8600	860	108	860	860	860
area (sq. m.)	2157	2183	2253	21572	2157	251	2157	2157	2157
(sq. ft.)	23220	23500	24250	232200	23220	2700	23220	23220	23220
thickness of barrier (ft)	3	3	3	3	3	3	1	2	3
Vapor point									
installation method	geoprobe	auger rig	bigger auger rig	geoprobe	geoprobe	geoprobe	geoprobe	geoprobe	geoprobe
Installation cost									
equipment	$14,900.00	$50,900.00	$145,000.00	$146,900.00	$14,900.00	$2,900.00	$14,900.00	$14,900.00	$14,900.0
expendables (backfill mix, tubing,	$26,280.00	$30,135.00	$39,000.00	$267,180.00	$26,280.00	$4,305.00	$26,280.00	$26,280.00	$26,280.0
labor (installation, oversite,	$37,758.00	$67,342.50	$103,941.00	$329,233.50	$37,758.00	$11,344.50	$37,758.00	$37,758.00	$37,758.0
SUBTOTAL	$78,938.00	$148,377.50	$287,941.00	$743,313.50	$78,938.00	$18,549.50	$78,938.00	$78,938.00	$78,938.0
Monitoring system									
rental ($2000/mo)	$20,000.00	$23,000.00	$26,000.00	$185,000.00	$20,000.00	$5,000.00	$8,000.00	$14,000.00	$20,000.0
mobilization	$6,000.00	$6,000.00	$6,000.00	$6,000.00	$6,000.00	$6,000.00	$6,000.00	$6,000.00	$6,000.00
set-up	$62,475.00	$70,020.00	$77,565.00	$477,450.00	$62,475.00	$24,750.00	$62,475.00	$62,475.00	$62,475.0
SUBTOTAL	$88,475.00	$99,020.00	$109,565.00	$668,450.00	$88,475.00	$35,750.00	$76,475.00	$82,475.00	$88,475.0
Test									
Tracer gas	$12,000.00	$14,000.00	$16,000.00	$122,000.00	$12,000.00	$2,000.00	$12,000.00	$12,000.00	$12,000.0
Lab	$43,080.00	$48,810.00	$54,540.00	$358,230.00	$43,080.00	$14,430.00	$43,080.00	$43,080.00	$43,080.0
SUBTOTAL	$55,080.00	$62,810.00	$70,540.00	$480,230.00	$55,080.00	$16,430.00	$55,080.00	$55,080.00	$55,080.0
Technical support, data analysis, report	$62,400.00	$69,925.00	$77,450.00	$476,275.00	$62,400.00	$24,775.00	$62,400.00	$62,400.00	$62,400.0
TOTAL	**$284,893.00**	**$380,132.50**	**$545,496.00**	**$2,368,268.50**	**$284,893.00**	**$95,504.50**	**$272,893.00**	**$278,893.00**	**$284,893.**
COST PER SQ. FT.	$12.27	$16.18	$22.49	$10.20	$12.27	$35.37	$11.75	$12.01	$12.27
NOTE: travel and labor costs associated	$59,538.00	$80,235.00	$104,346.00	$555,201.00	$59,538.00	$14,562.00	$59,538.00	$59,538.00	$59,538.0
percentage of total cost	20.90%	21.11%	19.13%	23.44%	20.90%	15.25%	21.82%	21.35%	20.90%
COST PER SQ. FT. WITHOUT	$9.71	$12.76	$18.19	$7.81	$9.71	$29.98	$9.19	$9.45	$9.71

Associated costs with difficulties in drilling are very hard to estimate, but effects on the overall cost would probably be similar to drilling to different depths. The demonstrations the system has been tested on to date would be considered small barriers. The cost model that was created matches these demonstrations well, and should also be fairly accurate for a medium sized barrier. The estimates for a large barrier are conservative. For a large barrier, one or more scanning systems would be purchased, rather than rented. The systems would be used simultaneously, reducing labor costs. Local personnel would be used, reducing travel costs.

Costs associated with the geographic location of the barrier are predominantly driven by travel costs to the site. Travel and labor costs associated with travel are estimated to be 15 – 20% of the overall cost of the demonstration. As this system moves out of the demonstration phase, SEA would opt to subcontract out much of the work that would require travel to the site, lowering the system cost. In each of the cases, the dollars associated with travel and the cost per sq. foot to monitor the barrier with these dollars removed has been included. For comparison with costs of other verification technologies or to installation costs of the barriers themselves, using the costs without travel provides a more accurate comparison.

The minimum size of the breach that must be detected and the barrier thickness both effect the systems cost by changing the monitoring time (the smaller the breach that must be detected and the thicker the barrier, the longer the monitoring time). Because the system automatically collects the data, increasing the monitoring time does not significantly increase the cost (see the case studies).

The final major item listed, whether the barrier has a cap or not, could effect the overall cost significantly. Puncturing a cap would require repair of all punctures, which could be very costly. Ideally any verification system would be used immediately upon completion of the barrier (prior to addition of a cap) so as to allow repair of flaws to be completed while the equipment used to form the barrier is still on location. Preservation of the injection wells during subsequent cap installation would allow the system to be used for long term monitoring.

Costs associated with using SEAtrace™ on a barrier will then range between $8 and $30 per square foot. These costs are roughly one-third to one-half of the cost to install a subsurface barrier. It is important to note that the same variables that drive the cost of the verification system will likewise effect the cost of barrier installation. Costs for other verification technologies presently being developed have not been published.

MSE Technologies recently completed an independent cost analysis of the system. Results are similar to those reported here. A cost comparison to a baseline technology (gaseous tracer testing where sampling and analysis are done manually) showed SEAtrace™ provided substantial cost savings (37%) over the baseline technology (MSE Technology Applications, Inc. 1999).

There are several ways to reduce the cost of SEAtrace™. Of the four major tasks associated with the system (vapor port installation, the monitoring system, testing, and data reporting) vapor port installation is the most costly. The number of monitoring wells required is inversely proportional to the desired detail of the results and the accuracy/range of the gas analyzer. If a different tracer gas / analyzer combination could be found that would allow accurate field analysis of lower concentrations, the ports could be spaced more coarsely for a desired resolution specification, resulting in a cost savings. The monitoring system / monitoring system setup is the second most expensive aspect of SEAtrace™. In its present design, the monitoring system costs about $100,000, with the gas analyzer accounting for about 1/3 of the cost. There are less expensive analyzers available, but none that were found to be field rugged / repeatable enough for the system. Analyzers are always being reviewed. Presently a field portable GC unit is the most likely replacement candidate. Incorporation of a GC would not only reduce the outright cost of the system, but would also reduce maintenance and power costs. Set-up of the monitoring system includes a number of things that must be done for each section of the barrier to be tested. These include manual checks of the monitoring ports, physical set-up and checks of the scanning system at the site, and generating/checking of the necessary files to run the inversion code. These files include assigning nearest neighbors to each port, providing coordinates for all ports, choosing ranges for all variables (including volumetric search ranges for each port), and providing background concentrations (if necessary). Presently, these files are time consuming to generate and check. The set-up also includes a number of things that only need to be done once for each site, including generating a test plan and developing a site specific injection scheme. Cost savings could be realized mainly in changes to the code to make it more user friendly and to perform logical tests on the input files to minimize the time to create the files. The final two tasks of the system, testing and report generation are roughly equal in cost. Some savings could be realized during the test period if a reliable, automatic injection system was created. Savings would be most pronounced in thick barriers where boost injections are necessary throughout the test duration to maintain a constant source concentration.

It should also be noted that there are other potential benefits of the system. First, the system is capable of performing long term monitoring of a barrier because the gas analyzer is capable of detecting volatile organic compounds. Port installation, file configurations, injection schemes, analysis templates, etc. will all be generated during the initial verification of the barrier, making monitoring less costly with time.

Second, because the gas analyzer can measure most contaminants the system can be used to monitor remediation efforts at a site. Sites in the active remediation and post-remediation stages require long-term monitoring. While results from the scanning system would not replace regulatory accepted laboratory analysis, it could provide cost savings in two ways:

1. The scanning system can provide both real time analysis and highly resolute histories of many parameters, helping sites determine how the remediation effort is progressing and enabling them to make changes to the system to enhance performance.

2. The data collected with the scanning system during active remediation and post-closure can be used as a screening tool for regulatory sampling programs, greatly reducing the number of required manual samples and the subsequent costs of processing, managing, reviewing, and preparing long term-monitoring programs.

Finally, it is possible (with some modifications) that the system could be used to verify/monitor the integrity of a surface cap if one is required at the site. There are significantly more surface barriers (caps) being constructed and used than there are subsurface barriers, and there are several DOE needs statements for long term monitoring of surface caps. Thus, a solution to reducing the cost of SEAtrace™ for a given site may lie in the ability of the system to serve dual purposes. In order to demonstrate these cost savings, additional demonstrations/implementations are required.

7. CONCLUSIONS

The SEAtrace™ system has been proven to provide accurate leak location and acceptable size information for subsurface barriers in the vadose zone. This technology can provide the assurance stakeholders need to accept the use of barriers at those sites where:

- The risk is too great to remove the contaminants
- The contaminants are too difficult to remove with current technologies
- The potential for movement of the contaminants to the water table is so high that immediate action needs to be taken to reduce health risks

To date, six demonstrations of the system have been completed. These include two demonstrations at the Waldo Test Facility, a demonstration at a colloidal silica barrier emplaced at Brookhaven National Laboratory, demonstrations on two thinwall diaphragm jet grouted barriers at the Dover Air Force Base, and the final developmental demonstration at the Brunswick Naval Facility. Each of these demonstrations was successful completed. SEAtrace™ found flaws in all but one of the barriers. Results from the system were corroborated with QA installation logs, geophysical, hydraulic, other tracer tests, and exhumation observations.

Under this contract option, SEA was tasked to perform a final developmental demonstration of the system and to perform a comparative study of the system with BNL's perfluorocarbon tracer technology.

The final developmental demonstration was conducted at the Naval Air Station in Brunswick, Maine. Prior to initiating the test modifications were made to the system's hardware and software. Hardware modifications included the addition of physical controls that would preclude the introduction of water into the sample manifold. Software modifications were made to accommodate the hardware changes, to recover more gracefully from unanticipated problems, and most importantly, to reduce the time required to perform a complete gas analysis scan of the ports. An aggressive effort to restructure the software, minimize set time delays in the code, and incorporate intelligence on what ports to sample and when extra purging steps were necessary resulted in a 25% reduction in the amount of time required to complete a full scan. The demonstration was uneventful. No breaches through the barrier were detected, although the gap between the top of the slurry wall and the bottom of the cap was observed.

Comparative tests between SEAtrace™ and BNL's PTF technology were conducted at the Waldo Test Facility. The tests were successful, with both technologies able to detect all six of the engineered breeches in the barrier. The results provided confirmation of the SEAtrace™ system in a number of ways:

- Automated SEAtrace™ results were confirmed by the manual PFT sampling and analysis.
- The SEAtrace™ data inversion methodology successfully inverted PFT data to locate barrier flaws, showing the codes independence of the tracer used.
- The SEAtrace™ inversion code was run on subsets of the data consisting of a much coarser monitoring port spacing, demonstrating how the results of the test

would have been affected if a less expensive sample array installation had been used. While the breaches were not found as accurately, the results were acceptable. The leaks that were large or that were not close to other leaks were found to within 0.75 m (versus 0.4 m) of the true leak location. Given the regrouting techniques that would be used to repair most barriers, this accuracy would be adequate.

SEAtrace™ is capable of locating flaws with typical positional accuracy of 1.6 feet (0.5 m). If the purpose of SEAtrace™ testing is to assist remediation of barrier flaws, this positional accuracy is sufficient to guide regrouting techniques to patch the holes in the barrier. The system can detect breaches in a barrier rapidly enough (days to weeks) so that results could be available prior to demobilization of emplacement rigs, yielding significant cost savings over needing to remobilize equipment. The system can be set-up, tested, and collect sufficient background data to begin a test in one week. This can be done as soon as the monitoring and injection ports are installed, which would be concurrent with barrier emplacement. The time required to test a barrier varies based on barrier size and thickness and the desired minimum breach size to be detected. In general, 1 to 6 weeks would be sufficient to complete the verification process.

It is estimated that verifying a barrier with the SEAtrace™ system will range between $8 and $30 per square foot. This price includes the total cost of installation, operation, and data analysis/reporting. The unit cost is highly dependent on a number of variables (barrier dimensions, the medium properties, regulatory concerns, etc), and will always be site specific. There are ways to lower the costs. Incorporation of a different tracer gas / analyzer, automation of the necessary files to run the inversion code, and creation of an automatic injection system could all lower the set-up and operating costs for the system. Additionally, dual use of the system could produce significant savings. The unit can be used to provide long term monitoring at sites, or can be adapted to monitor remediation efforts at the site. Finally, it is possible (with some modifications) that the system could be used to verify / monitor the integrity of a surface cap if one is required at the site.

SEAtrace™ is applicable to all impermeable barriers in the vadose zone. While the system has met the criteria established by DOE during the developmental process and has been successfully demonstrated at a multitude of sites, immediate application of the system is limited. Barriers are not being installed in the vadose zone, and even if they were, there are presently no regulatory drivers that require the capabilities of the system. It is possible (with some modifications) that the system could be used to verify/monitor the integrity of a surface cap. There are significantly more surface barriers (caps) being constructed and used than there are subsurface barriers, and there are several DOE needs statements for long term monitoring of surface caps.

8. ACKNOWLEDGMENTS

The authors wish to acknowledge the support of the FETC COR, Karen Cohen, during the course of this effort. In particular, her desire to use the SEA Waldo test facility for comparison testing of the tracer technologies and her patience in coordinating DOE approval to use the NASB site for the demonstration made those portions of this project possible.

The effort of a large number of people was required to make the SEAtrace™ demonstration at the NASB a reality. Emil Klawitter of the Northern Division, Naval Facilities Engineering command was instrumental in obtaining approval of the Navy to use the NASB site for the demonstration. His persistence and coordination between all parties involved in the demonstration were the driving force for making the demonstration possible. Michael Barry (US Environmental Protection Agency, Federal Facilities Superfund Section, Region I) and Claudia Schaffer (Maine Department of Environmental Protection, Federal Facilities Section) provided valuable input into the MOU for the demonstration. Without their support, the demonstration could not have happened. Greg Aprahamb, the Environmental Officer for the Naval Air Station Brunswick, Maine, provided the final approval to use the site. Tony Williams (Naval Air Station, Brunswick) coordinated the demonstration and, in general, assured it went smoothly. Tom Longly of Harding Lawson Associates, provided field support during the test.

We also appreciate the program interface help from Glenn Bastiaans of the Characterization, Monitoring, and Sensors Technology cross-cutting area out of the DOE Ames Laboratory.

Jerry Stockton, Veraun Chipman, and Tony Gallegos of SEA provided extensive field and instrumentation support. Ames Grissanti of SEA was responsible for changes in the coding. Finally, Linda Croom (SEA) provided final report preparation.

9. REFERENCES

Betsil, J. D., and R. D. Gruebel. 1995. "VAMOS, The Verification and Monitoring Options Study, Current Research Options for In-Situ Monitoring and Verification of Contaminant Remediation and Containment with in the Vadose Zone." TTP#AL2-2-11-07. Sandia National Laboratories, Albuquerque, NM.

Dalvit Dunn, Sandra, William Lowry, Bob Walsh, D.V. Rao, and Cecelia Williams. 1998. "Development of the SEAtrace™ Barrier Verification and Validation Technology Final Report." SAND98-1719. Sandia National Laboratories, Albuquerque, NM.

Dalvit Dunn, Sandra, Wiliam Lowry, Robert Walsh, Daniel Merewether, and Veraun Chipman. 1998. "Subsurface Barrier Validation with the SEAtrace™ System: Phase I Topical Report. SEA-SF-TR-97-176. Science & Engineering Associates, Santa Fe, NM.

Dalvit Dunn, Sandra, William Lowry, Veraun Chipman, Bob Walsh, Daniel Merewether, and Jerry Stockton. 1998. "Subsurface Barrier Validation of a Colloidal Silica and a Jet Grouted Barrier with the SEAtrace™ System." SEASF-TR-97-174. Science and Engineering Associates, Santa Fe, NM.

Falta, R., K. Pruess, S. Finsterle, and A. Barristelli. 1995. "T2VOC User's Guide." LBL-36400. Lawrence Berkeley National Laboratory, Livermore, CA.

Heiser, J. H. 1994 "Subsurface Barrier Verification Technologies." BNL-61127. Brookhaven National Laboratory, Upton, NY.

Lowry, William, Sandra Dalvit Dunn, Cecelia Williams, and David Ward. 1996. "Tracer Verification and Monitoring of Containment Systems." In *Nuclear and Hazardous Waste Management,"* 1342-49. Vol. 2. Proceedings of Spectrum '95, International Topical Meeting - Spectrum '96, August 18-23, Seattle, Washington. La Grange Park, IL: American Nuclear Society.

MSE Technology Applications. 1999. "Final Report - SEAtrace™ Cost Analysis." Butte, MT: MSE Technology Applications.

OHM Remediation Services Corp. 1996. *Remedial Action Final Report, Remediation of Sites 1, 3, 5, 6, and 8 Naval Air Station Brunswick, Maine.* Vol. 1. Prepared for Department of the Navy Northern Division, Naval Facilities Engineering Command. OHM Project 16285. Pittsburgh: OHM Remediation.

Ouenes, Ahmed. 1992. "Application of Simulated Annealing to Reservoir Characterization and Petrophysics Inverse Problems." Ph.D. Thesis. New Mexico Institute of Mining and Technology, Socorro, NM.

Rumer, R., and J. Mitchell, eds. 1995. *Assessment of Barrier Containment Technologies – A Comprehensive Treatment for Environmental Remediation Applications.* International Containment Technology Workshop, August 1995. National Technical Information Service Publication #PB96-180583.

Wilson, Ryan D., and Dpig;as M. Mackay. 1993. “The Use of Sulphur Hexafluoride as a Conservative Tracer in Saturated Sandy Media.” *Ground Water Journal* 31, no. 5 (September-October):719-24.

APPENDIX A:
THE INVERSION METHODOLOGY

Inverse modeling is used to reverse calculate flow and transport processes in an effort to understand unknown properties and flow conditions. This can be accomplished with numerical or analytical techniques, depending upon the complexity of the process and the detail required in the final result.

For this application a numerical method was chosen which would allow near real time assessment of recorded gas data. Consequently, the solution method chosen is readily programmed for use on a portable personal computer, which also performs the role of controlling data acquisition, archiving data, and reporting/transmitting the results.

The estimation of the size and location of a leak from measured concentration histories is an inverse problem of multiphase flow in porous media. From measured tracer concentrations C_{ik} taken at locations, $\underline{x}_i = (x_i, y_i, z_i)$ and times t_{ik} one seeks estimates for a set of parameters $\underline{p}$ that characterize the leak.

The inverse problem requires a leakage model

$$c(\underline{p};\ \underline{x},\ t)$$

that solves the forward problem; that is, it maps each point $\underline{p}$ from a multiparameter space into a set of predicted concentration histories. For example, an idealized leakage model for a vertical barrier surface described by $y = a+bx$ is

$$c\left(\underline{p};x,t\right) = \frac{r_o}{r} c_o \operatorname{erfc}\left(\sqrt{\frac{\left(r-r_o\right)^2}{4D\left(t-t_o\right)}}\right),\ r > r_o,\ t > t_o$$

where:

$r^2 = (x-x_o)^2 + (y-y_o)^2 + (z-z_o)^2,$

$y_o = a + bx_o,$

(x_o, y_o, z_o) is the location of the leak, t_o is the time that the leak began, r_o is the constant radius of the leak after time t_o, c_o is the uniform tracer concentration within the hemisphere of radius r_o after time t_o, D is the uniform diffusivity of the medium, and erfc(•) is the complement of the error function. In the idealized case at least the first four parameters are unknown. In a realistic application the model may be more complex, perhaps a finite element model, and there may be many unknown parameters.

The inverse problem can be cast in the form of a nonlinear global optimization problem. The objective function to be minimized may be taken as the sum of the squares of the differences between predicted and measured tracer concentrations:

$$E(\underline{p}) = \sum_{i,k} \left[c(\underline{p}; \underline{x}_i, t_{ik}) - C_{ik} \right]^2$$

The problem is made difficult by the fact that there may be more than one set of parameter values for which E achieves the minimum.

No algorithm can solve a general, smooth global optimization problem in finite time. This fact has lead to the use of stochastic methods, some of which are called Simulated Annealing (SA). An SA method has solved an inverse porous flow problem to obtain relative permeability and capillary pressure as a function of water saturation (Owens 1992). SEA has developed an SA method for estimating subsurface barrier leak size and location. This work is discussed below.

The simplest stochastic method for global optimization is to repeatedly select points in the parameter space at random, using a uniform probability distribution. The objective function is evaluated at each point; the minimum value and the point with the minimum value are remembered, all other information is discarded. Even with a large sample of points, the Pure Random Search method may not find the global minimum, but it *probably* will come close. As the sample increases, the probability of success converges to 1.

SA methods are similar to Pure Random Search. Points are selected at random and the best point is remembered. The difference is that an SA method does not use a uniform distribution to select points in the parameter space. Instead, the probability distribution depends in a complex way on the objective function of previous points.

In an SA method the probability distribution for the next point is centered around a particular point in parameter space, which we call the base point, by analogy to a base camp. As we shall see, the base point need not be the best point found so far. One way in which various SA methods differ from each other is in the exact form of the probability distribution.

The rule for determining the base point is responsible for the name "Simulated Annealing." If the objective function is smaller at the next point than it was at the base point, then the base point is moved to the new point. If the objective function is larger, we take a chance on moving the base point; we "roll the dice." If the objective function is much larger at the next point, the probability of moving the base point is less, because that probability is given by the following expression:

$$e^{-\Delta E / T}$$

This is analogous to the physical annealing process, where ΔE is the difference in energy states and T is proportional to the temperature. When T is relatively large, there is a good possibility that the base point will climb out of a local minimum to look for other

minima. If T is small, the base point is more likely to avoid "uphill" steps. In an SA method, the temperature is reduced as the process proceeds, just as in physical annealing.

SA methods not only differ in the form of the probability distribution used to select the new point, they also differ in the cooling schedule.

To select the next set of parameter values to be tested, each parameter is selected independently, using a probability distribution proportional to

$$e^{-w\left|p_j - q_j\right| / \left(M_j - m_j\right)}$$

where $\underline{p}$ and $\underline{q}$ are the new point and the base point, respectively, $[m_j, M_j]$ is the interval of allowed values of p_j, and W is a shape constant. This is a relatively simple probability distribution that satisfies the requirements that the probability density be positive over all possible parameters values and that the density be a maximum at the base point.

In a previous SA algorithm for an inverse porous flow problem, the "temperature" was periodically reduced by a factor between 0.7 and 0.95 (Owens 1992). Other studies suggest that the temperature should be proportional to:

$$E(\underline{p}_b) - E_o$$

where $\underline{p}_b$ is the most recent base point and E_o is an estimate of the minimum value for E. In order to assure that T converges to zero even when E_o is underestimated, the present algorithm uses

$$T = V \frac{E\left(\underline{p}_b\right) - E_o}{\ln(n+1)}$$

where n is the number of points for which E has been evaluated and V is a constant. The value for E_o is based on the fractional measurement errors e_i at the various monitors; that is

$$E_o = \sum_i e_i^2 \left(\sum_k C_{ik}^2 \right).$$

For the calculations reported here, V was set to 100. With this choice, the probability of accepting a point that would "double" the error is about 98.6 percent for n=1 and about 86 percent for n=2000.

An SA algorithm needs a stopping rule, which tends to be problem-dependent. The present algorithm stops a search when $E(\underline{p}) \le E_O$ or after a fixed number of evaluations N.

In order to estimate the uncertainty in the result, several sequences are run, each starting from the same initial $\underline{p}$ but using a different sequence of random numbers. Because of this repetition, it is reasonable to use a relatively small value of N for each search.

This iterative methodology was incorporated into a C++ code developed to run on a standard personal computer. Tests with simulated soil gas concentration histories from a one-dimensional spherical diffusion model were conducted to demonstrate the methodology.

APPENDIX B:
THE INVERSION CODE

The SEAtrace™ monitoring system detects leaks in subsurface barriers by measuring concentrations (outside the barrier) of a tracer gas that has been injected into the barrier. The main assumption is that if the tracer is detected, it passed through a breach in the barrier. Once a leak has been detected, it is necessary to determine various characteristics of the leak, including the time that the leak started, the location, and size of the leak. These are found through what is termed an "inversion" of the data. To perform an inversion of a data set, it is necessary to have a mathematical model, called the forward model, which describes the physical phenomena. The forward model uses model parameters and other information to generate an approximation of the physical quantity being measured. In the SEAtrace™ system, the quantity measured is the time and concentration of the tracer gas in the soil, so the forward model is used to predict what this concentration might be for a particular set of model parameters. The resulting data set is called the synthetic data, and it is compared to the measured data set through some type of a norm. For the SEAtrace™ system, an error functional of the form of an L2 norm is used, which is the square root of the sum of the differences squared between every data point in the measured and synthetic data sets. If the data sets match, then the model parameters are assumed to be the same parameters that are responsible for the measured data. In the barrier monitoring problem, the model parameters of primary interest are the leak location and size. Originally, the SEAtrace™ system used a simple one-dimensional spherical model. Section 3.2.2. *Forward Models* gives a detailed description of the model. In this model there are seven parameters, called model parameters, which in general, are unknown and must be supplied. The first three model parameters are the leak location coordinates, x_o, y_0, and z_0. The fourth model parameter is the radius of the leak, r_0. The fifth model parameter is the time at which the leak started, t_0. The sixth model parameter is the concentration of the tracer gas in the leak, c_0, and the seventh model parameter is the effective diffusivity of the soil at the site. While the one-dimensional spherical model was able to determine the location of the leak with accuracy, it was less accurate in determining the leak radius, source concentration, or time of the start of the leak. Calculational work showed that the barrier thickness could significantly limit the amount of tracer gas able to diffuse into the surrounding medium, causing the measured concentration histories in the medium to be much less than predicted by the one dimensional model. Consequently, a flux limited model was developed (Section 3.2.2. *Forward Models*). This model was incorporated into the inversion code. The flux limited forward model assumes that the barrier has a finite thickness, and treats the pathway through the barrier and the area outside the barrier as two separate regions. This model considers ten parameters. The first seven are the same as those for forward model #1. The remaining three model parameters are D_h, the effective diffusivity of the material in the barrier pathway, L_h, the length of the pathway, and C_b the concentration of tracer gas behind the barrier.

In addition to these model parameters, the locations of points in the surrounding media at which measurements of the concentration will be taken, as well as the times at which the measurements are to be taken, must be supplied to fully evaluate the forward model. For

purposes of monitoring at a disposal site where a subsurface barrier has been installed, only the locations of the monitoring points, the times at which measurements are taken and the measured concentrations are known. The model parameters are unknown. The SEAtrace™ SEAIM software uses a method called Simulated Annealing to determine the values of the model parameters to be used in the forward model, combined with the monitoring point locations, measurement times and measured concentrations, to produce the synthetic concentration data set.

Simulated annealing is a global optimization method. An optimization method is a method which optimizes some norm (parameter, function, or functional). For the SEAtrace™ system, simulated annealing is used to optimize the error functional, or the sum of squared differences between the measured and synthetic data set. The error functional is considered optimized when it is minimized. Because there are so many model parameters in the forward model (seven in the one-dimensional model and ten in the flux-limited model), the linear space in which this error functional exists is a seven or ten dimensional space. Because of the many dimensions, and because the interaction between each of the model parameters is not readily apparent, there may be multiple local minima in the error functional. Local minima are minima within the multi dimensional error functional space to which the inversion algorithm may converge, but are in fact incorrect answers. The nature of the simulated annealing algorithm allows it to sample many of these local minima without being trapped by them. In this way, the algorithm has a significantly improved chance of locating the desired absolute minima, which corresponds to the true answer, even in the presence of many local minima.

B.1 Code Benchmark

Benchmarking of the SEAIM code involved evaluating its ability to invert a synthetic data set to find the model parameters. This process is multi faceted, as each model parameter and each algorithm parameter interact with the others in a very complex way. As a way to better understand how the parameters interact, a large matrix of cases was run. They involved:

- Letting all parameters vary
- Setting one or more of the parameters at fixed values (which may or may not be their true values)
- Evaluating the effect of different constants on the mathematical scheme (in particular, varying the number of independent searches, the number of iterations per search, a cooling factor, and probability of acceptance constant)
- Evaluating the number of time sequences to be inverted

Synthetic data sets were generated using both the forward models and the T2VOC finite difference modeling code. Because of the stochastic nature of the simulated annealing algorithm, the complicated and unclear interactions among the model parameters, and the choice of error metric, exercising the code proved difficult. In particular, the interactions among the model parameters were the most difficult to understand and exploit.

B.1.1 Benchmarking SEAIM Using the Spherical One-Dimensional Forward Model.

A series of benchmark studies were performed on the one-dimensional forward model. These studies examined the ability of SEAIM to return accurate estimates of the model parameters for various settings of parameters and locations of leaks. A total of 18 separate studies were performed.

Results of the study showed SEAIM was able to return accurate estimates of the x_o, y_o, and z_o model parameters (leak location). The radius of the leak, r_o, and the source concentration were strongly coupled, and exerted significant influence on each other. In general, SEAIM was able to return order of magnitude estimates for each of these variables. The diffusivity of the soil, D, was usually accurate. Note that this parameter may be measured at a site, so it may be possible to fix the value of D within the inversion. Most difficult to understand of the studies results was the apparent lack of influence that the start time, t_0, exerted on the results of the inversion. In general the inversion generated results for the remaining model parameters which were within expectations regardless of the value at which t_0 was fixed. This lack of sensitivity to start time was determined to be an issue that was inherent in the forward model (the complimentary error function), and is therefore unavoidable. For purposes of barrier validation, however, start time is considered a less significant parameter.

B.1.2 Benchmarking SEAIM Using the Flux Limited Forward Model

The flux limited forward model differs from the one-dimensional model in that the barrier is treated as having a finite, non-zero thickness with a pathway through it approximated as a cylinder. This cylinder terminates on the outer face of the barrier. It was hoped that this new model would provide improved estimates of the concentration of tracer at the exit of the leak, which would lead to an improvement in the estimate for the radius of the leak. For the flux limited forward model, a less rigorous benchmark study was performed than for the initial one-dimensional spherical forward model. In general, the results of the benchmark study of the initial forward model were found to apply equally to the flux limited forward model. The code was found to perform better when no parameters were fixed, as opposed to fixing one or more parameters. As with the initial forward model, plots of the error functional vs. model parameter value were made for each of the model parameters. The results of this study showed that the behavior of the model parameters for the flux limited forward model were nearly identical to that of the one-dimensional forward model. An explanation for the lack of improvement with the flux limited forward model is that the expression for this model differs from that of the initial forward model only in that a more complicated expression for the source concentration is used. Other than this, there is no difference between the models, and therefore the behavior was similar. In particular, the formulation for the pathway through the barrier, with the three extra model parameters that it introduced into the inversion, did not enhance the ability of the inversion to find the leak location or radius.

B.2 Sources of Difficulty with the Forward Models on the Inversion of the Data

The ability of an inversion code to accurately solve for the desired model parameters is dependent upon the mathematical behavior of the forward model being used. Mathematical behavior in this context relates to how the model parameters interact with each other. For example, there are an infinite number of combinations of X/Y that equal 2, such as X=4, Y=2 or X=1, Y=0.5. It is easy to show that when the exact values of the model parameters are used, the error measure or L2Norm is close to or identically zero. However, when these parameters start to vary, then small changes in one or more of the model parameters may lead to large changes in the error measure. Therefore, it is desirable to minimize the number of model parameters, and to gain an understanding of their interaction. For both forward models being used in SEAIM, the main component of each model is the complementary error function. The argument for this function is the same for both forward models. Looking at the mathematical behavior of the complementary error function, its value varies for arguments from 0.01 to about 1.6, and then decreases asymptotically to zero. For the typical data acquisition process and data sets being acquired, the argument values are often greater than 1.0. This is a problem because the variations in the model parameters that make up the argument of the complementary error function do not yield significant variations in the value of the complementary error function. For the field system, data must be taken earlier in time or the monitoring points moved closer to the barrier to eliminate this problem. Attempts were made to modify the argument, such as using a binomial expansion on the square root term in the denominator, but these efforts did not yield any significant improvement. Another example of adverse model parameter interaction is the product of source concentration and radius, which shows up outside the error function. As long as the product of these two parameters remains relatively constant, they may vary in their individual magnitudes significantly. It is important to note that fixing model parameters at their true values does not solve the problem. To eliminate the interaction the model parameter must be completely eliminated. One source of possible error in the flux limited forward model is the treatment of the transition from the cylindrical path through the barrier to the spherical source radiating out into the medium.

Another source of difficulty is the choice of error measurement. The L2Norm is a satisfactory choice in the absence of extremely large experimental errors. In this instance, experimental error refers to the deviation from spherical of the tracer gas concentration profile. For SEAtrace™, this condition has yet to be validated. In the event that the profile is found to significantly deviate from spherical, an L1Norm may be a more appropriate metric.

B.3 Future Considerations

Several aspects of the code merit consideration for future modifications. The first is the choice of forward model. As mentioned previously, the complimentary error function is problematic. A formulation of the forward model in a Cartesian or cylindrical coordinate system will eliminate the complementary error function, and should increase sensitivity to leak location and radius. For field deployable systems, an analytic forward model is

essential. However, for an office based inversion system, a numerical approximation may be appropriate. A further analysis of the physical basis for spherical diffusion is required prior to determining this. A second consideration is the choice of the inversion algorithm. An adaptive simulated annealing algorithm, with some built in "learning" may lead to improvements. A genetic algorithm may also be appropriate.

APPENDIX C:
T2VOC MODELING

The objective of the modeling efforts has been to better understand how typical field conditions differ from the ideal model(s) which are used in the inversion code. A version of the Lawrence Berkeley National Laboratory TOUGH code, T2VOC, was used to model the diffusive transport processes. T2VOC is capable of modeling three-phase (gas, aqueous, NAPL), three-component (water, air, VOC), nonisothermal flow and transport through porous media (Falta, R., Pruess, K., Finsterle, S., Battistelli, 1995).

T2VOC was used to address the most significant differences between the forward model(s) used in the inversion code and reality. These include:

- The effect of flux rather than diffusion-limited flow of the tracer gas into the medium
- The effect of a non-constant source concentration
- Gravitational effects
- The effect of a heterogeneous medium
- The effect of non-constant diffusivity

C.1 Validation of the Flux Limited Forward Model

T2VOC, was used to validate the flux limited forward model (section 3.2.2. *Forward Models*). Barrier thickness, leak radius, and exit concentration were each addressed. Values or combinations of values were altered from a baseline T2VOC model, and resulting concentrations were compared to values predicted by the developed analytical model (Lowry et. al. 1994; Dunn et al. 1998). This is a brief summary of the results.

All the problems run used a radial 2-D mesh. A schematic of the mesh is given in figure C1. The baseline case had a constant source concentration of 0.304 kg/m^3 (50,000 ppm), a barrier thickness of 0.6 m (2 ft), and a leak radius of 0.152 m (6 in). The source volume was enclosed (e.g., a capped barrier was modeled). The medium (inside and outside the barrier) was homogeneous with a porosity of 30%, an effective diffusivity of 3.5e-9 m^2/s, a water saturation of 5% and a permeability of 9.87e-12 m^2. The barrier was homogenous with a very low porosity (1%) and permeability 9.87e-14 m^2. The leak through the barrier was cylindrical and on the center axis of the grid. All of the boundaries were no flow (zero diffusive transport).

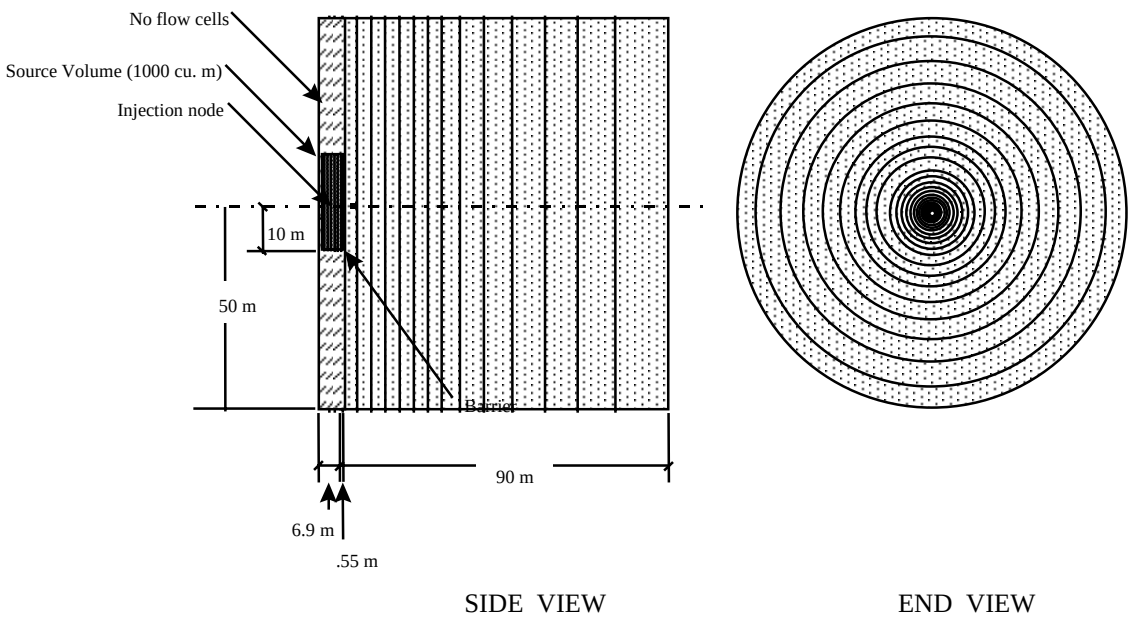

Figure C1. Schematic of the two-dimensional radial mesh used in the T2VOC modeling.

The preliminary T2VOC calculations performed to develop / validate the flux limited diffusion model included varying the barrier thickness and leak radius within the baseline T2VOC model, and comparing the resulting concentrations with those predicted from the analytical model. Results were promising, showing the analytical model was able to accurately predict the concentrations for distances 1 m or greater from the leak if the correct exit concentration for the leak was known. For the T2VOC model initially used in the testing, this concentration could be assumed to equal one-half the source concentration. Figure C2 shows a typical comparison between the analytical and numerical model. The relationship between the source and exit concentration was studied further. It was determined that changing the effective diffusivity would effect the exit concentration. Over the three order of magnitude range of effective diffusivities tested, the ratio of the exit to source concentration varied from 0.7 to 0.5. Figure C3 plots the effective diffusivity versus the concentration ratio. As the effective diffusivity increases the concentration decreases. This will result in lower calculated concentrations in the medium, i.e., as the effective diffusivity increases the resistance to diffusion decreases resulting in smaller concentration gradients. The tracer gas will move further into the medium with time, but the resulting concentrations will be smaller in magnitude. A best fit of the data resulted the relationship of:

$$C_{exit}/C_0 = 0.7 - 5{,}714D$$

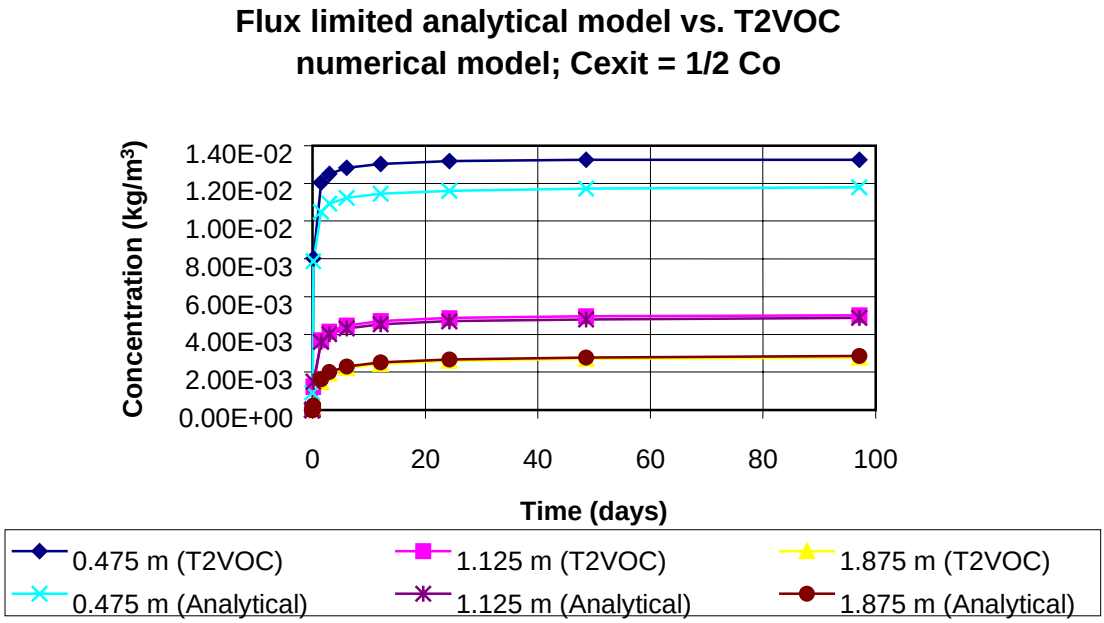

Figure C2. Comparison of the flux limited analytical model and the T2VOC numerical model.

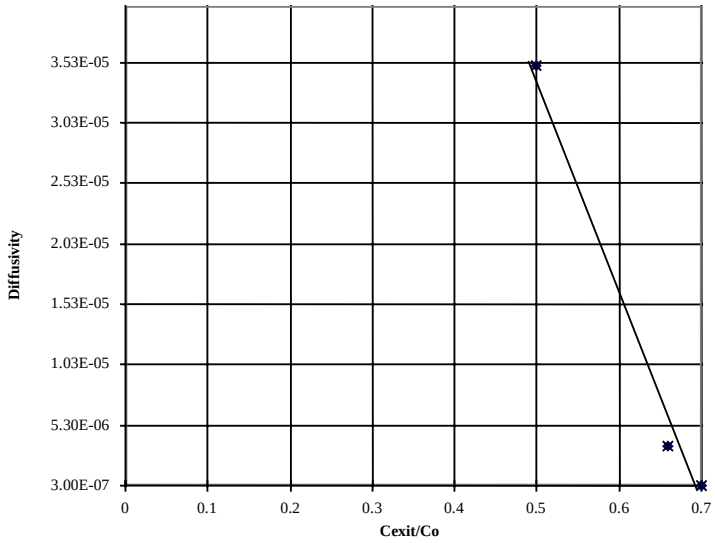

Figure C3. Effective diffusivity versus the concentration ratio for the flux limited forward model.

C.2 Effect of a Non-Constant Source Concentration

Unlike the model assumption, the concentration of the tracer gas inside the barrier will not be constant. Injection of the gas at specific points will create concentration gradients within the barrier. If there are leaks in the barrier, the gas will begin to diffuse into the surrounding medium before an equilibrium condition is reached inside the barrier. Even if the leak does not begin until after a quasi-equilibrium condition is reached, if the mass of tracer in the barrier is small relative to the mass which diffuses out of the barrier (through leaks or into the atmosphere, if the barrier is uncapped), the source concentration will be depleted with time. As the mass of the tracer gas is a function of the pore volume and the concentration, it is possible for even a large barrier (volume wise) to have only a relatively small mass of tracer gas.

To address how a non-constant source concentration will effect the concentration profiles outside the barrier, the following problems were modeled. Results are summarized after each model description.

C.2.1 Tracer Injection into a Capped Barrier with an Existing Leak

The baseline case for this model work was the same as that discussed in section C.1. *Validation of the Flux Limited Forward Model*, with the exception that the tracer gas was injected into the source volume over a 5-hour period. Results showed an initial pulse of tracer gas diffusing through the leak creating higher concentrations in the medium than seen in the baseline case. Figure C4 shows calculated concentration histories at three distances from the leak for the baseline case. Figure C5 shows the same information for the injection case. These higher concentrations began to slowly decay within 24 hours and asymptotically approached the values seen in the baseline case within a month of the injection. The results were explained by viewing the concentration of the tracer within the barrier. The injection of the gas into a point source created spherical diffusion from the injection point out into the source volume. When the concentration front reached the barrier it could not continue to expand in that direction except through the leak. The concentration at the barrier wall (the leak entrance) increased very rapidly, causing a pulse of tracer to diffuse through the leak. As the tracer began to equilibrate within the barrier, the concentration at the leak entrance began to diminish, causing less tracer to diffuse through the leak and the subsequent decay in the tracer concentration in the medium.

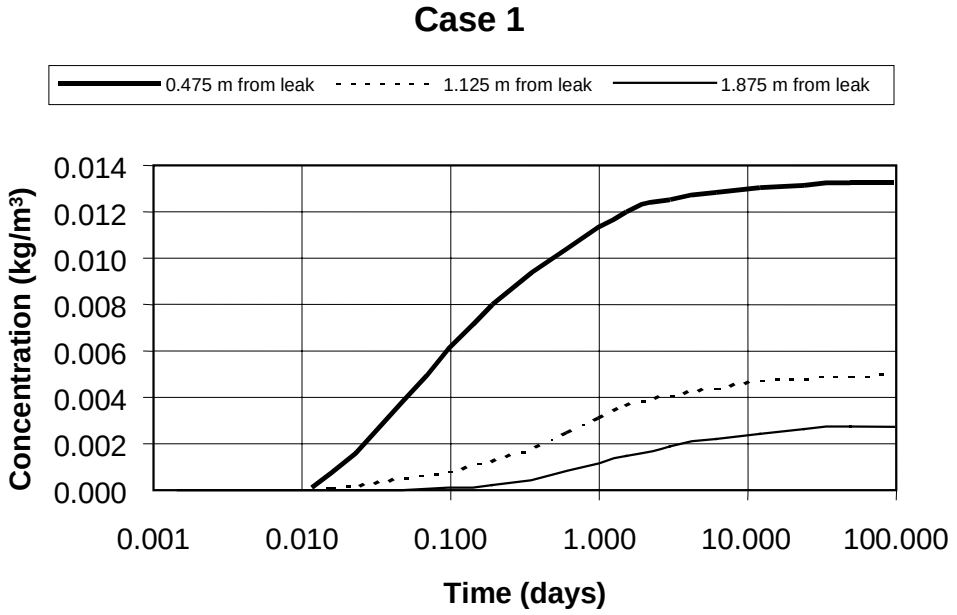

Figure C4. Calculated concentration histories at three distances from the leak for the baseline radial two-dimensional T2VOC case.

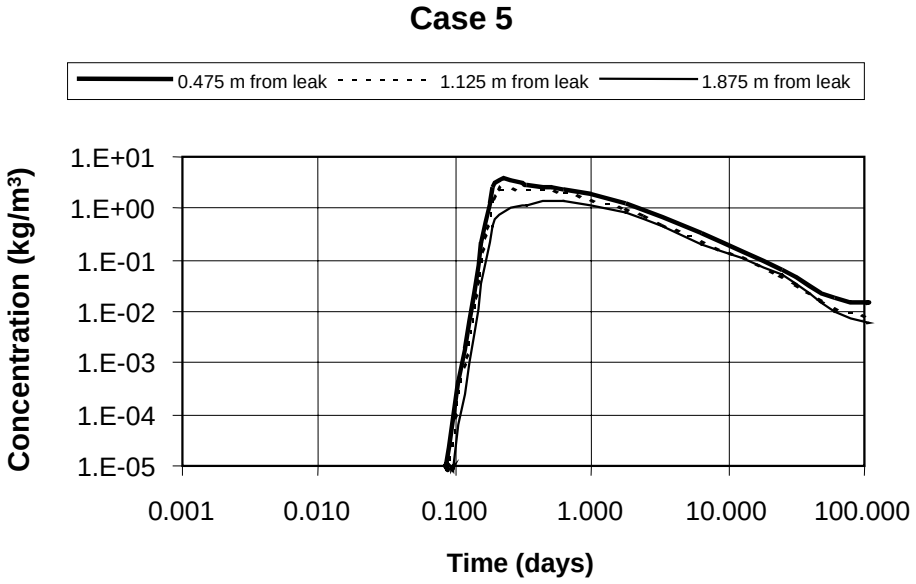

Figure C5. Calculated concentration histories at three distances from the leak for a case identical to the baseline with the exception that the injection of the tracer gas into the source volume through a single port is modeled.

The tracer within the barrier required almost 5 days to equilibrate. The magnitude of the increased concentration in the medium was a function of how close the injection port was to the leak, and how quickly the concentration in the source volume equilibrated. As the distance from an injection port to a leak is unknown, the solution to the problem lies in forcing the source concentration to rapidly equilibrate. A model simulating multiple injection ports throughout the barrier resulted in medium concentration profiles within 10-15% of the baseline case within one week of injection (figure C6).

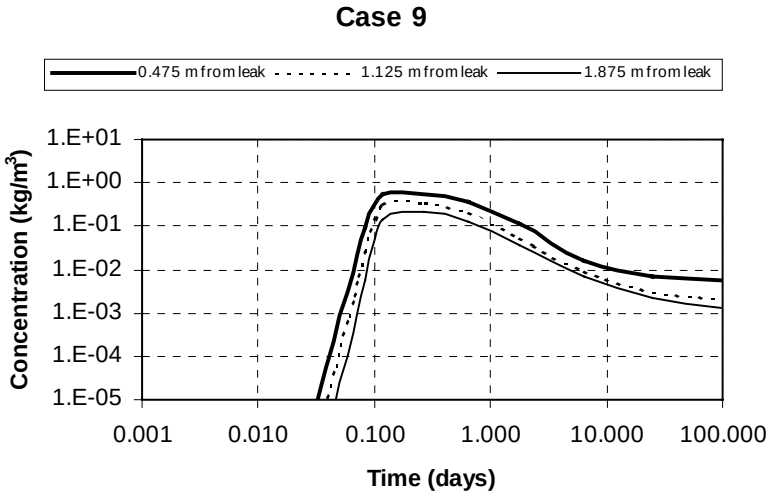

Figure C6. Calculated concentration histories at three distances from the leak for a case identical to the baseline with the exception that the injection of the tracer gas into the source volume through multiple ports is modeled.

C.2.2 Tracer Injection into an Uncapped Barrier with an Existing Leak

This simulation used the baseline case with the exception of having one surface of the source volume be a zero concentration rather than a no-flow boundary emulating exposure to surface air. Results showed that the source concentration rapidly diminished, causing the measured concentrations in the medium to be significantly less than in the baseline case. The model was then executed with tracer gas continuously injected in the source volume. While the concentration could be maintained in this manner, the amount of gas that required to be injected makes this approach expensive. Consequently, capping the barrier with a temporary, inexpensive plastic sheet has been used to conserve tracer gas.

C.3 Gravitational Effects

For the medium outside the barrier, conditions will likely be different than the model assumptions. Most geologic formations are not homogeneous, and in addition to molecular diffusion, there are several advective forces that can influence the movement of the tracer gas. These advective forces include density, pressure and temperature.

Depending on the molecular weight and concentration of the tracer, gravity will influence the isopleths.

The tracer gas of choice (sulfur hexafluoride), has a molecular weight of 146 gm/gm mole. At the concentrations anticipated to be measured at the monitoring ports (several hundred to several thousand ppm), it was thought that transport of the gas due to gravity could possibly be on the same order of magnitude as that of molecular diffusion. Because the gravitational force is directional, elliptical rather than spherical isopleths would develop. This would result in the code predicting the leak location to be lower than it actually is. It should be noted that gravity will also effect the distribution of the tracer gas inside the barrier. Because the source concentration (10,000 to 100,000 ppm) is much higher than the anticipated concentrations at monitoring ports, the effect will be much more pronounced inside the barrier. However, because the inversion code treats the source concentration as an unknown, the density induced gradient within the barrier is of little consequence to the SEAtrace™ system (the gradient will not cause the source concentration to be non-constant).

A conservative estimate at how gravity will effect the measured concentrations can be viewed by turning the two-dimensional cylindrical mesh on edge and adding gravity along the axis of the leak. This was done using the baseline model. Results are shown in figure C7. The overall magnitude of the measured concentration in the medium is larger than for the baseline case. This was found to be predominantly the result of the concentration gradient established within the source volume, not gravity. The true influence of gravity was determined by comparing the resulting concentrations in two cells the same radial distance from the leak (one cell on the leak axis, the other near the surface of the barrier). The difference in the measured concentrations in these cells indicates how non-spherical the resulting isopleths were due to gravity. It was found that there was only a small difference (less than 15%), as shown in Figure C8. As such, it was determined that given the anticipated concentrations in the medium, gravity will not significantly influence the results of the system.

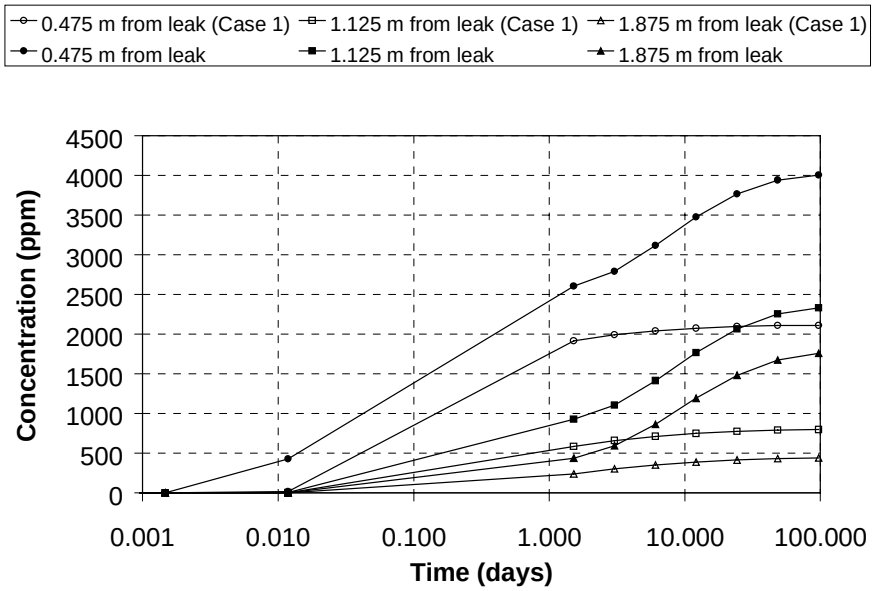

Figure C7. Calculated concentration histories at three distances from the leak for a case identical to the baseline with the exception that gravity is modeled.

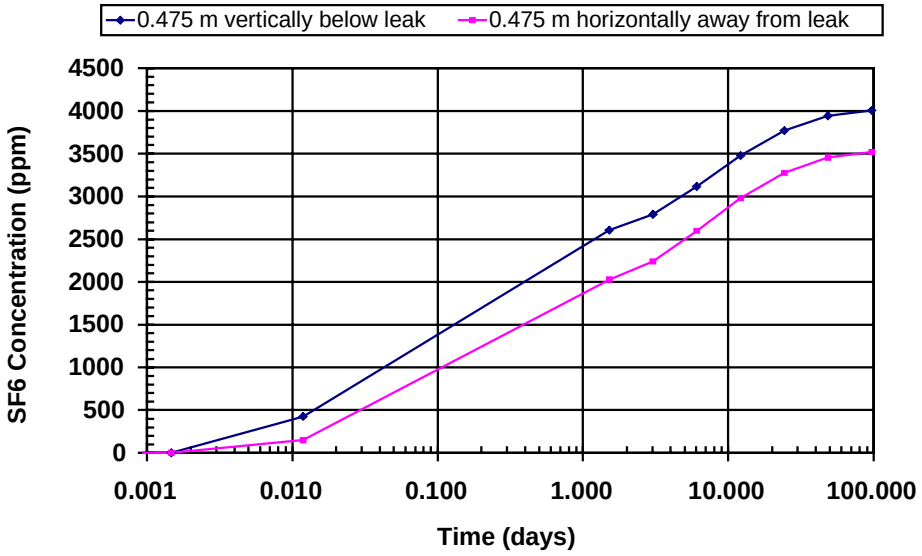

Figure C8. Calculated concentration histories at two points the same radial distance from the leak but at a right angle to one another for a case identical to the baseline with the exception that gravity is modeled.

Temperature and pressure gradients in the medium will also contribute to the transport of the tracer gas. These gradients are dependent on the depth of the barrier below ground surface and changing atmospheric conditions. For barriers near the ground surface (10m or less), these transport mechanisms may be important. Initial calculations have shown that temperature gradients are cyclical on a yearly period, and have a significant time lag with depth below ground surface. If temperature changes to the soil and the gases' properties are ignored, the advective motion of the tracer due to the gradient is small compared to molecular diffusion and gravity. Pressure gradients may be important if the heterogeneity of the medium is such that the barometric pumping of the soil gas results in something other than a cyclical motion of the tracer. It is also possible that the geometry of the barrier could cause preferential movement of the tracer during the inhalation / exhalation cycles of air into the medium.

C.4 Heterogeneous Soil Properties

Molecular diffusion is sensitive to heterogeneous gas diffusion properties. Layers of very low porosity (regions of high saturation, clay layers, etc.), regions in which pore spaces are not well connected, and areas where fracture flow is dominant can all impact the system results. Layers having different effective diffusivities will alter the shape of the isopleths in the medium. The greater the deviation from spherical isopleths, the less accurately the forward models used with the SEAtrace™ system will represent the data. It is important to note that the results of the system will only be effected by a layered medium if the ports used to calculate the properties of a breach are in different layers. SEAtrace™ solves for leak characteristics locally (using a search area of 1 to 2 m in radius).

Heterogeneous effects were modeled using a three-dimensional rectangular mesh. The model nodalization was based on a realistic but conservative layered medium (see figure C9a and C9b). Three cases were modeled. One is a baseline case with homogeneous soil gas diffusivity, adjusted for porosity and tortuosity, of 4.64e-6 m^2/s (the diffusivity of SF_6 in free air is 7.03e-6 m^2/s). The barrier is modeled as a 1m thick slant wall with a very low diffusivity (4.64e-9 m^2/s), extending up to the surface. An impermeable sheet to conserve tracer covers the top of the barrier. The initial concentration inside the barrier is 100,000 ppm SF_6 in soil air, and the leak is equivalent to a 9 cm diameter hole in the barrier.

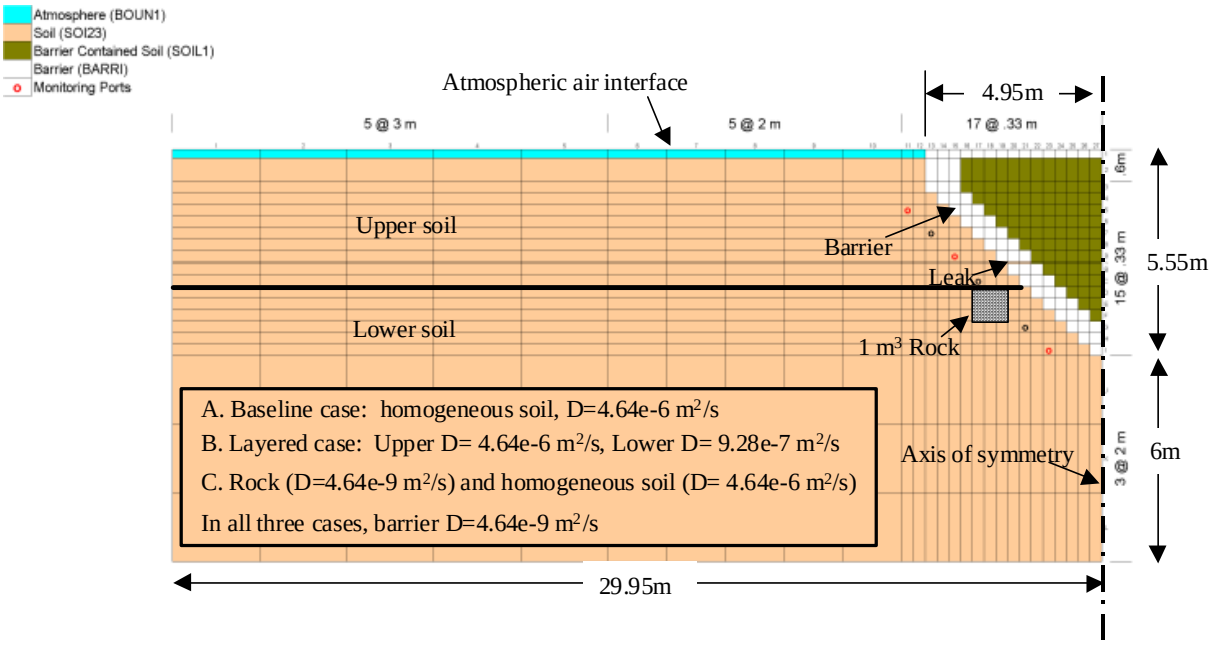

(a)

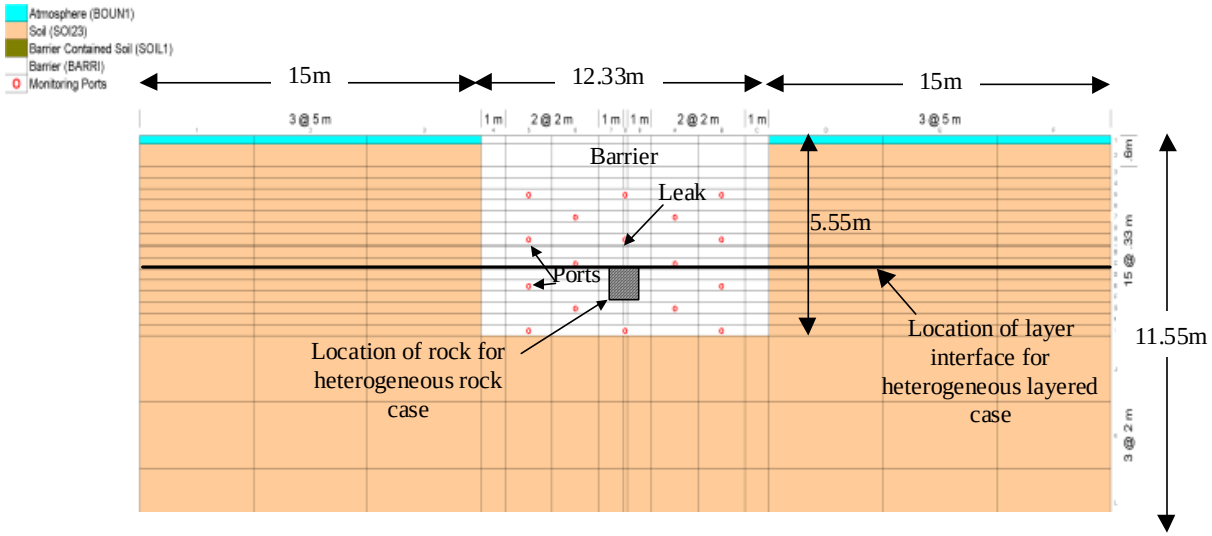

(b)

Figure C9. Schematic of the 2-D grid used in the T2VOC runs that compared calculated diffusiviites for homogeneous versus heterogeneous media: (a) side view (b) fron view.

The resulting concentration contours at 1, 7 and 30 days are shown in figure C10 through C12. Note the stair-stepped shape of the concentration profiles near the barrier, an artifact of the nodalization. Gravity is active in this simulation, drawing the isopleths downward slightly.

The second simulation considered a layered system, with a horizontal layer of soil of 1/5 the diffusivity of the baseline value extending downward from just below the leak (soil above the leak same as the baseline case). This contrast in diffusivity could be due to granular material of finer pore size or higher moisture content. Contours are plotted in figures C13 through C15. Note that the isopleths are not significantly distorted at the interface of the two soil types.

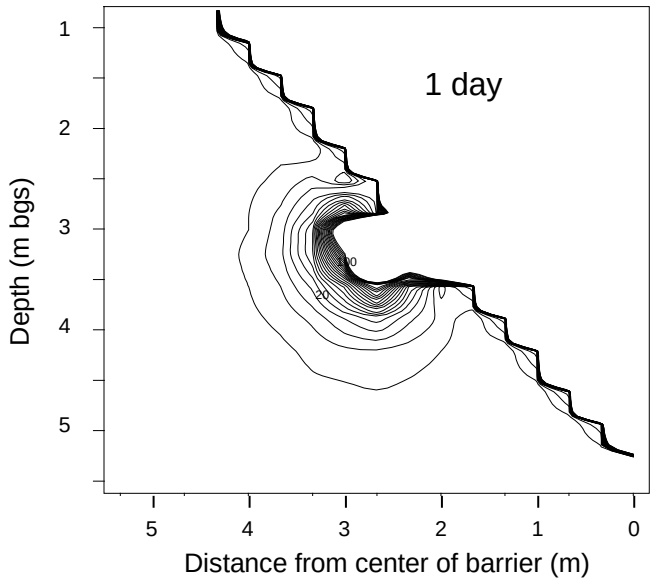

Figure C10. Contour plot of the calculated isopleths for the baseline, homogenous case after one day.

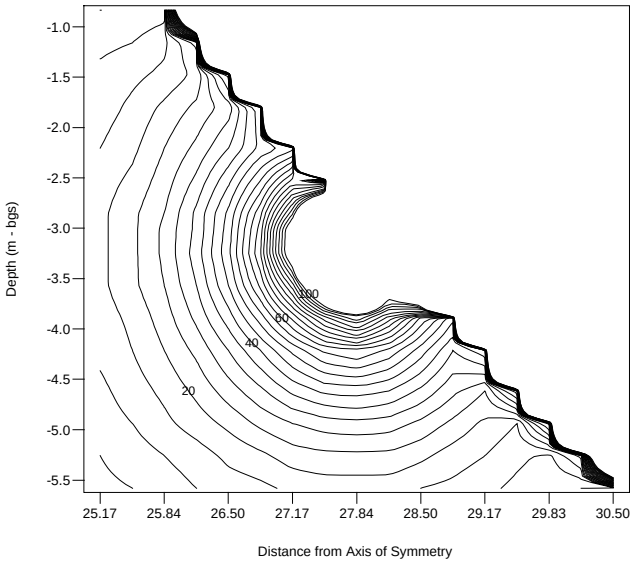

Figure C11. Contour plot of the calculated isopleths for the baseline, homogenous case after one week.

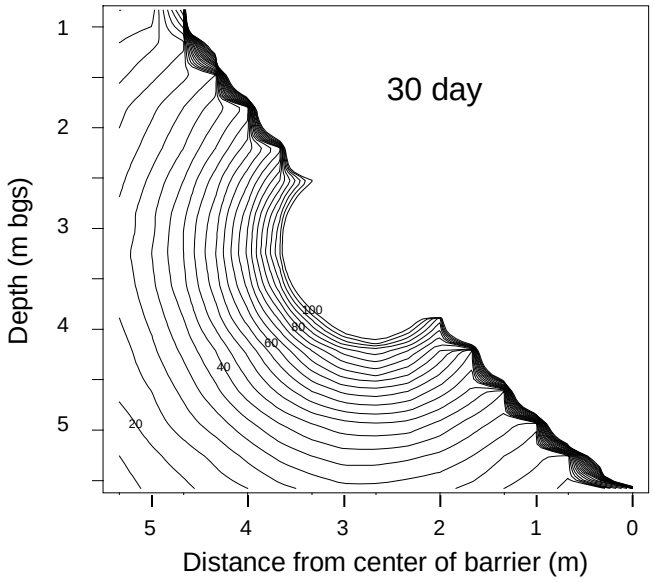

Figure C12. Contour plot of the calculated isopleths for the baseline, homogenous case after 1 month (30 days).

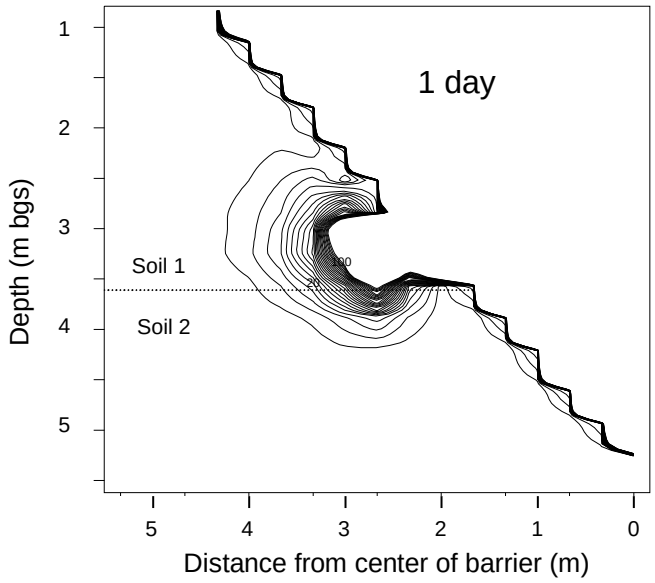

Figure C13. Contour plot of the calculated isopleths for the layered, heterogeneous case after 1 day.

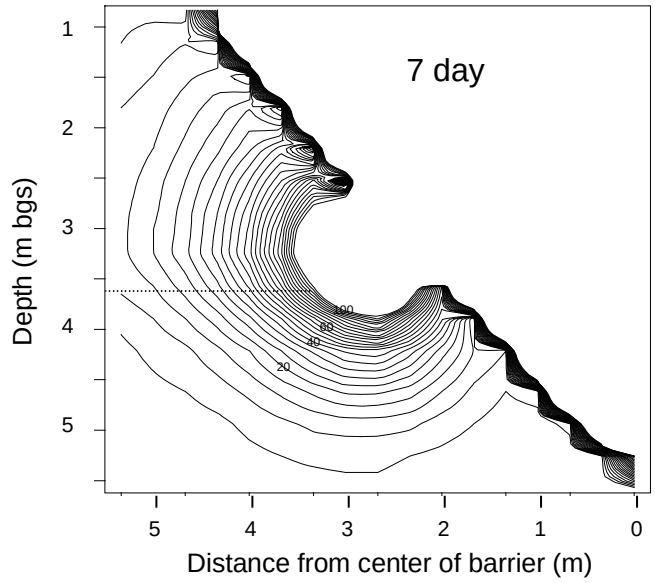

Figure C14. Contour plot of the calculated isopleths for the layered, heterogeneous case after 1 week.

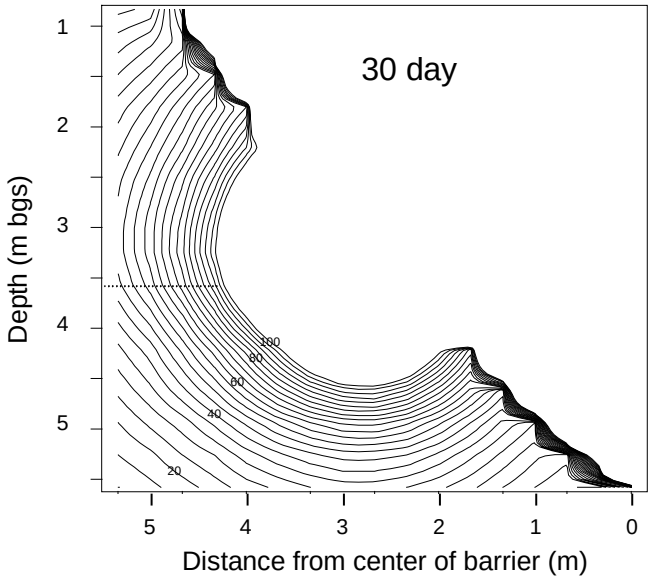

Figure C15. Contour plot of the calculated isopleths for the layered, heterogeneous case after 1 month (30 days).

A third simulation was conducted with an inclusion near the leak representing a 1 m^3 rock of diffusivity equal to the barrier wall material (very low). The concentration distributions shown in figures C16 through C18 show the effects of this perturbation.

The SEAIM code analyzed the output of the T2VOC simulations to determine the impact of the modeled heterogeneity on the code's ability to characterize the leaks. These results are summarized in table C1. The simulations ranged in locating accuracy from 0.6 to 1.2 m, and estimated the leak sizes to be 20.3 to 34.5 cm in diameter (with actual sizes ranging from 1.1 to 10.16 cm). Given the sampling port locations indicated in figure C9, the SEAIM code actually solved more accurately for the layered case than the homogeneous case. This is suspected due to gravitational effects, which would be most pronounced in the homogeneous case and less in the layered case (where the low diffusivity layer below the leak would restrict downward transport).

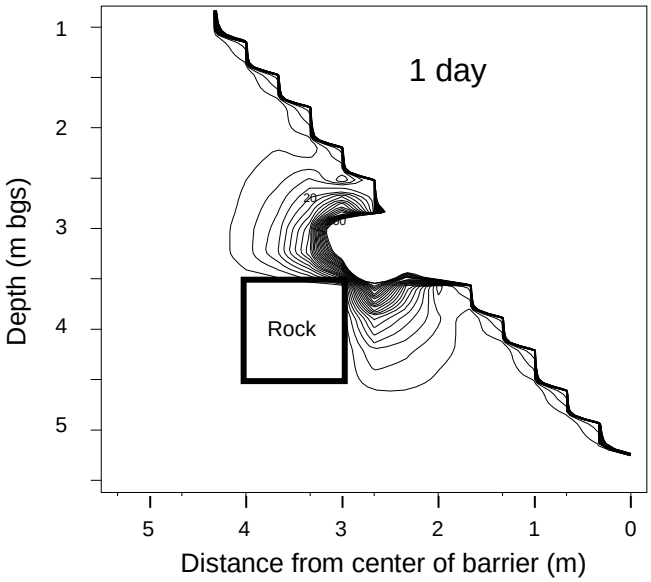

Figure C16. Contour plot of the calculated isopleths for the the boulder simulated within an otherwise homogenous medium case after 1 day.

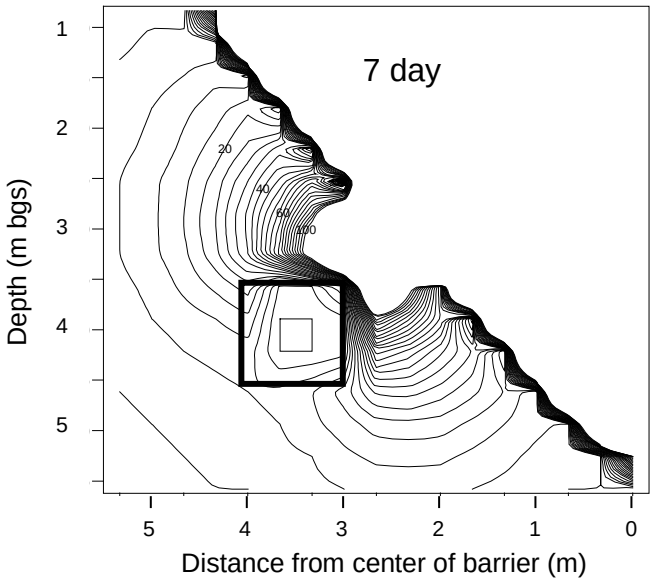

Figure C17. Contour plot of the calculated isopleths for the the boulder simulated within an otherwise homogenous medium case after 1 week.

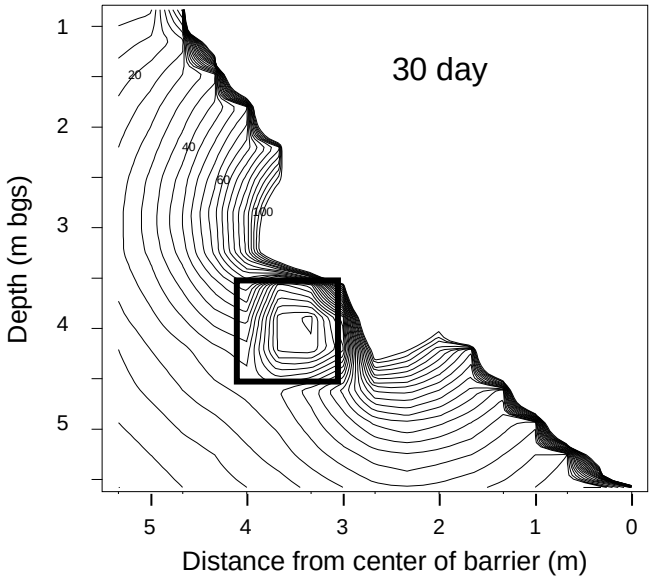

Figure C18. Contour plot of the calculated isopleths for the boulder simulated within and otherwise homogeneous medium case after 1 month (30 days).

Table C1. Calculated characteristics of a leak by the inversion code SEAIM using concentration histories predicted with T2VOC given a homogeneous medium, a medium having two geologic layers, and a medium with a large rock near the leak.

	position							
	X (m)	**Y (m)**	**Z (m)**	**radius (m)**	**start time (sec)**	**concentration (ppm)**	**diffusivity (mg/m^3)**	**Dist from leak (m)**
Time = 24 hours (1 day)								
homogeneous run	28.85	20.93	-2.31	0.05	1.7E+04	8.7E+04	4.5E-06	1.0
layered run	28.06	20.93	-2.44	0.00	2.5E+04	5.2E+04	9.5E-06	0.6
rock run	28.37	21.04	-2.78	0.01	1.6E+04	9.6E+04	6.1E-06	0.3
Time = 168 hours (7 days)								
homogeneous run	27.30	21.05	-3.63	0.00	1.4E+04	4.7E+04	6.9E-06	1.0
layered run	27.98	21.07	-2.71	0.00	6.1E+03	5.2E+04	4.7E-06	0.4
rock run	27.39	21.00	-3.50	0.00	1.5E+04	3.5E+04	3.8E-06	0.9
Time = 720 hours (30 days)								
homogeneous run	27.74	20.97	-3.23	0.00	2.3E+04	7.4E+04	1.8E-05	0.5
layered run	27.43	21.09	-3.40	0.00	2.5E+04	6.5E+04	3.3E-06	0.8
rock run	27.48	21.07	-3.49	0.00	9.4E+03	5.1E+04	4.2E-06	0.8

C.5 Effect of Non-Constant Diffusivity

The effective diffusivity of the leak itself and the medium surrounding the barrier could easily be different than that of the native soil. The diffusivity through the breach will likely be less than the surrounding medium, because of an increased saturation of the area caused by injection of the barrier material. The barrier material could also cause a halo effect around the barrier (a zone around the barrier of higher saturation due to the water content of the barrier material).

A two-dimensional cylindrical model was used to simulate each of these problems. Figure C1 is a schematic of the model, showing the pertinent grid dimensions. For the baseline case, the barrier volume, the leak, and the surrounding medium were modeled as a homogeneous medium with a porosity of 30% and an effective diffusivity of the tracer through the soil gas of 3.509e-5 m^2/s. The barrier itself was created with a very low porosity (.05%) giving an effective diffusivity of the tracer through the barrier that approached 0 m^2/s. Cells surrounding the barrier volume were decoupled from the barrier, and boundary cells around the medium were defined to be at a constant tracer concentration of 0 kg/m^3. A constant source concentration of .152 kg/m^3 (50,000 ppm at standard temperature and pressure), a barrier thickness of 0.6m (2 feet), and a leak radius of 0.15m (6 inches) was used.

In the first case, the diffusivity of the leak was altered to be an order of magnitude less than the effective diffusivity of the surrounding medium. Figure C19 shows the tracer gas concentrations versus time for this and the baseline runs (where the leak diffusivity was the same as the medium diffusivity). As expected, the results showed tracer gas concentrations significantly lower (approximately two orders of magnitude at steady state conditions) in the surrounding soil in the case where the leak diffusivity was lowered. The flux limited analytical model allows for the leak diffusivity to be set independently of the medium diffusivity. Calculations were completed using the flux limited analytical solution assuming the exit concentration could be calculated using the equation derived during prior numerical work (see section 3.2.2. *Forward Models*). These results are also presented in figure C19. The flux limited analytical results were fairly close to the T2VOC numerical results. The analytical model overpredicted the medium concentrations by 60 to 65%. This is believed to be caused by the overprediction of the exit concentration. Additional numerical modeling is required to understand how to adjust the analytical model to more accurately predict the medium concentrations under these conditions.

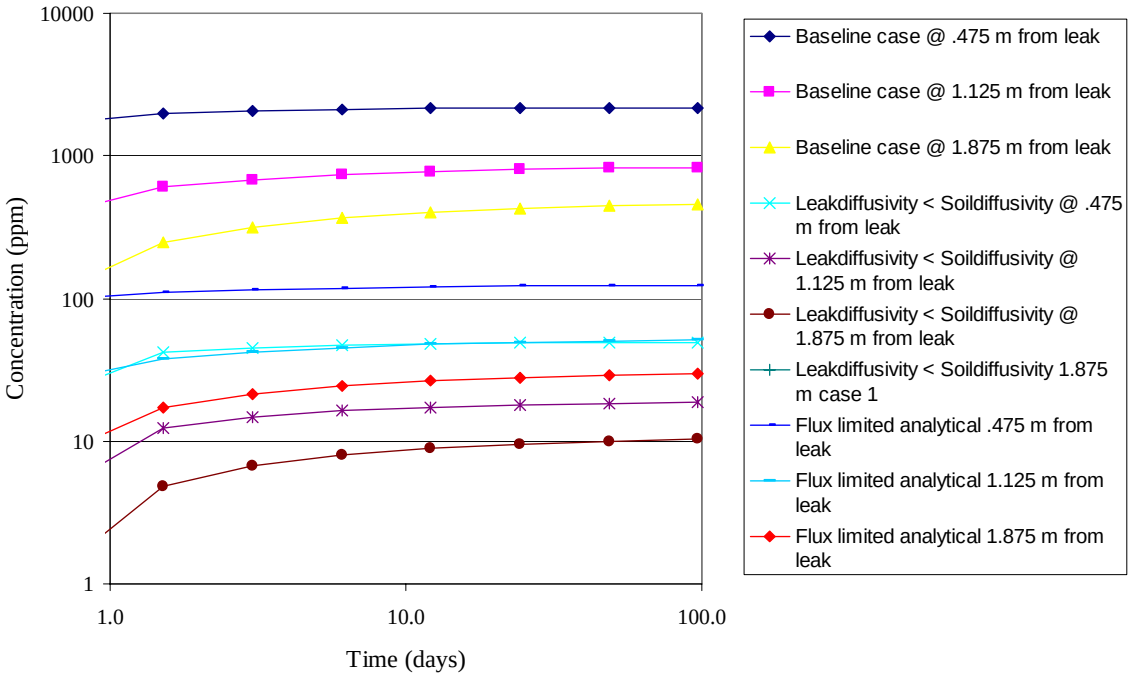

Figure C19. Calculated tracer gas concentrations versus time for numerical runs where the diffusivity of the leak is lower than that of the surrounding medium.

A saturated zone, or halo, would be caused by excess water from the grout injection during the construction of a grouted barrier. Based on the modeled soil parameters (permeability and porosity defined above in the baseline case), capillary effects were estimated to cause a semi-saturated thickness around the barrier of 0.5 m. For the numerical model, a region 0.5 m thick at a saturation of 50% was added to both sides of the barrier (and through the leak region). Figure C20 shows a plot of tracer concentration versus time for both the halo effect and the baseline case. At steady state conditions, the modeling results showed a reduced tracer gas concentration of about 1000 ppm (approximately 20%) for a point 0.15 m from the leak (within the saturated zone), and 1300 ppm (or approximately 3000%) for a point 0.725 m from the leak (outside the saturated zone). Additionally, it took much longer (days versus hours) for increased concentrations to be seen outside the leak.

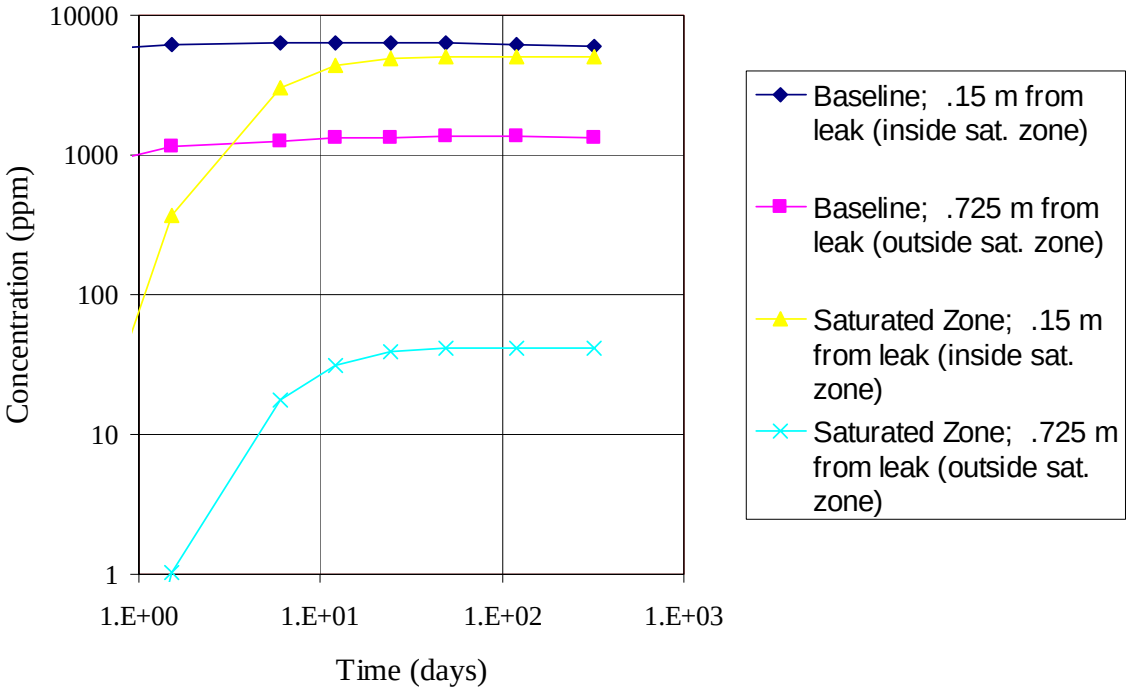

Figure C20. Calculated tracer gas concentrations versus time for numerical runs simulating a saturation halo around the barrier.

The results indicate the SEAtrace™ system would require a longer test duration to detect a leak, and would initially underestimate the size of a leak if the leak diffusivity was significantly lower than the medium diffusivity. If the leak area were to remain more highly saturated, contaminant migration would be minimized and this effect would not necessarily be problematic. However, with time the saturation within the leak would equilibrate with the surrounding medium, allowing the contaminants to migrate. Thus it is recommended that a barrier be tested both immediately after it is emplaced (to find large leaks and allow them to be repaired prior to equipment removal from the site) and at some time after emplacement when the liquid injected with the barrier material has dispersed into the medium and come to an equilibrium condition.

APPENDIX D:
RESULTS OF THE PFT TRACER TESTING AT THE WALDO TEST FACILITY

EWMG-SEA1-62599

Use of Perfluorocarbon Tracer (PFT) Technology
For Subsurface Barrier Integrity Verification at the Waldo Test Site

Prepared by

Terry Sullivan
John. Heiser
Gunnar Senum
and
Larry Milian

Brookhaven National Laboratory
Upton, NY 11973-5000

June 1999

USE OF PERFLUOROCARBON TRACER (PFT) TECHNOLOGY FOR SUBSURFACE BARRIER INTEGRITY VERIFICATION AT THE WALDO TEST SITE

D.1 Abstract

Testing of perfluorocarbon gas tracers (PFT) on a subsurface barrier with known flaws was conducted at the Waldo Test Site operated by Science and Engineering Associates, Inc (SEA). The tests involved the use of five unique PFTs with a different tracer injected along the interior of each wall of the barrier. A fifth tracer was injected exterior to the barrier to examine the validity of diffusion controlled transport of the PFTs. The PFTs were injected for three days at a nominal flow rate of 15 cm^3/min and concentrations in the range of a few hundred ppm. Approximately 65 liters of air laced with tracer was injected for each tracer. The tracers were able to accurately detect the presence of the engineered flaws. Two flaws were detected on the north and east walls, and one flaw was detected on the south and west walls. In addition, one non-engineered flaw at the seam between the north and east walls was also detected. The use of multiple tracers provided independent confirmation of the flaws and permitted a distinction between tracers arriving at a monitoring port after being released from a nearby flaw and non-engineered flaws. The PFTs detected the smallest flaw, 0.5 inches in diameter. Visual inspection of the data showed excellent agreement with the known flaw locations and the relative size of the flaws was accurately estimated. Simultaneous with the PFT tests, SEA conducted tests with another gas tracer sulfur hexafluoride (SF_6).

D.2 Introduction

One of the more promising remediation options available to the DOE waste management community is subsurface barriers. Some of the uses of subsurface barriers include surrounding and/or containing buried waste, as secondary confinement of underground storage tanks, to direct or contain subsurface contaminant plumes and to restrict remediation methods, such as vacuum extraction, to a limited area. Subsurface barriers will improve remediation performance by removing pathways for contaminant transport due to ground water movement, meteorological water infiltration, vapor- and gas-phase transport, transpiration, etc. Subsurface barriers are a remediation option for many of the DOE defense sites and are also considered an important remediation option by the USEPA [1].

To be most effective, the barriers should be continuous and depending on use, have few or no breaches. A breach may be formed through numerous pathways including discontinuous grout application, from joints between panels and from cracking due to grout curing or wet-dry cycling. The ability to verify barrier integrity is valuable to the DOE, EPA, and commercial sector and will be required to gain full public acceptance of subsurface barriers as either primary or secondary confinement at waste sites.

To fully assess a technology, the stakeholders must have tools available to measure the performance capabilities of the technology. The goal of any barrier installation should be

a product that is continuous, having as few holes as possible. Until now, no suitable method existed for the verification of an emplaced barrier's integrity. The large size and deep placement of subsurface barriers makes detection of leaks challenging. This becomes magnified if the permissible leakage from the site is low. Detection of small cracks (fractions of an inch) at depths of 100 feet or more has not been possible using existing surface geophysical techniques. Compounding the problem of locating flaws in a barrier is the fact that no placement technology can guarantee the completeness or integrity of the emplaced barrier. Several of the DOE programs are investigating variations of permeation grouting and jet grouting to emplace grout barriers. Permeation grouting is plagued by short-circuiting the flow of grout, which can leave large untreated areas. Jet grouting methods require straight boreholes and sufficient overlap of columns to maintain barrier continuity. Often the borehole wanders or the jet is partially obstructed by cobble or varying soil types, leaving a gap in the final barrier. Panel jet grouting may leave gaps between panels and/or at the junctions of horizontal and vertical barrier walls. Cementitious grouts are subject to desiccation and wet-dry cycling cracks. Additionally, at the time of gel formation, separations or "tears" may occur if localized settling takes place.

DOE has a need to develop/refine barrier verification methods to determine the existence, size, and location of breaches in a subsurface barrier. After such determinations, the effect of the breaches may be factored into the performance assessment of the waste site, or, more appropriately, the breaches could be repaired (and the repairs qualified with the same technology).

Gas tracers are a promising technology for barrier verification. Tracers can be injected inside of the barrier and detected in monitoring ports outside of the barrier. The concentrations on the outside can then be related to the integrity of the barrier. Gas tracers can provide information on the location and size of flaws in a matter of days to weeks. During this study, perfluorocarbon tracers (PFTs) were used to detect barrier imperfections.

D.3. Perfluorocarbon Tracers

A tracer is any substance that can be easily or clearly monitored (traced) in the study media. Tracer technologies can be used in transport/dispersion studies, leak detection studies, and material location. Leak detection studies use tracers to locate and estimate leak rates in various scenarios. These can be as simple as colored dyes used to visually locate cracks and holes in tanks or as complex as mass spectroscopy detection of helium to find leaks in vacuum systems. In transport and dispersion studies, tracers are used to tag a medium to determine how it is being dispersed in a surrounding matrix.

Brookhaven National Laboratory (BNL) has developed a suite of PFTs and has incorporated them into barrier continuity verification tests. These tracers were originally used in atmospheric and oceanographic studies and have since been applied to a great variety of problems, including detecting leaks in buried natural gas pipelines and locating radon ingress pathways in residential basements [3].

PFTs can be detected at extremely low levels. Parts per quadrillion are routinely measured. This allows detection of very small breaches in the barrier. A breach can be located by injecting a series of tracers on one side of a barrier wall and monitoring for those tracers on the other side. The injection and monitoring of the tracers can be accomplished using conventional low-cost monitoring methods, such as existing vadose zone monitoring wells or multilevel monitoring ports, placed using cone penetrometer techniques (e.g., Hydropunch). The amount and type of tracer detected on the monitoring side of the barrier will determine the size and location of a breach. It is easy to see that the larger the opening in a barrier, the greater the concentration of tracer is transported across the barrier. Locating the breach requires more sophistication in the tracer methodology. Multiple tracer types can be injected at different points along the barrier, in both vertical and horizontal directions. Investigation of the spectra of tracers coming through a breach then gives a location relative to the various tracer injection points.

PFT technology consists of the tracers themselves, injection techniques, samplers, and analyzers. PFTs have the following advantages over conventional tracers:

- Negligible background concentrations of PFTs in the environment. Consequently, only small quantities are needed.
- PFTs are nontoxic, nonreactive, nonflammable, environmentally safe (contains no chlorine), and commercially available.
- PFT technology is the most sensitive of all nonradioactive tracer technologies and concentrations in the range of 10 parts per quadrillion of air (ppq) can be routinely measured.
- PFT technology is a multi-tracer technology allowing up to six PFTs to be simultaneously deployed, sampled, and analyzed with the same instrumentation. This results in a lower cost and flexibility in experimental design and data interpretation. All six PFTs can be analyzed in 15 minutes on a laboratory-based gas chromatograph.

Typically, the PFTs are measured by a capillary adsorbent tracer sampler (CATS) which is a small cigarette-sized glass tube containing a carbonaceous adsorbent specific for the PFTs. This sampler can be used dynamically (flowing a sample through the CATS) or passively (opening only one end to allow the CATS to sample by diffusion). The passive mode allows a time-integrated PFT concentration to be measured in a simple manner. The CATS are shipped back to the laboratory for PFT analysis.

PFTs allow locating and sizing of breaches at depth and have a detection capability of flaws less than an inch in radius. The tracers themselves have regulatory acceptance and are used commercially for nonwaste management practices (e.g., detecting leaks in underground power cables). The major use of tracers will be to verify placement continuity of a freshly emplaced barrier and to recheck corrective actions that may be used to seal or repair a breach. PFTs may also prove useful in measuring some performance parameters (e.g., diffusion coefficient) of some higher permeability grouts (e.g., Portland cement) and will be useful to monitor a barrier to determine the long-term integrity of the walls. Tracers would allow determination of performance losses in containment over the life of the barrier.

D.4 Waldo Site Experimental Plan

The objective of this set of tests was to be able to determine the accuracy with which PFTs could locate and size known flaws in a subsurface barrier. SEA installed a test facility for this purpose; a complete description of the facility and test plan for this project can be found in Reference [4]. The test facility was originally designed to exercise the SEAtrace^{TM} system under conditions similar to those that would be encountered at a "real" barrier. The test volume consisted of a small-scale barrier with monitoring points both internal and external to the barrier. The shape and the dimensions of the barrier were chosen to be realistic, easily constructed, and capable of allowing a multitude of leak combinations to be tested. A V-shaped trench roughly 5-meters deep and 15-meters long was excavated (figure D1). The side walls and ends of the trench were sloped roughly 45^{o} from horizontal.

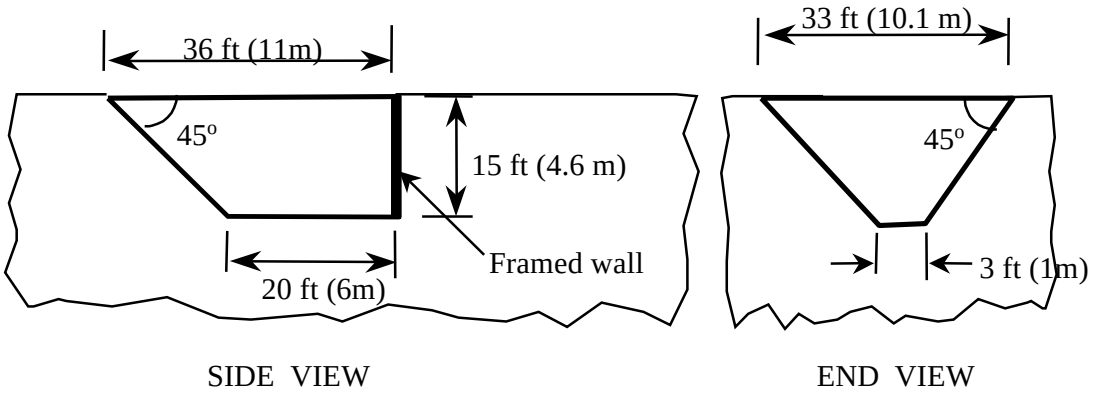

Figure D1. Schematic Overview of the Waldo Subsurface Test Site

After excavation, the south, east, and west walls of the trench were lined with a 4-inch layer of shotcrete, then a 30-mil thick sheet of plastic to create an impermeable barrier. The north wall, designated as the Framed Wall in figure 1, was covered with plastic. The region outside of the Framed Wall in figure 1 was backfilled and is more permeable than the native soils. Once the barrier was completed, the trench was also backfilled.

A series of 23 monitoring wells are placed exterior to the barrier. The wells are separated by approximately six feet at the surface. Within each well, there was one to four monitoring ports at different depths. The distance between ports within a well is also approximately six feet. In total, there are 62 external ports (figure D2). The depths of the monitoring ports were staggered between wells to provide more efficient coverage of the subsurface region (figure D2).

The test barrier had six known flaws open during the test. The flaws location and size are presented in table D1 and figure D3.

Table D1. Properties of the engineered leaks in the Waldo test barrier.

	LOCATION		LEAK RADIUS		LEAK DIAMETER		LEAK AREA		BARRIER THICKNESS	
PANEL	LATERAL, RELATIVE TO PANEL	DEPTH, RELATIVE TO PANEL	(IN)	(CM)	(IN)	(CM)	(IN^2)	(CM^2)	(FT)	(M)
EAST	CLOSEST TO NORTH PANEL	CENTER	7.5	19.1	15.0	38.1	176.7	1140.1	2	0.6
EAST	CLOSEST TO SOUTH PANEL	CENTER	2.0	5.1	4.0	10.2	12.6	81.1	4	1.2
SOUTH	CENTER	CENTER	2.0	5.1	4.0	10.2	12.6	81.1	0	0
WEST	CLOSEST TO SOUTH PANEL	CENTER	1.5	3.8	3.0	7.6	7.1	45.6	2	0.6
NORTH	CLOSEST TO EAST PANEL	CENTER	0.5	1.3	1	2.5	0.79	5.07	0	0
NORTH	CLOSEST TO WEST PANEL	CENTER	0.22	0.56	0.44	1.20	0.15	0.97	0	0

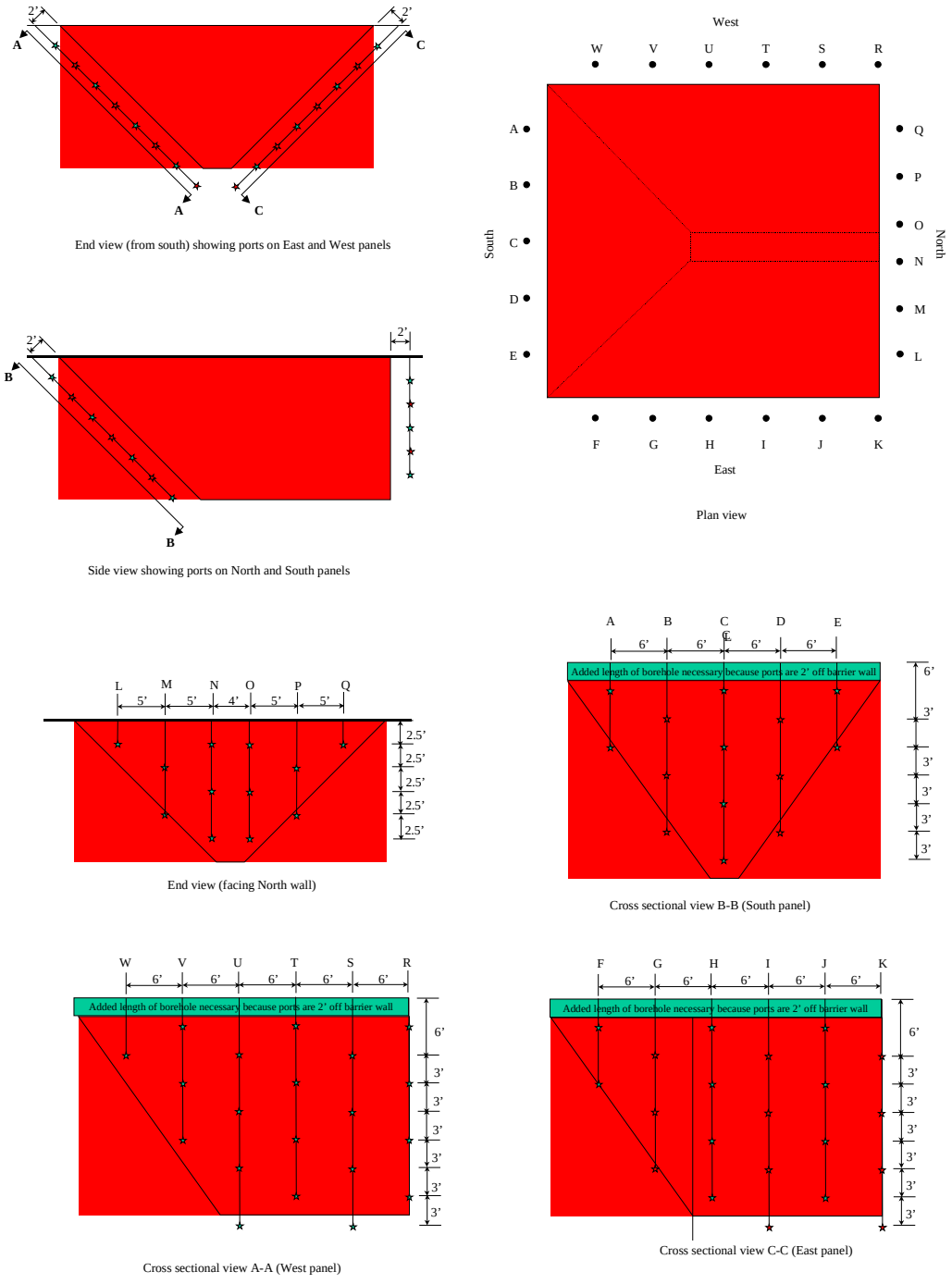

Figure D2. Scaled drawings of the well emplacement and designations. Side and end views of the test facility are shown in the upper right hand corner. A plan view is shown in the upper left-hand corner. Cross sectional views of the slant walls and a side view of the north wall are shown on the bottom half of the page.

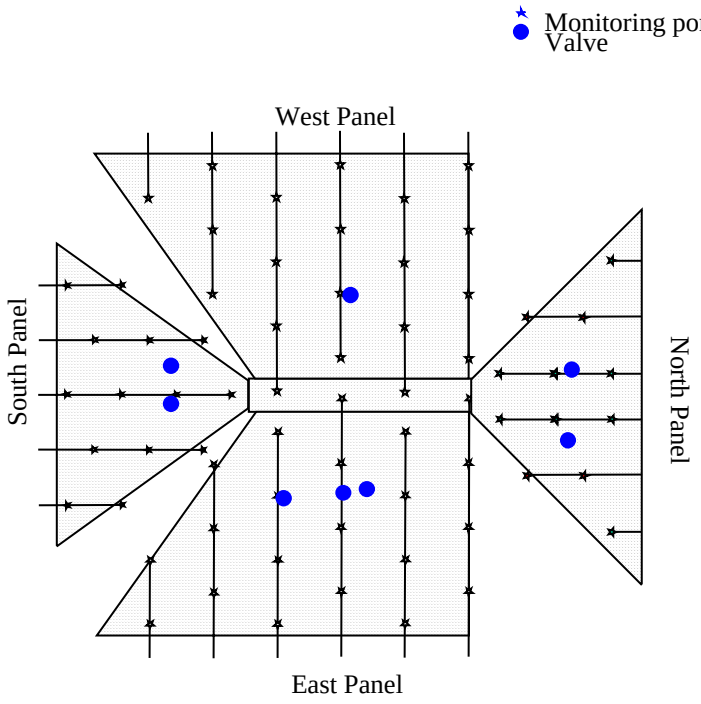

Figure D3. Engineered flaws in the Waldo test site for the PFT tests.

D.5 Experiment

D.5.1 Injection Schedule

One injection sequence was conducted as part of the test. The test began on November 4, 1998 with the injection of five different PFTs: PMCH, ocPDCH, p-PDCH, PTCH, and PMCP (table D2). The tracer concentrations in the injected air range from a few ppm to approximately one thousand ppm (table D3). The tracers injection flow rates are close to the design air flow rate of 15 cm^3/min (table D3). Four of the tracers were injected in the center region of the barrier near the centroid of each wall approximately one to two feet below grade. The fifth tracer, PTCH, was injected outside of the barrier in the fractured shale layer at monitoring port 52 on the west wall (table D2). This tracer will be used in an attempt to gain a better understanding of flow through this layer and the clay and alluvial layers above. The injection continued for three days until November 7, 1998. The location of each injection and monitoring port is labeled in figure D4. Injection ports are labeled IS, IE, IN, and IW for the four principle directions, south, east, north, and west, respectively. The relative mass as normalized to the PDCB mass of each tracer injected is also presented in table D3.

Table D2. Chemical acronym, name and formula for PFT tracers used in this study.

Chemical Acronym	Chemical Name	Chemical Formula
PDCB[1]	Perfluorodimethylcyclobutane	C_6F_{12}
PMCP[1]	Perfluoromethylcyclopentane	C_6F_{12}
PMCH	Perfluoromethylcyclohexane	C_7F_{14}
pt-PDCH	Perfluorotrans 1,4 dimethylcyclohexane	C_8F_{16}
PTCH	Perfluorotrimethylcyclohexane	C_9F_{18}

[1]PDCB and PMCP are chemically distinct isomers.

Table D3. Injection location, concentration, flow rate, and relative mass injected

TRACER	**LOCATION**	**INJECTION CONCENTRATION (PPM)**	**AVERAGE FLOW RATE (CM^3/MIN)[1]**	**RELATIVE MASS INJECTED[2]**
PDCB	SOUTH INTERIOR	141	13.1	1
PMCP	EAST INTERIOR	936	25.95	13.1
PTPDCH	NORTH INTERIOR	318	12.5	2.15
PMCH	WEST INTERIOR	447.5	13.45	3.26
PTCH	WEST EXTERIOR (MONITORING PORT 52)	122	4.15	0.27

[1]Flow rate measurements were taken initially and after one day. Difficulties with the flow meter prevented further testing. Reported values are the average of the two measurements.

[2]The relative mass is the product of the injection concentration and average flow rate of the tracer divided by the injection concentration and average flow rate of PDCB.

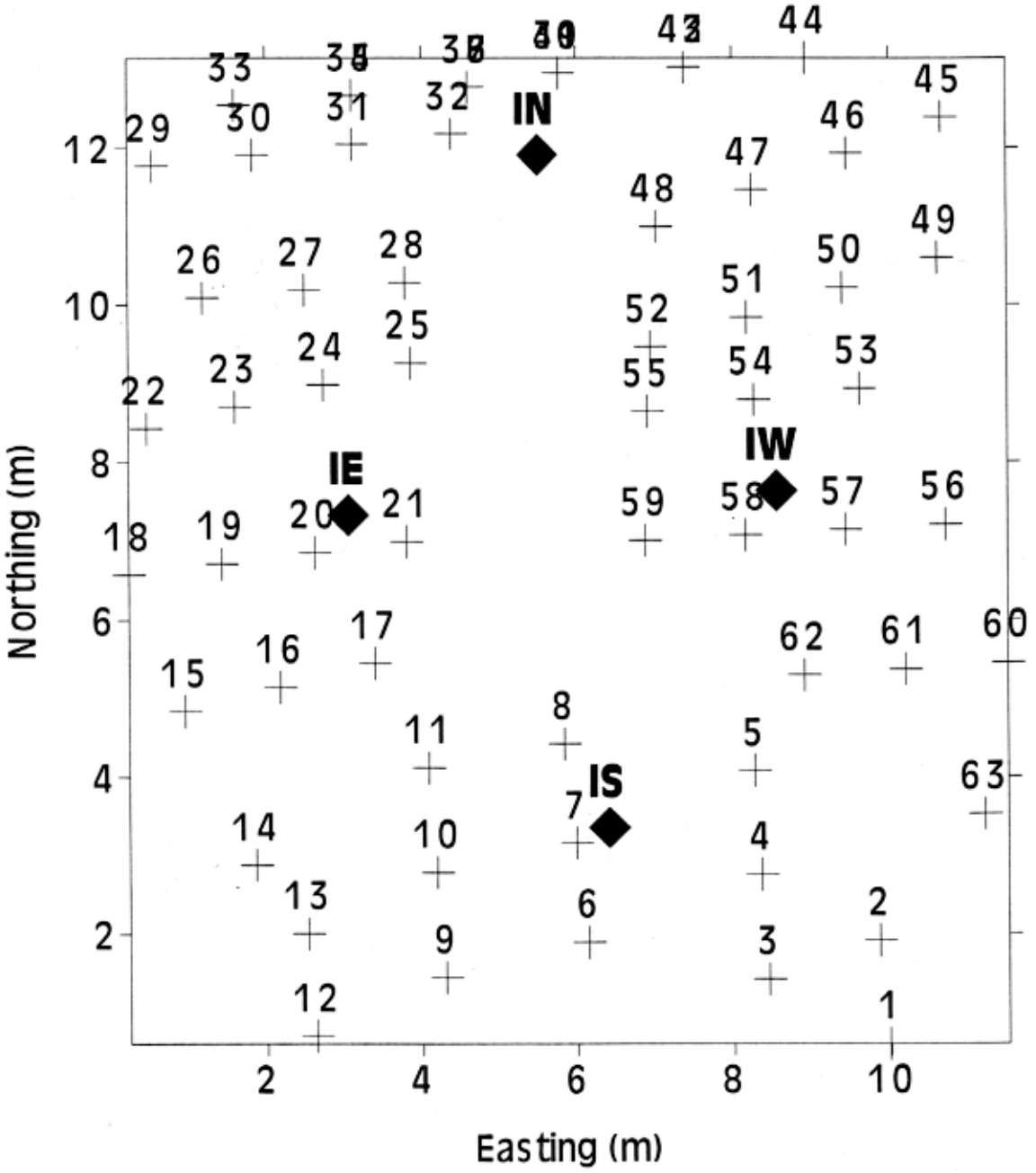

Figure D4. Plan view of injection and monitoring ports at the SEA Waldo test site.

D.5.2 Sampling Procedure

The sampling procedure included all monitoring ports on a one-day cycle. Monitoring began the day after the injection was started, November 5, 1998, and continued for two weeks, stopping on November 18, 1998. Samples were taken, placed on CATS, and shipped back to BNL for analysis. Sampling of interior ports was necessary to determine the distribution of contaminants inside the barrier after injection. Interior wells were sampled every other day after completion of the injection. A total of 846 samples were taken during the data collection phase of this study.

D.5.3 Results

The data were analyzed using a gas chromatograph to determine the concentrations of the tracers in each sample. This data was organized by the location of each sample point and a two-dimensional contour plot was generated for each day, wall, and contaminant using Surfer™. Over 100 contour plots were produced to examine the outcome of the test. The following figures, figure D5 through D9, are representative of the findings.

The PTCH tracer that was injected on the outside of the barrier demonstrated diffusion-controlled behavior on the exterior. It was only detected on the interior at one location during one sample collection period. This indicates that the area for flow into the barrier is small compared to the area for flow outside of the barrier. This is consistent with the small flaw sizes as compared to the total area.

Figures D5, D6, and D7 show the time evolution of PMCH detected in the monitoring ports on the west wall. PMCH was the tracer injected closest to the west wall and appears on the first day of sampling outside of the barrier. The concentrations show a remarkably consistent pattern for the duration of the experiment with the normalized concentration increasing from 10^{-5} to almost 10^{-4} after 5 days. There is a slow decrease in concentration for the remainder of the experiment. The data support a single flaw in the barrier located at 8.8 m (Northing) and -2.65 m depth.

Figures D8 and D9 show the time evolution of PDCB detected in the monitoring ports on the west wall. PDCB was injected in the interior near the south wall approximately five meters from the injection location of the PMCH. In figure D8, at early times, PDCB is detected at normalized concentrations of $3\ 10^{-7}$ at the lower left corner region of the diagram. This is near the intersection of the south and west walls. The PDCB normalized concentration is two orders of magnitude lower than the levels of PDCB on this wall. At Day 9, PDCB is detected in the region of the flaw detected by PMCH. The normalized concentration in this region increases to a maximum of $2\ 10^{-6}$, and it is the highest measured PDCB concentration on this wall. This PDCB data independently confirms the flaw at 8.8 m Northing and –2.65 m in depth. The concentrations at the lower left corner could be from a leak at the seam or from spill over from the hole on the south wall of the barrier. The concentration data for PDCB from the south wall indicate that this is due to movement around the outside of the barrier originating from the flaw in the south wall. This is further supported by the absence of any indication of a leak at the seam from the PMCH data. The use of distinct tracers was essential in determining if the concentration in this region was due to a flaw at the seam or due to transport around the outside of the barrier of tracer originating from another flaw.

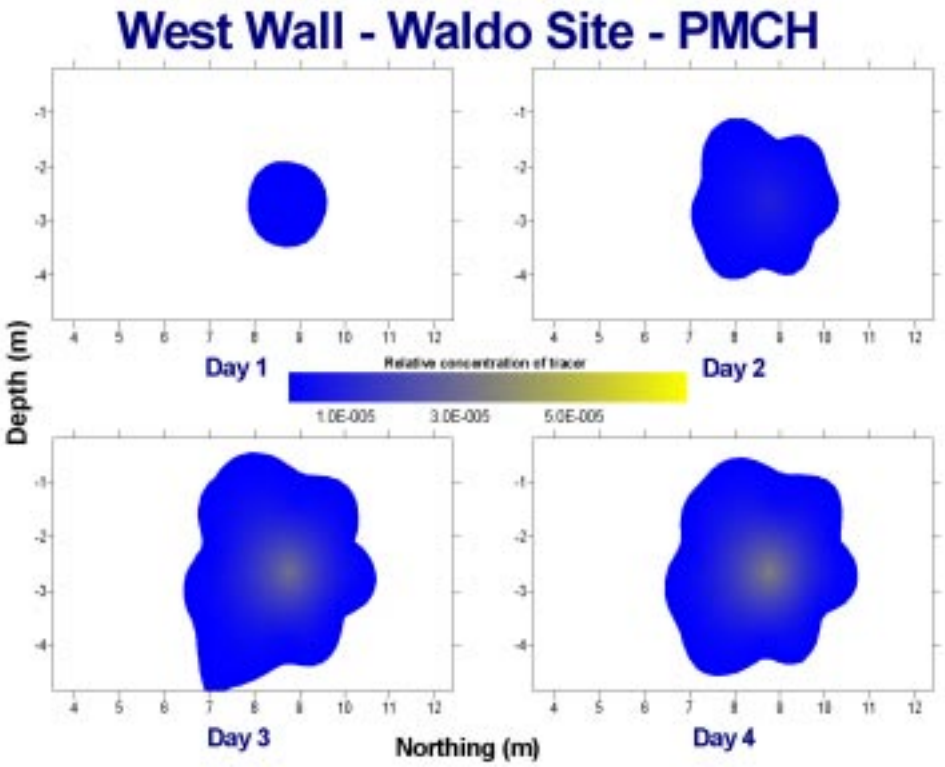

Figure D5. PMCH contours on days 1 –4 at the west wall.

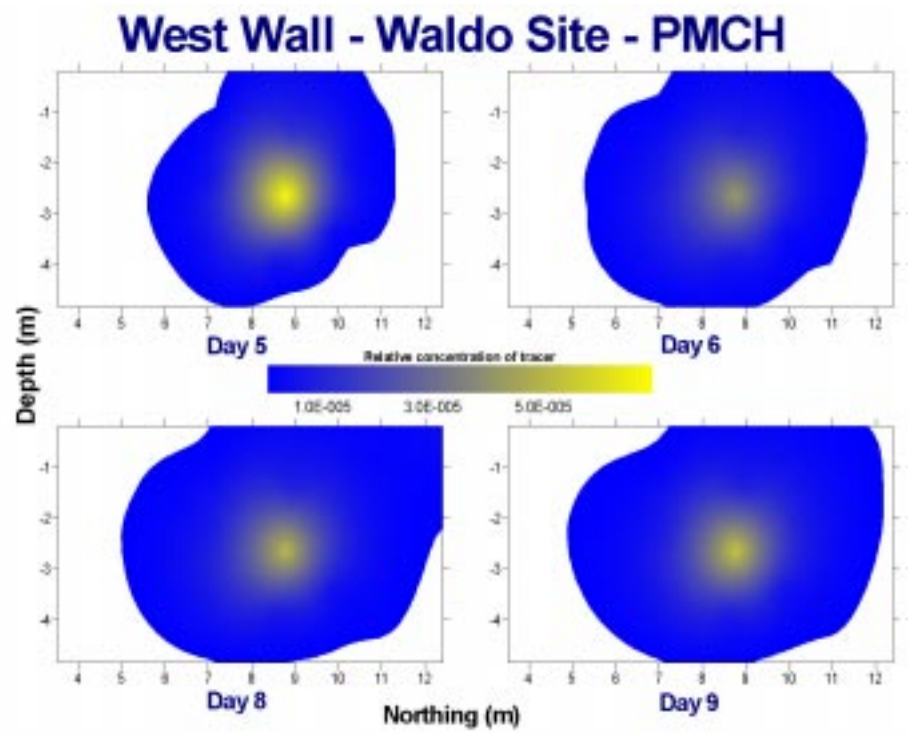

Figure D6. PMCH contours on eays 5 – 9 at the west wall.

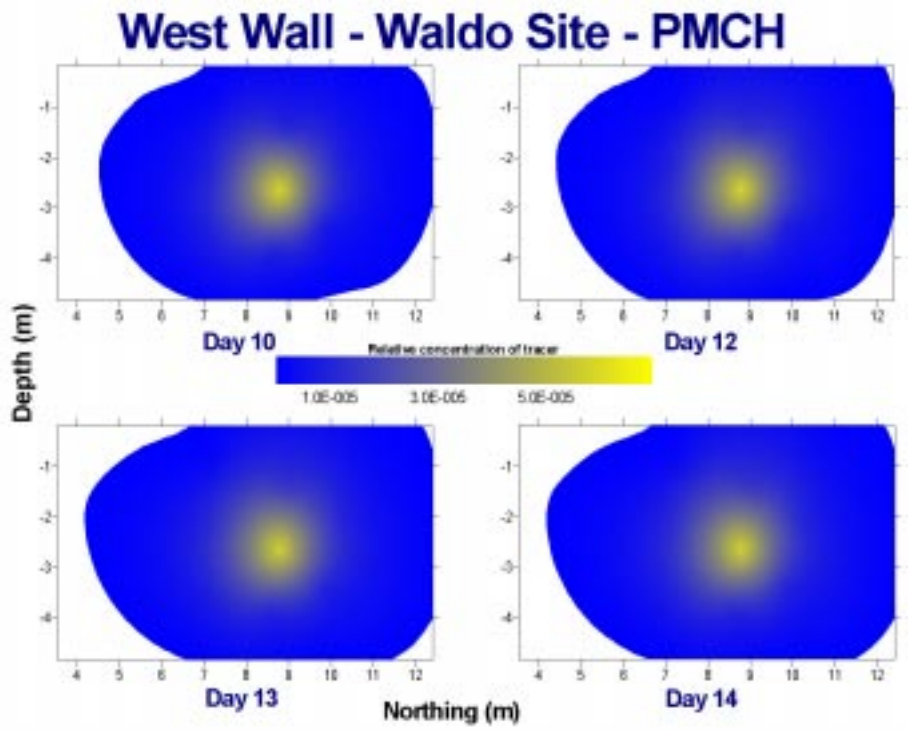

Figure D7. PMCH contours on days 10 – 14 at the west wall.

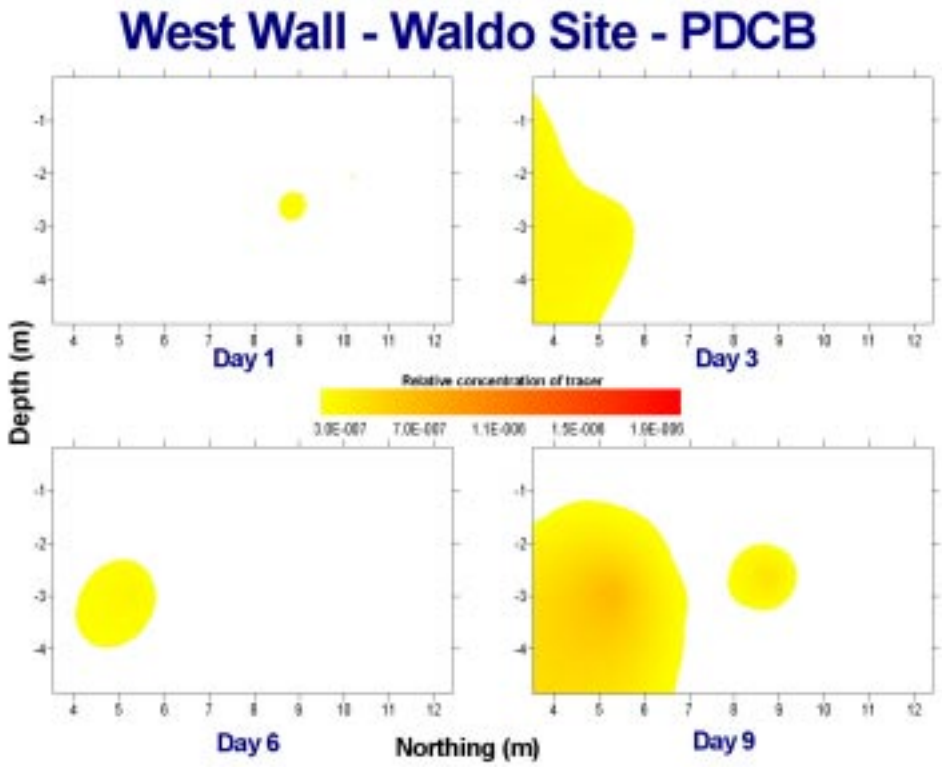

Figure D8. PDCB contours on days 1 – 9 at the west wall.

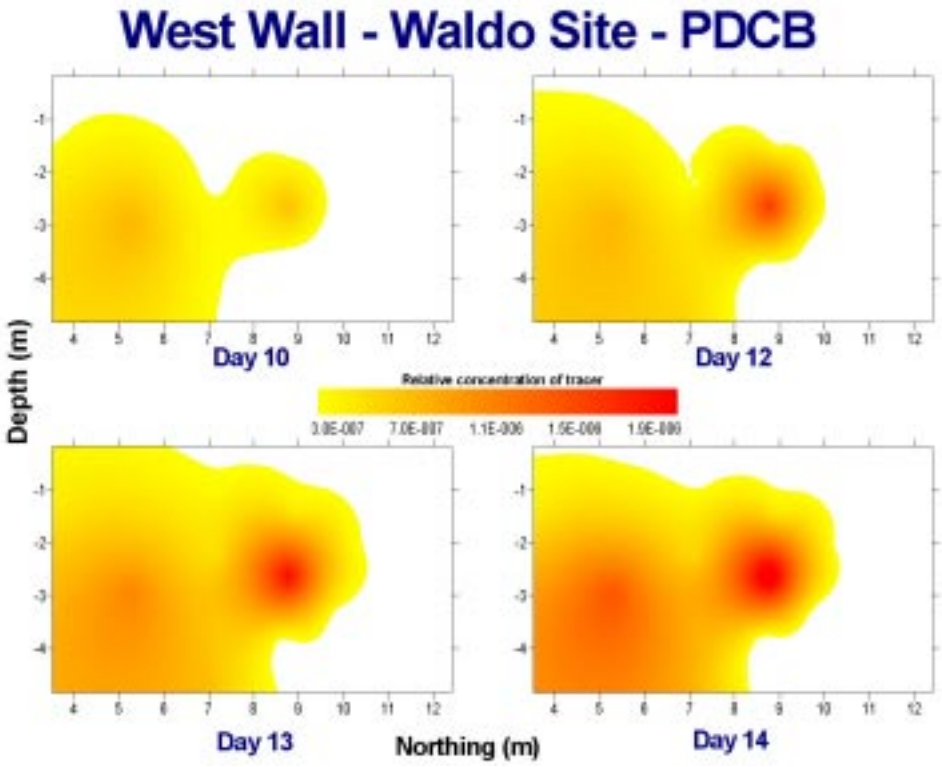

Figure D9. PDCB contours on days 10 - 14 at the west wall.

Data from other walls showed similar results. The south wall also had one flaw that was easily detected with the PFTs. The north wall had two small holes that were located by the PFTs. The east wall had three flaws. Two of these were engineered flaws, and the third occurred at the seam between the north and east walls. The non-engineered leak was confirmed by the ptPDCH injected on the north wall and the PMCP injected on the east wall. Table D4 presents the best estimate of the flaw locations in the plane of the monitoring ports based on the PFT data.

Table D4. Flaw locations in the plane of the monitoring ports.

ID	EASTING (M)	NORTHING (M)	DEPTH (M)
S1	6.0	3.1	-3.2
E1	3.1	12.1	-3.2
E2	3.6	9.6	-3.6
E3	2.6	7.0	-3
N1	5.8	13.0	-1.5
N2	4.6	12.8	-1.4
W1	8.25	8.8	-2.65

Flaw locations in table D4 are defined in the plane of the monitoring ports by direction (Easting, Northing, and Depth). For the north wall, reduce Northing by 0.7 m (2 ft) to get location on the wall. For other walls, projection is complicated by the 45-degree slope of the wall and the fact that the walls are not exactly parallel to the north or east axis. However, as a first approximation, assume that the walls are parallel. In this case, for the east and west walls, the depth is decreased by 0.5 m, and the Northing is reduced by 0.5 m on the west wall and increased by 0.5 m on the east wall. For the south wall, the Depth and Easting are increased by 0.5 m.

Figures D10 through D14 present the flow locations projected on the plane of the barrier. Figure D10 presents the plan view with all flaw locations. Figures D11 through D14 represent the side view for the south, east, north, and west walls, respectively.

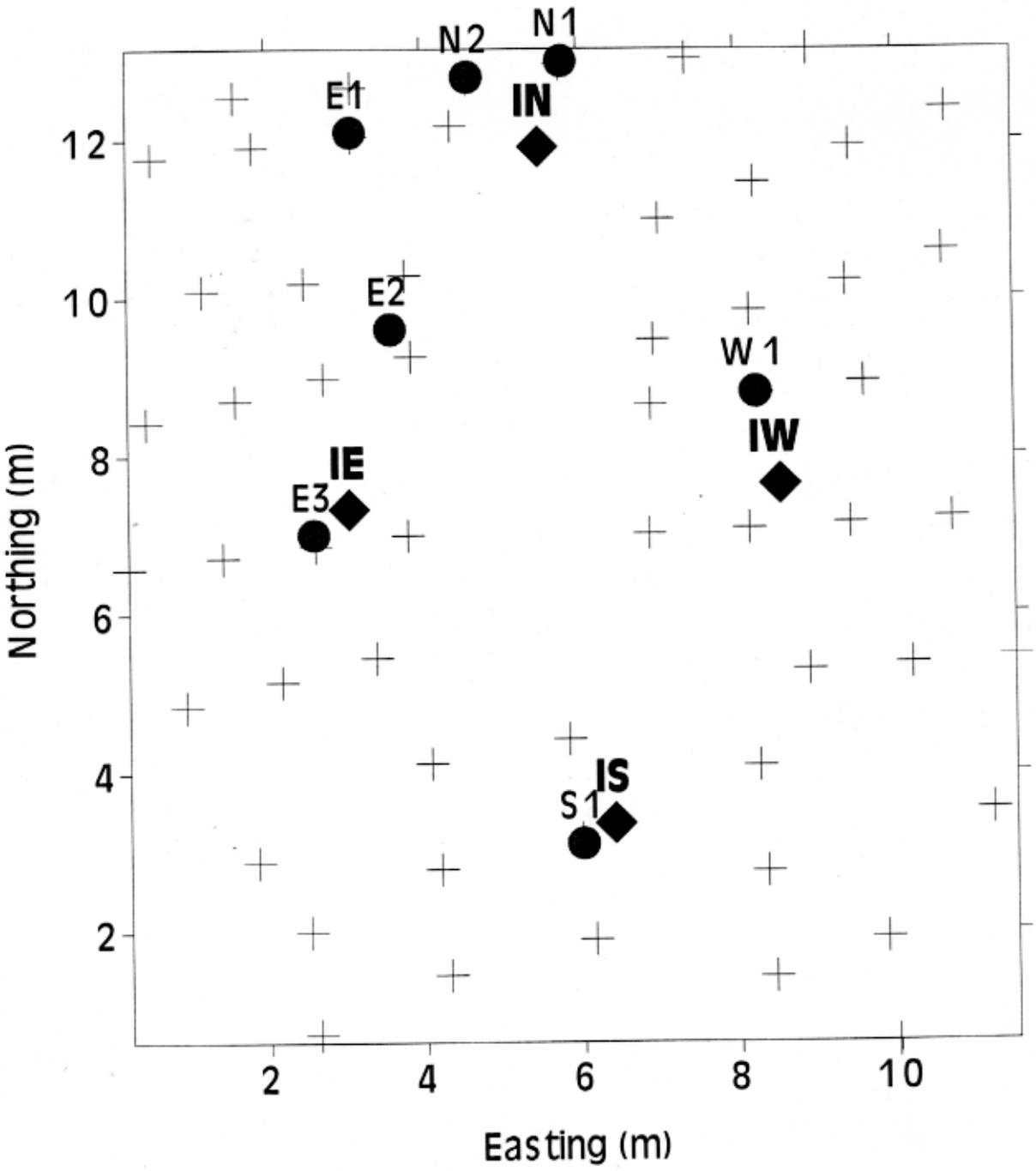

Figure D10. Plan view of injection port, monitoring port, and flaw locations.

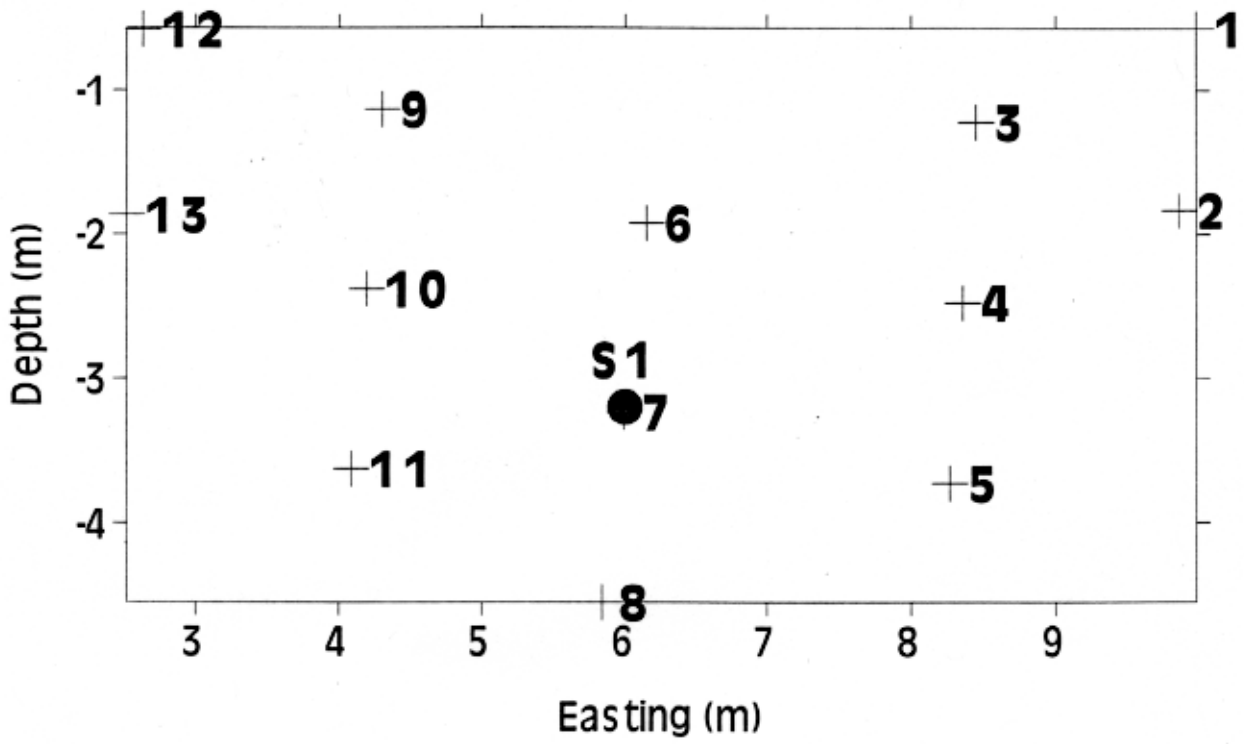

Figure D11. Side view of the flaw (circle) and monitoring port (+) locations on the south wall.

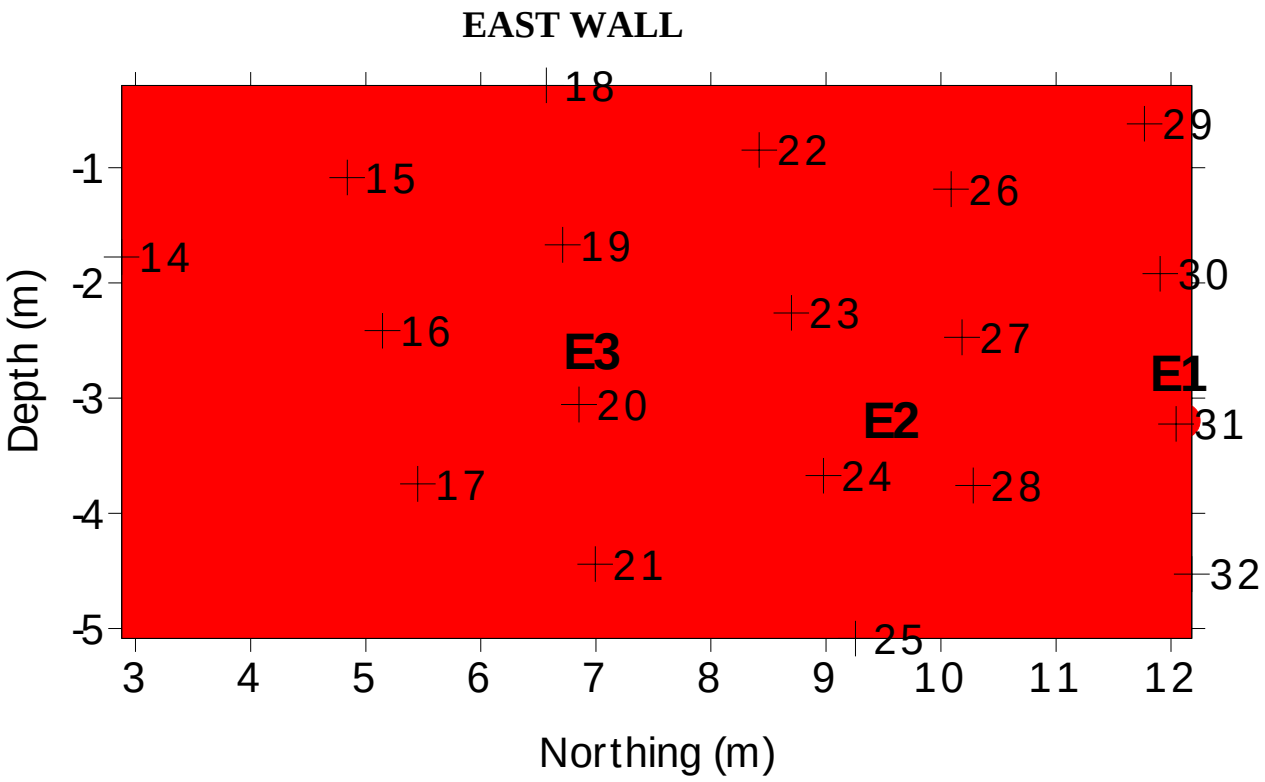

Figure D12. Side view of the flaw (circle) and monitoring port (+) location on the east wall.

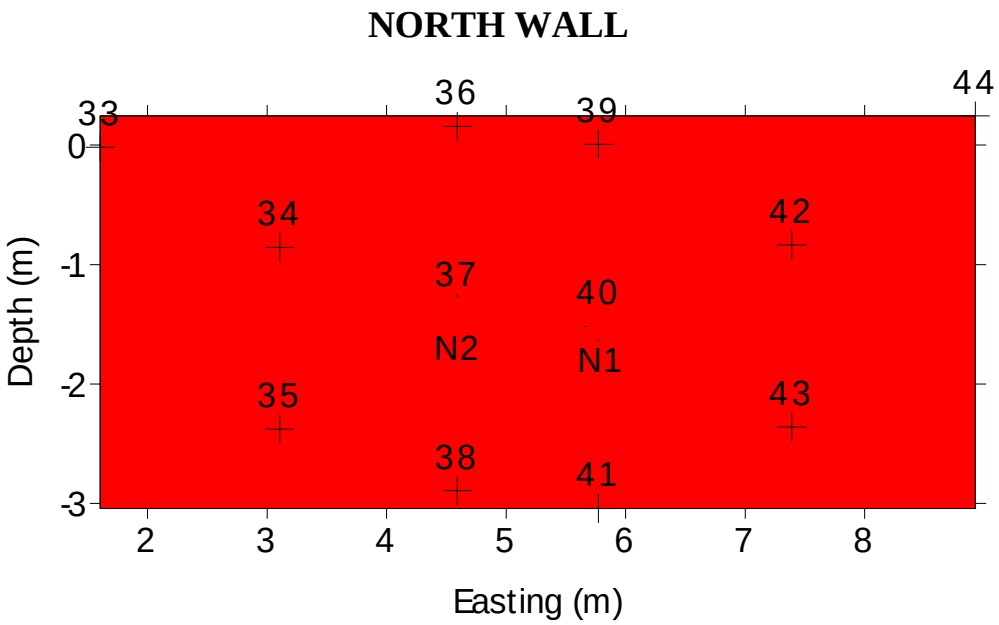

Figure D13. Side view of flaw (circle) and monitoring port (+) location on the north wall.

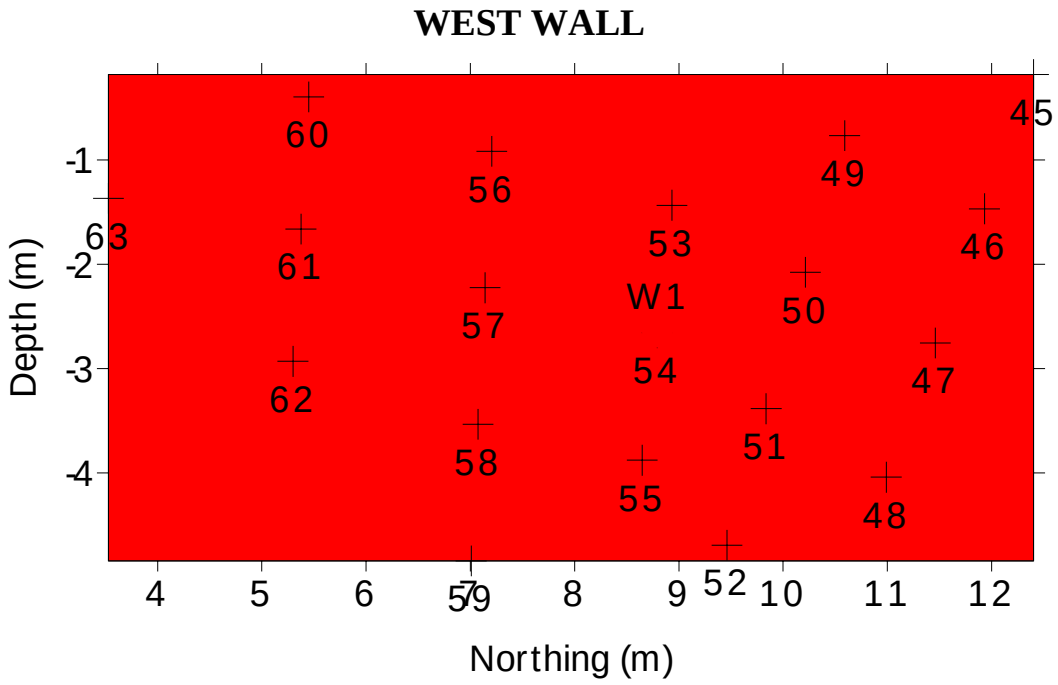

Figure D14. Side view of flaw (circle) and monitoring port (+) locations on the west wall.

Comparison of the projected flaw locations and the locations of the flaws as detailed in table D1 and figure D3 shows excellent agreement. The location of the six flaws is projected within one or two feet of the actual location. This estimate could be enhanced by numerical modeling of the movement of the PFTs in the subsurface. One non-engineered flaw was detected at the seam between the north and east walls.

Without detailed numerical modeling, it is not possible to estimate the flaw size. However, it is possible to examine the relative size of the flaws directly from the data. Assuming that the flaw is small in comparison to the size of the wall, it can be assumed that there is a uniform concentration across the flaw on the interior of the barrier. For a unit concentration on the interior of the barrier, the amount of mass that passes through the wall is directly proportional to the area of the wall. Therefore, to first approximation, the ratio of peak normalized concentrations inside and outside of the barrier is a measure of the area of the flaw, equation (1). Table D5 presents the peak internal, external, and measured concentrations normalized to injection concentration for each wall.

$$Area \propto \frac{Peak\ Exterior\ Normalized\ Concentration}{PeakInteriorNormalizedConcentration} \qquad \text{(Eq.1)}$$

Table D5. Peak internal and external measured concentrations normalized to injection concentration

WALL	TRACER	PEAK EXTERNAL CONCENTRATION	PEAK INTERNAL CONCENTRATION	PEAK CONCENTRATION RATIO
SOUTH	PDCB	2.90E-05	7.80E-03	3.72E-03
EAST	PMCP	3.50E-04	2.50E-03	1.40E-01
NORTH	PTPDCH	4.80E-06	1.00E-02	4.80E-04
WEST	PMCH	7.10E-05	9.20E-03	7.72E-03

Taking the peak normalized concentration ratio for each wall, the relative size of the flaw areas can be obtained. The area ratio can be obtained from the normalized concentration ratios, correcting for the different flow rates of injection (this is required to place everything on the same basis) as follows, Equation (2):

$$Area\ Ratio = \frac{Interior\ to\ Exterior\ Ratio\ \ for\ Wall\ X}{Interior\ to\ Exterior\ Ratio\ \ for\ East\ Wall} \bullet \frac{East\ Injection\ Gas\ Flow\ Rate}{Wall\ X\ \ Gas\ Flow\ Rate} \quad \text{(Eq.2)}$$

The average measured gas injection rates were presented in table D3. Using the flow rates and the normalized concentration ratios, an estimate of the flaw size can be obtained. Three cases are considered. In the first case, the largest flaw is normalized to a unit area. Thus, this column of the table gives the ratio of flaw areas. In the second case, it is assumed that the flaw is circular and the radius of the flaw is estimated normalizing the largest radius to 1. The third case considered the largest flaw to be circular with a 7.5-inch radius. The results are in table D6.

Table D6. Relative flaw area and flaw radius for each wall (sizes normalized to the largest flaw on the east wall)

Wall	Tracer	Area with Maximum Normalized to 1	Radius with Maximum Normalized to 1	Radius with Maximum Radius Normalized to 7.5 Inches.
SOUTH	PDCB	0.053	0.23	1.7
EAST	PMCP	1	1	7.5
NORTH	PTPDCH	0.00713	0.084	0.63
WEST	PMCH	0.106	0.32	2.4

The data show reasonable agreement with the actual flaw sizes. Normalizing the largest radius to 1 (East wall), the relative radius for the largest hole on each wall is 0.27 for the south and west walls, and 0.067 for the North wall. The data measured the relative flaw size within 25% of the actual relative flaw sizes.

D.6 Conclusion

Five PFTs were injected in and around a four-sided subsurface barrier that was approximately 10 m by 10 m at the surface and 5 m deep in the test facility at the Waldo Test Site operated by SEA, Inc. Four tracers were injected in the interior of the barrier, one in the center of each wall. The fifth was injected on the outside to confirm that diffusion controlled transport was the controlling transport mechanism. The tests involved a three-day injection scheme followed by a 14-day monitoring period. Monitoring began one day after the start of the injections.

The major findings of the experiment are:

- The PFTs were used to detect a total of seven flaws. This included the six engineered flaws and one non-engineered flaw at a seam between the north and east walls. Multiple flaws were detected on the east (three flaws) and north (two flaws) walls.
- The use of multiple tracers provided simultaneous and independent confirmation of flaw locations.
- The use of multiple tracers allowed monitoring of transport around the barrier. This permitted differentiation between tracers originating from flaws on the other sides of the barrier moving underneath the barrier and flaws in seams of the barrier.
- The PFT data were used to accurately determine the relative size of the flaws in each barrier. The east wall clearly had the largest flaw, the south and west walls had similar size flaws, and the north wall had the smallest flaws.

Numerical modeling of the hole sizes and locations was beyond the scope of work for this project. However, it is needed to improve definition of flaw size and location.

D.7 References

[1] Siskind, B., and J. Heiser, "Regulatory Issues and Assumptions Associated with Barriers in the Vadose Zone Surrounding Buried Waste," Environmental and Waste Technology Center, Brookhaven National Laboratory, February 1993, BNL-48749(I).

[2] Heiser, J., "Verification of Subsurface Barrier Integrity Using Perfluorocarbon Tracers," TTP CH3-5-PR-19, proposal to U.S. Department of Energy, Office of Technology Development, In Situ Remediation Integrated Program, March 1994.

[3] Deitz, R.N., “Perfluorocarbon Tracer Technology, Regional and Long-Range Transport of Air Pollution,” Elsevier Science Publishers, B.V. Amsterdam, The Netherlands, 215-247.

[4] Dunn, S.D., W. Lowry, V. Chipman, and T. Sullivan, “Draft Phase II Test Plan for the Gaseous Tracer Comparative Tests Conducted at the Waldo Subscale Barrier Test Facility”, SEA-SF-TR-98, October 1998.

APPENDIX E:
DRAFT PHASE II TEST PLAN FOR THE GASEOUS TRACER COMPARATIVE TESTS CONDUCTED AT THE WALDO SUBSCALE BARRIER TEST FACILITY

E.1 Introduction

Because of the importance of the containment integrity of subsurface barriers, the DOE has funded multiple verification / validation technologies. Two of these technologies involved testing the barrier with a gaseous tracer. Science and Engineering Associates (SEA) developed a system called SEAtrace™, and Brookhaven National Laboratory (BNL) has pioneered the use of perfluorocarbon tracers and highly sensitive detection equipment to verify the integrity of subsurface barriers.

The SEAtrace™ system is an integrated, real time gaseous tracer system. The methodology incorporates gaseous tracer injection inside the contained volume of soil with analysis of tracer arrival at sampling points outside of the barrier walls. Solar powered, remotely accessible, and capable of multimonth standalone operation, SEAtrace™ collects soil gas samples with an automated multipoint soil gas sampling and analysis system, then immediately analyzes this data to locate and size flaws in the barrier construction. Since the approach uses real time analysis to characterize flaws, immediate repair of the barrier may be conducted with the appropriate remedial method. Presently, the tracer gas used with SEAtrace™ is sulfur hexafluoride (SF_6). SF_6 is readily available, non-hazardous, and relatively inexpensive. It is easily detected with the photoacoustic gas analyzer used in the system. The gas analyzer is also capable of measuring volatile organic compounds in the gas phase, so the system is also well suited to long term monitoring of the barrier's integrity.

Brookhaven National Laboratory (BNL) has developed a host of perfluorocarbon tracers (PFT). As with the SEAtrace™ system, this methodology involves gaseous tracer injection inside the contained volume of soil with analysis of tracer arrival at sampling points outside of the barrier walls. With the PFTs, multiple tracer types can be injected at different points along the barrier (both vertical and horizontal). Investigation of the spectra of tracers coming through a breach then gives a location relative to the various tracer injection points. Soil gas samples are collected and analyzed manually. PFTs can be detected at extremely low levels, and parts per quadrillion are routinely measured. This allows detection of very small breaches in the barrier. The amount and type of tracer detected on the monitoring side of the barrier will determine the size and location of a breach. The key advantages of the PFTs are multiple tracers, regulatory acceptance, extreme sensitivity, and proven technology with commercial acceptance and use.

The two methodologies are similar to one another in many ways. SEA has focused primarily on autonomous, economical, real time data collection and analysis. SEAtrace™ is capable of producing locations and size estimates of breaches very quickly (within 12 – 24 hours after injection of the tracer gas. This quick turn around time would allow for the

initial verification of the barrier to be completed prior to equipment removal by the installation vendor, resulting in significant cost savings if breaches are found and need to be repaired. Conversely, BNL's focus has been predominantly concerned with the tracer gas and detection equipment. Perfluorocarbons can be detected in very low concentrations, requiring very little tracer to be injected into the contained barrier volume. Because there are numerous types of perfluorocarbon tracers that can be used, multiple verification tests can be completed either simultaneously or over time.

Both technologies have shown promise, so in addition to the original scope of this phase of the contract, DOE chose to fund a side by side comparison of the methodologies. The comparison is to be completed at the Waldo test facility built under the initial phase of this contract.

E.2 Description of the Test

The test facility was originally designed to exercise the SEAtrace™ system under conditions similar to those that would be encountered at a "real" barrier. The test volume consisted of a small-scale barrier with monitoring points both internal and external to the barrier. The shape and the dimensions of the barrier were chosen to be realistic, easily constructed, and capable of allowing a multitude of leak combinations to be tested. A V-shaped trench roughly 5 meters deep and 15 meters long was excavated (figure E1). The roughly 45^{o} from horizontal - a slope side walls and ends of the trench were sloped shallow enough to minimize construction hazards but steep enough that it would be economically viable to use at a real site. The trench was excavated using a trackhoe. Inspection of the trench afterward revealed three distinct geologic layers. The upper layer (approximately one third of the total depth) was an alluvial deposit; the middle layer (approximately one third of the total depth) a clay layer, and the bottom third was a dense but highly fractured shale. A vertical wall was formed at one end of the trench after the trench had been excavated. As soon as the trench was completed, holes for the exterior monitoring ports were emplaced perpendicular to the walls using a hand held K-V penetrometer. Holes were roughly 1" in diameter and 2' deep. Three-quarter inch PVC pipe was used to keep the holes open until the points were surveyed and the ports emplaced. Ports were connected to the monitoring system via 1/8 inch o.d., 1/16 inch i.d. polyethylene tubing. The annulus around the ports/tubing was backfilled with a bentonite/sand mixture (immediately around the sample locations only sand was used). After the ports were installed, the trench was sprayed with a 3-4" layer of gunnite concrete. The gunnite stabilized the trench walls, held the flanges for the valves (part of the engineered leaks) in place, and provided a smooth surface for the membrane to lay against. A 30 mil plasticized polyvinylchloride geomembrane composed the primary barrier to gas migration. A professional landfill company installed the membrane. After the liner was in place, the valves were attached to the flanges to act as controllable, known leaks sources of various sizes. Figure E2 is a schematic of a typical valve assembly, and figure E3 is a photograph of two of the valves after they were emplaced. The different lengths of soil-filled pipes incorporated in each valve assembly simulate various barrier thicknesses. Boots of the liner material were used to seal around the valve assemblies. The barrier was then backfilled. Finally, the trench area was covered with a surface seal (40 mil high density polyethylene plastic sheeting) to prevent both excessive

loss of the tracer to the atmosphere and water infiltration. The surface seal was covered with a 2-3" layer of native soil for protection. Figure E4 is a schematic of the completed test barrier.

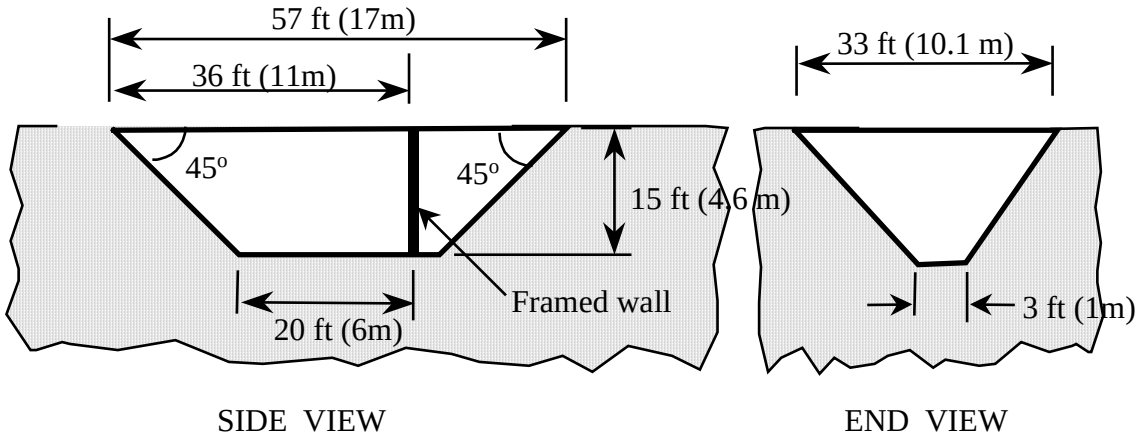

Figure E1. Approximate dimensions of the test facility at the Waldo site.

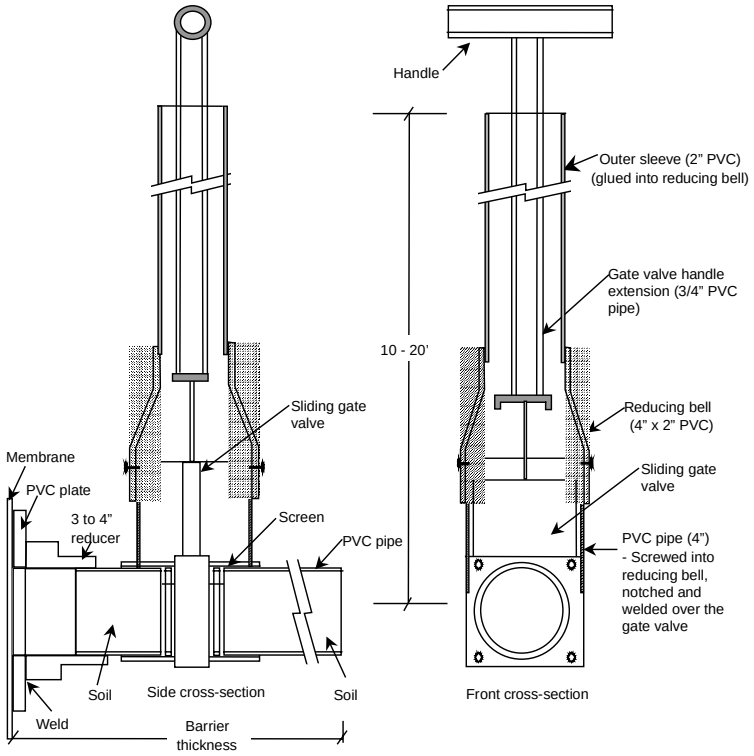

Figure E2. Typical gate valve assembly used to define the engineered leaks at the Waldo site test barrier.

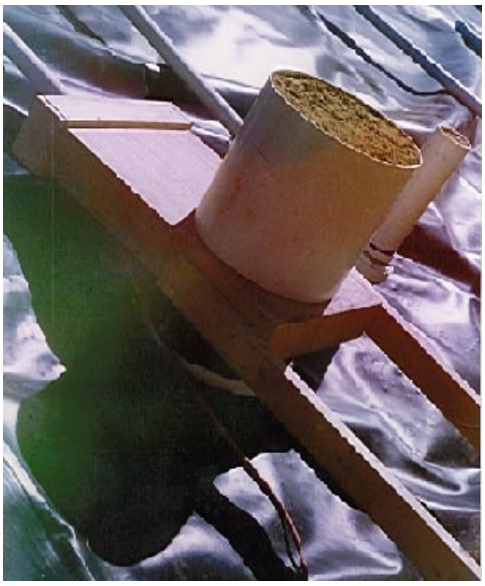

Figure E3. Photograph of engineered leak valve assemblies. Assembly in the foreground simulates a 15" diameter leak, in a 2' thick barrier. Assembly in the background simulates a 4" diameter leak in a 2' thick barrier.

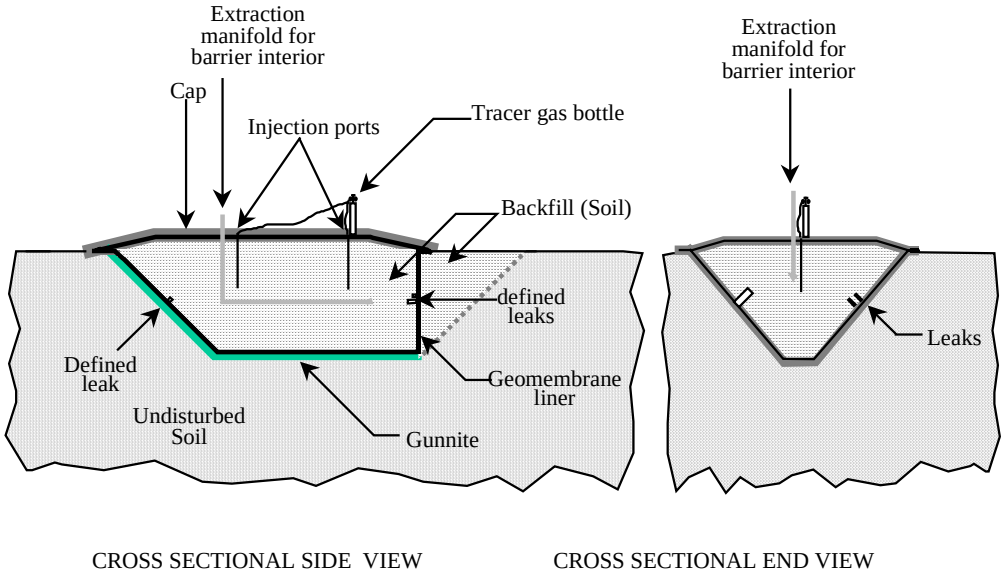

Figure E4. Sketch of the completed test facility at the Waldo site.

There are six engineered leaks within the test barrier. Table E1 lists the leak radius and corresponding wall thickness along with other pertinent information of each defect. It is important to note that the design of the engineered leaks allows for all but the smallest leak (on the north panel) to be closed.

Between the time that the original work at the test facility was completed (October 1997) and the time that the DOE opted to perform the comparison tests (July 1998) the test facility incurred some damage. Cattle grazing around the facility damaged or moved much of the protective pipe around the sample tubing, leaving the tubing exposed. Rodents chewed through much of the tubing. Rather than try to repair the tubing and then deduce what port it was connected to, the decision was made to install new ports around the barrier. Figures E5 and E6 show the new designed port installation. Ports on the east, west and south panels will be spaced on 6 foot (1.8 meter) intervals on a plane parallel to and 2 feet (0.61 meters) from the barrier panels. Rows of ports will be offset 3 feet (0.9 meters) from one another. The port spacing on the north panel will be slightly different from the other panels. This panel is smaller than the others, and the spacing previously described does not provide the best coverage for the number of ports available. The ports will be emplaced as shown in figure E5. Boreholes will be formed with a 4 in hollow stem auger.

Table E1. Properties of the engineered leaks in the Waldo test barrier.

	LOCATION		LEAK RADIUS		LEAK DIAMETER		LEAK AREA		BARRIER THICKNESS	
PANEL	LATERAL, RELATIVE TO PANEL	DEPTH, RELATIVE TO PANEL	(IN)	(CM)	(IN)	(CM)	(IN^2)	(CM^2)	(FT)	(M)
EAST	CLOSEST TO NORTH PANEL	CENTER	7.5	19.1	15.0	38.1	176.7	1140.1	2	0.6
EAST	CLOSEST TO SOUTH PANEL	CENTER	2.0	5.1	4.0	10.2	12.6	81.1	4	1.2
SOUTH	CENTER	CENTER	2.0	5.1	4.0	10.2	12.6	81.1	0	0
WEST	CLOSEST TO SOUTH PANEL	CENTER	1.5	3.8	3.0	7.6	7.1	45.6	2	0.6
NORTH	CLOSEST TO EAST PANEL	CENTER	0.5	1.3	1	2.5	0.79	5.07	0	0
NORTH	CLOSEST TO WEST PANEL	CENTER	0.22	0.56	0.44	1.20	0.15	0.97	0	0

Ports will be connected to the monitoring system via 1/8" od, 1/16" id polyethylene tubing. The number of ports to be emplaced in each well will be bundled prior to emplacement. Tubing in the bundle will be held apart from one another with T-clips. The clips provide a defined space that will allowed backfill material to flow between the tubes, forming a more complete vertical seal. After the tubes are lowered in place, the borehole will be backfilled using a mixture of 2 parts bentonite flour to 5 parts silica sand by weight. Under the first phase of this contract, the effective air permeability of the different geologic layers at the site and the proposed backfill material were measured. Results are given in table E2. The permeability of the backfill material was equal to or lower than the medium surrounding the ports, which will minimize preferential removal of pore gas from the borehole during sample collection. Note that permeability data was not obtained for the fractured shale geologic layer as it was not possible to obtain a good sample for the laboratory tests. Subsequent air extraction from this layer has shown that soil gas can move easily through this layer, presumably through the fractures. As such, the backfill material that will be used should provide adequate protection against creation of a short circuit pathway along the borehole during sample collection. However, it is also highly likely that tracer gas movement in this region will be dominated by flow along the discrete fractures. Figure E6 roughly shows the different geologic layers at the sites, the engineered leak locations, and the port locations. The sketch shows the panels

as if they were rotated around the bottom panel and laid flat. Port locations are then superimposed over panels.

Tubing will be routed from individual monitoring wells into a common 2" pvc pipe. The 2" pipe will terminate near the scanning system. The pipe will protect the tubing from ultraviolet light and other forms of damage.

Table E2. Laboratory measured effective air permeabilities of the different soils at the barrier test facility in Waldo, NM.

MEDIUM DESCRIPTION	**MEASURED PERMEABILITY (DARCIES)**
Alluvium (top geologic layer)	10
Clay (middle geologic layer)	4
Crusher fines (backfill behind north wall)	25 – 40
Backfill (5:2 silica sand/bentonite flour)	3

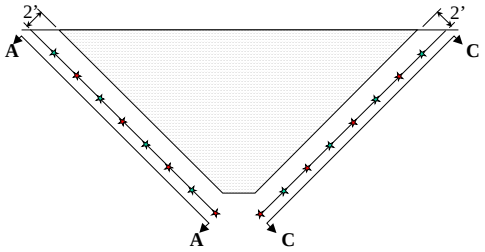

End view (from south) showing ports on East and West panels

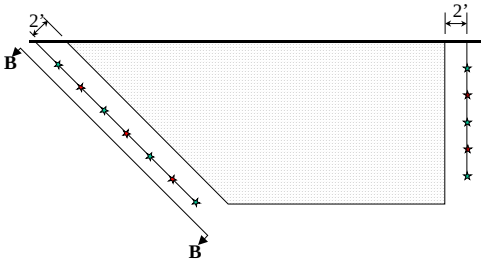

Side view showing ports on North and South panels

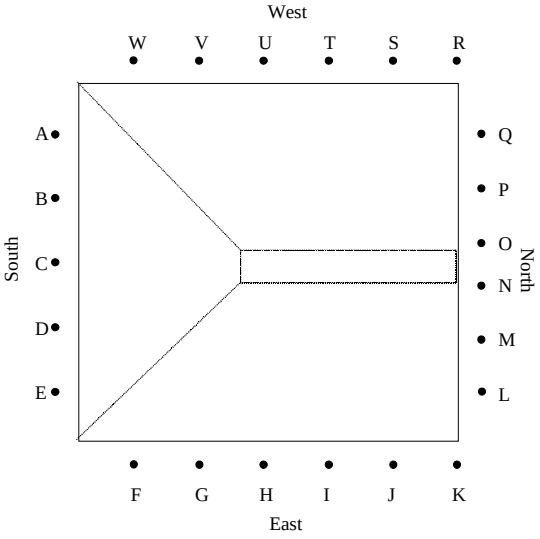

Plan view

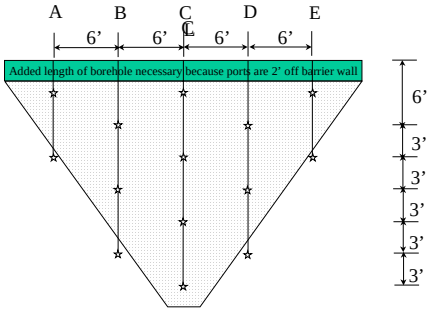

Cross sectional view B-B (South panel)

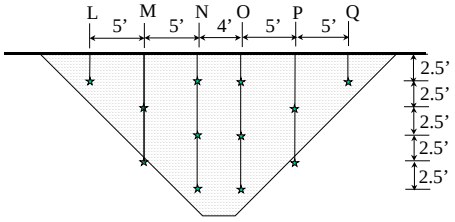

End view (facing North wall)

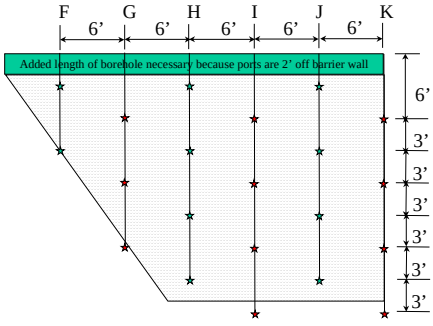

Cross sectional view C-C (East panel)

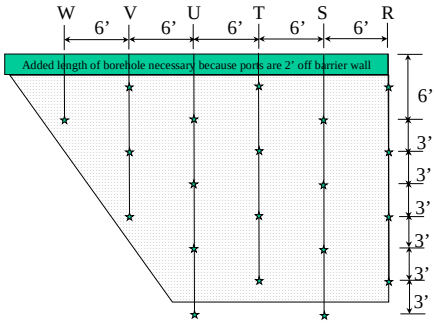

Cross sectional view A-A (West panel)

Figure E5. Scaled drawings of the proposed well/monitoring port emplacement and designations.

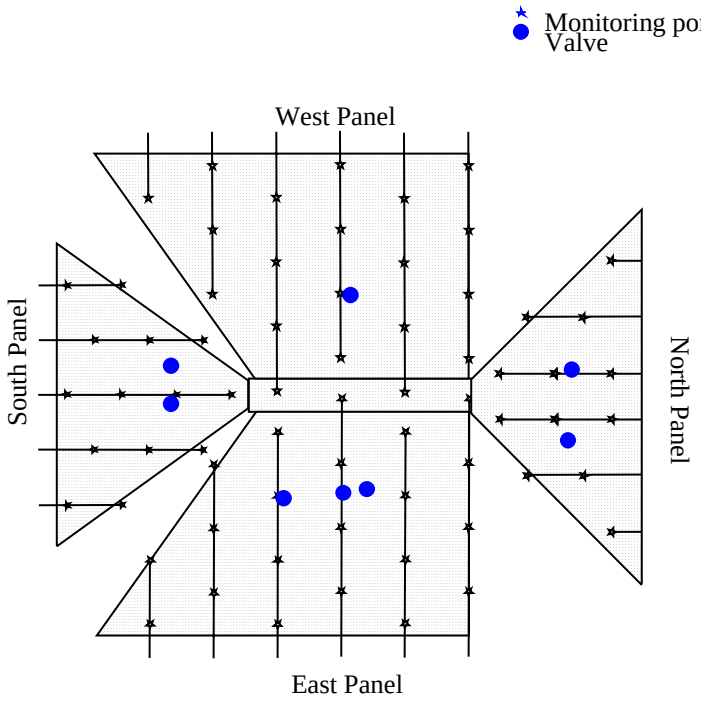

Figure E6. Proposed locations of the new monitoring ports (shown as stars on the schematic), viewed as if the panels were opened around the bottom of the barrier. The existing engineered leaks are depicted as circles.

E.3 Experiment Design

The SEAtrace™ and PFT tests will be conducted in series after the site is prepared for testing to assure the injection of the SF_6 does not interfere with the PFT tracer. The total duration of the test program is expected to be four to six weeks.

E.3.1 SEAtrace™/SF_6

The SEAtrace™ methodology and testing experience is described in SEAtrace™, A Solution to subsurface Barrier Validation[1]. The basic design for the SEAtrace™ system installation is driven by the size of the leak that must be detected given the various parameters that influence that value. The design includes:

- Determining the monitoring port placements
- Determining the method of port emplacement and appropriate backfill of the boreholes
- Determining the injection port placements and the overall injection scheme
- Determining a means to verify that the monitoring system is functioning properly

[1] Lowry et. al, *SEAtrace™ A Solution to Subsurface Barrier Validation*, Science and Engineering Assoc., Santa Fe, NM; SEASF-TR-98-188.

The first two issues were discussed above, but a more detailed description of how the port spacing was chosen will be given below. The injection port placements, injection scheme, and means to verify the monitoring system will also be discussed below.

E.3.1.1 Monitoring Port Spacing and Locations for the Demonstration. The primary design issues in the application of SEAtrace™ are the gas sample port locations and spacing. Determining the port spacing is very critical to the success of the SEAtrace™ system, and there are numerous things that must be considered. Uncontrollable variables (from the system's viewpoint) include medium properties (diffusivity, porosity, tortuosity, permeability), barrier properties (diffusivity, porosity, tortuosity, permeability), barrier dimensions (thickness as well as the overall area which must be verified), and barrier construction. Many of these variables are unknown, and estimates must used in the calculations. Other variables that influence port spacing include the source concentration (which is limited only by the amount of soil gas that could realistically be replaced with the tracer), the allowable measurement time to complete the verification, and the minimum size of the leak that is desired to be detected.

The initial step in determining the port spacing is to calculate the minimum area each monitoring port must cover. This is a function of the area of barrier to be tested at a given time, and the number of available monitoring ports. The test barrier in question is small enough that the entire barrier can be monitored at once. The total area of the barrier is roughly 2,000 sq. ft. Given 64 available monitoring ports, this requires a minimum area for each port to cover of approximately 30 sq. ft. Because of the shape of the barrier panels, and the need to have monitoring ports below or near the edges of the panels to provide adequate coverage of those edges, the area each port will need to cover will be greater than the minimum. In order to minimize the necessary test period, a port spacing that provided coverage per port near the minimum value (figure E5) was used in numerical calculations to predict the minimum leak size that could be found by the system given certain assumptions. These calculations are described below.

A flux limited forward model and a spherical diffusion model (Section 3.2.2. *Forward models*) were used to estimate resulting medium concentration histories for different input parameters. In particular, calculations were completed for several combinations of source concentration, barrier thickness and the minimum detectable concentration required to be recorded at the maximum distance between a leak anywhere on the barrier and at least three monitoring ports. Details of the calculations can be found in attachment A. Table 3 is a summary of the results. The table shows the smallest leak that could be found for the various cases. The highlighted cells show when, during the test sequence, the system would detect the different engineered leaks given a maximum test duration of one week for each source concentration. If the measured background concentration of the tracer gas, SF_6, is very low, then any measured tracer at the exterior monitoring ports can be assumed to be from a leak in the barrier. Under these conditions, all of the engineered leaks except the 2" diameter, 4' thick leak on the East panel would be seen after the initial low concentration source injection (2500 ppm). That leak would only be seen after the second stepped injection (7500 ppm). If the measured background concentrations at the monitoring ports are not zero, then the SEAtrace™ system will

"see" a leak as the concentrations at the ports exceed the background concentration. The maximum anticipated background value of the tracer at any of the ports is assumed to be 10 ppm. Using this value as the minimum assumed detection limit, none of the engineered leaks will be seen after the initial low concentration source injections (2,500 ppm and 7,500 ppm). The small diameter leaks on the north wall would be seen after the source concentration is increased to 20,000 ppm. The remaining engineered leaks would not be seen until the source concentration was stepped up to the maximum target concentration.

Initial results from the SEAtrace™ system will be calculated based on concentration measurements recorded at all of the exterior monitoring ports. In addition, the inversion code will be run on subsets of the data to determine how a much coarser grid of monitoring ports would effect the results of the system.

Table E3. Summary of the calculational results completed with the forward diffusion models for the Waldo demonstration. Values were calculated for a port grid of 6' horizontal by 6' vertical grid, where adjacent columns of ports are skewed 3' from one another. The plane of the sampling ports is 2' from the barrier wall. The minimum distance the tracer must be able to be detected for this port spacing is slightly less than 2.0 meters.

Assumed Detection Limit (ppm)	**Barrier Thickness (feet)**	**Min. Leak Radius that Could be Seen Given a Source Concentration of:**							
		2500 ppm, 7 day test		**7500 ppm, 7 day test**		**20,000 ppm, 7 day test**		**100,000 ppm, 7 day test**	
		(cm)	**(in)**	**(cm)**	**(in)**	**(cm)**	**(in)**	**(cm)**	**(in)**
1	0	2.0E-1	7.8E-2	7.0E-2	2.8E-2	2.5E-2	1.0E-2		
1	2	6.0	2.4	3.5	1.4	2.2	0.9		
1	4	8.5	3.4	5.0	2.0	3.0	1.2		
10	0	2.0	7.0E-1	6.5E-1	2.6E-1	2.5E-1	1.0E-1		
10	2	19.0	7.5	11.0	4.3	5.7	2.3	3.0	1.2
10	4	27.0	10.6	15.5	6.1	9.5	3.7	4.2	1.7

E.3.1.2 Injection Port Spacing and Locations for the Demonstration. Tests completed under the initial phase of this contract coupled with research of typical "real" barrier installations showed a need for a more structured injection scheme for the tracer gas than initially used. During the initial testing of the system, emphasis was placed on injecting the tracer gas through a limited number of centrally located ports in the barrier interior. The assumption with this approach was that the tracer would equilibrate rapidly within the contained volume creating a constant source concentration. Research showed that

barriers are often emplaced around tens to hundreds of acres at a contaminated site. The volume contained by these barriers would make creating a constant source concentration throughout the entire volume prohibitive, both from cost and time standpoints. Additionally, field results showed that it was possible (probable) that immediate injection of the tracer to a high target concentration would result in exterior medium concentrations from large leaks high enough at distant monitoring ports that smaller leaks in the barrier would be masked. Thus the most complete verification of barriers would include multiple injection steps that would create a relatively constant concentration at the barrier wall for a given period of time. Multiple injection ports would be needed, with each port generating a source concentration over a defined area of the barrier wall. The initial injection would be a low concentration to check for large leaks. Areas of the barrier where leaks are found would be maintained at the low source concentration until adequate data is collected. The source concentration at other areas of the barrier would be increased incrementally until the target concentration is achieved. This method of injection would increases the detail of SEAtrace™ results without flooding the medium with the tracer and without the need to maintain a constant concentration throughout the entire barrier volume.

Numerical calculations were performed with T2VOC[2] to establish a relationship between the mass of tracer / injection port location / equilibration time / duration of the "constant" concentration. These calculations are discussed in Attachment B.

Testing the new injection scheme at the Waldo test facility will be difficult due to the small size of the barrier. Numerical calculations showed injection ports could be spaced on 18 foot centers under typical test conditions. However, this spacing at the Waldo facility would result in creating a constant concentration throughout the entire barrier volume. Placement of the injection ports was scaled down to 9 foot centers.

The starting concentration for the injection scheme will be 2,500 ppm. After 7 days, additional gas will be injected to increase the source concentration to 7,500 ppm for areas of the barrier where no leaks (or very small leaks) were detected. After 7 days, the source concentration will be increased to 20,000 ppm. Finally, after an additional 7 days, the source concentration will be raised to the target demonstration concentration of 80,000 to 100,000 ppm in any areas of the barrier that leaks have not been detected.

E.3.1.3 Leak Anomaly. Acceptance of the SEAtrace™ systems results by regulators will be dependent on the belief that the system is working as designed. Testing a controlled leak best validates this, particularly if actual validation testing shows a barrier to be integral. Thus SEA has adopted the practice of installing an engineered leak (leak anomaly) near any barrier that is to be tested. The leak anomaly will be located in close proximity (within 50 ft.) to the barrier. A small container is buried to a shallow depth (5 to 10 ft below ground surface). The container acts as the source volume. A gate valve attached to the container forms the "leak." A 1.5-inch diameter valve will be used.

[2] Falta, R., K. Pruess, S. Finsterle, and a. Barristelli. 1995. *T2VOC User's Guide*. Lawrence Berkeley, CA: LBL-36400, Lawrence Berkeley National Laboratory.

Small diameter tubing from the surface to the container is used to inject the tracer gas into the source volume. The test commences with the opening of the "leak". Monitoring ports are installed near the leak anomaly, at the same spacing used to monitor the barrier. The leak anomaly will be tested immediately after completion of barrier validation.

E.3.2 Perfluorocarbons

Use of perfluorocarbon (PFT) gaseous tracers shows promise as an excellent means of demonstrating barrier integrity. This technique was pioneered by Brookhaven National Laboratory[3]. In a typical experiment, the tracers are injected on one side of a barrier and monitoring ports, located on the other side of the barrier, are used to measure the release of the gas through the barrier. The test facility developed by SEA has been prepared by introducing flaws of known size and location. This experiment focuses on the use of PFTs to detect the flaws.

E.3.2.1 Injection Schedule. One injection sequence will be conducted as part of the test. The test design calls for injection of five different PFTs: PMCH, ocPDCH, p-PDCH, PTCH, and PMCP. These tracers may change based on their availability at the time of the experiment. The tracer concentrations in the injected air range from a few ppm to approximately one thousand ppm. All tracers will be injected at a nominal air flow rate of 15 cm^3/min for a period of three days. Four of the tracers will be injected in the center region of the barrier near the centroid of each wall. The fifth tracer will be injected outside of the barrier in the fractured shale layer. This tracer will be used in an attempt to gain a better understanding of flow through this layer and the clay and alluvial layers above. If experimental problems are encountered in detecting a tracer, or anamolous results are occurring a sixth tracer may be injected after the start of the experiment to help resolve the encountered problem.

E.3.2.2 Sampling Procedure. The sampling procedure will initially sample all monitoring ports on a one-day cycle. Samples will be taken, placed on CATS, and shipped back to Brookhaven for analysis. The turnaround time should be two days. All samples will be archived in case problems arise with the first sample. It is anticipated that the travel times to the exterior monitoring points from the injection point will be on the order of a few days to a week. Based on sample results, a revised sampling schedule may be developed. Termination of the experiment will be based on the data. Typically for experiments of this size, the concentrations outside of a flaw reach their peak at one to two weeks after injection. After this time, there is a slow steady decline at that location. When the data indicates that the declining regime is occurring, the experiments will be discontinued. This is expected to take approximately two weeks from the injection period.

[3] Heiser, J. H. 1994. *Subsurface Barrier Verification Technologies*, BNL-61127. Brookhaven National Laboratory.

E.3.2.3 Interior Sampling. Sampling of interior ports is necessary to determine the distribution of contaminants inside the barrier after injection. This may be particularly important if the SF_6 injections occur after the PFT injections causing advective transport on top of diffusive transport. Interior wells will be sampled every other day.

E.4 Experimental Results

The purpose of the test is to allow two similar technologies to be tested under the same conditions. A comprehensive comparison of the technologies will not be addressed. This comparison could only be completed if system costs, ease of use, timeliness of the systems results, and overall accuracy of the systems were reviewed. However, data will be represented in similar formats such that the DOE can make an evaluation of the accuracy with which each technology/type of tracer can detect the location and size of the flaws. Data reported for each technology will include:

- Test chronology (injection, sampling, analysis)
- Injected tracer mass(es) and injection timing
- Concentration histories at sampling locations
- Resulting leak locations and sizing information, presented versus the actual locations and sizes
- Results of additional post test analysis

E.5 Attachment A -- Calculations to Determine Sample Port Spacing

The primary design issue in the application of SEAtrace™ is the gas sample and injection port locations. Determining the spacing of the sample ports is very critical to the success of the SEAtrace™ system, and there are numerous things that must be considered. Uncontrollable variables (from the system's viewpoint) include medium properties (diffusivity, porosity, tortuosity, permeability), barrier properties (diffusivity, porosity, tortuosity, permeability), barrier dimensions (thickness as well as the overall area which must be verified), and barrier construction. Many of these variables are unknown, and estimates must be used in the calculations. Other variables that influence sample port spacing include the source concentration (which is bounded by the amount of soil gas that could realistically be replaced with the tracer, and is a function of the injection port location, mass injection rate, and medium properties), the measurement time of verification, and the minimum size of the leak that is desired to be detected.

A flux limited forward model (Section 3.2.2. *Forward Models*) was used to estimate resulting medium concentration histories for different input parameters for cases where the barrier thickness was not negligible. A spherical diffusion forward model (Section 3.2.2. *Forward Models*) was used to estimate resulting medium concentration histories for the input parameters for the cases of negligible barrier thickness. Assumptions / ranges for the input parameters included:

1. The effective diffusivity of the leak/medium was assumed to be 5.0e-6 m^2/s based on results from prior testing at the site and laboratory measurements.
2. Source concentrations used in the calculations were 2500, 7500, 20,000 and 100,000 ppm. These values correspond to the target injection concentrations. The exit concentration was calculated using the relationship $C_{exit} = C_{source}$ (.7 –

5714D). This relationship was developed using results from numerical modeling and was shown to be accurate if the medium diffusivity was equal to the leak diffusivity.

3. Barrier thickness' were chosen to be 0, 2 and 4 feet. These values correspond to the thickness' of the engineered leaks.
4. Leak radius was varied to find the minimum value that would allow a detectable amount of tracer (assumed to be 1 ppm) to be seen a distance of 6.3 feet (roughly 2.0 m) from the leak. This distance is the maximum distance a leak would be from at least 3 ports closest to it given a 6' horizontal x 6' vertical skewed grid port spacing that was 2' from the barrier.
5. The time used for each calculation corresponded to the anticipated delay between the different injection pulses. The initial target concentrations of 2,500, 7,500 and 20,000 ppm will sequentially be maintained for a period of 3 days each after a 4 day equilibration period (assuming that tracer is not detected at any of these concentrations). The final target concentration of 100,000 ppm will be maintained for the duration of the test time.
6. The minimum assumed detection limit at the monitoring ports used in the calculations was either 1 or 10 ppm. The 1 ppm limit assumes that there is no existing tracer in the medium prior to the initiation of the test. Because tracer was injected at the facility during previous tests, it is likely that this assumption will not be true. Spot measurements at the site show a background concentration around 10 ppm. Thus additional calculations were performed using 10 ppm as the detection limit, e.g. the increase in tracer seen at a port would need to be of the same order of magnitude as the background concentration for the system to easily locate the leak.

Results are summarized in table E-A1. Figures E-A1 through E-A20 graph the calculational results for the various cases.

Table E-A1. Summary of the calculational results completed with the forward diffusion models for the Waldo demonstration. Values were calculated for a port grid of 6' horizontal by 6' vertical grid, where adjacent columns of ports are skewed 3' from one another. The plane of the sampling ports is 2' from the barrier wall. The minimum distance the tracer must be able to be detected for this port spacing is less than 2.0 meters.

ASSUMED DETECTION LIMIT (PPM)	BARRIER THICKNESS (FEET)	MIN. LEAK RADIUS THAT COULD BE SEEN GIVEN A SOURCE CONCENTRATION OF:							
		2500 PPM, 7-DAY TEST		7500 PPM, 7-DAY TEST		20,000 PPM, 7-DAY TEST		100,000 PPM, 7-DAY TEST	
		(CM)	(IN)	(CM)	(IN)	(CM)	(IN)	(CM)	(IN)
1	0	2.0E-1	7.8E-2	7.0E-2	2.8E-2	2.5E-2	1.0E-2		
1	2	6.0	2.4	3.5	1.4	2.2	0.9		
1	4	8.5	3.4	5.0	2.0	3.0	1.2		
10	0	2.0	7.0E-1	6.5E-1	2.6E-1	2.5E-1	1.0E-1		
10	2	19.0	7.5	11.0	4.3	5.7	2.3	3.0	1.2
10	4	27.0	10.6	15.5	6.1	9.5	3.7	4.2	1.7

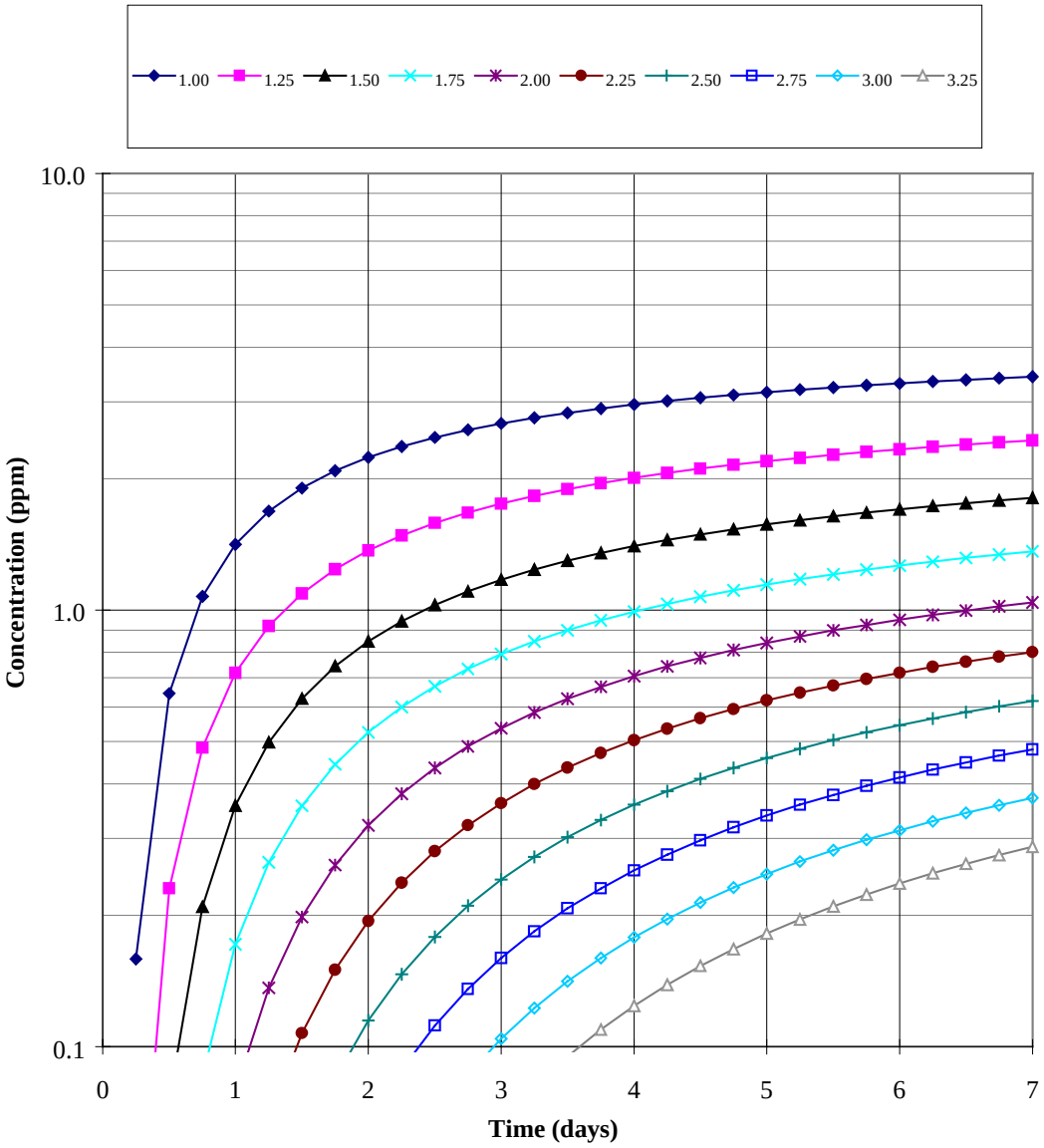

Medium Diffusivity	5.00E-06 m^2/sec		
Source Concentration	2500 ppm	15175 mg/m^3	
Barrier Thickness	0.00 feet	0.00 meters	
Leak Radius	0.2 cm	2.0E-03 meters	7.9E-02 inches
Leak Area	0.13 sq. cm.	1.9E-02 sq. in.	

Figure E-A1. Results from the spherical diffusion model showing the minimum leak size that could be detected at a 2.0-m detection distance, given the conditions listed above (2,500 ppm source concentration, 0' thick barrier).

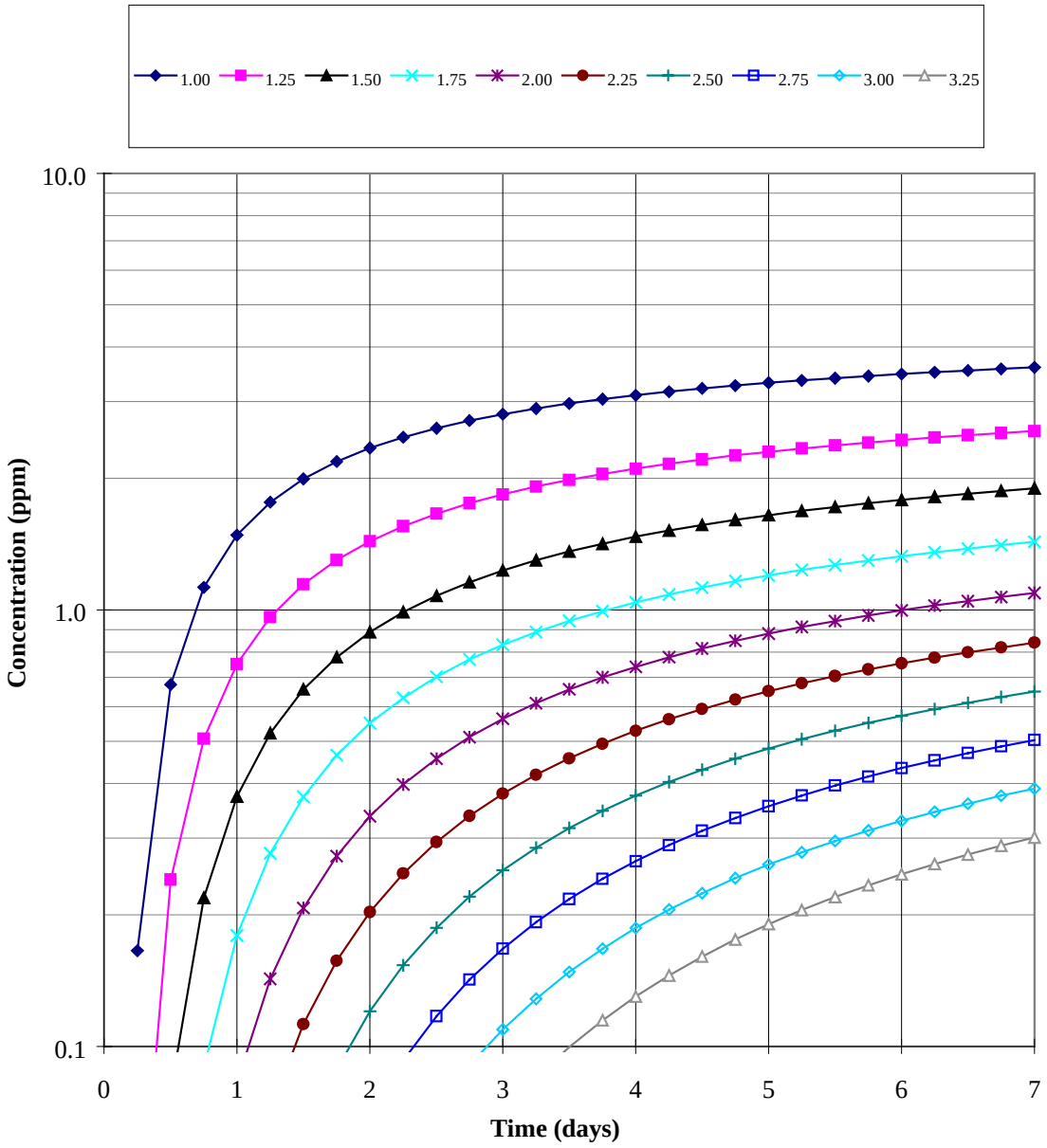

Medium Diffusivity	5.00E-06 m^2/sec		
Source Concentration	7500 ppm	45525 mg/m^3	
Barrier Thickness	0.00 feet	0.00 meters	
Leak Radius	0.07 cm	7.0E-04 meters	2.8E-02 inches
Leak Area	0.02 sq. cm.	2.4E-03 sq. in.	

Figure E-A2. Results from the spherical diffusion model showing the minimum leak size that could be detected at a 2.0-m detection distance, given the conditions listed above (7,500 ppm source concentration, 0' thick barrier).

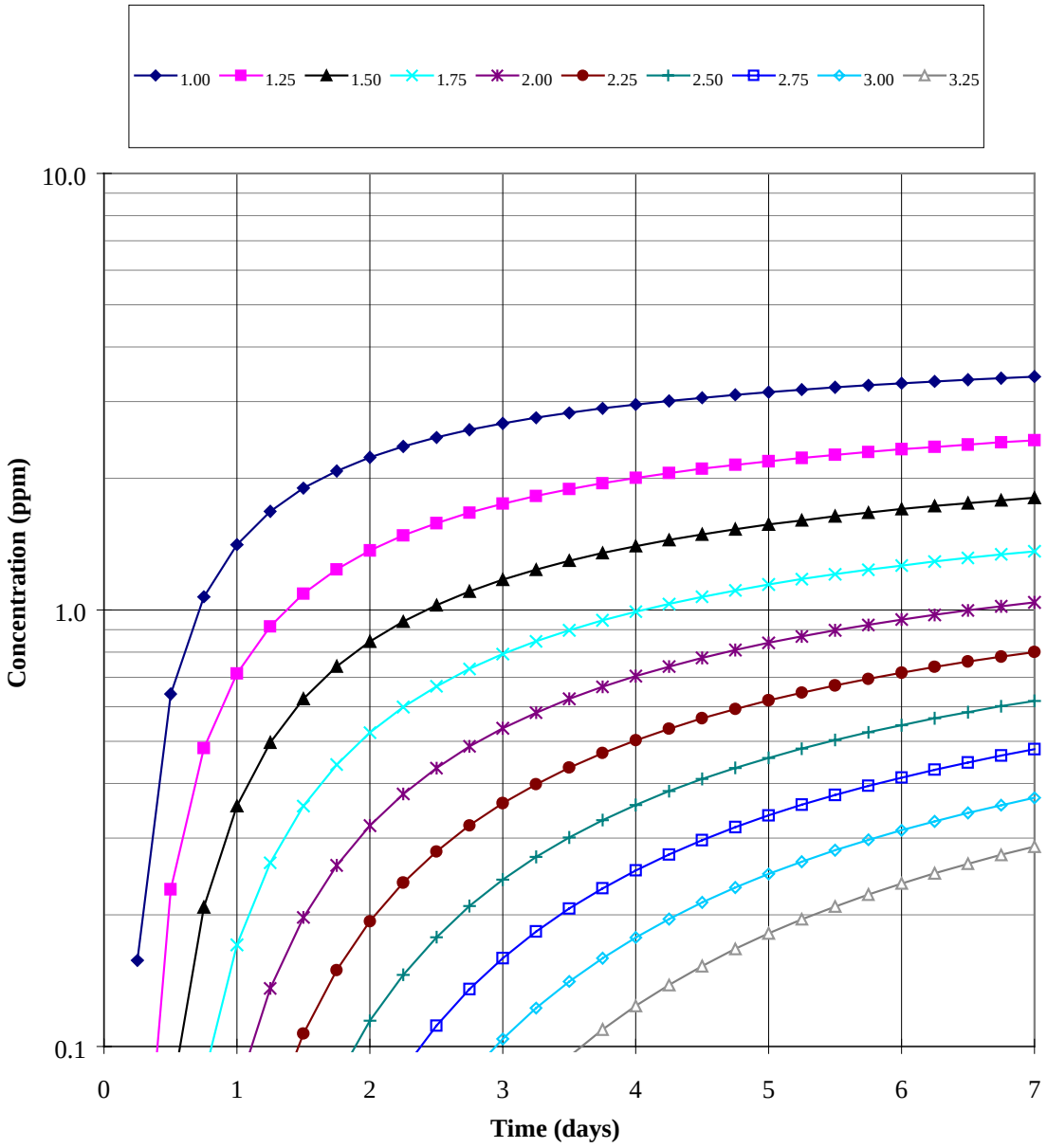

Medium Diffusivity	5.00E-06 m^2/sec		
Source Concentration	20000 ppm	121400 mg/m^3	
Barrier Thickness	0.00 feet	0.00 meters	
Leak Radius	0.025 cm	2.5E-04 meters	9.8E-03 inches
Leak Area	0.00 sq. cm.	3.0E-04 sq. in.	

Figure E-A3. Results from the spherical diffusion model showing the minimum leak size that could be detected at a 2.0-m detection distance, given the conditions listed above (20,000 ppm source concentration, 0' thick barrier).

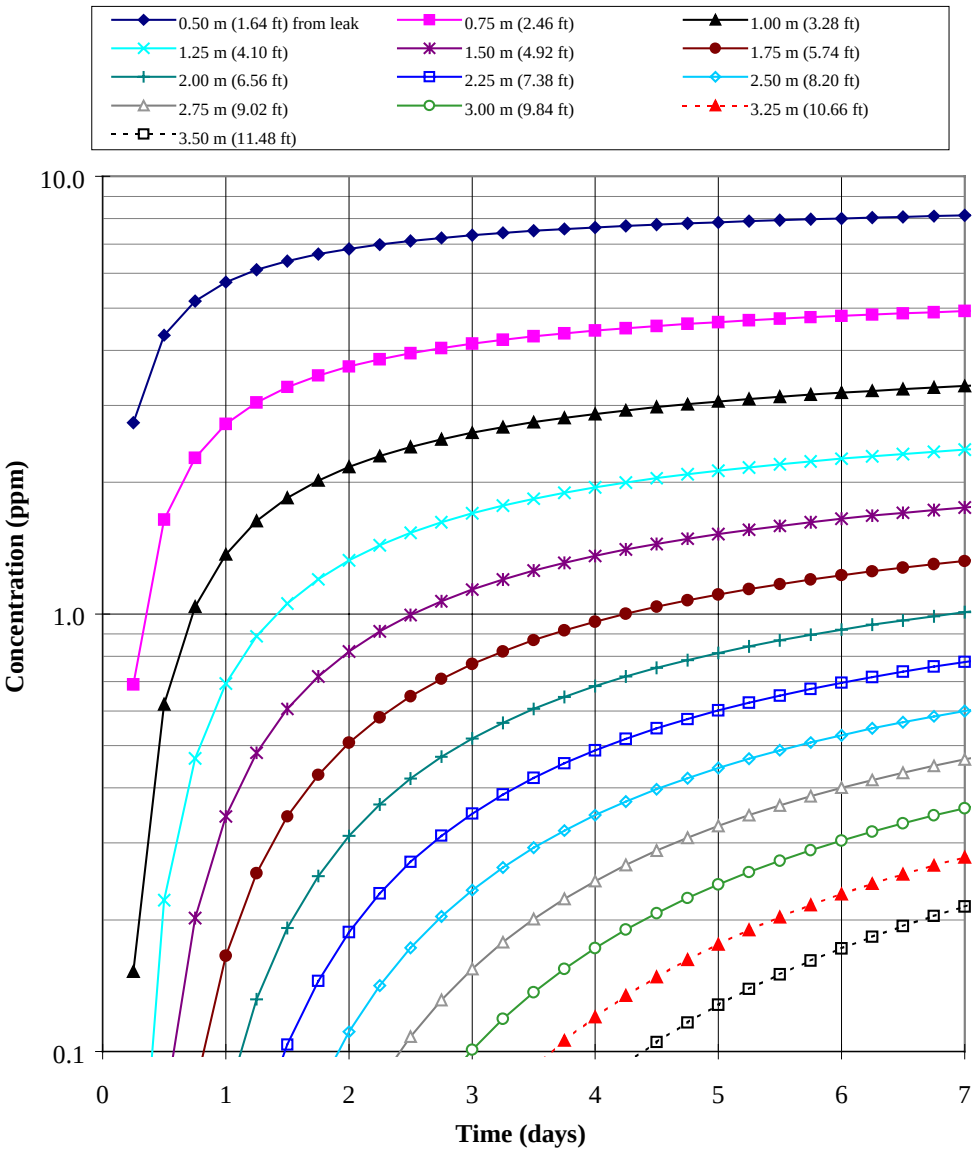

Leak Diffusivity:	5.00E-06 m^2/sec	0.018 m^2/hour	
Medium Diffusivity	5.00E-06 m^2/sec		
Source Concentration	2500 ppm	15175 mg/m^3	
Exit Concentration	1679 ppm	10189 mg/m^3	
Barrier Thickness	2.00 feet	0.61 meters	
Exit flux (mg/m^2/s)	4.09E-02		
Leak Radius	6 cm	6.00E-02 meters	2.3622 inches
Leak Area	113.10 cm^2		

Figure E-A4. Results from the flux limited diffusion model showing the minimum leak size that could be detected at a 2.0-m detection distance, given the conditions listed above (2,500 ppm source concentration, 2' thick barrier).

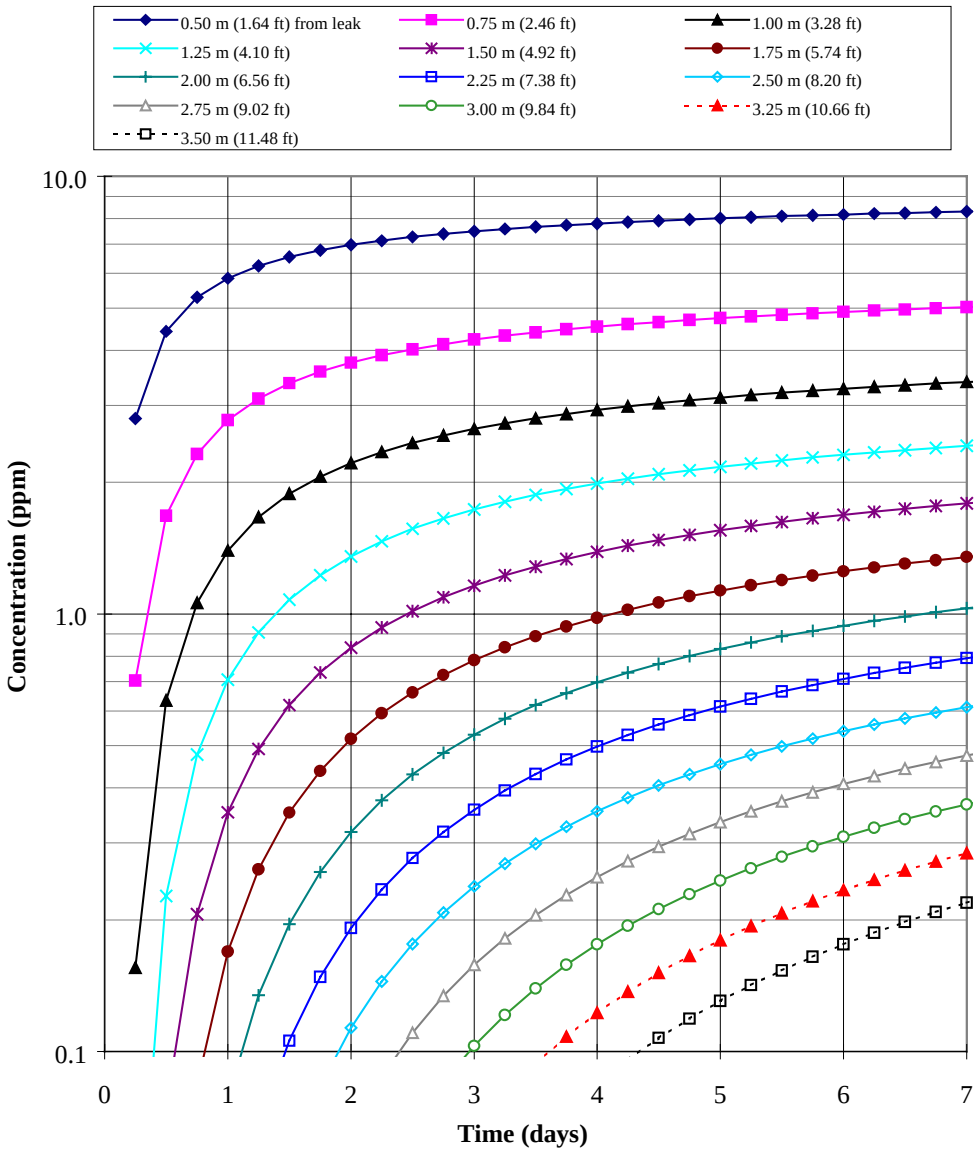

Leak Diffusivity:	5.00E-06 m^2/sec	0.018 m^2/hour	
Medium Diffusivity	5.00E-06 m^2/sec		
Source Concentration	7500 ppm	45525 mg/m^3	
Exit Concentration	5036 ppm	30567 mg/m^3	
Barrier Thickness	2.00 feet	0.61 meters	
Exit flux (mg/m^2/s)	1.23E-01		
Leak Radius	3.5 cm	3.50E-02 meters	1.37795 inches
Leak Area	38.48 cm^2		

Figure E-A5. Results from the flux limited diffusion model showing the minimum leak size that could be detected at a 2.0-m detection distance, given the conditions listed above (7,500 ppm source concentration, 2' thick barrier).

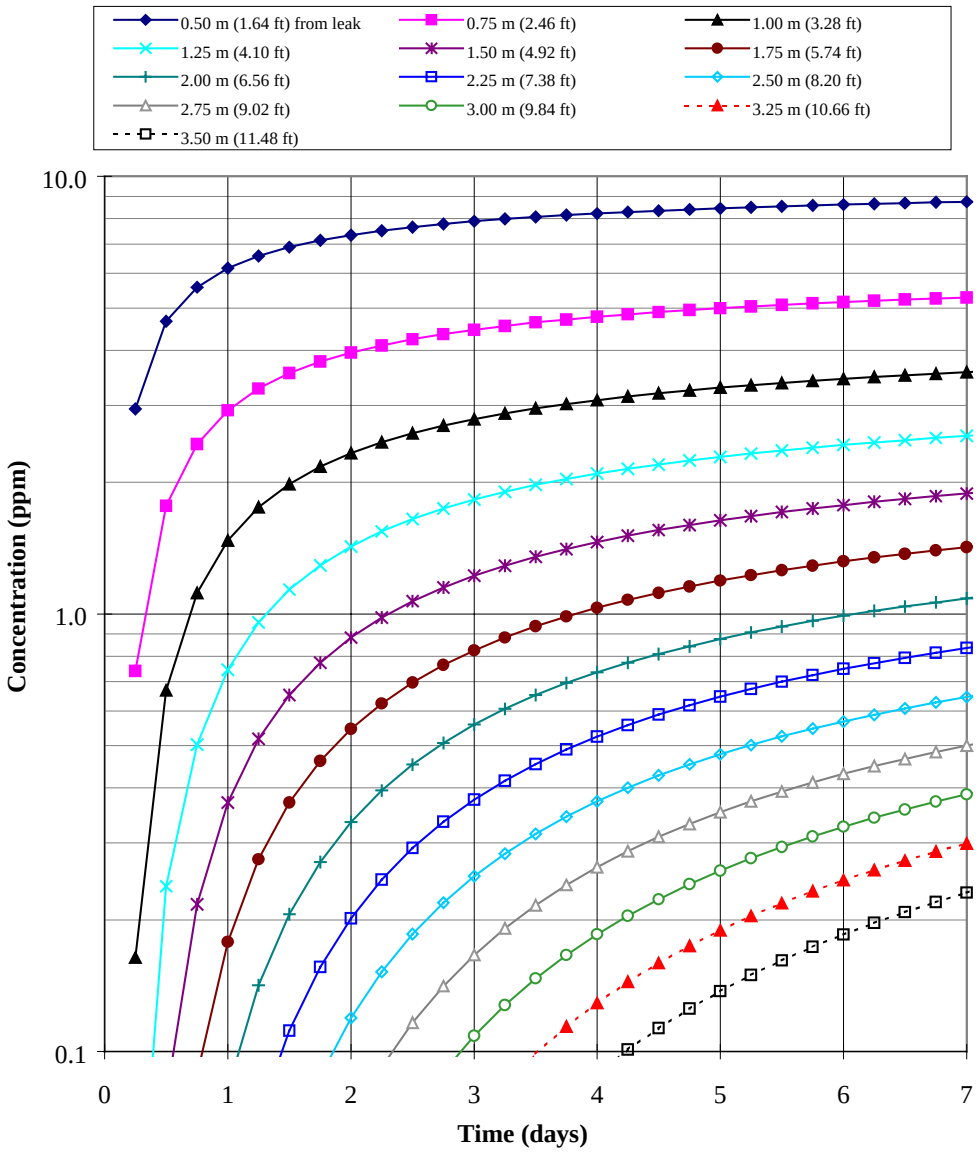

Leak Diffusivity:	5.00E-06 m^2/sec	0.018 m^2/hour	
Medium Diffusivity	5.00E-06 m^2/sec		
Source Concentration	20000 ppm	121400 mg/m^3	
Exit Concentration	13429 ppm	81512 mg/m^3	
Barrier Thickness	2.00 feet	0.61 meters	
Exit flux (mg/m^2/s)	3.27E-01		
Leak Radius	2.2 cm	2.20E-02 meters	0.86614 inches
Leak Area	15.21 cm^2		

Figure E-A6. Results from the flux limited diffusion model showing the minimum leak size that could be detected at a 2.0-m detection distance, given the conditions listed above (20,000 ppm source concentration, 2’ thick barrier).

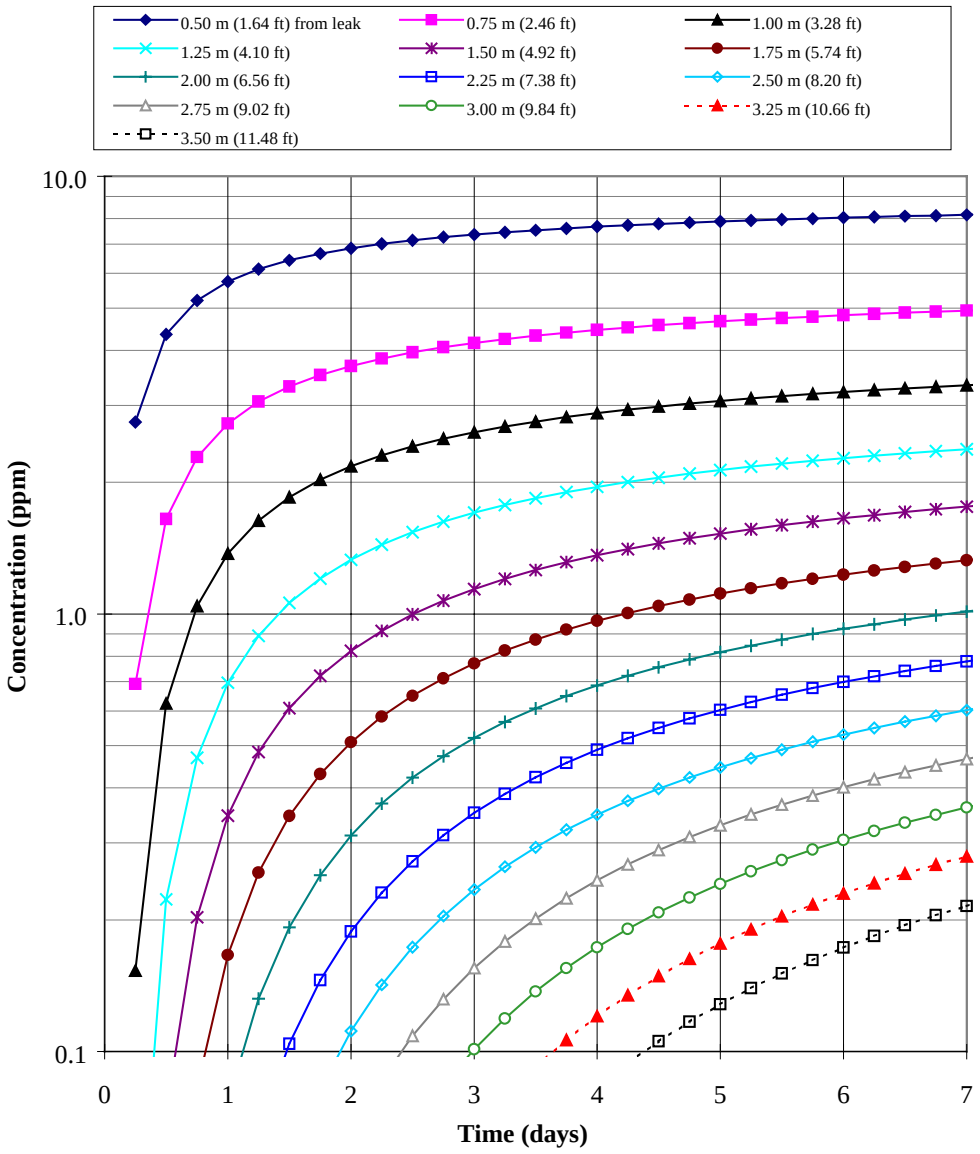

Leak Diffusivity:	5.00E-06 m^2/sec	0.018 m^2/hour	
Medium Diffusivity	5.00E-06 m^2/sec		
Source Concentration	2500 ppm	15175 mg/m^3	
Exit Concentration	1679 ppm	10189 mg/m^3	
Barrier Thickness	4.00 feet	1.22 meters	
Exit flux (mg/m^2/s)	2.04E-02		
Leak Radius	8.5 cm	8.50E-02 meters	3.34646 inches
Leak Area	226.98 cm^2		

Figure E-A7. Results from the flux limited diffusion model showing the minimum leak size that could be detected at a 2.0-m detection distance, given the conditions listed above (2,500 ppm source concentration, 4’ thick barrier).

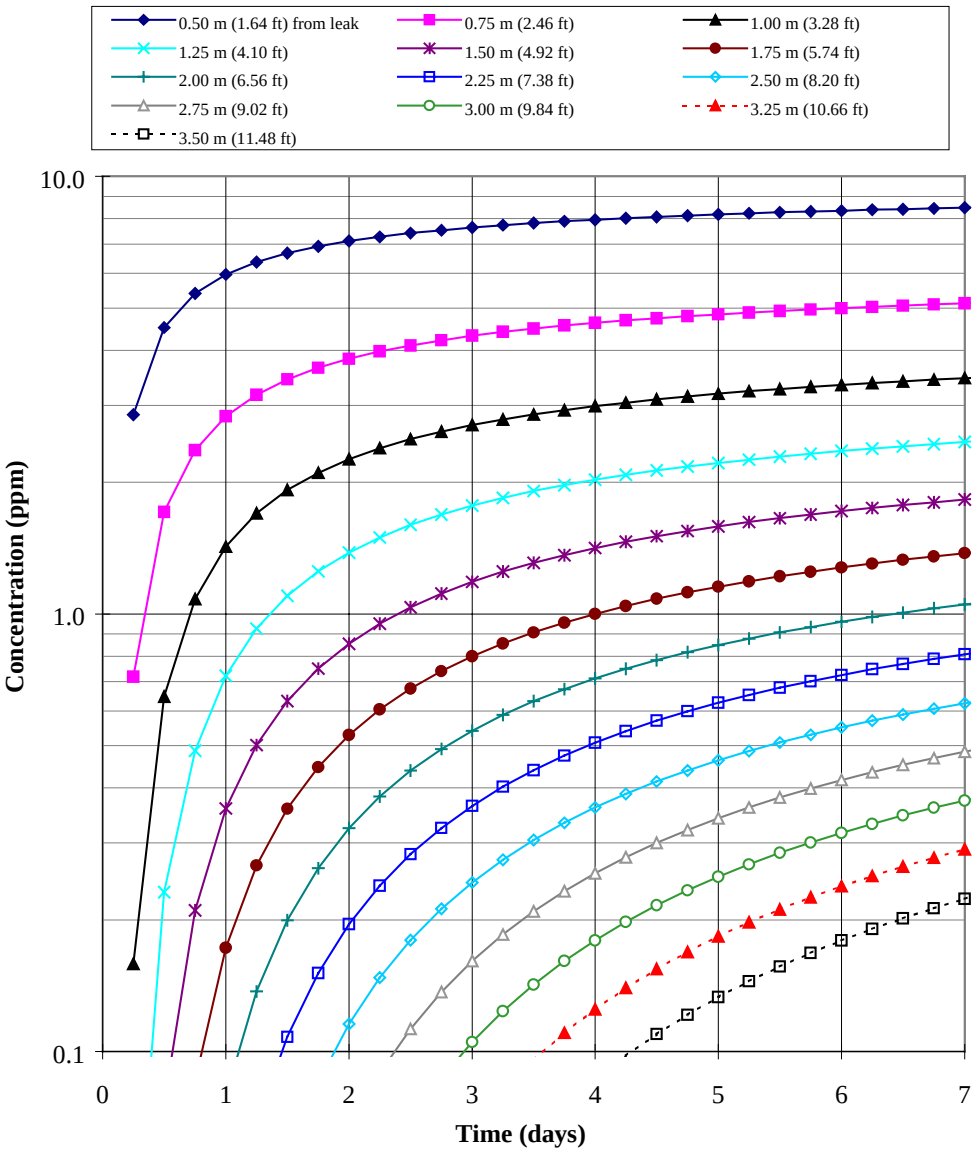

Leak Diffusivity:	5.00E-06 m^2/sec	0.018 m^2/hour	
Medium Diffusivity	5.00E-06 m^2/sec		
Source Concentration	7500 ppm	45525 mg/m^3	
Exit Concentration	5036 ppm	30567 mg/m^3	
Barrier Thickness	4.00 feet	1.22 meters	
Exit flux (mg/m^2/s)	6.13E-02		
Leak Radius	5 cm	5.00E-02 meters	1.9685 inches
Leak Area	78.54 cm^2		

Figure E-A8. Results from the flux limited diffusion model showing the minimum leak size that could be detected at a 2.0-m detection distance, given the conditions listed above (7,500 ppm source concentration, 4' thick barrier).

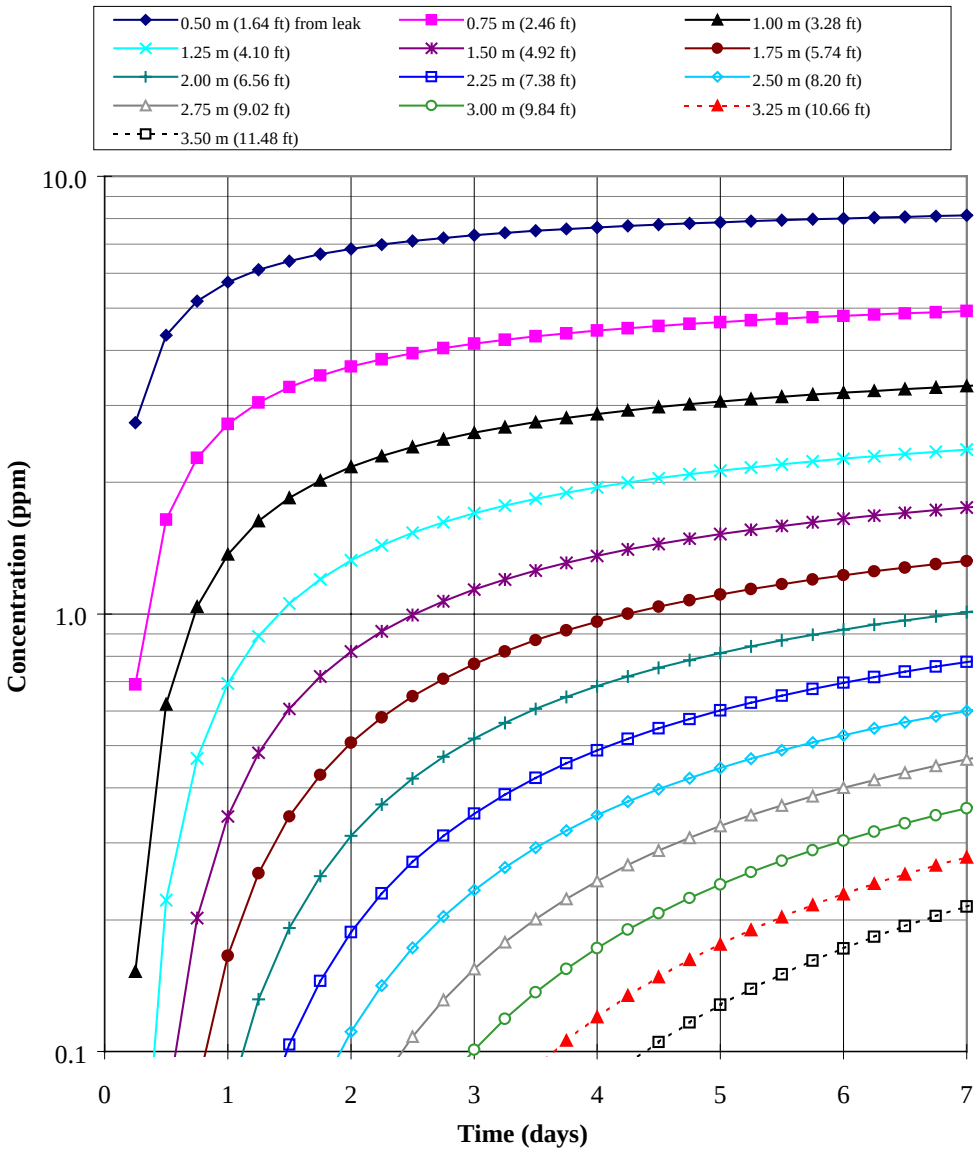

Leak Diffusivity:	5.00E-06 m^2/sec	0.018 m^2/hour	
Medium Diffusivity	5.00E-06 m^2/sec		
Source Concentration	20000 ppm	121400 mg/m^3	
Exit Concentration	13429 ppm	81512 mg/m^3	
Barrier Thickness	4.00 feet	1.22 meters	
Exit flux (mg/m^2/s)	1.64E-01		
Leak Radius	3 cm	3.00E-02 meters	1.1811 inches
Leak Area	28.27 cm^2		

Figure E-A9. Results from the flux limited diffusion model showing the minimum leak size that could be detected at a 2.0-m detection distance, given the conditions listed above (20,000 ppm source concentration, 4’ thick barrier).

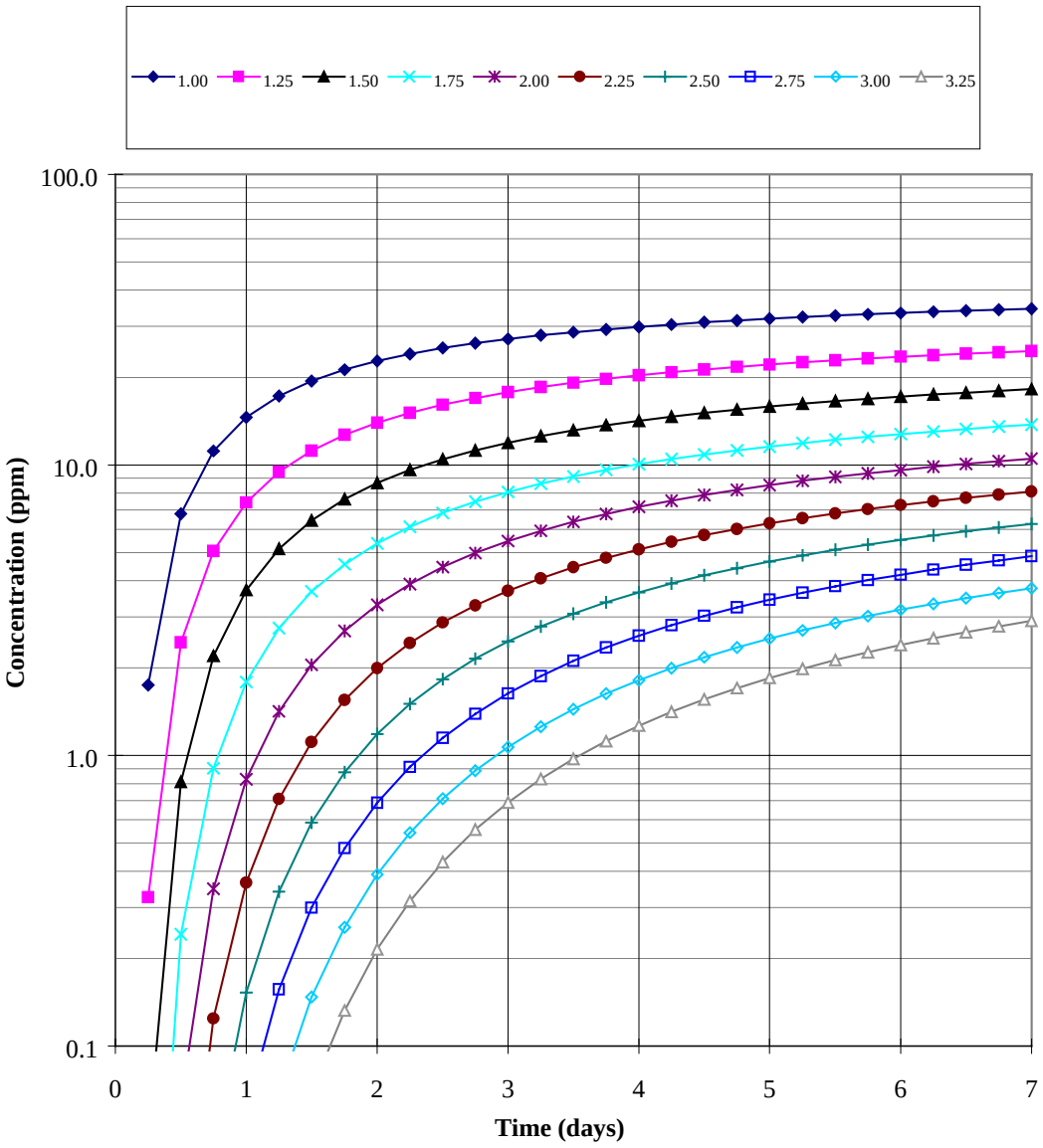

Medium Diffusivity	5.00E-06 m^2/sec		
Source Concentration	2500 ppm	15175 mg/m^3	
Barrier Thickness	0.00 feet	0.00 meters	
Leak Radius	2 cm	2.0E-02 meters	7.9E-01 inches
Leak Area	12.57 sq. cm.	1.9E+00 sq. in.	

Figure E-A10. Results from the spherical diffusion model showing the minimum leak size that could be detected at a 2.0-m detection distance, given the conditions listed above (2,500 ppm source concentration, 0' thick barrier).

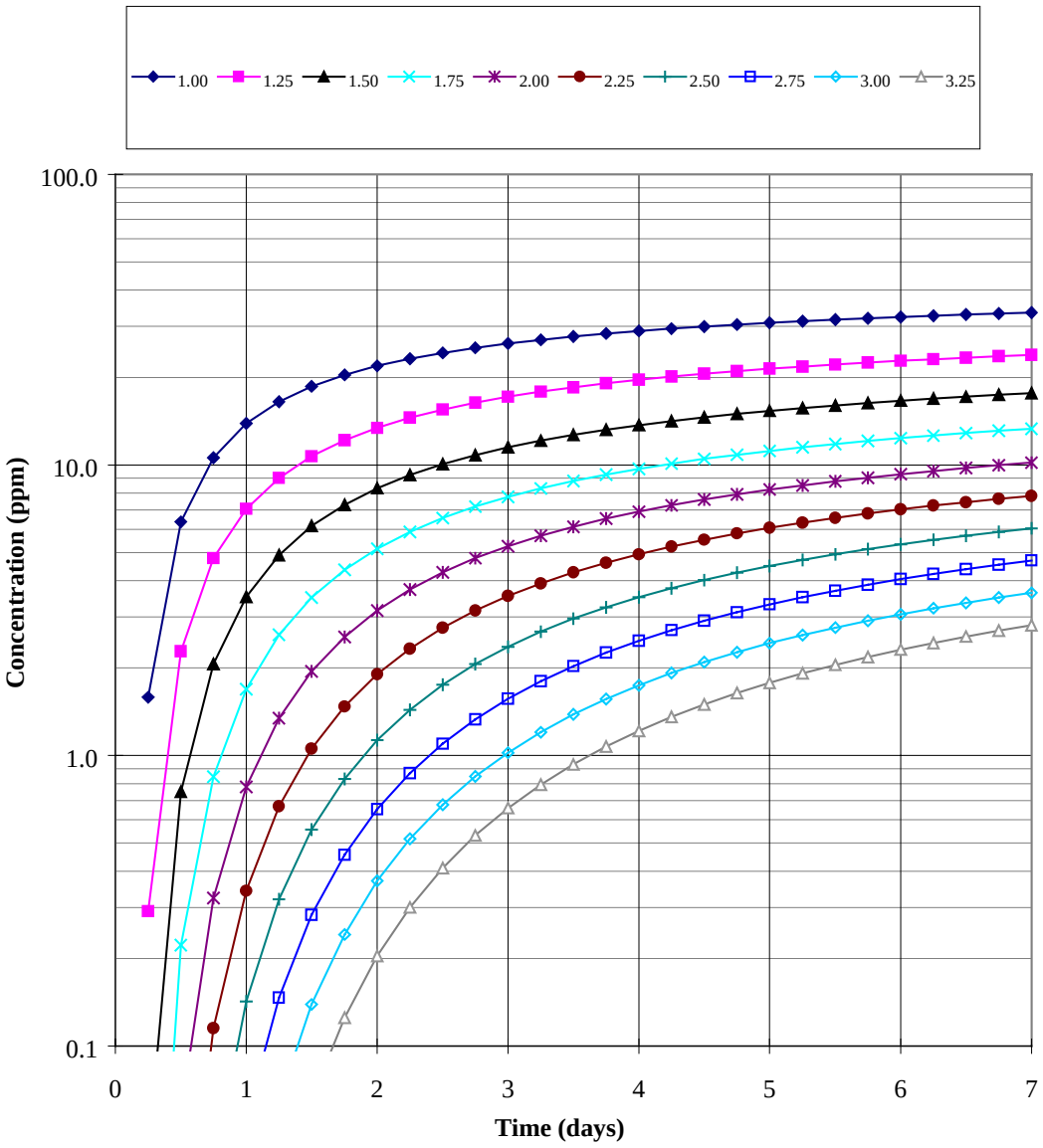

Medium Diffusivity	5.00E-06 m^2/sec		
Source Concentration	7500 ppm	45525 mg/m^3	
Barrier Thickness	0.00 feet	0.00 meters	
Leak Radius	0.65 cm	6.5E-03 meters	2.6E-01 inches
Leak Area	1.33 sq. cm.	2.1E-01 sq. in.	

Figure E-A11. Results from the spherical diffusion model showing the minimum leak size that could be detected at a 2.0-m detection distance, given the conditions listed above (7,500 ppm source concentration, 0' thick barrier).

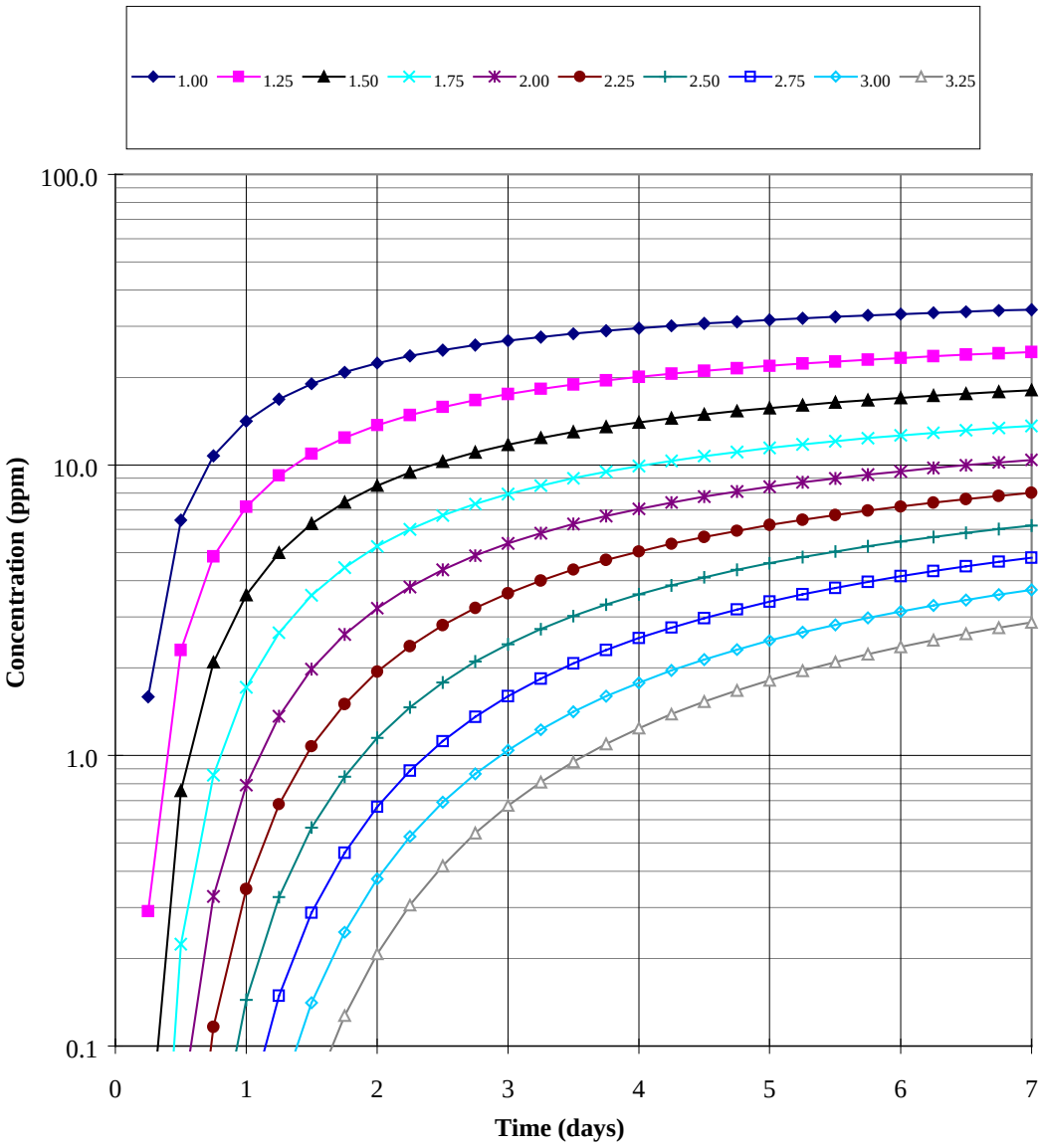

Medium Diffusivity	5.00E-06 m^2/sec		
Source Concentration	20000 ppm	121400 mg/m^3	
Barrier Thickness	0.00 feet	0.00 meters	
Leak Radius	0.25 cm	2.5E-03 meters	9.8E-02 inches
Leak Area	0.20 sq. cm.	3.0E-02 sq. in.	

Figure E-A12. Results from the spherical diffusion model showing the minimum leak size that could be detected at a 2.0-m detection distance, given the conditions listed above (20,000 ppm source concentration, 0' thick barrier).

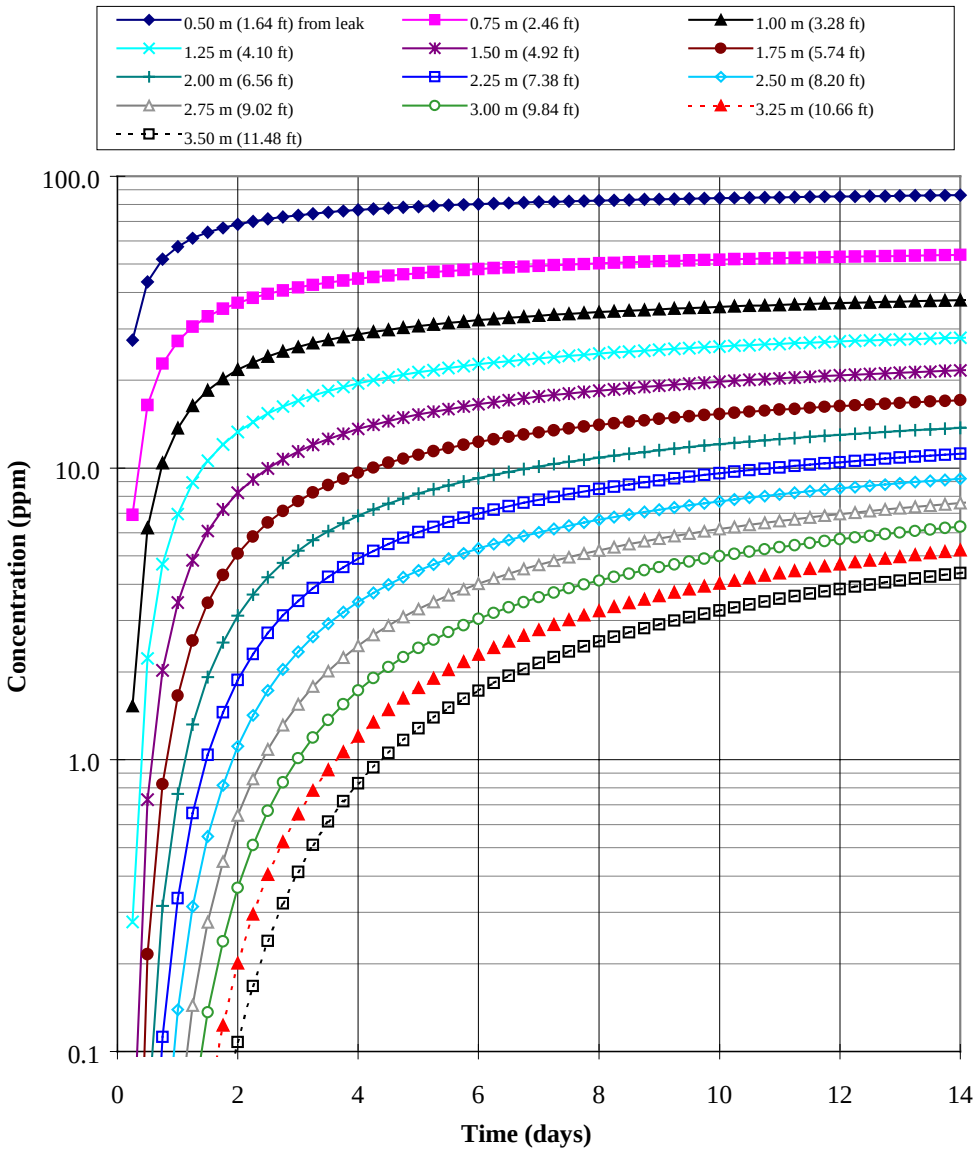

Leak Diffusivity:	5.00E-06 m^2/sec	0.018 m^2/hour	
Medium Diffusivity	5.00E-06 m^2/sec		
Source Concentration	2500 ppm	15175 mg/m^3	
Exit Concentration	1679 ppm	10189 mg/m^3	
Barrier Thickness	2.00 feet	0.61 meters	
Exit flux (mg/m^2/s)	4.09E-02		
Leak Radius	19 cm	1.90E-01 meters	7.48031 inches
Leak Area	1134.11 cm^2		

Figure E-A13. Results from the spherical diffusion model showing the minimum leak size that could be detected at a 2.0-m detection distance, given the conditions listed above (2,500 ppm source concentration, 2’ thick barrier).

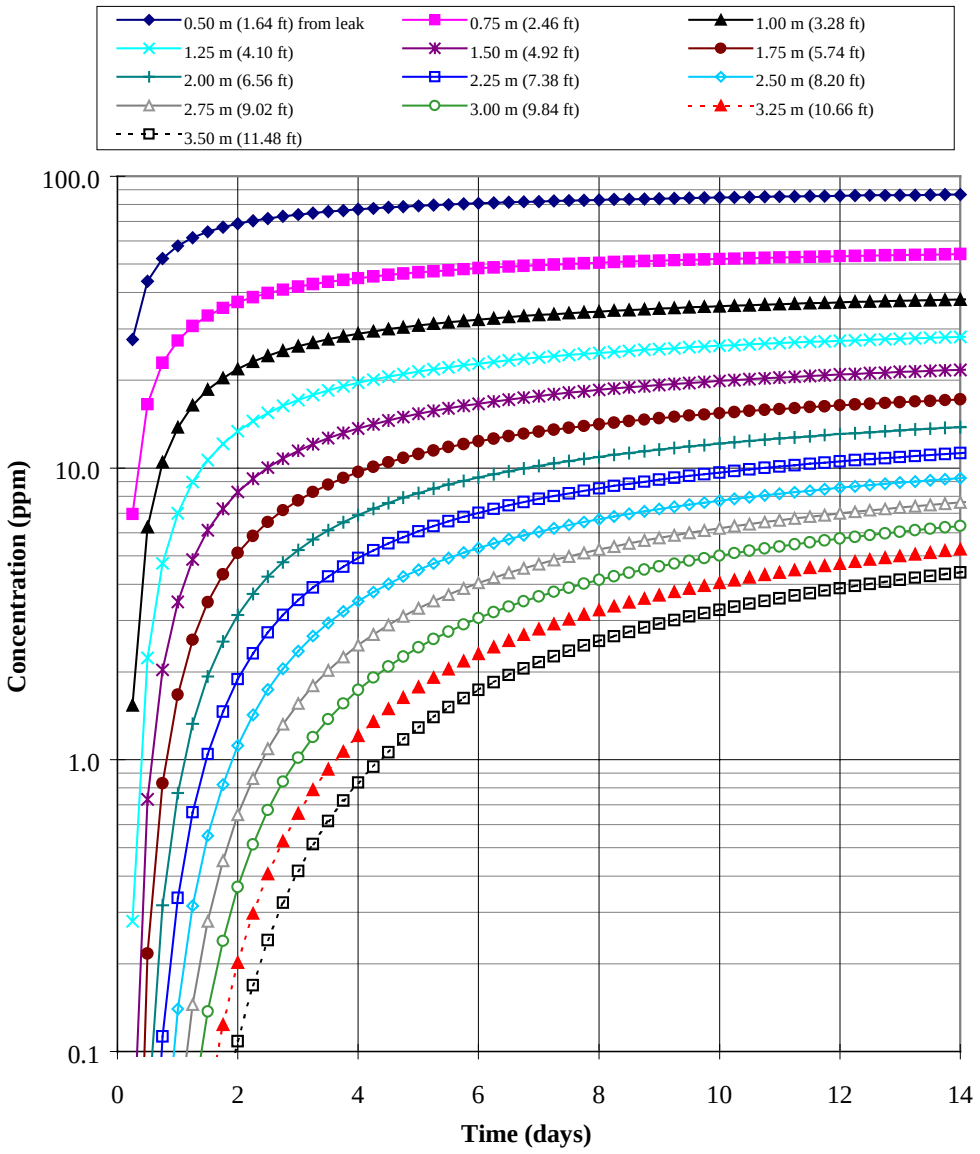

Leak Diffusivity:	5.00E-06 m^2/sec	0.018 m^2/hour	
Medium Diffusivity	5.00E-06 m^2/sec		
Source Concentration	7500 ppm	45525 mg/m^3	
Exit Concentration	5036 ppm	30567 mg/m^3	
Barrier Thickness	2.00 feet	0.61 meters	
Exit flux (mg/m^2/s)	1.23E-01		
Leak Radius	11 cm	1.10E-01 meters	4.33071 inches
Leak Area	380.13 cm^2		

Figure E-A14. Results from the spherical diffusion model showing the minimum leak size that could be detected at a 2.0-m detection distance, given the conditions listed above (7,500 ppm source concentration, 2' thick barrier).

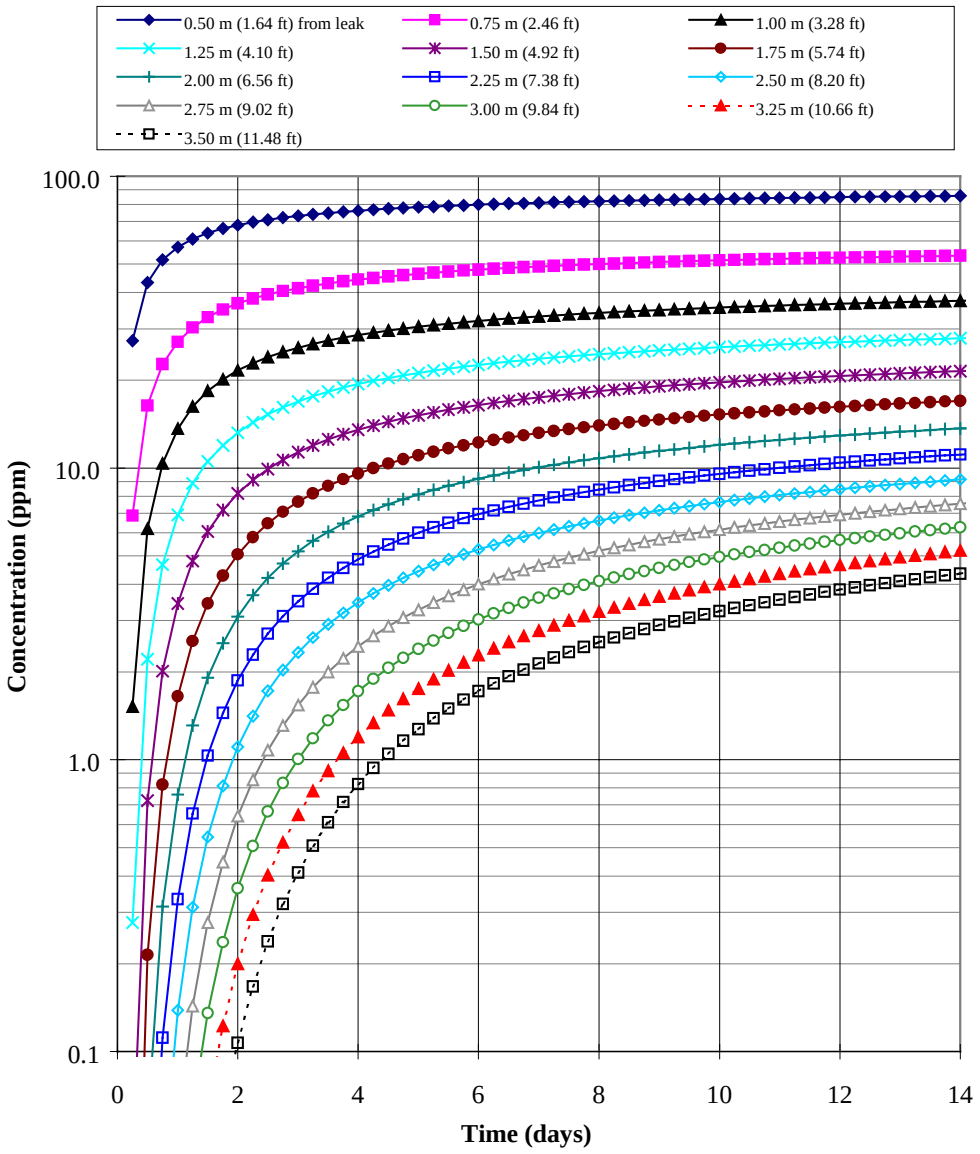

Leak Diffusivity:	5.00E-06 m^2/sec	0.018 m^2/hour	
Medium Diffusivity	5.00E-06 m^2/sec		
Source Concentration	20000 ppm	121400 mg/m^3	
Exit Concentration	13429 ppm	81512 mg/m^3	
Barrier Thickness	2.00 feet	0.61 meters	
Exit flux (mg/m^2/s)	3.27E-01		
Leak Radius	6.7 cm	6.70E-02 meters	2.6378 inches
Leak Area	141.03 cm^2		

Figure E-A15. Results from the spherical diffusion model showing the minimum leak size that could be detected at a 2.0-m detection distance, given the conditions listed above (20,000 ppm source concentration, 2’ thick barrier).

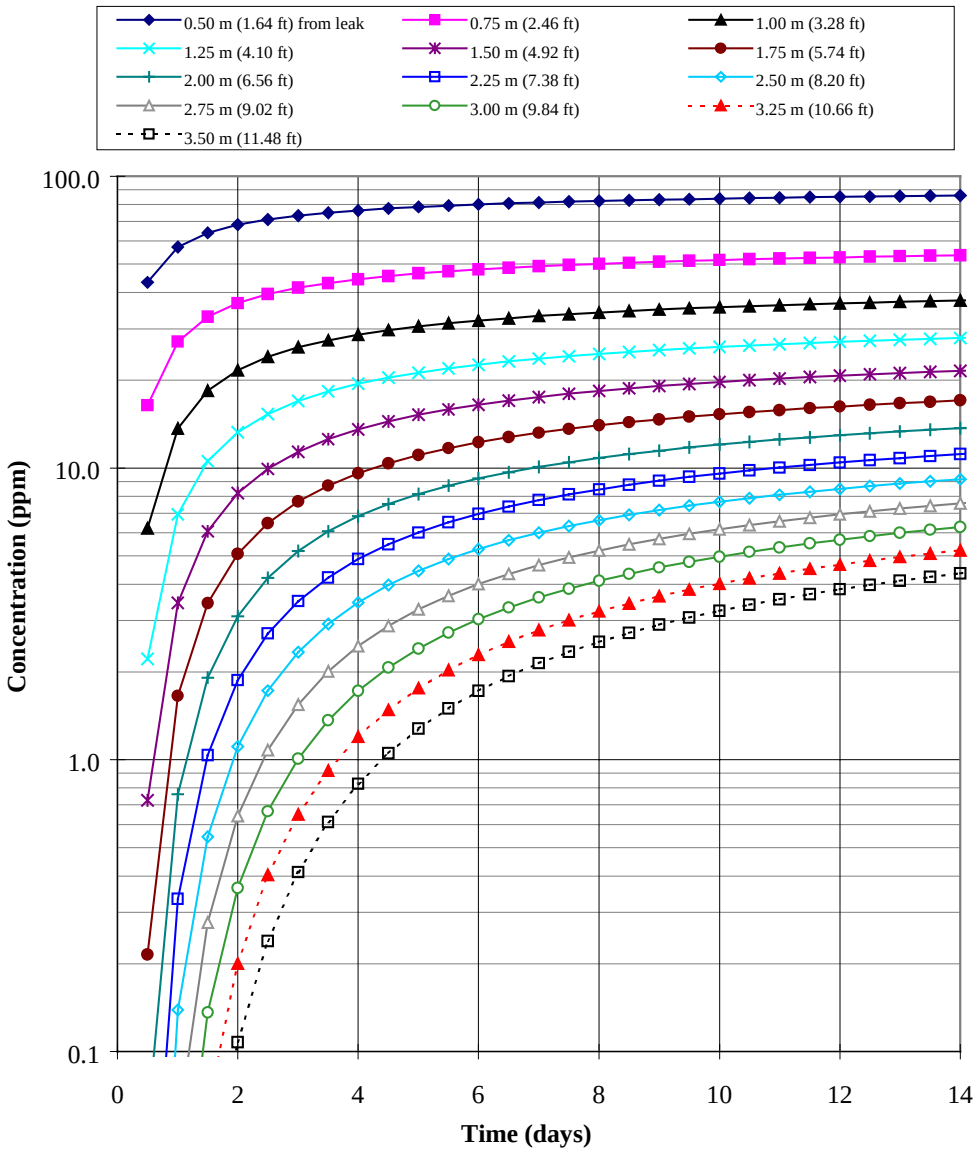

Leak Diffusivity:	5.00E-06 m^2/sec	0.018 m^2/hour	
Medium Diffusivity	5.00E-06 m^2/sec		
Source Concentration	100000 ppm	607000 mg/m^3	
Exit Concentration	67143 ppm	407558 mg/m^3	
Barrier Thickness	2.00 feet	0.61 meters	
Exit flux (mg/m^2/s)	1.64E+00		
Leak Radius	3 cm	3.00E-02 meters	1.2 inches
Leak Area	28.27 cm^2		

Figure E-A16. Results from the spherical diffusion model showing the minimum leak size that could be detected at a 2.0-m detection distance, given the conditions listed above (100,000 ppm source concentration, 2' thick barrier, 7 day test period).

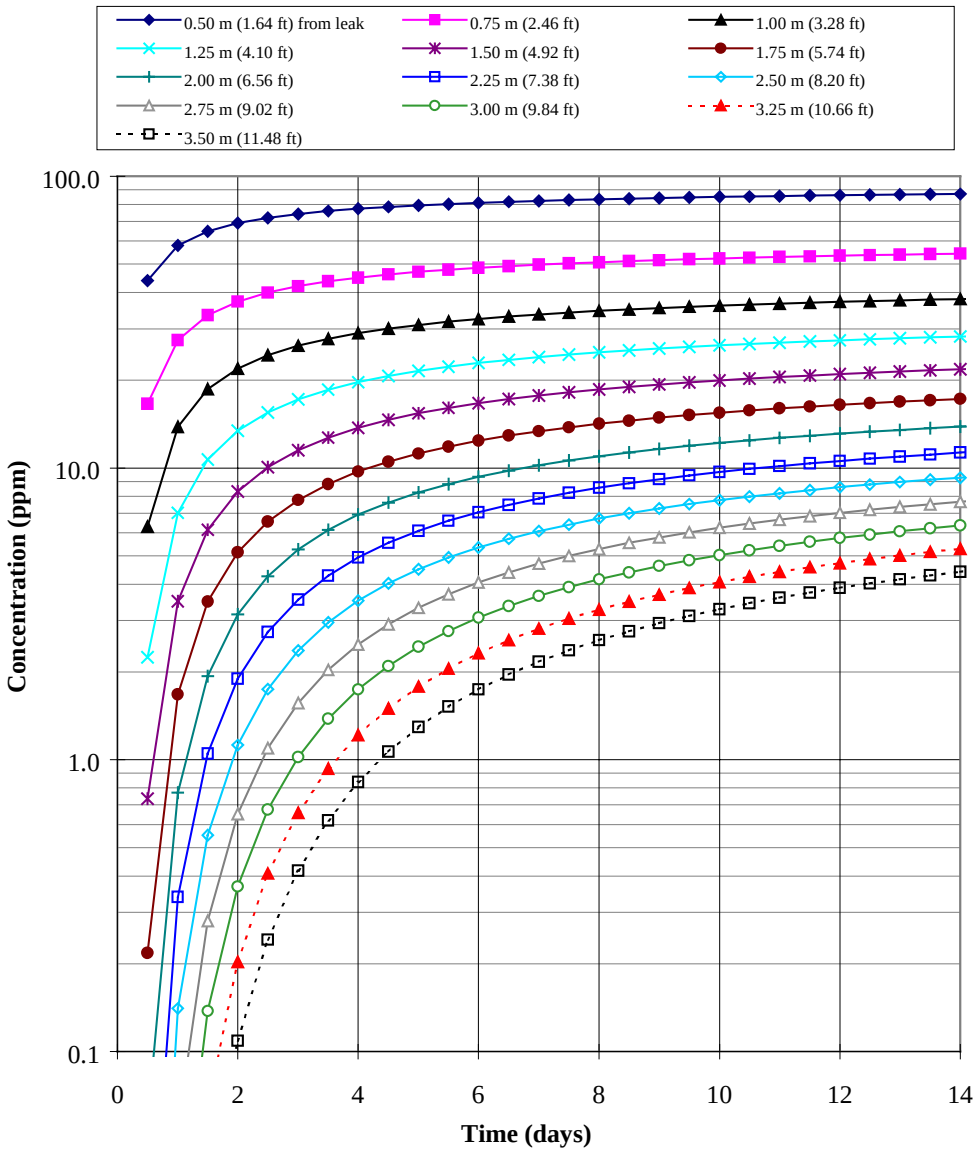

Leak Diffusivity:	5.00E-06 m^2/sec	0.018 m^2/hour	
Medium Diffusivity	5.00E-06 m^2/sec		
Source Concentration	2500 ppm	15175 mg/m^3	
Exit Concentration	1679 ppm	10189 mg/m^3	
Barrier Thickness	4.00 feet	1.22 meters	
Exit flux (mg/m^2/s)	2.04E-02		
Leak Radius	27 cm	2.70E-01 meters	10.6 inches
Leak Area	2290.22 cm^2		

Figure E-A17. Results from the spherical diffusion model showing the minimum leak size that could be detected at a 2.0-m detection distance, given the conditions listed above (2,500 ppm source concentration, 4’ thick barrier, 7 day test period).

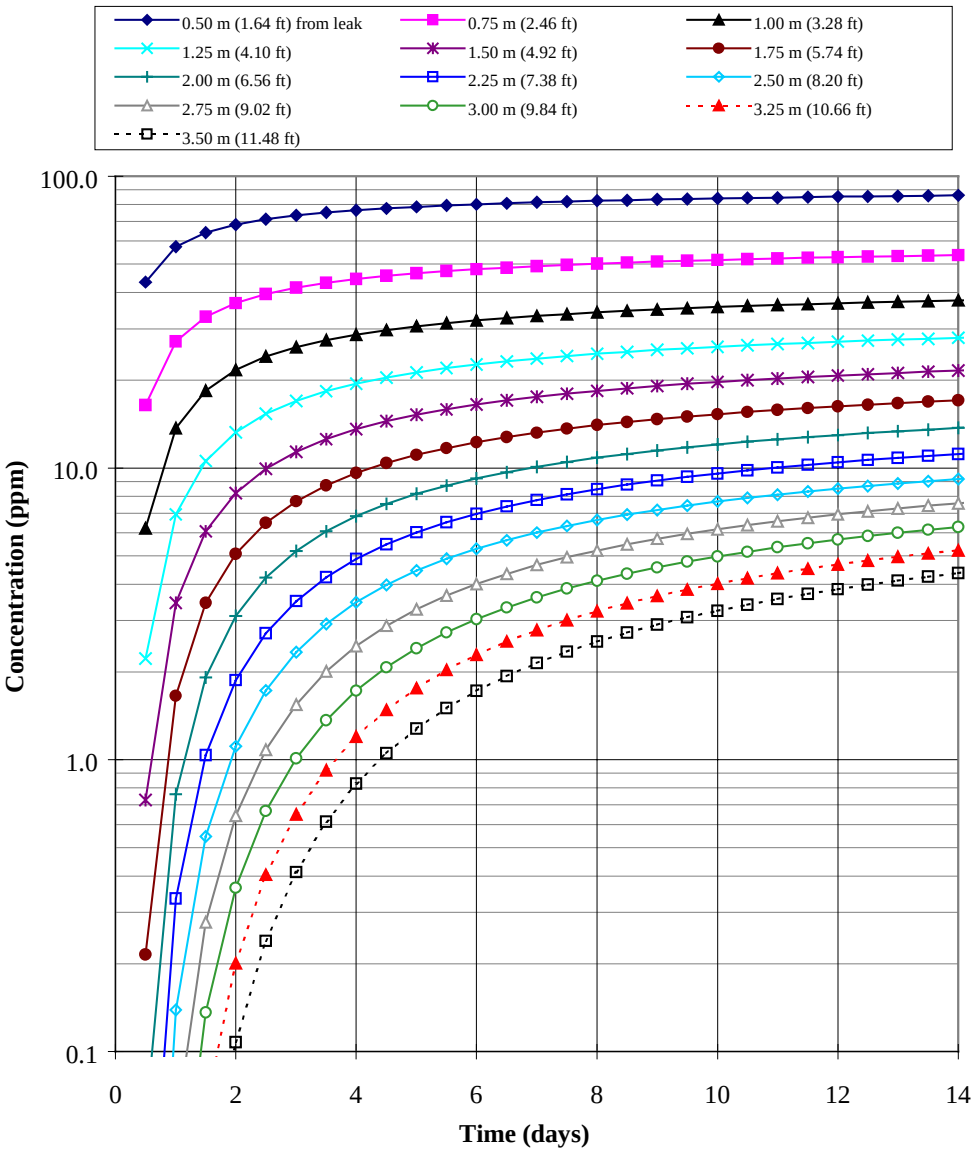

Leak Diffusivity:	5.00E-06 m^2/sec	0.018 m^2/hour	
Medium Diffusivity	5.00E-06 m^2/sec		
Source Concentration	7500 ppm	45525 mg/m^3	
Exit Concentration	5036 ppm	30567 mg/m^3	
Barrier Thickness	4.00 feet	1.22 meters	
Exit flux (mg/m^2/s)	6.13E-02		
Leak Radius	15.5 cm	1.55E-01 meters	6.1 inches
Leak Area	754.77 cm^2		

Figure E-A18. Results from the spherical diffusion model showing the minimum leak size that could be detected at a 2.0-m detection distance, given the conditions listed above (7,500 ppm source concentration, 4’ thick barrier, 7 day test period).

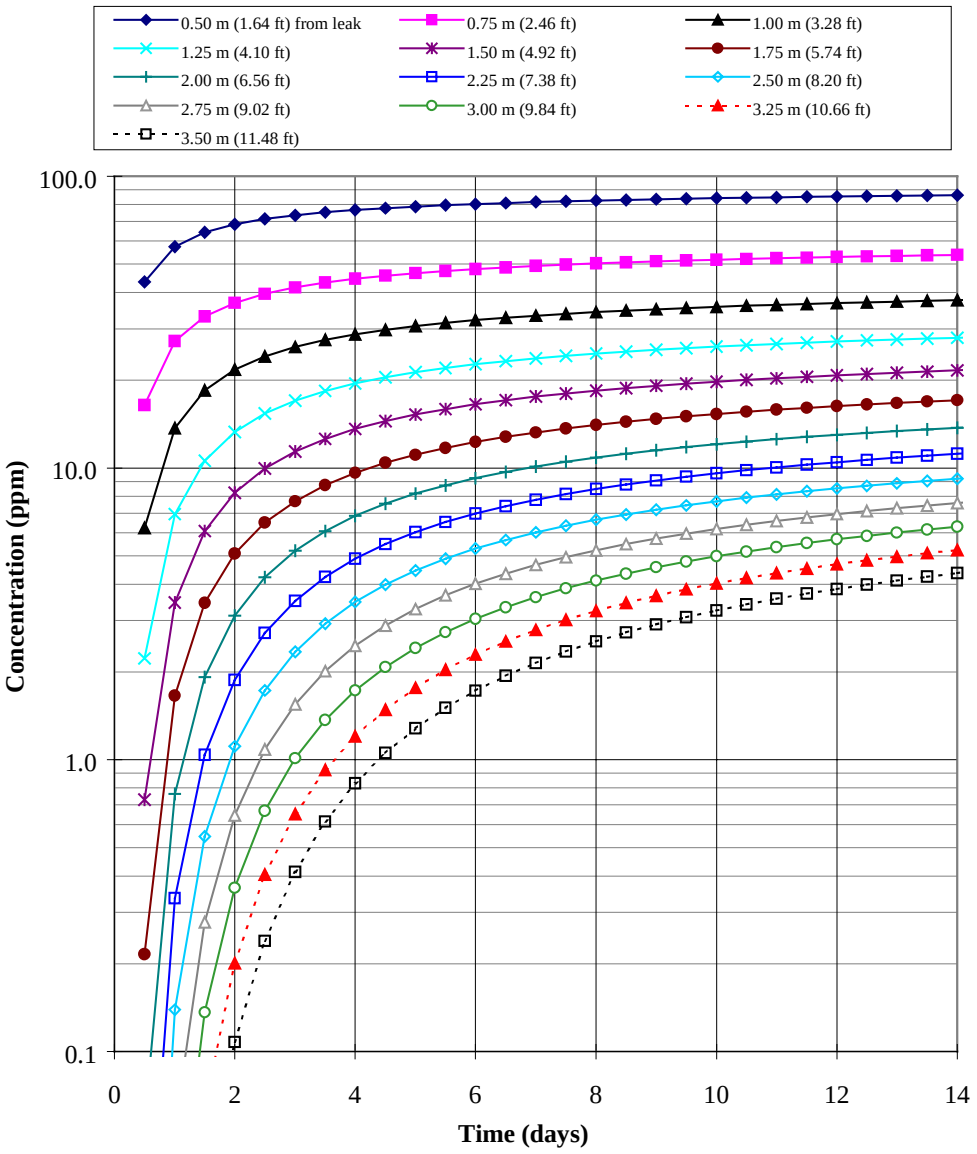

Leak Diffusivity:	5.00E-06 m^2/sec	0.018 m^2/hour	
Medium Diffusivity	5.00E-06 m^2/sec		
Source Concentration	20000 ppm	121400 mg/m^3	
Exit Concentration	13429 ppm	81512 mg/m^3	
Barrier Thickness	4.00 feet	1.22 meters	
Exit flux (mg/m^2/s)	1.64E-01		
Leak Radius	9.5 cm	9.50E-02 meters	3.7 inches
Leak Area	283.53 cm^2		

Figure E-A19. Results from the spherical diffusion model showing the minimum leak size that could be detected at a 2.0-m detection distance, given the conditions listed above (20,000 ppm source concentration, 4’ thick barrier, 7 day test period).

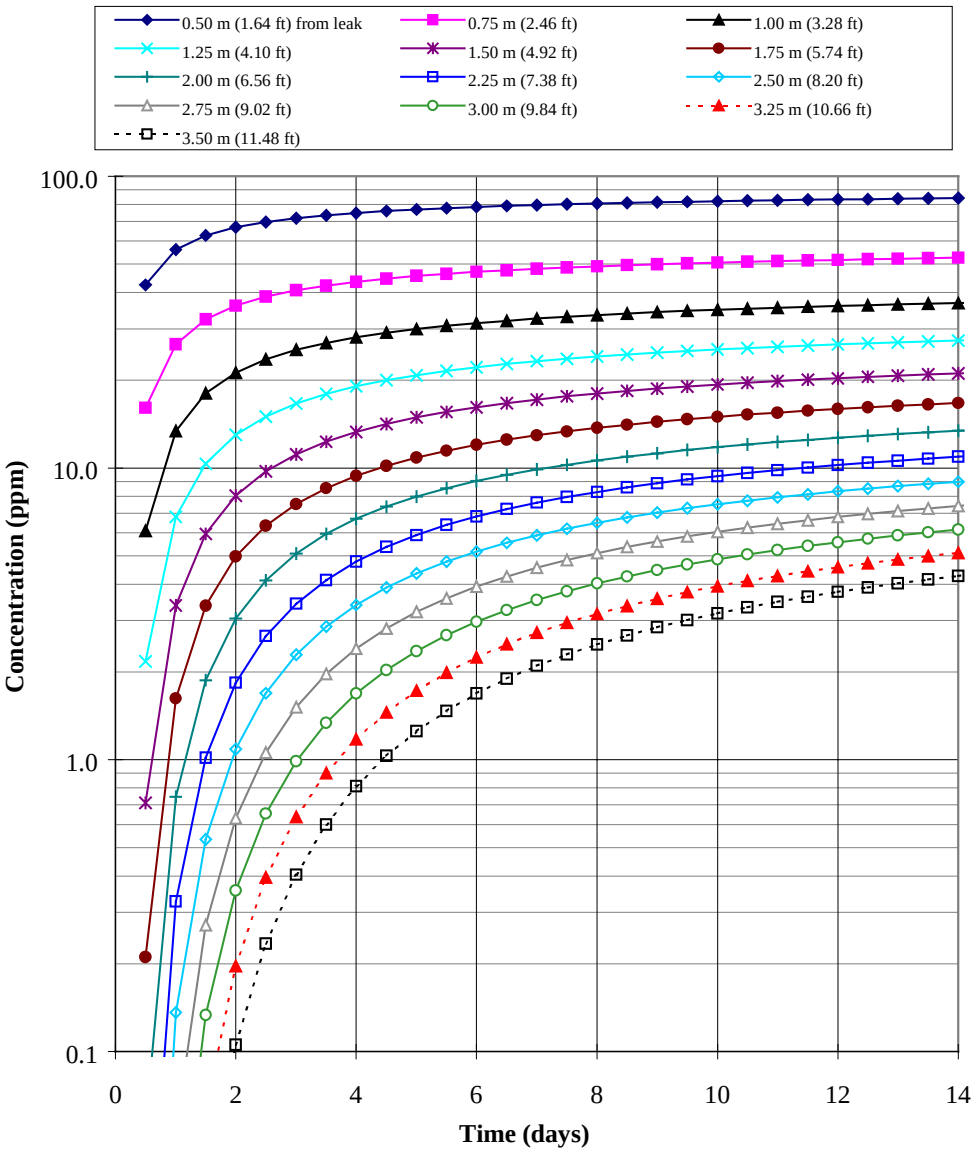

Leak Diffusivity:	5.00E-06 m^2/sec	0.018 m^2/hour	
Medium Diffusivity	5.00E-06 m^2/sec		
Source Concentration	100000 ppm	607000 mg/m^3	
Exit Concentration	67143 ppm	407558 mg/m^3	
Barrier Thickness	4.00 feet	1.22 meters	
Exit flux (mg/m^2/s)	8.18E-01		
Leak Radius	4.2 cm	4.20E-02 meters	1.7 inches
Leak Area	55.42 cm^2		

Figure E-A20. Results from the spherical diffusion model showing the minimum leak size that could be detected at a 2.0-m detection distance, given the conditions listed above (100,000 ppm source concentration, 4’ thick barrier, 7 day test period).

E.6 ATTACHMENT B – Calculation of Injection Point Spacing

Tracer gas injection schemes for barrier validation using the SEAtrace™ system were initially designed to create a uniform tracer concentration inside an enclosed volume of soil. However, experience gained from SEAtrace™ field demonstrations at Dover Air Force Base, Brookhaven National Laboratory, and the Waldo site in New Mexico identified limitations in this type of injection scheme. Primarily, large leaks in the barriers prevented uniform tracer concentrations inside the contained volume, and caused significant tracer concentrations outside the barrier which flooded the gas analyzer and masked smaller flaws. In addition, typical barriers are very large scale, subsurface walls enclosing acres of soil rather than the relatively small barriers tested at Dover AFB, BNL, and the Waldo site. Using an injection scheme designed to fill an enclosed volume of soil with a uniform tracer concentration on large scale barriers would not be feasible. These facts have led to a modification of the injection scheme designed to create a uniform concentration of tracer at the barrier wall itself rather than within the volume of enclosed soil. Injection should occur in slow, controlled, staged steps. Initial injection at a low concentration allows detection of relatively large flaws, if they exist, without flooding the gas analyzer. This also prevents too large of a background concentration to accumulate in the soil outside the barrier for subsequent testing. Subsequent testing at higher tracer concentrations, achieved by pulse injections near the barrier walls, allows monitoring for successively smaller leaks. This type of injection scheme allows discrete sections of very large barriers to be tested, and the detection of progressively smaller leaks. Injection port spacing, distance from the barrier wall to the injection ports, and the injection rate become coupled parameters which can be optimized to test site specific barrier walls of varying size and orientation. The Waldo field demonstration will attempt to validate this type of injection scheme.

Although the Waldo barrier is small, the injection scheme was designed to test discrete sections of the barrier walls rather than the entire barrier as a whole. One purpose of the demonstration was to validate the injection methodology for a large scale barrier using the relatively small scale Waldo site. The injection port spacing, proximity of the injection ports to the barrier walls, and the injection rate were scaled down and optimized using a numerical model. Also, in designing the injection scheme, care was take to initially avoid large known flaws in the Waldo barrier in order to test the injection methodology.

A numerical model was used to determine a scheme for slow, stepped injection of tracer gas that would create progressively higher, and relatively uniform concentrations along the barrier wall. The target concentrations for the first, second, and third injections were determined to be between 2000 to 5000 parts per million (ppm), 5000 to 10,000 ppm, and 10,000 to 30,000 ppm respectively. T2VOC, a finite difference numerical simulator capable of modeling three-phase (gas, aqueous, NAPL), three component (water, air, volatile organic compound), nonisothermal flow and transport through porous media (Falta, Pruess, Finsterle, Battistelli 1995), was used to determine the proper location of the injection ports with respect to each other and the barrier interior walls.

A three-dimensional Cartesian mesh was used to represent a barrier volume of homogeneous and isotropic soil. The permeability of the soil was chosen to be $1e^{-13}$ m^2 with a 30% porosity and negligible moisture content. Sulfur hexaflouride (SF_6) was used as the tracer gas and had a diffusivity of $7.03e^{-6}$ m^2/s in the soil. The mesh boundaries were chosen to simulate no flow boundaries, one of which was the barrier wall, around a single injection port. A volume of influence from only a single injection port was modeled because in an evenly spaced array of injection ports where each injection rate is equal, no flow boundaries exist at the interfaces between advancing spherical tracer gas fronts assuming homogeneous and isotropic soil conditions. The distances from a single injection port to its no flow boundaries and the barrier wall were varied to represent different spacing between other injection ports and the barrier wall.

The desired concentration at the barrier interior wall for the first injection was found by systematically changing the injection port spacing (the distance from the single injection port to the no flow boundary), the distance from the injection port to the barrier wall, and the mass of tracer injected. After the initial pulse of tracer gas, the system was allowed to equilibrate for a period of time before the next injection. The following scenario was found to deliver the desired tracer concentrations at the barrier wall:

- 9 foot (on center) injection port spacing
- 4 foot spacing from the injection port to the barrier wall
- Initial tracer injection of 0.2 pounds for 1 hour (allowed to equilibrate for 96 hours)
- Second tracer injection of 0.4 pounds for 1 hour (allowed to equilibrate for another 96 hours)
- Third tracer injection of 1.0 pounds for 1 hour (allowed to equilibrate for another 96 hours)

After the first injection, tracer concentration at the barrier varied between 2674 ppm to 2719 ppm. Figure E-B1 shows the distribution of SF_6 at the barrier wall after this the initial pulsed injection was allowed to equilibrate. Subsequent injections, also illustrated in figure E-B1 showed tracer concentrations to be between 7393 ppm and 7487 ppm, and 18,989 ppm and 19,196 ppm. It is also significant to notice that the tracer SF_6, whose molecular weight is heavier than air, tends to sink downward with time due to gravity.

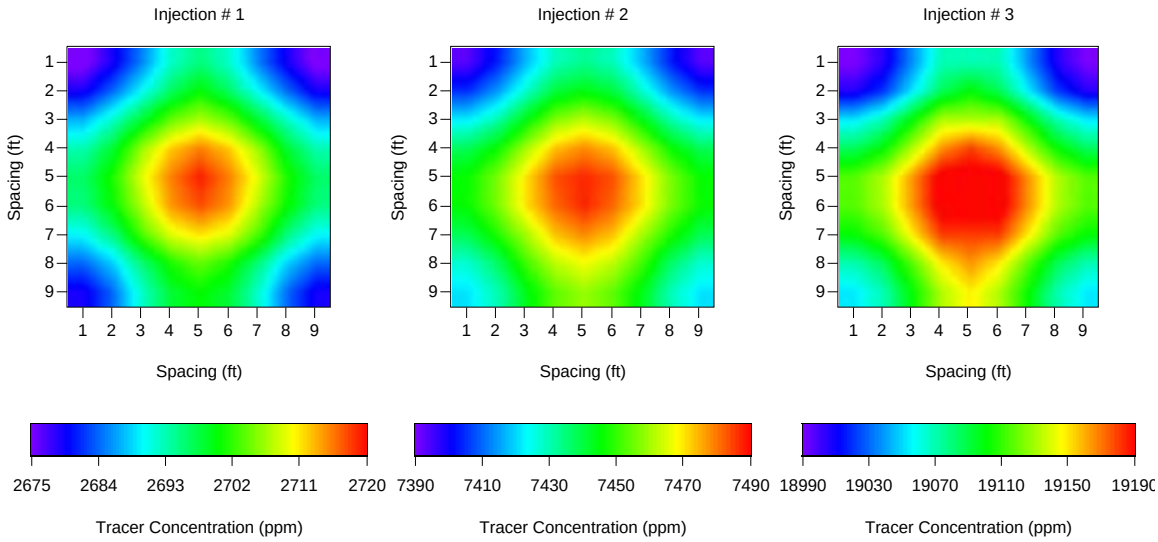

Figure E-B1. Tracer concentrations after each injection and a period of equilibration were found to be relatively uniform across the barrier wall.

APPENDIX F:
MEMORANDUM OF UNDERSTANDING FOR SEATRACE™ DEMONSTRATION AT BRUNSWICK NAVAL AIR STATION

Memorandum of Understanding (MOU)
Vadose Zone Barrier Verification and Monitoring System Demonstration
of Site 1&3 (OU1) Slurry Wall,
Naval Air Station, Brunswick, ME

Purpose: To document an understanding between the signatories regarding a vadose zone barrier verification and monitoring system demonstration using Site 1&3 (OU1) landfill slurry wall at Naval Air Station, Brunswick, ME

Background: While barriers have been used historically to stop contaminant transport beneath the water table (where favorable hydraulic gradients can be maintained), they are less common in stopping transport in unsaturated media. However, many of the containment problems facing the Department of Energy (DOE) are in the vadose zone. As such, DOE is currently developing in-situ barrier emplacement techniques and materials for the containment of high-risk contaminants in soils. These include slurry walls, grout barriers, soil-mixed walls, cryogenic barriers, and other forms of impermeable barriers. Because of their relatively high cost, barriers are intended for use in high-risk circumstances. These include cases where the risk is too great to remove the contaminants, the contaminants are too difficult to remove with current technologies, or the potential for movement of the contaminants to the water table is so high that immediate action needs to be taken to reduce health risks. Consequently, barriers are primarily intended for use in the high-risk sites where few viable alternatives exist to stop the movement of contaminants in the near term. Assessing the integrity of a barrier in the vadose zone once it is emplaced, and during its anticipated life, is a very difficult but necessary requirement. They cannot be tested with water fill to determine if they are flawed, since doing so would mobilize the contaminants they are intended to contain. Geophysical techniques can image the barrier installation but cannot attain adequate spatial resolution to detect small flaws. Without an assessment mechanism or historical data, the use of barriers in the vadose zone is often not considered an adequate control measure. Thus the DOE has actively sought methods that could be used to verify the integrity of a barrier. In response to this need, Science and Engineering Associates, Inc. (SEA) developed a system, SEAtrace™, based on gaseous diffusion. Gaseous tracer testing can detect in barrier structures without risking mobilization of the contaminants, and can, with rigorous analysis, determine both the size and location of the flaws.

The development of the SEAtrace™ system has progressed rapidly through several stages of maturation. Last fall the system was demonstrated at several experimental barriers. The test results were very well received. DOE, through the Federal Energy Technology Center (FETC), has asked SEA to make final adjustments to the system and perform a final field demonstration on a full size barrier. Unfortunately,

because of the issues addressed above, the DOE doesn't have a suitable facility to perform the test so a suitable host site had to be found. After considerable research, a slurry wall emplaced at the Naval Air Station in Brunswick, Maine, proved to be one of the most viable options.

Demonstration Objective: The objective is to demonstrate a vadose zone barrier monitoring system. The slurry wall at Sites1&3 is controlling the movement of groundwater around the contaminants, not controlling gaseous phase transport of the contaminants. The demonstration at this site is a test of the verification system, not the slurry wall. The methodology relies on the predictable process of binary diffusion of a tracer in the soil gas. A known concentration of tracer gas would be placed on one side of the barrier wall and soil gas samples would be drawn from known locations on the other side. Using inverse modeling methodology, the history of soil gas concentration at the various sampling locations allows determination of the leak location and its size. The function of the slurry wall is controlling the movement of groundwater around the contaminants, not controlling gaseous phase transport of the contaminants. I.e., the demonstration at this site is a test of the verification system, not the barrier.

Demonstrator Name and Address:
Science and Engineering Associates, Inc.
6100 Uptown Blvd. NE, Suite 700
Albuquerque NM 87110
Point of Contact: Sandra Dalvit Dunn (505) 424-6955

DOE Federal Energy Technology Center
Point of Contact: Karen Cohen, FETC, DOE Pittsburgh office, at (412)892-6667 or email at"cohen@fetc.doe.gov"

Understandings:

1. The demonstration at this site is a test of the monitoring system, not the barrier. Therefore the EPA and MEDEP will not require the Navy to take any actions resulting solely from the data generated in demonstration of the monitoring system.
2. Approximately seven monitoring wells or ports will be required inside the slurry wall through the landfill cap and approximately eighteen wells or ports outside the slurry wall. SEA, Inc., will be responsible for installation and closure of these wells, using approved procedures and an approved contractor.
3. SEA, Inc. will be responsible for landfill cap repairs in the area of these monitoring wells or ports. When testing is completed, SEA Inc. will repair the landfill cap liner to its original specifications with an approved contractor. All repairs shall be completed by June 1, 1999.
4. SEA, Inc. will follow all NAS Brunswick policies and procedures especially related to security.
5. SEA, Inc. certifies that the indicator gas used in the test SF_6 is a non-hazardous substance as defined by ME DEP and EPA regulations.

6. All funding for the test shall be provided by Science and Engineering Associates, Inc. who is under contract with the DOE Federal Energy Technology Center to perform this work. SEA Inc. will be responsible for securing and providing payment to the aforementioned contractor.
7. The Navy will be allowed to review the report, but not alter conclusions of test data prior to report finalization.

APPENDIX G:
SUBSURFACE BARRIER VALIDATION WITH THE SEATRACE™ SYSTEM: PROPOSED TEST PLAN OF THE SYSTEM AT THE NAS BRUNSWICK SITE

G.1 Introduction

While barriers have been used historically to stop contaminant transport beneath the water table (where favorable hydraulic gradients can be maintained), they are less common in stopping transport in unsaturated media. However, many of the containment problems facing the Department of Energy (DOE) are in the vadose zone. As such, DOE is currently developing in-situ barrier emplacement techniques and materials for the containment of high-risk contaminants in soils. These include slurry walls, grout barriers, soil-mixed walls, cryogenic barriers, and other forms of impermeable barriers. Because of their relatively high cost, barriers are intended for use in high-risk circumstances. These include cases where the risk is too great to remove the contaminants, the contaminants are too difficult to remove with current technologies, or the potential for movement of the contaminants to the water table is so high that immediate action needs to be taken to reduce health risks. Consequently, barriers are primarily intended for use in the high-risk sites where few viable alternatives exist to stop the movement of contaminants in the near term. Assessing the integrity of a barrier in the vadose zone once it is emplaced, and during its anticipated life, is a very difficult but necessary requirement. They cannot be tested with water fill to determine if they are flawed, since doing so would mobilize the contaminants they are intended to contain. Geophysical techniques can image the barrier installation but cannot attain adequate spatial resolution to detect small flaws. Without an assessment mechanism or historical data, the use of barriers in the vadose zone is often not considered an adequate control measure. Thus the DOE has actively sought methods that could be used to verify the integrity of a barrier. In response to this need, Science and Engineering Associates (SEA) developed a system, SEAtrace™, based on gaseous diffusion. Gaseous tracer testing can detect in barrier structures without risking mobilization of the contaminants, and can, with rigorous analysis, determine both the size and location of the flaws.

The development of the SEAtrace™ system has progressed rapidly through several stages of maturation. Last fall the system was demonstrated at several experimental barriers. The test results were very well received. DOE, through the Federal Energy Technology Center (FETC), has asked SEA to make final adjustments to the system and perform a final field demonstration on a full size barrier. Unfortunately, because of the issues addressed above, the DOE doesn't have a suitable facility to perform the test so a suitable host site had to be found. After considerable research, a slurry wall emplaced at the Naval Air Station in Brunswick, Maine, proved to be one of the most viable options.

G.2 Description of the Naval Air Station, Brunswick Site

NAS Brunswick is located south of the Androscoggin River between Brunswick and Bath, Maine. The topography at the site is characterized by low, undulating hills with

deeply incised brooks. The ground surface elevation ranges between mean sea level to over 110 ft. A 2,300-lineal-foot, soil-bentonite slurry has been emplaced at the site. The purpose of the slurry wall is to provide a subsurface barrier to prevent groundwater from flowing through subsurface contaminants contained within the landfill area[4], and all indications show that the barrier is successfully meeting this criteria. However, there is a portion of the barrier where the depth to the groundwater is approximately 20 ft. below the top of the barrier. This section of the barrier could be used to demonstrate the SEAtrace™ system. Because the results from the demonstration cannot be correlated with the effectiveness of the slurry wall and cap system (as SEAtrace™ is based on gaseous diffusion and the slurry wall is designed to mitigate hydraulic flow) a memorandum of understanding between SEA, NAS Brunwick and the regulatory agencies involved at the site will be negotiated prior to initiation of the demonstration. This letter of intent will essentially say that NAS Brunswick will not be required to complete any action based on the results of the demonstration.

G.3 Description of the SEAtrace™ System

SEAtrace™ is predicated on the relatively simple and predictable transport process of gaseous diffusion in porous media. Diffusion is an attractive process to utilize for leak detection because the tracer concentration histories measured at locations distant from the source are highly sensitive to both the size of the breach and the distance from the leak source. This sensitivity allows a global optimization modeling methodology to iterate to a leak geometry and location by minimizing errors in a relatively simple transport model.

A schematic of the SEAtrace™ system is shown in figure G1. Multiple sample points are located outside the barrier, as well as one or more injection and sample ports inside the barrier. These ports are connected to a stand-alone data acquisition and analysis system. A non-hazardous tracer gas (sulfur hexafluoride) is injected into the barrier, creating a large source volume of the tracer. If the barrier has a breach open to gas phase transport, the tracer will diffuse into the surrounding medium and the exterior sample ports will measure the amount of tracer in the soil gas with time. Once concentration history data has been collected, it must be analyzed if any tracer gas was detected outside the barrier. SEAtrace™ uses a global optimization technique to effectively search multidimensional "space" to simultaneously find the best fit solution based on all of the input parameters. These parameters include the measured concentration histories, the sample port locations, medium properties, and the source concentration. The code iterates to find a best-fit solution given the input parameters.

[4] OHM Remediation Services Corp. 1996. *Remedial Action Final Report, Remediation of Sites 1, 3, 5, 6, and 8 Naval Air Station Brunswick, Maine.* Vol. 1. Prepared for Department of the Navy Northern Division, Naval Facilities Engineering Command. OHM Project 16285. Pittsburgh; OHM Remediation.

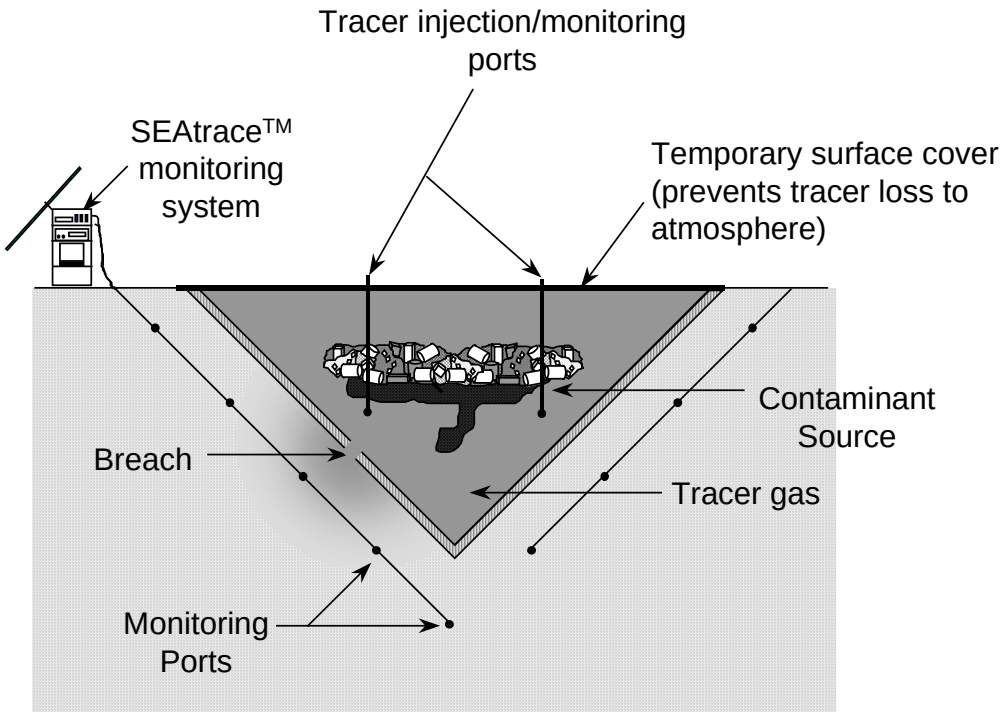

Figure G1. Schematic of a SEAtrace™ system installation.

Solar powered, remotely accessible, and capable of multimonth standalone operation, SEAtrace™ is ideal for the field. Since the approach uses real time analysis to characterize flaws, immediate repair of the barrier may be conducted with the appropriate remedial method. The gas analyzer used by the SEAtrace™ system is also capable of measuring volatile organic compounds in the gas phase, so the system is also well suited to long term monitoring of the barrier's integrity.

G.4 Design of the Demonstration

SEAtrace™ was developed to be capable of both verifying the integrity of a barrier immediately upon completion of its emplacement, and monitoring the long-term performance of the barrier. For both of these cases, the primary issue that must be addressed to develop the test plan is how small a leak the system must be able to detect in a given time frame. The size of leak that must be detectable will be dictated by regulatory concerns. The time allotted to detect the leak will be of greatest concern for the initial verification of the barrier (detecting a breach in the barrier prior to the removal of the emplacement equipment from the site will result in significant cost savings). For long term monitoring, the testing time will typically not be of importance. For the NAS Brunswick demonstration, no regulatory agencies are requiring a minimum detectable leak size because the barriers primary function is controlling the movement of groundwater around the contaminants, not controlling gaseous phase transport of the contaminants. For example, the demonstration at this site is a test of the verification system, not the barrier. Because the barrier is already emplaced, there is not a constraint on the time required to test the barrier due to cost. However, because of the typically

severe winters at the site, SEA would prefer to complete the testing to a relatively short period of time. SEA is estimating that site preparation could be completed in two weeks or less (depending on the mechanism used for emplacing the ports), inclusive of a ground penetrating radar survey needed to accurately locate the barrier. The tracer test itself would be completed over a six week period. Allowing a week for site abandonment, the total time required to complete the demonstration is approximately two months. Figure G2 shows an abbreviated milestone schedule for the proposed demonstration.

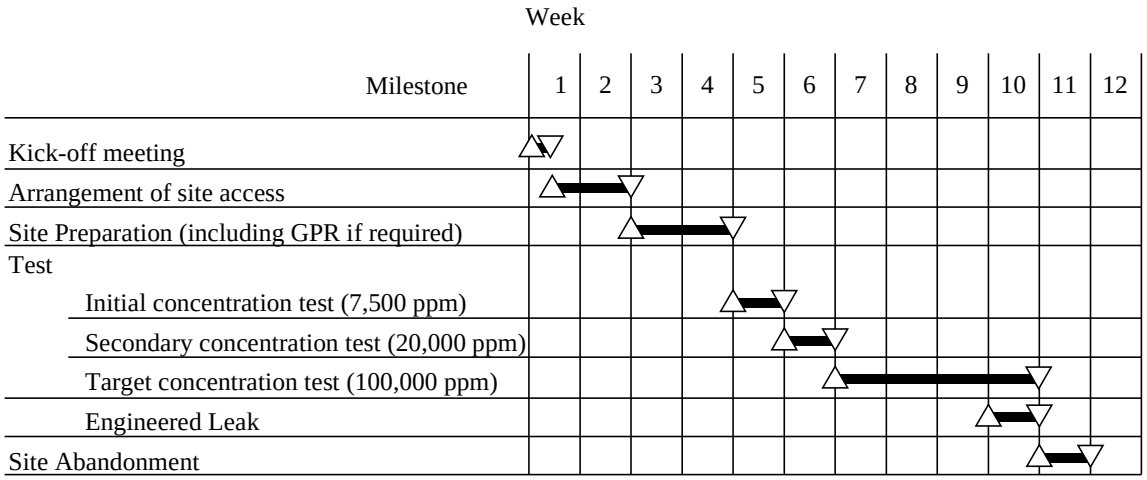

Figure G2. Abbreviated milestone schedule for the proposed SEAtrace™ demonstration.

G.4.1 Monitoring Port Spacing and Locations for the Demonstration

Given that a 5 week (maximum) test period is the driving constraint in the test design, calculations were performed to estimate what minimum size leak could be found by the system given several different test configurations, assuming a stepped injection sequence of the tracer. These calculations are attached as appendix A. After reviewing the calculational results, a 6 ft. horizontal x 6 ft. vertical skewed grid of ports offset 4 ft. from the barrier is recommended (figure G3). Offsetting the ports 4 ft. from the barrier wall allows a considerable safety zone that minimizes any chances of inadvertently drilling through the barrier during port emplacement. The 6 ft. x 6 ft. grid allows for relatively small diameter leaks to be found over the test period. The calculations performed predict that the system will be able to see a leak as small as 1.85 sq. in. (equivalent radius of 0.77 in.) over the test sequence. A review of design drawings of the barrier show the maximum distance between the top of the barrier wall and the ground water to be approximately 20 ft. This depth to the ground water exists roughly between stations 1650 and 2200 on the west side of the barrier. As SEAtrace™ is a vadose zone monitoring system, some portion of this 550 foot section of the barrier would be the preferred demonstration area. Spacing the ports on a 6' horizontal x 6' vertical interval would require a total of 18 monitoring wells to be installed, each with 3 ports (for a total of 54 ports) to test roughly a 100 ft. section of the barrier.

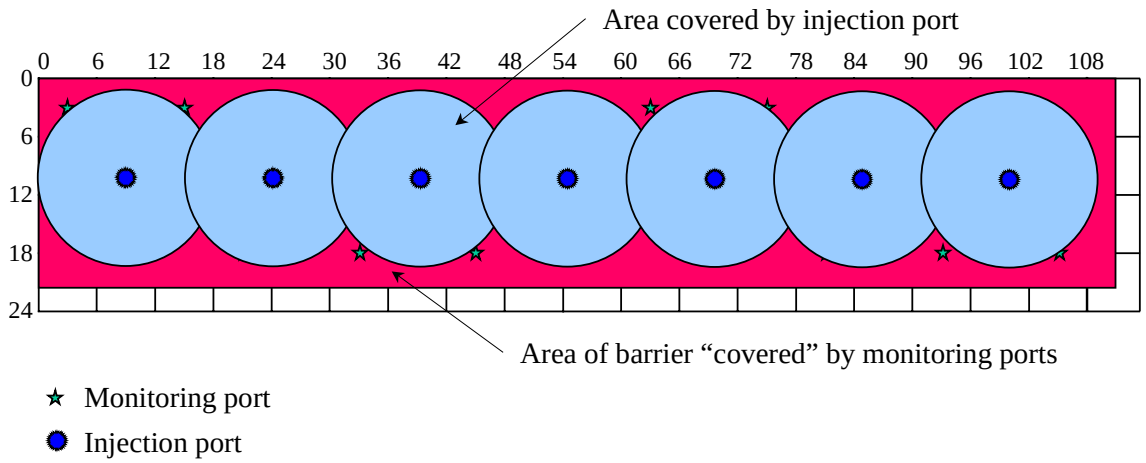

Figure G3. Schematic of the proposed monitoring port/injection port layout for the NAS Brunswick demonstration. The monitoring ports are outside of the volume contained by the barrier. The injection ports are inside the barrier volume.

G.4.2 Injection Port Spacing and Locations for the Demonstration

Injection ports will be spaced inside the NAS Brunswick barrier to provide as constant a tracer source concentration as possible along the length of the wall that will be covered, using the fewest number of ports possible. Spacing from port to port, and from the port to the walls was guided by the modeling exercise discussed in appendix B. Given the maximum area of barrier that will be tested (roughly 100 ft. x 20 ft.), 7 injection ports would be needed (spaced approximately 15 ft. apart from one another). Each of the ports would be installed to a depth of 10-12 ft. (as referenced from the top of the barrier wall as opposed to the ground surface) approximately 4 ft. away from the interior edge of the barrier wall. Figure G3 schematically depicts the area of influence of each injection port.

The tracer gas injection scheme for the SEAtrace™ system is designed to create a uniform concentration of tracer along the barrier wall itself rather than within the volume of the enclosed soil. Injection occurs in slow, controlled, staged steps. Initial injections at one or more low concentrations allows detection of relatively large flaws, if they exist, without the possibility of flooding the medium with such high concentrations of the tracer that the maximum detection limit of the gas analyzer is exceeded. Subsequent testing at higher tracer concentrations allows the system to search for successively smaller leaks. While the typical starting concentration is 2,500 ppm, calculations showed that the overall distance between the injection and the monitoring ports for the NAS Brunswick barrier would preclude any but extremely large leaks to be seen within the allotted time. Thus the starting concentration will be 7,500 ppm. After seven days, if no tracer has been detected at any sampling ports, additional gas will be injected to increase the source concentration to 20,000 ppm. After an additional seven days, the source concentration will be raised to the target demonstration concentration of 80,000 to 100,000 ppm. Tracer will be injected periodically over the duration of the test to maintain the target concentration.

G.4.3 Injection/Sampling Port Installation

Given the shallow depth required for the ports (the maximum port depth would be 18 ft. below the top of the barrier wall), it is possible that all of the ports could be installed using a hand held penetrometer. The penetrometer creates a 1.25 in. diameter hole. The medium to the desired depth of installation is described as being a homongeneous sand, which is ideal for a push type port installation if the hole can stay open long enough for installation of the ports. The ports used with the system consist of a small filter (3/8" diameter by 1 ¼" long) that is attached to a small diameter (1/8" o.d. x 1/16" i.d) polyethylene tubing. The tubing is lowered into the open hole to the desired depth, and then the borehole is backfilled with a mixture of either dry bentonite powder and sand or silica flour and sand. The only requirement of the backfill seperating the monitoring points, from an experimental standpoint, is that it be less permeable to the soil gas than the surrounding medium. The upper 1.5 – 2 ft. of the hole will be cased with 2 inch diameter schedule 40 PVC pipe. This casing is connected together above ground using standard tee fittings and pipe. Sample tubing is run inside the pipe to the scanning system, as a means to protect the flexible tubing from damage during the test.

Even if the soil is not stable enough to remain open for a short period of time, the penetrometer can still be used if a disposable tip is used. If this were necessary, each port would be installed independently (rather than having multilpe monitoring ports in each borehole). If the medium proves to be unsuitable for the hand operated direct push probe, a rotary drill rig would be used. The smallest diameter bit available would be used, typically 4 or 6 inch diameter. The boreholes would be backfilled as described above. No boreholes will penetrate to the site ground water table.

Penetrating the surface cap to emplace the injection ports would be done under the supervision of a company with expertise in covers. A tentative plan for installation of the ports includes:

- Removal of overlying soil from the cap in the area where the borehole is to be made.
- Removal of a small section of the geomembrane within the cleared area.
- Installation of the injection port, preferably with the penetrometer. Using a push technique to form the borehole will eliminate drilling spoils.
- Backfill the borehole. A short PVC casing (extending 2 – 3 ft. below the surface of the geomembrane) will be installed during the backfill procedure. This allows a seal to be formed between the casing and the geomembrane with a boot.

After completion of the test, the casing and boot will be removed, and the geomembrane will be repaired. Repairs will be tested. Finally, the overburden soil will be replaced.

G.4.4 Possible Adjustments to the Proposed Demonstration Configuration

The proposed demonstration configuration may need to be adjusted due to conditions at the site not being the same as those assumed in the calculations. The actual thickness of the barrier, the diffusivity of the tracer through the soil gas, and the depth to the ground water are the parameters most likely to require adjustments to be made. However, the

overall number of monitoring/injection wells would not increase. In fact, the final configuration of the demonstration can be adjusted in several ways, if the proposed configuration is unacceptable to the host site:

1. Minimize penetrations through the barrier cap
2. Minimize the number of monitoring wells exterior to the barrier
3. Increase the proposed standoff distance between the ports and the barrier to assure the barrier will not be inadvertently damaged during port installation

G.4.5 Leak Anomaly

To validate the ability of the system to function as designed in the event that no leaks are detected in the barrier during the test duration, an engineered leak (leak anomaly) will be constructed. The leak anomaly will be located in close proximity (within 50 ft.) to the portion of the barrier that will be used for the demonstration. Essentially, the anomaly consists of (please reword) fabricating a known leak (both location and size) near the slurry wall (typically within 50 to 75 feet of the outside the contained volume. A small container is buried to a shallow depth (5 to 10 ft below ground surface). The container acts as the source volume. A gate valve attached to the container forms the "leak." A 1.5 inch diameter valve would be used. Small diameter tubing from the surface to the container is used to inject the tracer gas into the source volume. The test is commenced with the opening of the "leak." Monitoring ports are installed near the leak anomaly, at the same spacing used to monitor the barrier.

G.4.6 Site Abandonment

After the demonstration is completed, the scanning system will be removed, as will the protective pipe running between the boreholes and the scanning system. All of the borehole casing will be removed. The small diameter flexible tubing will be terminated several inches below the ground surface. If desired, the tubing can be capped. All repairs of the landfill cap liner will be completed to its original specifications using an approved contractor.

G.5 Health and Safety Plan

The Engineering firm HLA (Harding Lawson and Associates, Inc), with help from SEA employees, will complete installation of the demonstration sampling and monitoring ports. HLA is an established entity at NAS Brunswick, and, among other tasks, performs necessary checks and repairs to the surface cap at the barrier site. Because of this existing work, they presently have in place a site specific Health and Safety Plan. The work for this demonstration will be performed in accordance with that plan and an HLA employee will be on site whenever SEA personnel are there. In addition, HLA will assume the responsibility for disposal of all wastes generated during the demonstration.

G.6 Attachment A -- Calculations to Determine Sample Port Spacing

The primary design issue in the application of SEAtrace™ is the gas sample and injection port locations. Determining the spacing of the sample ports is very critical to the success of the SEAtrace™ system, and there are numerous things that must be considered.

Uncontrollable variables (from the system's viewpoint) include medium properties (diffusivity, porosity, tortuosity, permeability), barrier properties (diffusivity, porosity, tortuosity, permeability), barrier dimensions (thickness as well as the overall area which must be verified), and barrier construction. Many of these variables are unknown, and estimates must be used in the calculations. Other variables that influence sample port spacing include the source concentration (which is bounded by the amount of soil gas that could realistically be replaced with the tracer, and is a function of the injection port location, mass injection rate, and medium properties), the measurement time of verification, and the minimum size of the leak that is desired to be detected.

A flux limited forward model was used to estimate resulting medium concentration histories for different input parameters. Assumptions/ranges for the input parameters included:

- The effective diffusivity of the leak/medium was assumed to be the same value because the barrier has been in place for a considerable amount of time (e.g. any moisture added to the medium during barrier emplacement should have equilibrated by now). The medium in question is described as sand.[5] The effective diffusivity of the tracer through the soil gas that was chosen was conservative (1e-6 m^2/s) for this type of soil (the diffusivity of SF_6 in air is 7.03e-6 m^2/s).
- Source concentrations used in the calculations were 2500, 7500, 20,000 and 100,000 ppm. These values correspond to the target injection concentrations. The exit concentration was calculated using the relationship $C_{exit} = C_{source}$ (.7 – 5714D). This relationship was developed using results from numerical modeling and was shown to be accurate if the medium diffusivity was equal to the leak diffusivity.
- Barrier thickness was chosen to be 5 feet. The "*Remedial Action Final Report, Remediation of Sites 1, 3, 5, 6, and 8 Naval Air Station Bruswick, Maine*" report states "To maintain stable surficial soil conditions during trench excavation, the surficial sideslopes of the trench were routinely sloped and/or benched back. As a result, the top of the slurry wall was significantly wider than the minimum width of 3 feet that was defined by the project technical specifications and design drawings." The document does not define what "significantly wider" is, so a value of 5 feet was assumed.
- Leak radius was varied to find the minimum value that would allow a detectable amount of tracer (assumed to be 1 ppm) to be seen distances of 2.0 m and 3.0 m from the leak. These distances were chosen after looking at various port spacing plans and determining the maximum distance a leak would be from at least 3 ports closest to it. Port spacings of 6' horizontal x 6' vertical and 8' horizontal and 8' vertical skewed grids were reviewed. For each of the grids, the standoff distances of 2', 4' and 6' of the ports from the barrier were used.

[5] OHM Remediation Services Corp. 1996. *Remedial Action Final Report, Remediation of Sites 1, 3, 5, 6, and 8 Naval Air Station Brunswick, Maine*. Vol. 1. Prepared for Department of the Navy Northern Division, Naval Facilities Engineering Command. OHM Project 16285. Pittsburgh; OHM Remediation.

- The time used for each calculation corresponded to the anticipated delay between the different injection pulses. The initial target concentrations of 7,500 and 20,000 ppm will sequentially be maintained for a period of 3 days each after a 4 day equilibration period (assuming that tracer is not detected at any of these concentrations). The purpose of the low concentration, stepped injections is to assure there is no gross leakage across the barrier prior to injection of the tracer gas to the desired source concentration. The final target concentration of 100,000 ppm will be maintained for the duration of the test time (approximately 4 weeks).

Results are summarized in table G-A1. Figures G-A1 through G-A13 graph the calculational results for the various cases.

Table G-A1. Summary of the calculational results completed with the forward diffusion model for the NAS Brunswick .

Grid [A]	Port Stand-off[B] (ft)	Min. required detection dist,[C] (m)	Detection distance used in calc.[D] (m)	Min. leak radius that could be seen given a source concentration of:							
				2500 ppm, 3 day test		7500 ppm, 3 day test		20,000 ppm, 3 day test		100,000 ppm, 28 day test	
				(cm)	(in)	(cm)	(in)	(cm)	(in)	(cm)	(in)
6' X 6'	2	1.93	2.00	86	33.9	50	19.7	31	12.2	1.65	0.65
	4	2.20	2.25	160	63.0	95	37.4	57	22.4	1.95	0.77
	6	2.59	2.75	--	--	--	--	225	88.6	2.60	1.02
8' X 8'	2	2.51	2.50	--	--	180	70.9	110	43.3	2.20	0.87
	4	2.73	2.75	--	--	--	--	225	88.6	2.60	1.02
	6	3.05	3.00	--	--	--	--	--	--	3.00	1.18

A Values listed are horizontal spacing by vertical spacing, for a skewed grid

B Distance of ports from barrier wall

C Distance tracer must be able to be detected (m) for the system to function properly given the grid spacing and distance between the ports and the barrier

D Detection distance used in calculating the minimum leak radius that could be detected (the values in column C rounded to the nearest ¼ m)

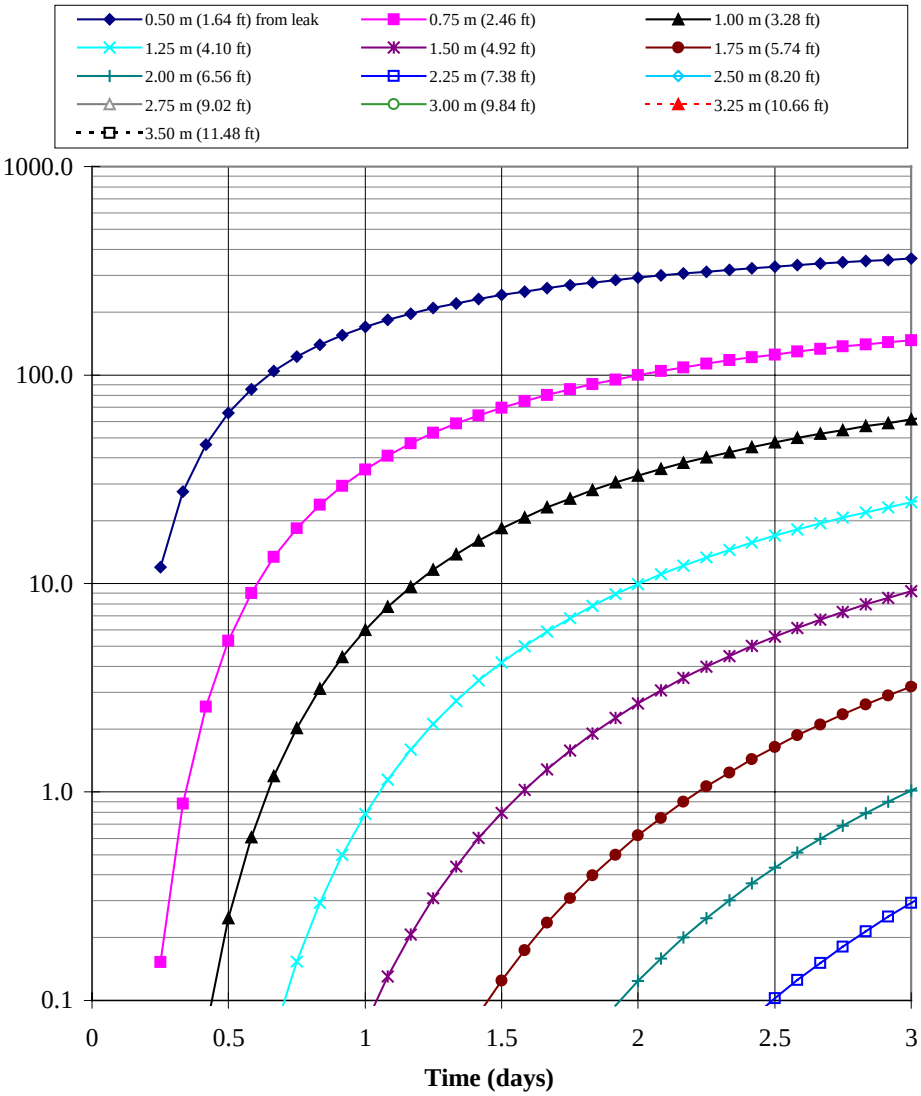

Leak Diffusivity:	1.00E-06	m^2/sec	0.0036	m^2/hour
Medium Diffusivity	1.00E-06	m^2/sec		
Source Concentration	2500	ppm	15175	mg/m^3
Exit Concentration	1736	ppm	10536	mg/m^3
Barrier Thickness	5.00	feet	1.52	meters
Exit flux (mg/m^2/s)	3.04E-03			
Leak Radius	86	cm	8.60E-01	meters
Leak Area	23235.22	cm^2		

	33.86 inches

Figure G-A1. Results from the flux limited diffusion model showing the minimum leak size that could be detected at a 2-m detection distance, given the conditions listed above (source concentration of 2,500 ppm).

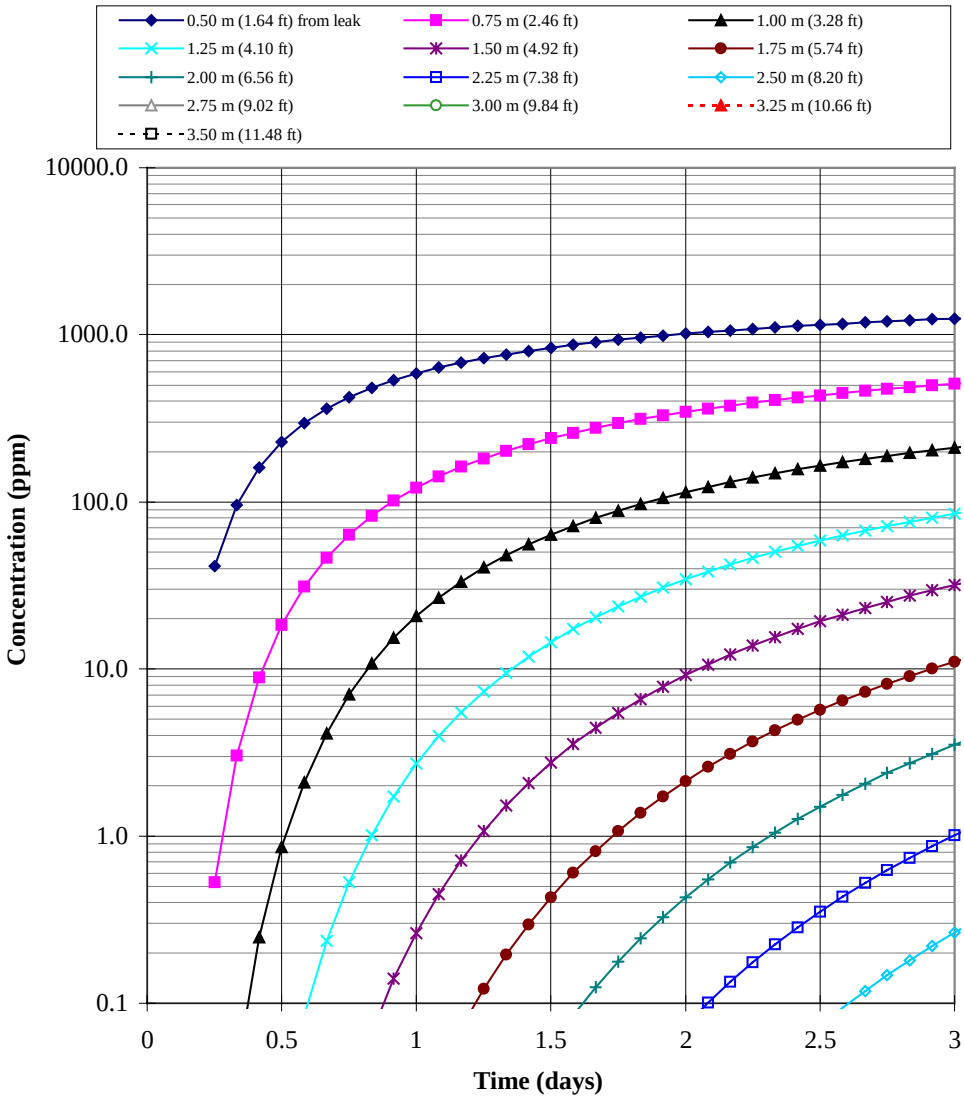

Leak Diffusivity:	1.00E-06	m^2/sec	0.0036	m^2/hour	
Medium Diffusivity	1.00E-06	m^2/sec			
Source Concentration	2500	ppm	15175	mg/m^3	
Exit Concentration	1736	ppm	10536	mg/m^3	
Barrier Thickness	5.00	feet	1.52	meters	
Exit flux (mg/m^2/s)	3.04E-03				
Leak Radius	160	cm	1.6E+00	meters	62.99 inches
Leak Area	80424.77	cm^2			

Figure G-A2. Results from the flux limited diffusion model showing the minimum leak size that could be detected at a 2.25-m detection distance, given the conditions listed above (source concentration of 2,500 ppm).

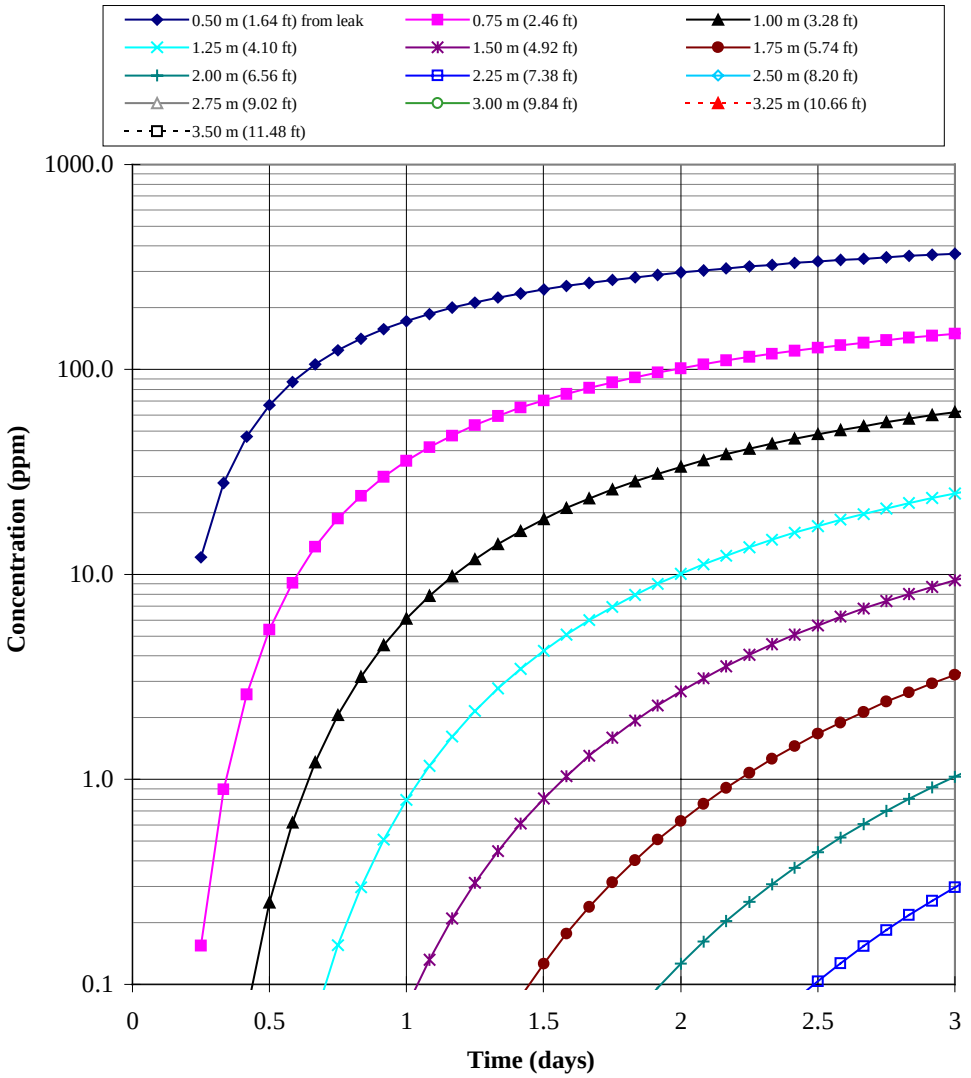

Leak Diffusivity:	1.00E-06	m^2/sec	0.0036	m^2/hour	
Medium Diffusivity	1.00E-06	m^2/sec			
Source Concentration	7500	ppm	45525	mg/m^3	
Exit Concentration	5207	ppm	31607	mg/m^3	
Barrier Thickness	5.00	feet	1.52	meters	
Exit flux (mg/m^2/s)	9.13E-03				
Leak Radius	50	cm	5.0E-01	meters	19.69 inches
Leak Area	7.85E+03	cm^2			

Figure G-A3. Results from the flux limited diffusion model showing the minimum leak size that could be detected at a 2-m detection distance, given the conditions listed above (7500 ppm source concentration).

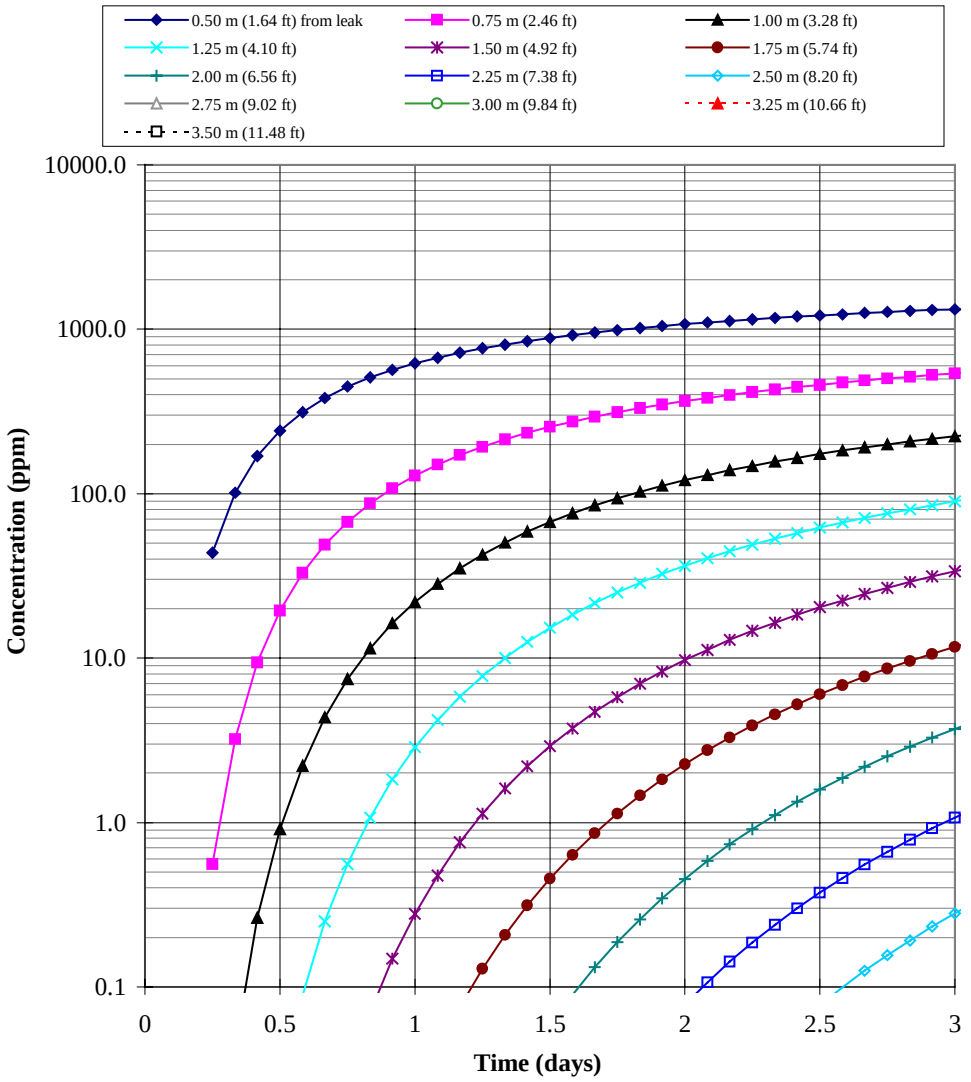

Leak Diffusivity:	1.00E-06	m^2/sec	0.0036	m^2/hour	
Medium Diffusivity	1.00E-06	m^2/sec			
Source Concentration	7500	ppm	45525	mg/m^3	
Exit Concentration	5207	ppm	31607	mg/m^3	
Barrier Thickness	5.00	feet	1.52	meters	
Exit flux (mg/m^2/s)	9.13E-03				
Leak Radius	95	cm	9.5E-01	meters	37.40 inches
Leak Area	2.84E+04	cm^2			

Figure G-A4. Results from the flux limited diffusion model showing the minimum leak size that could be detected at a 2.25-m detection distance, given the conditions listed above (7500 ppm source concentration).

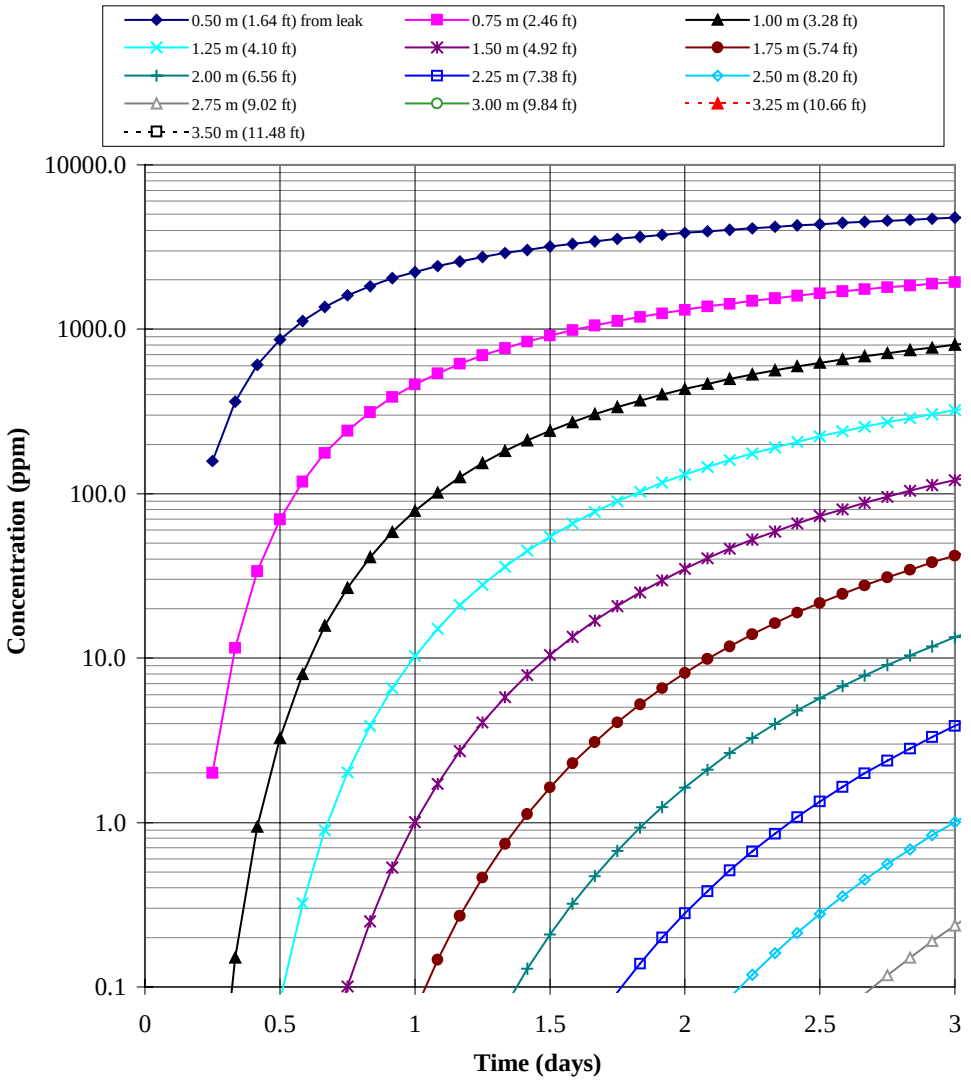

Leak Diffusivity:	1.00E-06	m^2/sec	0.0036	m^2/hour	
Medium Diffusivity	1.00E-06	m^2/sec			
Source Concentration	7500	ppm	45525	mg/m^3	
Exit Concentration	5207	ppm	31607	mg/m^3	
Barrier Thickness	5.00	feet	1.52	meters	
Exit flux (mg/m^2/s)	9.13E-03				
Leak Radius	180	cm	1.8E+00	meters	70.87 inches
Leak Area	1.02E+05	cm^2			

Figure G-A5. Results from the flux limited diffusion model showing the minimum leak size that could be detected at a 2.75-m detection distance, given the conditions listed above (7500 ppm source concentration).

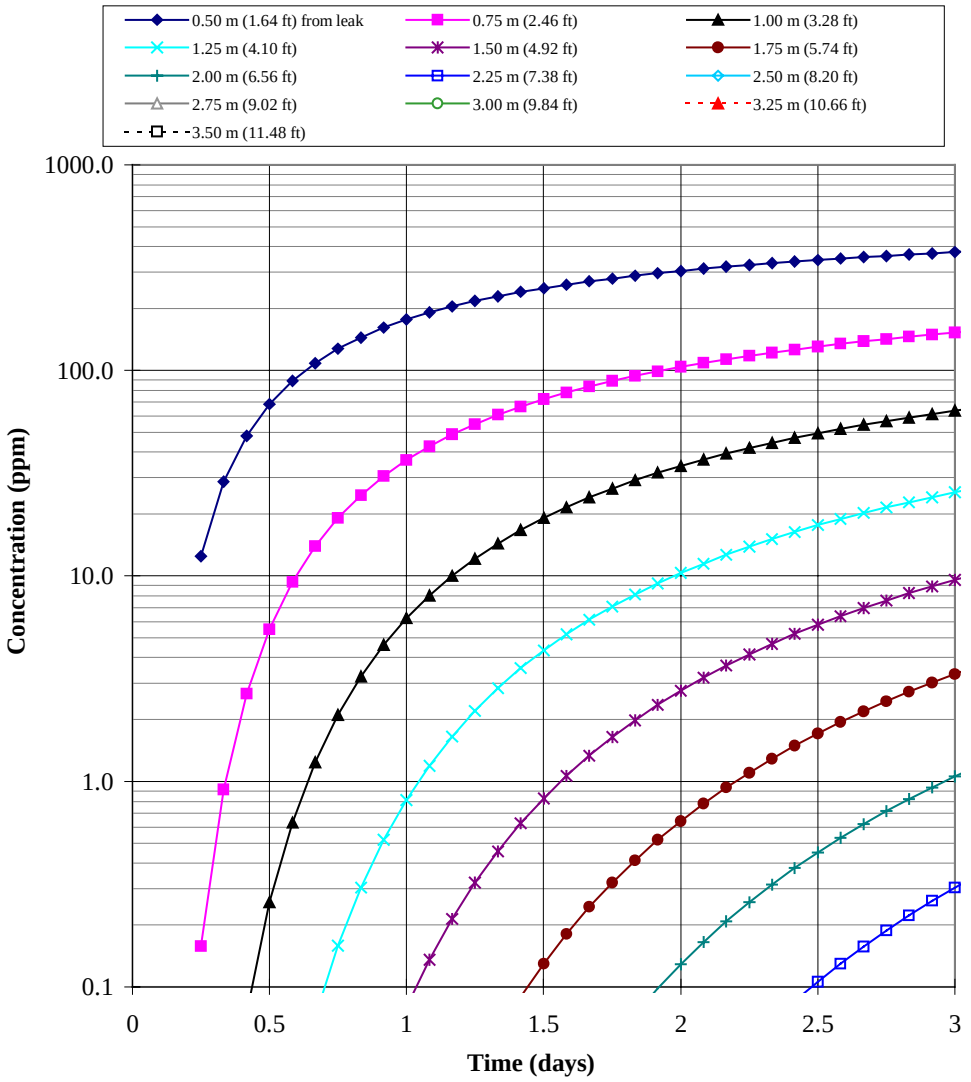

Leak Diffusivity:	1.00E-06	m^2/sec	0.0036	m^2/hour	
Medium Diffusivity	1.00E-06	m^2/sec			
Source Concentration	20000	ppm	121400	mg/m^3	
Exit Concentration	13886	ppm	84286	mg/m^3	
Barrier Thickness	5.00	feet	1.52	meters	
Exit flux (mg/m^2/s)	2.44E-02				
Leak Radius	31	cm	3.1E-01	meters	12.20 inches
Leak Area	3.02E+03	cm^2			

Figure G-A6. Results from the flux limited diffusion model showing the minimum leak size that could be detected at a 2-m detection distance, given the conditions listed above (20,000 ppm source concentration).

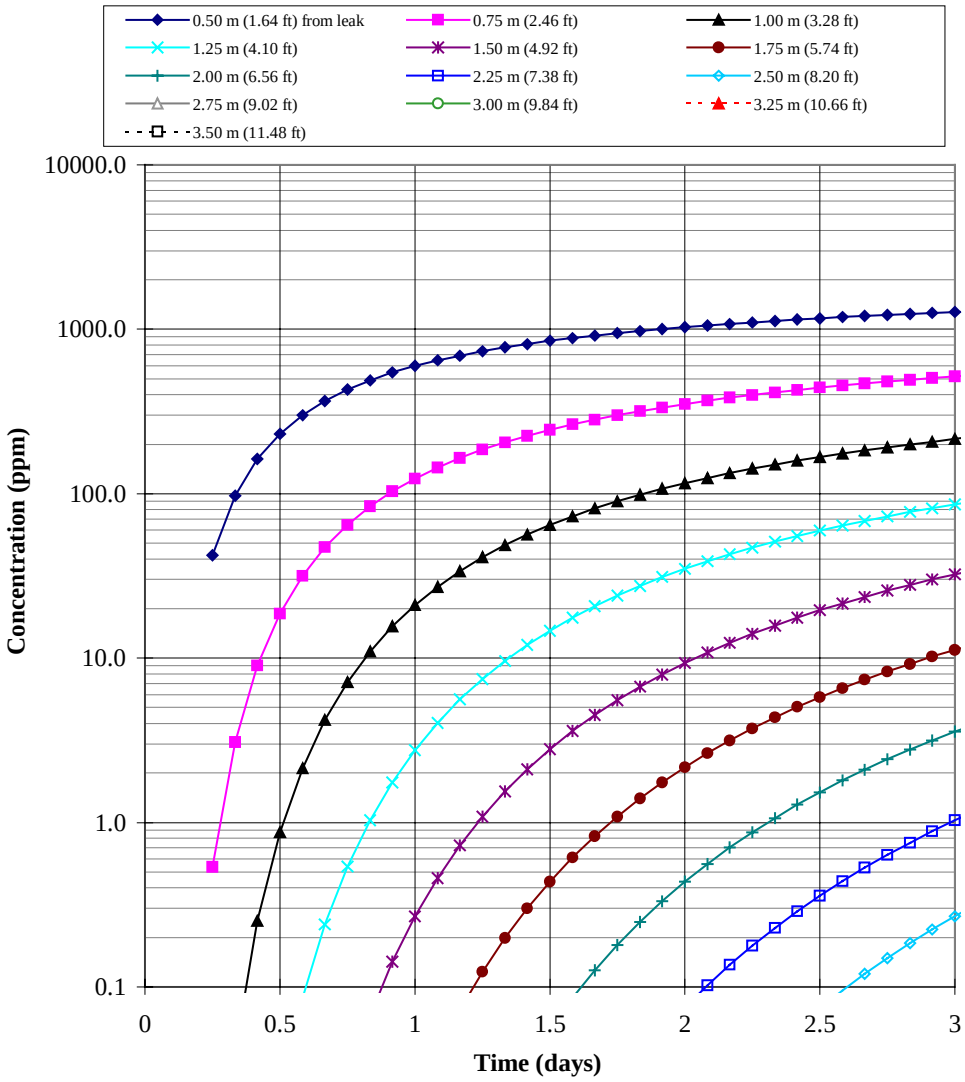

Leak Diffusivity:	1.00E-06	m^2/sec	0.0036	m^2/hour	
Medium Diffusivity	1.00E-06	m^2/sec			
Source Concentration	20000	ppm	121400	mg/m^3	
Exit Concentration	13886	ppm	84286	mg/m^3	
Barrier Thickness	5.00	feet	1.52	meters	
Exit flux (mg/m^2/s)	2.44E-02				
Leak Radius	57	cm	5.7E-01	meters	22.44 inches
Leak Area	1.02E+04	cm^2			

Figure G-A7. Results from the flux limited diffusion model showing the minimum leak size that could be detected at a 2.25-m detection distance, given the conditions listed above (20,000 ppm source concentration).

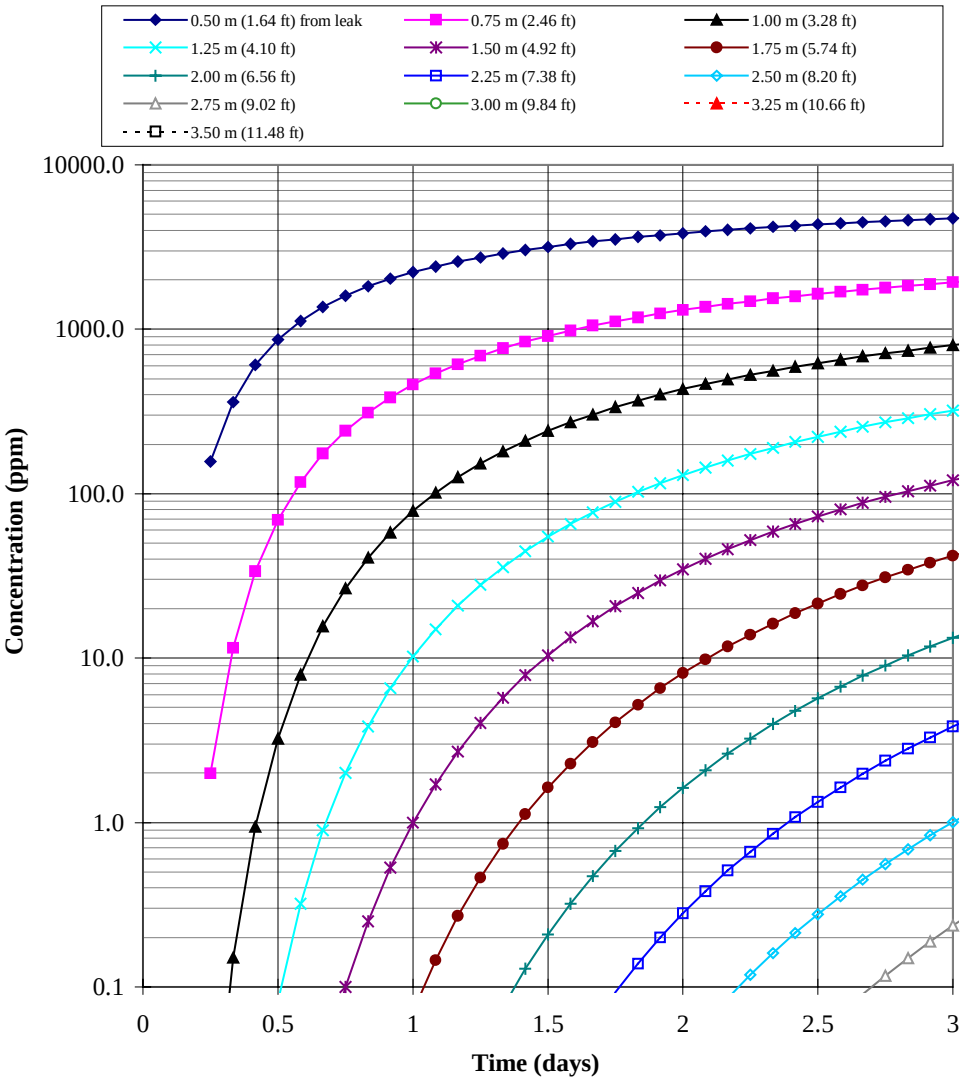

Leak Diffusivity:	1.00E-06	m^2/sec	0.0036	m^2/hour	
Medium Diffusivity	1.00E-06	m^2/sec			
Source Concentration	20000	ppm	121400	mg/m^3	
Exit Concentration	13886	ppm	84286	mg/m^3	
Barrier Thickness	5.00	feet	1.52	meters	
Exit flux (mg/m^2/s)	2.44E-02				
Leak Radius	110	cm	1.1E+00	meters	43.31 inches
Leak Area	3.80E+04	cm^2			

Figure G-A8. Results from the flux limited diffusion model showing the minimum leak size that could be detected at a 2.50-m detection distance, given the conditions listed above (20,000 ppm source concentration).

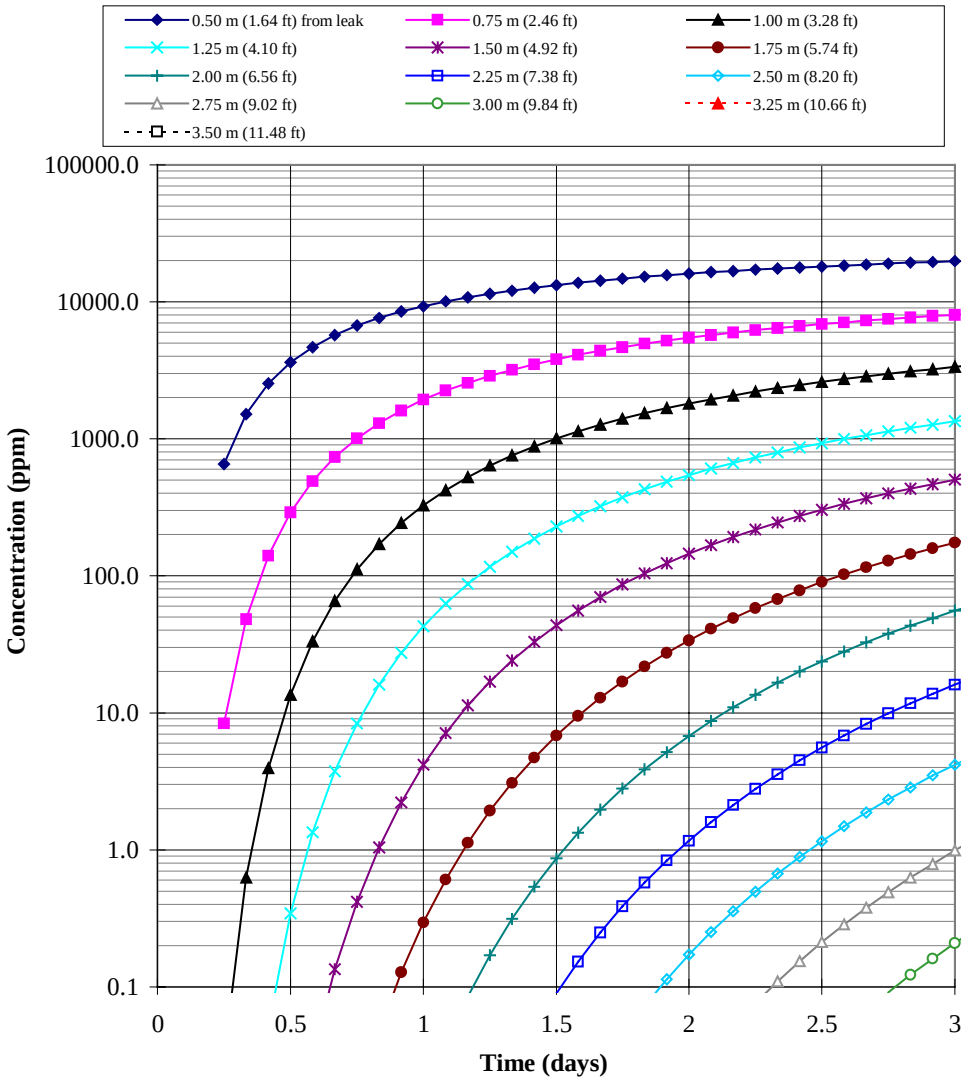

Leak Diffusivity:	1.00E-06	m^2/sec	0.0036	m^2/hour
Medium Diffusivity	1.00E-06	m^2/sec		
Source Concentration	20000	ppm	121400	mg/m^3
Exit Concentration	13886	ppm	84286	mg/m^3
Barrier Thickness	5.00	feet	1.52	meters
Exit flux (mg/m^2/s)	2.44E-02			
Leak Radius	225	cm	2.3E+00	meters 88.58 inches
Leak Area	1.59E+05	cm^2		

Figure G-A9. Results from the flux limited diffusion model showing the minimum leak size that could be detected at a 2.75-m detection distance, given the conditions listed above (20,000 ppm source concentration).

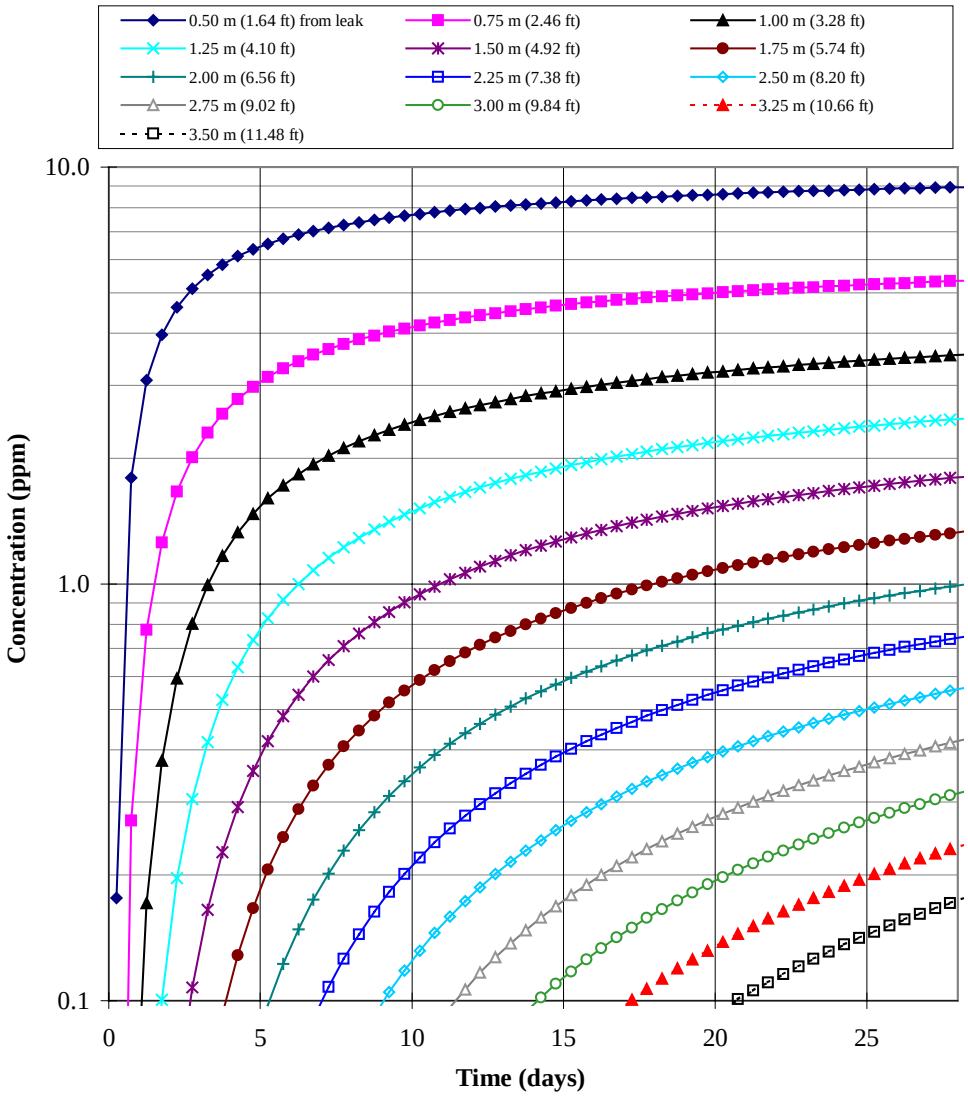

Leak Diffusivity:	1.00E-06	m^2/sec	0.0036	m^2/hour	
Medium Diffusivity	1.00E-06	m^2/sec			
Source Concentration	100000	ppm	607000	mg/m^3	
Exit Concentration	69429	ppm	421432	mg/m^3	
Barrier Thickness	5.00	feet	1.52	meters	
Exit flux (mg/m^2/s)	1.22E-01				
Leak Radius	1.65	cm	1.65E-02	meters	0.65 inches
Leak Area	8.55	cm^2			

Figure G-A10. Results from the flux limited diffusion model showing the minimum leak size that could be detected at a 2-m detection distance, given the conditions listed above (100,000 ppm source concentration).

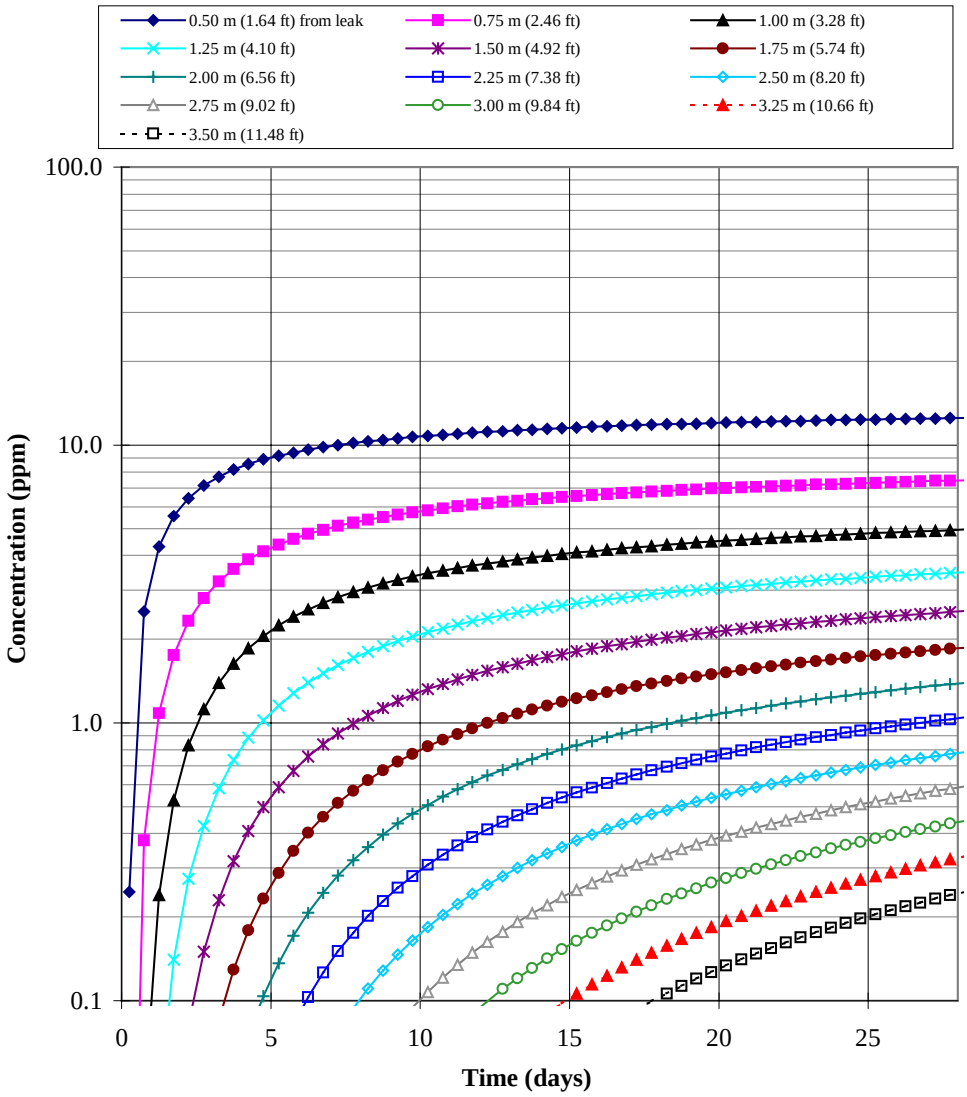

Leak Diffusivity:	1.00E-06	m^2/sec	0.0036	m^2/hour	
Medium Diffusivity	1.00E-06	m^2/sec			
Source Concentration	100000	ppm	607000	mg/m^3	
Exit Concentration	69429	ppm	421432	mg/m^3	
Barrier Thickness	5.00	feet	1.52	meters	
Exit flux (mg/m^2/s)	1.22E-01				
Leak Radius	1.95	cm	1.95E-02	meters	0.77 inches
Leak Area	11.95	cm^2			

Figure G-A11. Results from the flux limited diffusion model showing the minimum leak size that could be detected at a 2.25-m detection distance, given the conditions listed above (100,000 ppm source concentration).

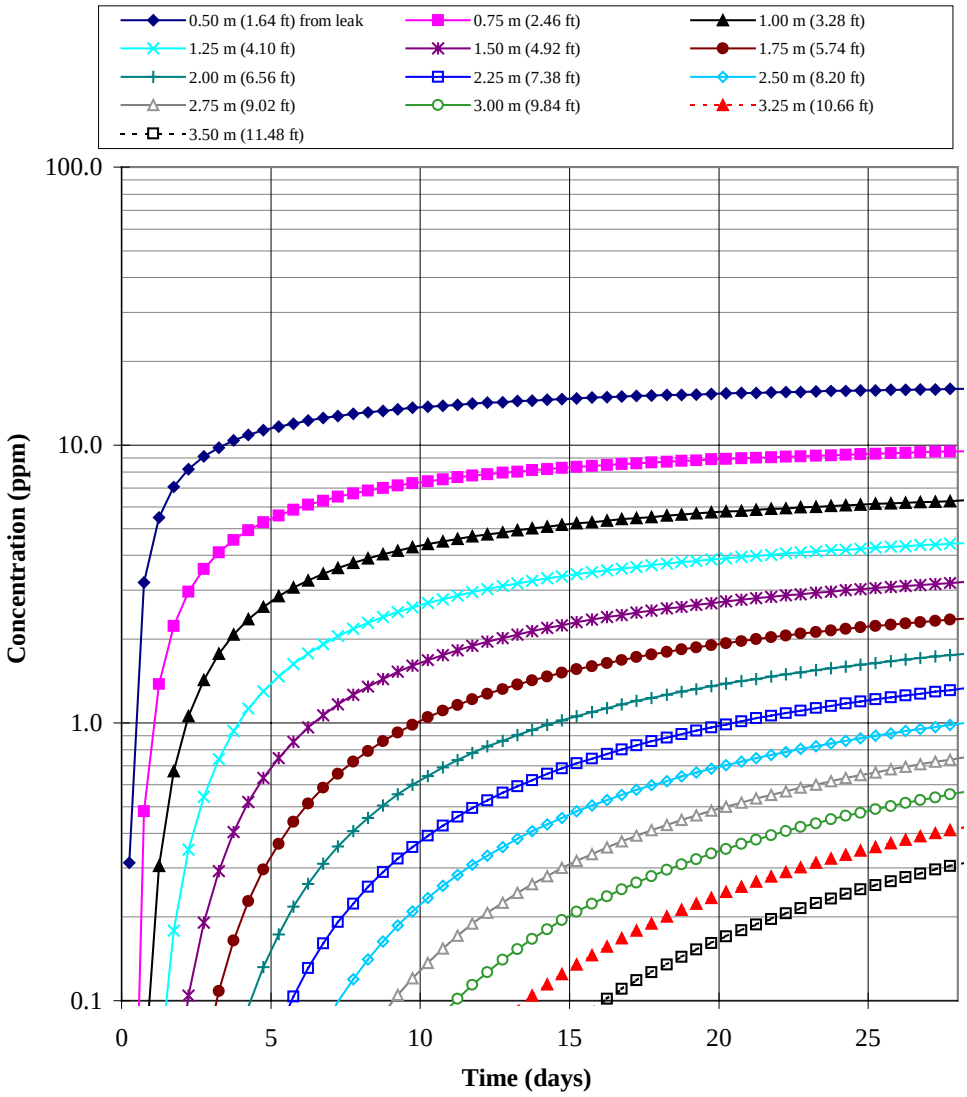

Leak Diffusivity:	1.00E-06	m^2/sec	0.0036	m^2/hour	
Medium Diffusivity	1.00E-06	m^2/sec			
Source Concentration	100000	ppm	607000	mg/m^3	
Exit Concentration	69429	ppm	421432	mg/m^3	
Barrier Thickness	5.00	feet	1.52	meters	
Exit flux (mg/m^2/s)	1.22E-01				
Leak Radius	2.2	cm	2.20E-02	meters	0.87 inches
Leak Area	15.21	cm^2			

Figure G-A12. Results from the flux limited diffusion model showing the minimum leak size that could be detected at a 2.50-m detection distance, given the conditions listed above (100,000 ppm source concentration).

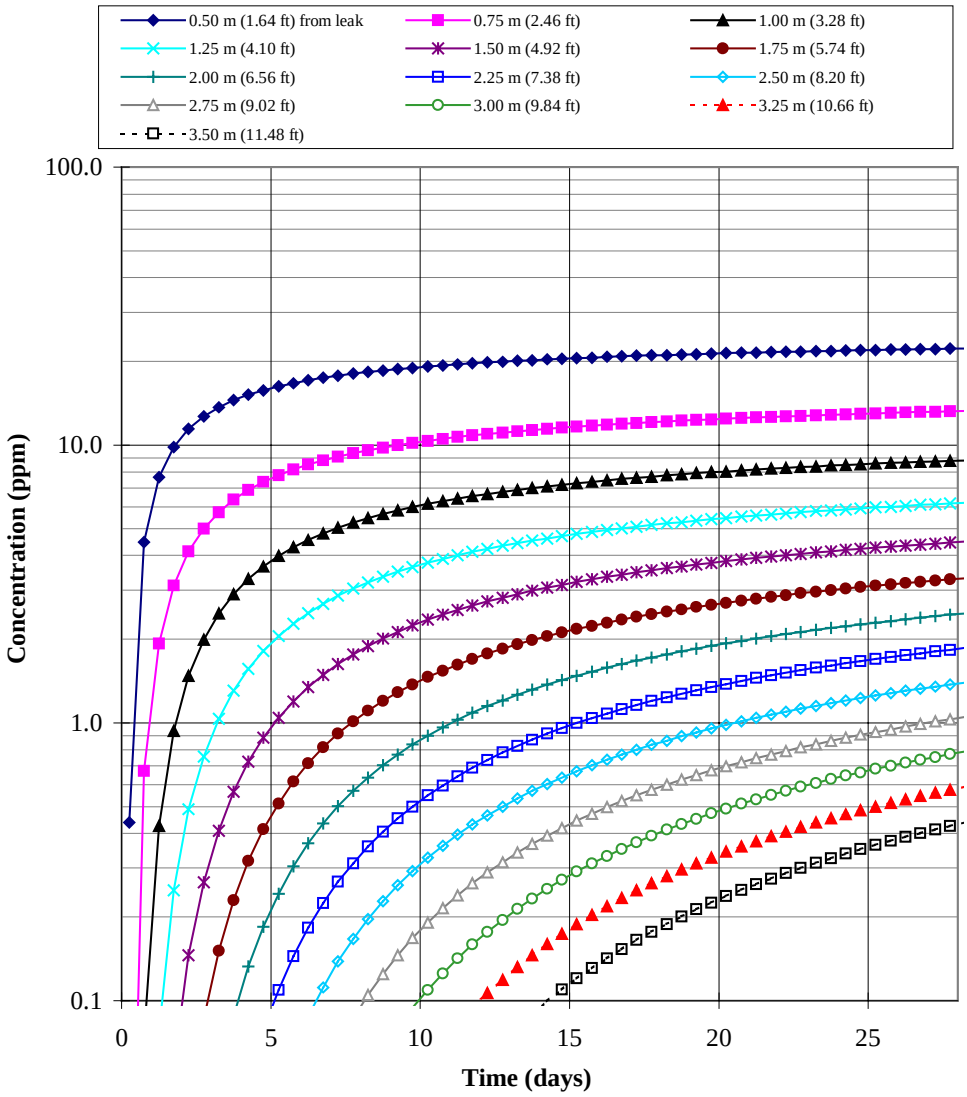

Leak Diffusivity:	1.00E-06	m^2/sec	0.0036	m^2/hour	
Medium Diffusivity	1.00E-06	m^2/sec			
Source Concentration	100000	ppm	607000	mg/m^3	
Exit Concentration	69429	ppm	421432	mg/m^3	
Barrier Thickness	5.00	feet	1.52	meters	
Exit flux (mg/m^2/s)	1.22E-01				
Leak Radius	2.6	cm	2.60E-02	meters	1.02 inches
Leak Area	21.24	cm^2			

Figure G-A13. Results from the flux limited diffusion model showing the minimum leak size that could be detected at a 2.75-m detection distance, given the conditions listed above (100,000 ppm source concentration).

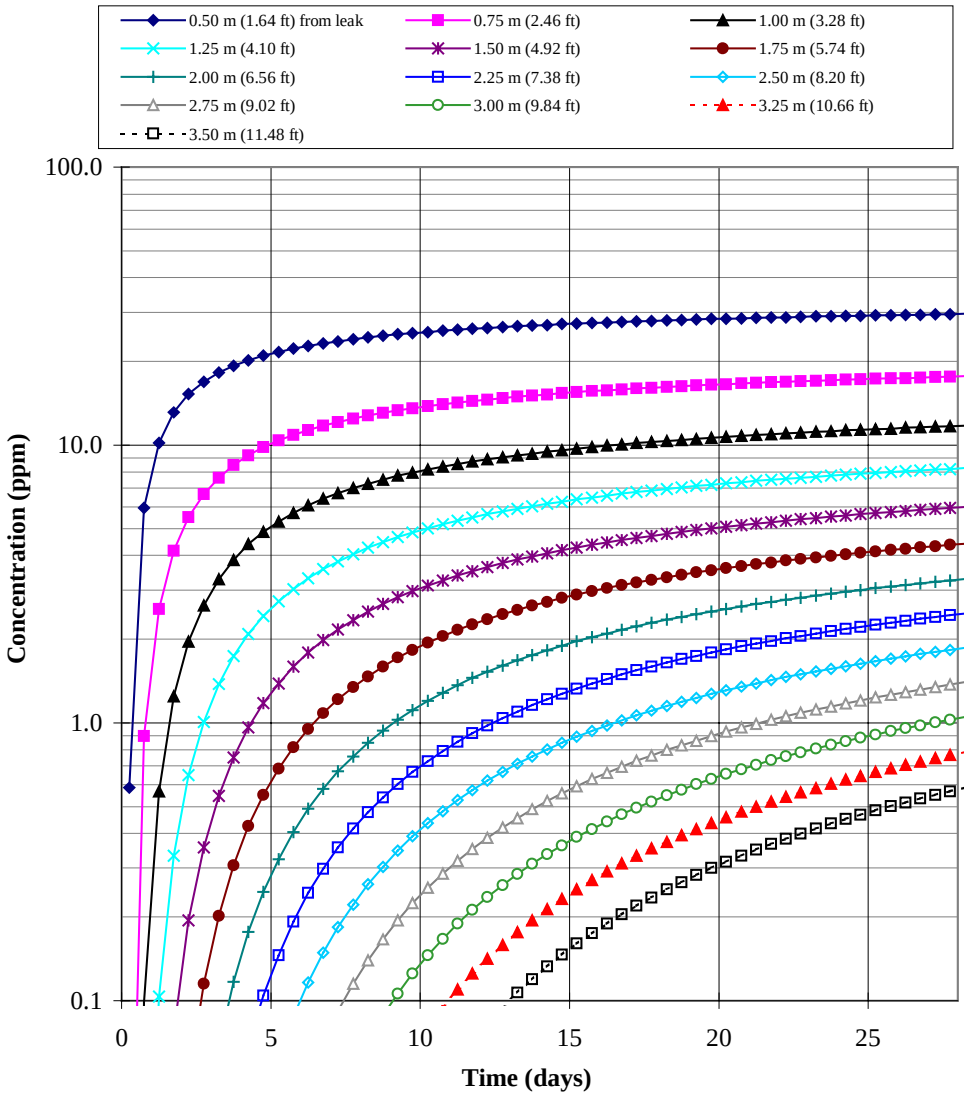

Leak Diffusivity:	1.00E-06	m^2/sec	0.0036	m^2/hour	
Medium Diffusivity	1.00E-06	m^2/sec			
Source Concentration	100000	ppm	607000	mg/m^3	
Exit Concentration	69429	ppm	421432	mg/m^3	
Barrier Thickness	5.00	feet	1.52	meters	
Exit flux (mg/m^2/s)	1.22E-01				
Leak Radius	3	cm	3.00E-02	meters	1.18 inches
Leak Area	28.27	cm^2			

Figure G-A14. Results from the flux limited diffusion model showing the minimum leak size that could be detected at a 3-m detection distance, given the conditions listed above (100,000 ppm source concentration).

G.7 Attachment B – Calculation of Injection Point Spacing

A numerical model was used to determine a scheme for slow, stepped injection of tracer gas that would create progressively higher, and relatively uniform concentrations along the barrier wall. The target concentrations for the first, second, and third injections were determined to be between 2000 to 5000 parts per million (ppm), 5000 to 10,000 ppm, and 10,000 to 30,000 ppm respectively. T2VOC, a finite difference numerical simulator capable of modeling three-phase (gas, aqueous, NAPL), three component (water, air, volatile organic compound), nonisothermal flow and transport through porous media (Falta, Pruess, Finsterle, Battistelli 1995), was used to determine the proper location of the injection ports with respect to each other and the barrier interior walls.

A three-dimensional Cartesian mesh was used to represent a barrier volume of homogeneous and isotropic soil. The permeability of the soil was chosen to be $1e^{-13}$ m^2 with a 30% porosity and negligible moisture content. Sulfur hexaflouride (SF_6) was used as the tracer gas and had a diffusivity of $7.03e^{-6}$ m^2/s in the soil. The mesh boundaries were chosen to simulate no flow boundaries, one of which was the barrier wall, around a single injection port. A volume of influence from only a single injection port was modeled because in an evenly spaced array of injection ports where each injection rate is equal, no flow boundaries exist at the interfaces between advancing spherical tracer gas fronts assuming homogeneous and isotropic soil conditions. The distances from a single injection port to its no flow boundaries and the barrier wall were varied to represent different spacing between other injection ports and the barrier wall.

The desired concentration at the barrier interior wall for the first injection was found by systematically changing the injection port spacing (the distance from the single injection port to the no flow boundary), the distance from the injection port to the barrier wall, and the mass of tracer injected. After the initial pulse of tracer gas, the system was allowed to equilibrate for a period of time before the next injection. The following scenario was found to deliver the desired tracer concentrations at the barrier wall:

- 9 foot (on center) injection port spacing
- 4 foot spacing from the injection port to the barrier wall
- Initial tracer injection of 0.2 pounds for 1 hour (allowed to equilibrate for 96 hours)
- Second tracer injection of 0.4 pounds for 1 hour (allowed to equilibrate for another 96 hours)
- Third tracer injection of 1.0 pounds for 1 hour (allowed to equilibrate for another 96 hours)

After the first injection, tracer concentration at the barrier varied between 2674 ppm to 2719 ppm. Figure G-B1 shows the distribution of SF_6 at the barrier wall after this the initial pulsed injection was allowed to equilibrate. Subsequent injections, also illustrated in figure G-B1 showed tracer concentrations to be between 7393 ppm and 7487 ppm, and 18,989 ppm and 19,196 ppm. It is also significant to notice that the tracer SF_6, whose molecular weight is heavier than air, tends to sink downward with time due to gravity.

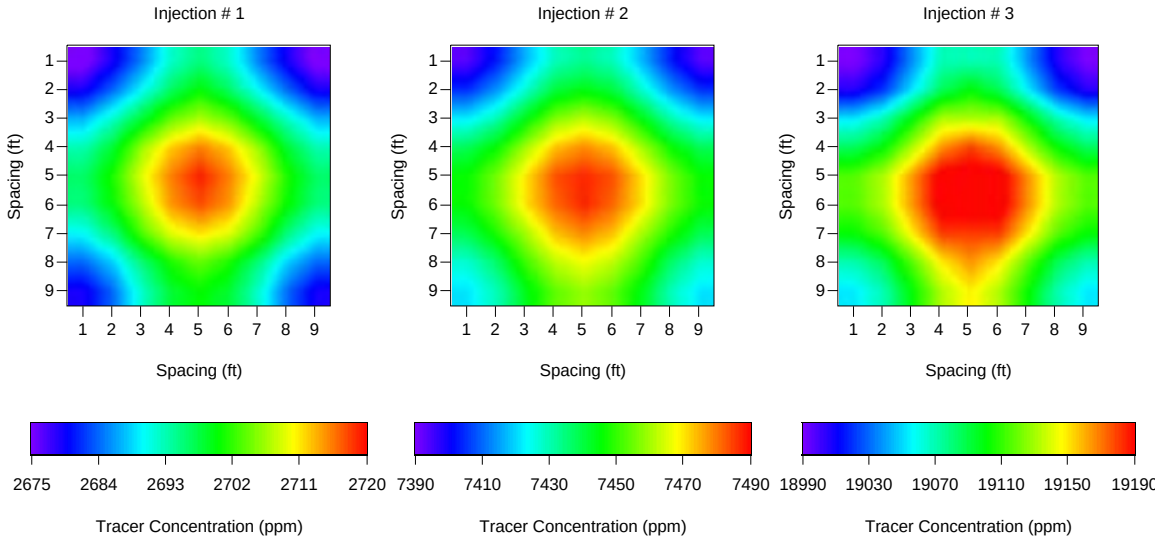

Figure G-B1. Tracer concentrations after each injection and a period of equilibration were found to be relatively uniform across the barrier wall.